

Test Stand for Synchronous Hydraulic-Motor Drive

Bachelor project

MAS302

Lars Alexander Eikeland

Thomas Børseth

Kjetil Lohne Bakke

Supervisor

Hamid Reza Karimi

Eivind Arne Johansen

This Bachelor's Thesis is carried out as a part of the education at the University of Agder and is therefore approved as a part of this education. However, this does not imply that the University answers for the methods that are used or the conclusions that are drawn.

University of Agder, 2013

Faculty of Engineering and Science

Department of Mechatronics

Preface

This bachelor thesis has been highly educational at all aspects of an engineering feat.- Not only has the group been working with an engineering perspective, but also been following up on the economical and constructional part of the equation. Moreover, this project also demonstrated the importance of team work, communication and personal behavior in the work place.

The project required several disciplines of engineering knowledge. This has helped the authors to distribute the work between themselves, and then work in a parallel fashion. This could only be achieved with good cooperation and a sense of friendship.

A special thanks to the assistant participants during this project

Supervisors: Hamid Reza Karimi, UiA

Eivind Arne Johansen, UiA

Assisting supervisor: Michael Rygaard Hansen, UiA

Mechanical construction assistant: Roy Werner Folgerø, UiA

22.05.2013

Kjetil Lohne Bakke

Lars Alexander Eikeland

Thomas Børseth

Abstract

It is not always practical or even possible to synchronize multiple actuators with a mechanical connection. Therefore, it is ideal to experimentally try to improve or explore new ways to a successful result. This report covers the work performed to solve the problem of a bachelor thesis written by the University of Agder. The thesis "*Test Stand for Synchronous Hydraulic-Motor Drive*" involves synchronizing two hydraulic motors regardless of load distribution. The project prompts the authors to investigate the problems associated with a non-mechanical connection.

This report present the results of the students' solution to synchronize two hydraulic motors using a hydraulic system, regulated with a PID controller, and implemented in a student-constructed test stand. A test stand is designed, manufactured and assembled in accordance with an acceptable budget limitation. Furthermore, the group designed the hydraulic system controlling the motors. All components of the hydraulic system had to be selected according to safety, cost and not least, functionality. A mathematical model was created as the basis of the control system. The control system was simulated in LabVIEW and later applied to the stand.

Testing of the stand showed the physical result of a simulated theory. In turn, the testing also displayed the significant impact of discrepancies and noise. The test stand and the system in its entirety showed the students firsthand the possibility of synchronizing multiple actuators without a mechanical connection.

Table of contents

List of Figures.....	6
List of Tables.....	8
List of Notations	9
1 Introduction.....	13
1.1 Background	13
1.2 Motivation.....	13
1.3 Problem statement	14
2 Mechanical design	15
2.1 Mechanical components.....	16
2.1.1 Steel.....	16
2.1.2 Beam.....	17
2.1.3 Gear	18
2.1.4 Shaft coupling.....	19
2.1.5 Bearing.....	19
2.1.6 Winch.....	20
2.2 SolidWorks simulation	21
2.2.1 Test stand	21
2.2.2 Beam.....	23
2.3 Weld calculations	25
3 Hydraulic Design	27
3.1 Hydraulic components.....	27
3.1.1 Pump.....	27
3.1.2 Motor.....	27
3.1.3 Overcenter valve	28
3.1.4 Proportional valve group.....	30
3.1.5 Pressure transducer.....	30
3.1.6 Pressure relief valve	30
3.1.7 Hydraulic lines	31
3.2 Hydraulic circuit	33
4 Instrumentation.....	34
4.1 Instruments.....	34
4.1.1 National Instrument	34

4.1.2	Horizontal accelerometer.....	35
4.1.3	Distance sensor	35
4.1.4	Pressure transducer.....	35
4.1.5	Voltage amplifier	35
4.2	Electrical wiring	36
5	Control design.....	38
5.1	Mathematical model.....	38
5.1.1	Mechanical system applied to hydraulic system.....	38
5.1.2	Motor equations.....	42
5.1.3	Valve equations	43
5.1.4	Hydro-mechanical system	45
5.2	Control system	47
5.2.1	Closed loop control.....	48
5.2.2	Controller design	53
5.3	Real time simulations.....	55
6	Concluding remarks	59
6.1	Results.....	59
6.2	Discussion.....	59
6.3	Conclusion.....	59
7	Reference list	60
Appendix A,	Final Accounts	62
Appendix B,	Electrical wiring diagram.....	63
Appendix C,	Data sheets.....	64

List of Figures

Figure 1:	Test Stand for Synchronous Hydraulic-Motor Drive	15
Figure 2:	3D-model of the mechanical design.....	16
Figure 3:	Beam Assembly	17
Figure 4:	Worm gear.....	18
Figure 5:	Rotex coupling.....	19
Figure 6:	PASEY45 Bearing Housing & Bearing.....	19
Figure 7:	Winch.....	20
Figure 8:	Wire coupling	20
Figure 9:	Test Stand, Von Mises simulation	21
Figure 10:	Test Stand, Displacement simulation	22
Figure 11:	Beam unit, Von Mises simulation.....	23
Figure 12:	Beam unit, displacement simulation.....	24
Figure 13:	Free body diagram, cable drum	25
Figure 14:	Weld Figure	26
Figure 15:	Pump.....	27
Figure 16:	Motor.....	28
Figure 17:	Overcenter valve	28
Figure 18:	Proportional valves, normally closed and normally open, respectively	30
Figure 19:	Pressure transducer.....	30
Figure 20:	Pressure relief valve	30
Figure 21:	Hydraulic flow diagram.....	33
Figure 22:	Amplifier Sketch	35
Figure 23:	Mechanical lifting system, angles and lengths.....	39
Figure 24:	Mechanical lifting system, moments and forces.....	40
Figure 25:	Mechanical lifting system, accelerations and angular acceleration.....	40
Figure 26:	Hydraulic system	44
Figure 27:	Valve operations block diagram	47
Figure 28:	Closed loop of inclination	48
Figure 29:	Closed loop with time delay of inclination	48
Figure 30:	Simulation of the uncompensated systems Gvmh.....	52
Figure 31:	Simulation of the PI compensated systems Gvmh.....	53
Figure 32:	Simulation of the PID compensated systems Gvmh	54

Figure 33:	Simulations of the three PID controllers	54
Figure 34:	Real time simulation, unloaded.....	56
Figure 35:	Real time simulation, 400kg in position x=0.44	57
Figure 36:	Block Diagram.....	58
Figure 37:	Front Panel	58

List of Tables

Table 1:	HPU specifications	27
Table 2:	Calculation of hydraluc lines	32
Table 3:	Electrical signal specifications	34
Table 4:	Signal cord connections.....	37

List of Notations

Constant	Value	Unit	Description
β	1100	MPa	Bulk modulus, oil stiffness
η_{hmM}	0.91	–	Hydro-mechanical efficiency coefficient motor
η_{vM}	0.94	–	Volumetric efficiency coefficient motor
ρ	875	kg / m ³	Density of the hydraulic fluid
ρ_p	3	–	Pilot ratio overcenter valve
Δp_{ocv}	3	bar	Pressure drop @ 5l / min, overcenter valve
ν	32	cSt	Kinematic viscosity, hydraulic fluid
μ	30	cP	Dynamic viscosity, hydraulic fluid
γ	0.82	–	Dynamic efficiency, wormdrive
τ	0.120	s	Time constant
$A_{d0,M}$	4.23	mm ²	Discharge area master PVG slade
$A_{d0,S}$	14.82	mm ²	Discharge area slave PVG slade
C_d	0.62	–	Discharge coefficient
D	32	cm ³ / rev	Stroke displacement motor
g	9.81	m / s ²	Gravitational constant
L_B	1.8	m	Length of beam
L_L	2500	mm	Line length
m_B	20	kg	Mass of the beam
m_d	7.1	kg	Mass of the drum assembly
m_L	780	kg	Mass of payload
N	20	–	Gearing ratio
p_s	$100 \cdot 10^5$	Pa	Supply pressure
Q_P	23.0	l / min	Max flow from pump
$Q_{M,\max}$	5	l / min	Max flow through master PVG
$Q_{S,\max}$	25	l / min	Max flow through slave PVG
r	0.035	m	Radius of drum
Re_T	2300	–	Reynolds number, threshold in circular lines
U_{offset}	2.5	V	Voltage corresponding to 0 acceleration
$U_{sensitivity}$	4	V	Voltage range from the accelerometer
U_{sup}	24	V	Supply voltage PVG
$V_{L,in}$	0.970	l	Volume of hydraulic oil in pipelines, A-port
$V_{L,out}$	1.41	l	Volume of hydraulic oil in pipelines, B-port

Parameter	Unit	Description
$\Delta p_{B \rightarrow T}$	Pa	Pressure drop from port B to port T
Δp_{cv}	Pa	Pressure drop across the check valve
$\Delta p_{M,M}$	Pa	Pressure drop across master motor
$\Delta p_{M,S}$	Pa	Pressure drop across slave motor
$\Delta p_{P \rightarrow A}$	Pa	Pressure drop from port P to port A
Δp_{Q_p}	bar	Pressure drop in the line from the pump side
$\Delta p_{Q_{M,\max}}$	bar	Pressure drop in the line from the PVG _M
$\Delta p_{Q_{S,\max}}$	bar	Pressure drop in the line from the PVG _S
Δp_v	Pa	Pressure drop across the PVG valve
θ_{acc}	rad	Inclination angle in the beam
θ_M	rad	Angle position of master drum
θ_S	rad	Angle position of slave drum
ω_M	rad / s	Angular velocity of master motor
ω_S	rad / s	Angular velocity of slave motor
η_{ys}	—	Factor of safety for yield stress
η_w	—	Factor of safety for yield stress in weld
$\sum M_A$	Nm	Sum of momentum located at point A
$\sum F_Y$	N	Sum of force in direction Y
σ_e	MPa	Equivalent stress from either simulation or calculation
σ_f	MPa	Yield strength of the weakest material
σ_{ys}	MPa	Yield strength of material
$\sigma_{N\perp}$	MPa	Normally experienced yield stress perpendicular to the weld length
$\tau_{N\perp}$	MPa	Normally experienced shear stress perpendicular to the weld length
σ_\perp	MPa	Total yield stress perpendicular to the weld length
τ_\perp	MPa	Total shear stress perpendicular to the weld length
λ	—	Friction factor in circular lines
a	m / s^2	Acceleration
a_c	m / s^2	Acceleration of the centre of mass
a_w	mm	Weld thickness
a_1	m / s^2	Acceleration on the edge of the beam on master side
a_2	m / s^2	Acceleration on the edge of the beam on slave side
A	mm^2	Area of the circular lines
C	$m^4 \cdot s^2 / kg$	Capacitance of hydraulic system
F	N	Force
F_1	N	Vertical force acting between wire and beam on master side
F_2	N	Vertical force acting between wire and beam on slave side

F_L	N	Static load acting between the beam and wire on master side
F_N	N	Force experienced in the weld normally to the weld thickness line
F_P	N	Force experienced in the weld perpendicular to the weld thickness line
F_y	N	Total acting forces on the beam, y-direction
J	kgm^2	Mass moment of inertia around the centre of mass
J_B	kgm^2	Mass moment of inertia of the beam
$J_{eff,M}$	$kg \cdot m^2$	Effective mass moment of inertia applied to motor, master side
$J_{eff,S}$	$kg \cdot m^2$	Effective mass moment of inertia applied to motor, slave side
J_d	$kg \cdot m^2$	Mass moment of inertia, drum
K_{qu}	m^3 / s	Flow gain
K_{qp}	$m^4 \cdot s / kg$	Flow pressure gain
K_c	—	Controller gain
L	mm	Possible length of weld
L_e	mm	Assumed effective length of weld
m	kg	Mass
m_1	kg	Effectiv mass pulling in wire, master side
m_2	kg	Effectiv mass pulling in wire, slave side
M_1	Nm	Momentum on the edge of the beam, master side
M_2	Nm	Momentum on the edge of the beam, slave side
M_c	Nm	Momentum acting around center of mass
M_M	Nm	Momentum applied by motor to motor shaft, master side
M_S	Nm	Momentum applied by motor to motor shaft, slave side
$M_{L,M}$	Nm	Momentum on load holding shaft, master side
$M_{L,S}$	Nm	Momentum on load holding shaft, slave side
$M_{M,M}$	Nm	Momentum applied by load to motor shaft, master side
$M_{M,S}$	Nm	Momentum applied by load to motor shaft, slave side
p_{pil}	bar	Pilot pressure, overcenter valve
Q_{corr}	m^3 / s	Corrective flow through slave PVG to ensure equal flow
$Q_{M,M}$	m^3 / s	Flow across master motor
$Q_{M,S}$	m^3 / s	Flow across slave motor
Re	—	Reynolds number
R_{A_Y}	N	Reaction force at point A in direction Y
R_{B_Y}	N	Reaction force at point B in direction Y
T_i	s	Integration time, controller
T_d	s	Derivative time, controller
T_L	Nm	Static torque applied on the load-bearing shaft
T_M	Nm	Motor torque

u_{corr}	—	Corrective position of the spool in slave PVG due to inclination in beam
u_M	—	Normalized position of the spool in master PVG
u_S	—	Normalized position of the spool in slave PVG
v	m / s	Velocity at a given point
v_{Q_p}	m / s	Velocity of the hydraulic oil at the pumpside
$v_{Q_{M,\max}}$	m / s	Velocity of the hydraulic oil after the PVG_M
$v_{Q_{S,\max}}$	m / s	Velocity of the hydraulic oil after the PVG_S
x	m	Distance between Master and payload
x_c	m	Distance in x-direction on the beam to the centre of mass
y_1	m	Distance from beam to drum, master
y_2	m	Distance from beam to drum, slave
y_e	m	Difference in distance between y_1 and y_2

1 Introduction

The crane as we know it was invented by the Greeks in the 6th century BC. [1] As technology improves and our knowledge of mechanical physics enhances, the crane has become the mega-structure among constructional tools.

Challenging building designs and offshore performance requirements demand tools of an unconventional and reliable nature. Based on these requirements, the group has been assigned to find an alternative solution to synchronize two hydraulic motors, without a mechanical fix. The motors hoist an object of a non-homogenous load. The project gives the students the opportunity to implement hydraulics, programming, design and instrumentation into a single solution. The report require basic understanding within the field of mechatronics and is adapted as such.

1.1 Background

The dissertation compelled the students to think around a direct solution to a simple task. The ability to synchronize motors with a mechanical composition was not an option. The next closest option to synchronize the motors would be by controlling the hydraulic valves with a control system. The development of the control system was considered to be the key to a stable, reliable and functional end result. The control system was also expected to be the main source of discrepancies. However, all disciplines of the system were expected to have sources for discrepancies. Some of these sources are wire extension, sensor deviation, valve reaction time and also motor efficiency at different pressures.

The thesis examines all disciplines to mechatronics. To ensure a steady work progress it is important to examine all disciplines simultaneously. To do so, each student would focus on the discipline best suited for their areas of expertise. However, the beginning of the project started with all three students working on the development of the hydraulic system. Several ideas were discussed on how to synchronize the motors, such as series coupling, parallel coupling using two servo valves and also parallel coupling using two PVG valves. A series coupling would cause unacceptable discrepancies, and servo valves were an overly expensive solution. The final solution built on the last suggestion combined with the Master-Slave principle.

1.2 Motivation

The project at hand was picked out to be the favourite among thirty-two bachelor assignments. The group selected this project due to its relevance to future work in the oil industry. The mechanic and hydraulic disciplines were the part which caught the groups' fancy. However, the control part is interesting on account of the relevance to the offshore industry. The group has been working together since the first day at the university. In time, this has become a great asset in accordance with collaboration and communication. Furthermore, two of the group members have a mechanical certificate from previous work experience. The experience with lathe, milling, welding and mounting along with efficient teamwork encouraged the students to choose an educational yet challenging bachelor project.

1.3 Problem statement

This project addresses a problem where two hydraulic motors are to run synchronized in the event of an unequal strain. In order to solve this problem the group had to design and construct a test stand implemented with a hydraulic system and regulated with a control system. In order to accomplish the task in accordance with the University's demand the group had to work closely with the following disciplines.

- Mechanics
- Hydraulics
- Control system

Mechanics

The ingenuity of design was unlimited besides permission for a mechanical connection between the engines. The group was required to design, buy, machine and compile all parts necessary to complete the project task of constructing a test stand. All welding and machining was done in the workshop of the University of Agder under supervision of the workshop supervisors. The test stand required use of gears and bearing as well as equipment approved for lifting. The stand was also required to be designed in accordance with the hydraulic system implemented to the construction.

Hydraulics

A series connection in order to synchronize the hydraulic motors is not acceptable in terms of leakage and loss of pressure. A parallel connection of the motors is therefore the only possible solution. This type of system creates several challenges in terms of choosing the appropriate components. Furthermore, the group had to be aware of safety and create a redundant system at an acceptable level considering the construction is subjected to a suspended load.

Control system

The control system is expected to require the most attention in this project and may be considered as the brain of the entire system. The synchronous hydraulic-motor drive requires mathematical models, simulations and control design in order to work appropriately. One of the major difficulties encountered in the design of the control system is implication of linear solutions to a non-linear problem.

2 Mechanical design

This chapter addresses the mechanical part of the task. It includes a short explanation of the various components and connections, static simulations and weld calculations. The mechanical design is made in accordance to the project specification under the mechanical supervisor guidance. Therefore, it is required to build a test stand properly not only for the use of this years' assignment, but also for assignments years to come.

The project required use of hydraulic motors already available at the workshop. These motors are not capable of handling the force and torque of the load directly as promoted in the thesis. For that reason, the group was allowed to find a solution that contravenes the thesis required solution. The solution adopted is the use of gearboxes.

The construction is made of square pipes adding to a solid framework. The completed stand can be seen in a real time picture in Figure 1. The construction allows the possibility to attach the external load at several locations on the beam. The stand was constructed primarily by the students of the group. However, some assistance was given by the workshop supervisors. The reason for this aid was because of time constraints and use of machinery outside the students' field of expertise.

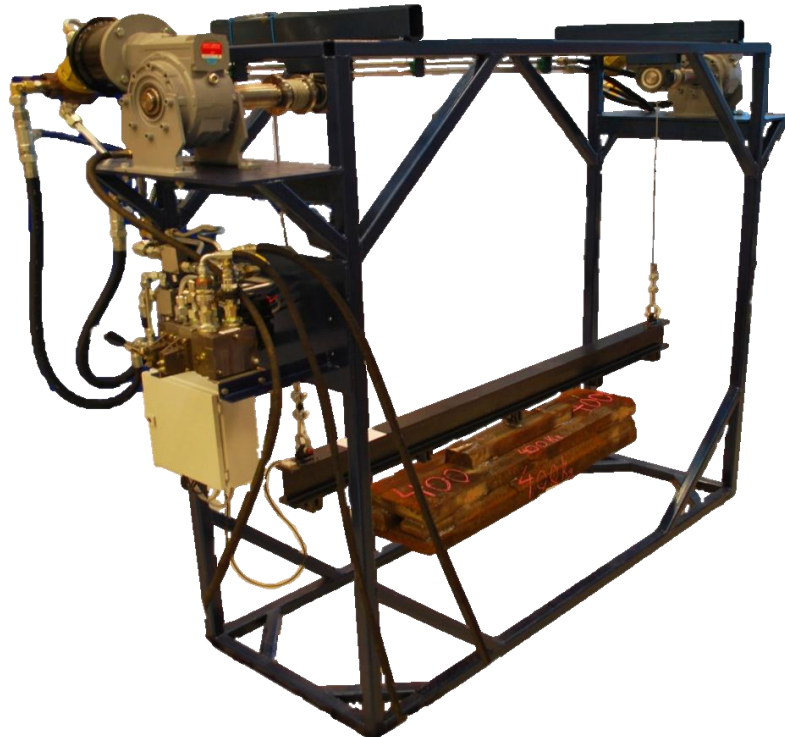


Figure 1: Test Stand for Synchronous Hydraulic-Motor Drive

2.1 Mechanical components

All vital parts and components of the mechanical structure are described in this subsection. To see production drawings for the construction see the included folder to the report.

2.1.1 Steel

The stand is built out of square pipes in material S355J2H. The dimensions of these pipes are based on the forces inflicting the test stand. The material of the pipes is bounded to the dimension, due to the product list of Leif Hübert. All steel components for this project were purchased from Leif Hübert. The final result of the mechanical design can be seen in Figure 2. The 3D model includes wire, gearboxes and hydraulic motors.

There were multiple factors to consider while dimensioning the various parts of the stand. Availability, cost, force resistance and assembly simplicity were the main factors. Considering force resistance, SolidWorks simulations were used in order to determine the minimum dimensions required of the varying parts. The simulation results are described in chapter 2.2.



Figure 2: 3D-model of the mechanical design

2.1.2 Beam

The beam is the most eye-gripping part of the construction during testing, seeing as the beam is the part used to measure the angle during lifting.

Getting the lifting angle to zero is physically impossible. There will always be discrepancies influencing the result. One of these expected discrepancies is the bend in the beam. Therefore, the beam must be sturdy enough to stay within acceptable bending limits. Furthermore, the beam assembly as a unit must be sturdy enough to endure changing forces, as both the magnitude and area of effect changes.

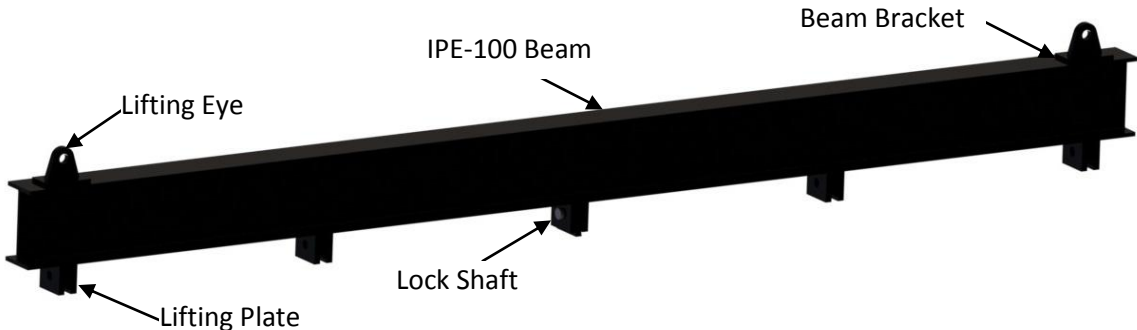


Figure 3: Beam Assembly

The group chose the beam type IPE due to recommendation from the mechanical supervisor. However, this decision was non-essential. Testing the different beam standards started with creating the beam in SolidWorks. The material of the beam is S355J2G3. In order to determine the correct measurements for the various standards of IPE beams the group used the site “*Structural Drafting Net Expert*” [2]. Simulation results showed the use of IPE-100 was acceptable. The simulation results are illustrated in chapter 2.2.

2.1.3 Gear

In order to lift a payload and yoke of combined 800kg the group had to come up with a solution to decrease the torque and the radial force on the output shaft of the motor. The motor used in this project can handle a torque of 178Nm with a pressure drop of 350bar and an radial force of 5400N. The maximum static radial force on the shaft holding the payload and beam is estimated to be 8525N. In this case, the load is hanging on the edge of the beam. The torque will in this case be 298Nm, as calculated at (2.1).

$$F_L(0) = 8525N$$

$$\begin{aligned} T_L(x) &= F_L(x) \cdot r \\ T_L(0) &= 8525N \cdot 0.035m = \underline{\underline{298Nm}} \end{aligned} \quad (2.1)$$

For this reason, the group found it necessary to place the load on an external shaft and use a gear box to comply the torque and the radial force limits. For great ratio and small volume, a worm drive was considered most suitable for this project. The force $F_L(0)$ is calculated at (2.2).

Worm drives are used when large gear reductions are needed. The hydraulic motors used in this project require high operating speed in order to reach ideal. Therefore, a large gear reduction will reduce the speed on the output shaft of the gearbox. Another advantage with the worm drive is the automatic breaking mechanism. The output shaft of the gear is only able to rotate when the input shaft rotates [3]. The gearboxes used in the project are worm drives from Hydromec. For more information about the worm drives see Appendix C.1.

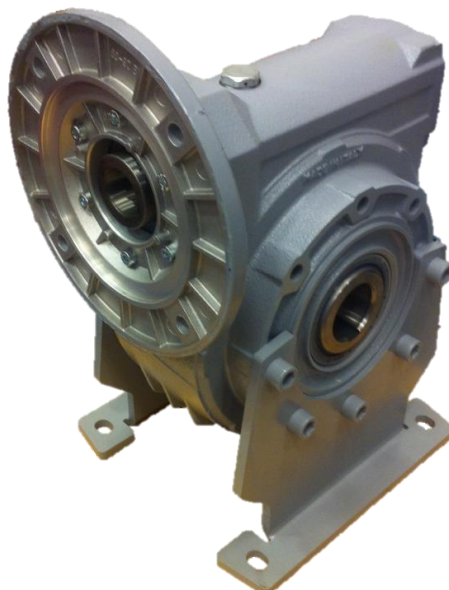


Figure 4: Worm gear

2.1.4 Shaft coupling

The hydraulic motors' output shaft is not connectable to the input of the gearbox considering both size and shape. The A2FM32 motor has a splines shaft, whereas the gearbox has a wedge input. A coupling is required in order to connect these two components. The workshop had two matching couplings already available for the motor side. The couplings are from Rotex and therefore a matching coupling for the gearbox side was purchased. The coupling is a torsionally flexible jaw-type with taper clamping sleeve of size 3138K98. For more information about the coupling see Appendix C.2, or visit www.ktr.com. The appropriate axle connecting the coupling and the gearbox was machined in the workshop. Covering the shaft and coupling is a protective drum mounted to support the weight of the motor.



Figure 5: Rotex coupling[24]

2.1.5 Bearing

To ensure low frictional rotation of the shafts the group decided to implement bearings to the mechanical construction. The bearings are mounted in bearing housings. The maximum force carried in the bearing is 6650N, see weld calculations chapter 2.2. The required size of the shaft and the force applied to the bearing is decisive when choosing a bearing for this project. However, a bearing along with housing was already available for use in the workshop. Therefore, this test stand uses the radial insert ball bearings, GAY45-NPP-B. This bearing can handle much larger forces than our minimum requirement. For datasheet of this bearing see Appendix C.3. The matching housing for this type of bearing is the PASEY45. For more information about the housing, see Appendix C.4.

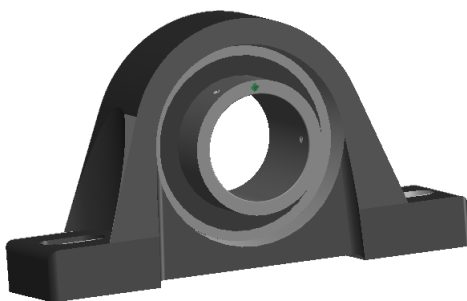


Figure 6: PASEY45 Bearing Housing & Bearing

2.1.6 Winch

In order to twirl the wire the group had to come up with a solution for design of a winch. The SolidWorks illustration can be seen in Figure 7. The drum is welded to a machined shaft, this shaft is connected to the gearbox shaft using a sleeve and wedges. All machined components for the winch can be found in the included folder.

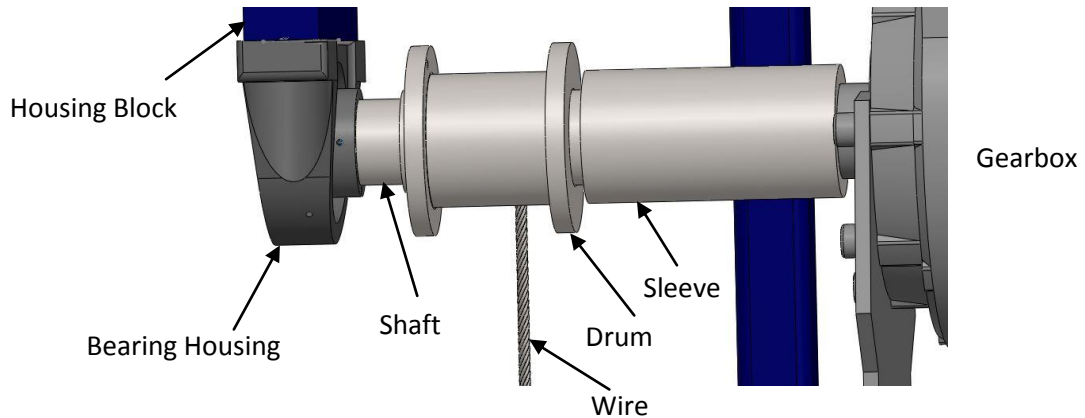


Figure 7: Winch

The wire is lead through a hole on the side of the drum and fixed using a small wire clamp. In turn, the wire is twisted around the drum four times, this is the primary attachment between the drum and wire. Opposite side of the wire has a small thimble of 24mm diameter. The thimble is created using two Iron Grip wire clamps, for more information about the mounting of the wire clamps, see Appendix C.5. Finally the wire is connected to the beam using a shackle. The result can be seen below in Figure 8.



Figure 8: Wire coupling

2.2 SolidWorks simulation

This section deals with the static simulations from SolidWorks of the test stand and the beam. The load bearing force is set to 8800N and the torque in winch is set to 330Nm. All forces have been added 10% for safety reasons. The deformation scale is 100 in all simulation illustrations.

2.2.1 Test stand

The simulations can be seen below in Figure 9 and Figure 10, and includes worm drives and hydraulic motors. Figure 9 illustrates the physical strain to the stand during static load bearing. The simulation illustrates the original solution to design of the test stand. However, the housing block, see Figure 7, has been replaced by square pipe. The use of square pipe results in unacceptable stress, $\eta_{ys} = 1.8$.

This problem was ignored due to the payload supplied was changed from 780kg to 400kg.

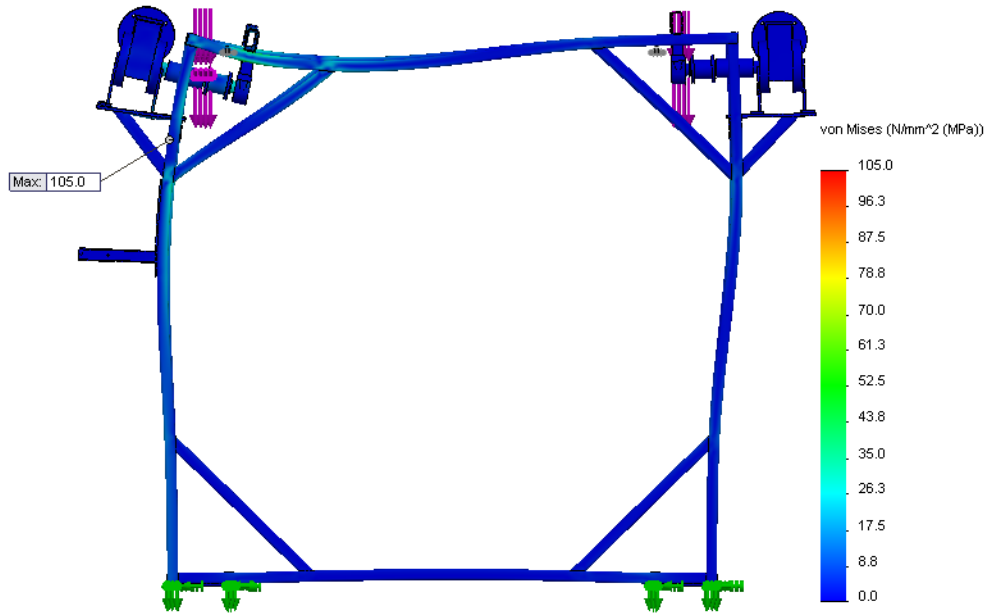


Figure 9: Test Stand, Von Mises simulation

The weight of the beam is 20kg, whereas the attached load could originally be as heavy as 780kg. Maximum static load on one of the two wires is therefore 790kg. For safety reasons the forces exerting are simulated with a 10% increase. The forces in the simulation are also increased slightly for the sake of simplicity, hereby leaving a margin for start acceleration in the beam.

$$F_L(x) = \left(\frac{m_B}{2} + m_L \left(\frac{L_B - x}{L_B} \right) \right) \cdot g \cdot 110\% \quad (2.2)$$

$$F_L(0) = \left(\frac{20\text{kg}}{2} + 780\text{kg} \left(\frac{1.8\text{m} - 0\text{m}}{1.8\text{m}} \right) \right) \cdot 9.81\text{m/s}^2 \cdot 110\% = \underline{\underline{8525\text{N}}}$$

The maximum force in the simulation was set to 8800N with a sinusoidal bearing distribution, leaving a margin for the start acceleration of 0.35m/s^2 , calculated below.

$$F_{margin} = F_{simulation} - F_L(0) = 8800\text{N} - 8525\text{N} = 275\text{N} \quad (2.3)$$

$$a = \frac{F}{m} \quad (2.4)$$

$$a_{margin} = \frac{F_{margin}}{\left(\frac{m_B}{2} + m_L\right)} = \frac{275\text{N}}{790\text{kg}} = \underline{\underline{0.35\text{m/s}^2}}$$

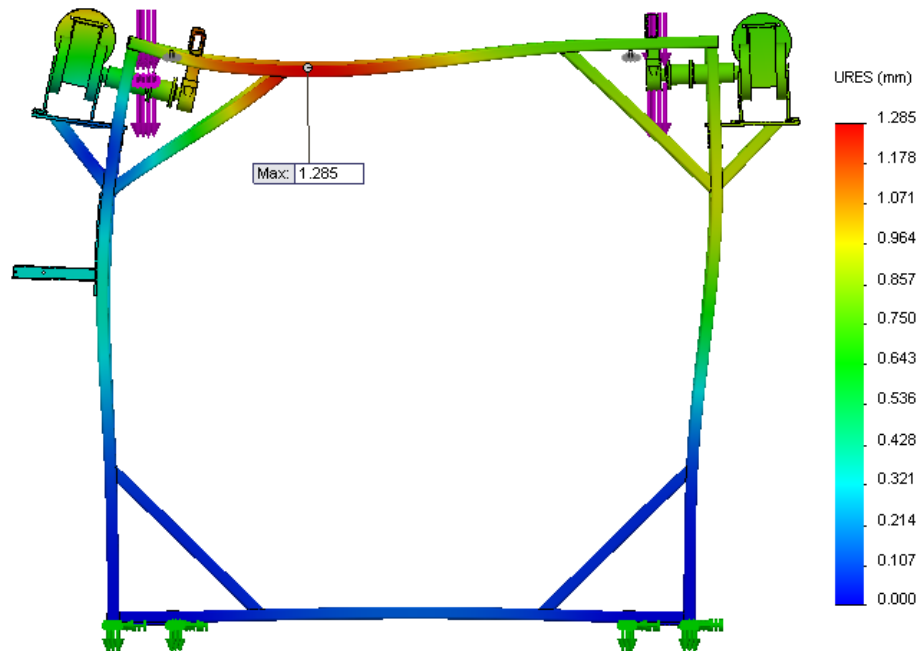


Figure 10: Test Stand, Displacement simulation

The von Mises study in Figure 9 shows a maximum annotation of 105.0MPa on the edge of the supporting pipe underneath the plate. Factor of safety in terms of yield stress is simply calculated.

$$\eta_{ys} = \frac{\sigma_{ys}}{\sigma_e} \quad (2.5)$$

$$\eta_{ys} = \frac{355\text{MPa}}{105\text{MPa}} = 3.38$$

The factor of safety for this project is considered acceptable at 3.0. The simulation results show acceptable stress in the material. Further investigation concludes no other areas of the structure subjected to stress of a significant magnitude. Considering the displacement illustrated in Figure 10, the deformation is largest in the upper pipes resulting in a bend of 1.285mm. The resulting bend is acceptable considering the pipes' function. Furthermore, the displacement of the winch components is acceptable at approximately one millimetre due to the bearing housings' ability to compensate for static misalignment.

2.2.2 Beam

The von Mises simulation illustrated in Figure 11 shows the maximum stress in the beam assembly is 151.2MPa. This stress is located on the bottom edge of the lifting eye. Factor of safety in terms of yield stress is simply calculated at (2.4).

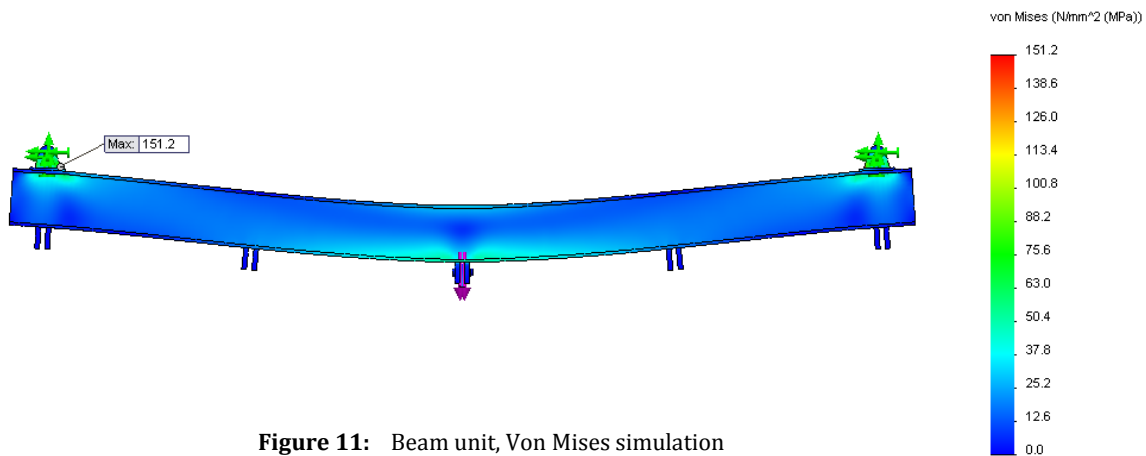


Figure 11: Beam unit, Von Mises simulation

The von Mises simulation illustrated in Figure 11 shows the maximum stress in the assembly is 151.2MPa. This stress is located on the bottom edge of the lifting eye. Factor of safety in terms of yield stress is simply calculated at (2.6).

$$\eta_{ys} = \frac{\sigma_{ys}}{\sigma_e} \quad (2.6)$$

$$\eta_{ys} = \frac{235MPa}{151.2MPa} = 1.55$$

The calculation shows the assembly is likely to work in terms of its function. However, in terms of safety this is not an acceptable result. An alternative solution to design is recommended in the case of working further on this construction in following projects years to come. However, the load used in this project was changed from 800kg to 400kg by order of our mechanical supervisor. The reason for this change is due to financial reasons. The load reduction of 400kg results in a maximum stress of 75.6MPa. The new factor of safety is calculated using the formula at (2.6).

$$\eta_{ys} = \frac{235MPa}{75.6MPa} = 3.1$$

Calculations prove the magnitude of stress to be at an acceptable level.

The simulation in Figure 12 illustrates the resulting bend in the beam. The group consider the maximum possible bending of 0.749mm as acceptable. The magnitude of force in the simulation is 8800N and applied at the centre of the assembly. Should the load be applied further to either side of the assembly would the stress and displacement diminish.

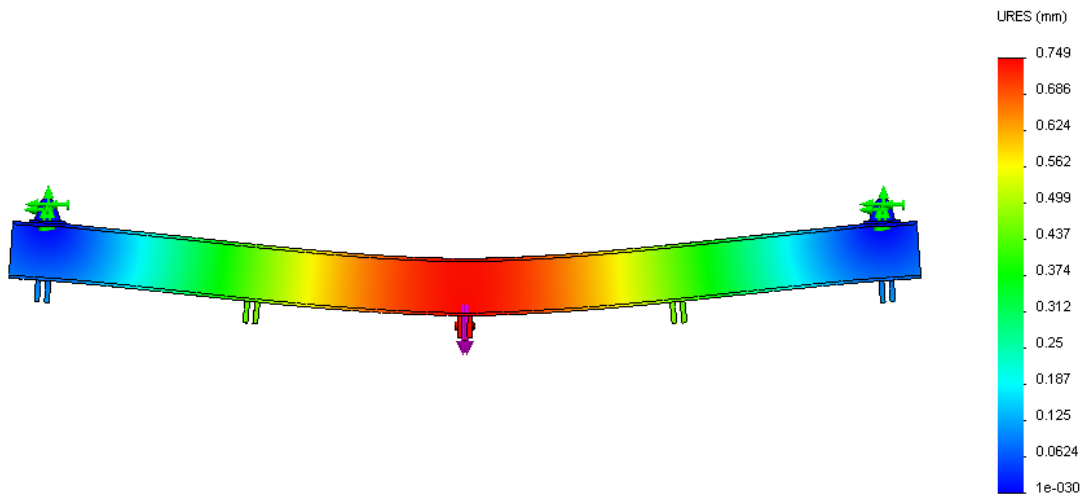


Figure 12: Beam unit, displacement simulation

This concludes the static force simulations in SolidWorks. The following section addresses the weld calculations.

2.3 Weld calculations

From visual inspection bending moment can be disregarded from all welds in the construction. Therefore, the most critical of welds is determined to be the weld carrying the bearing house. This fillet weld is exposed to the largest radial force and also of the minimal length, 40mm. The following calculations of this force are determined by the measurements taken from SolidWorks, shown in the figure below. All figures are simplified and are not proportional to the actual sizes.

Cable Drum Measurements

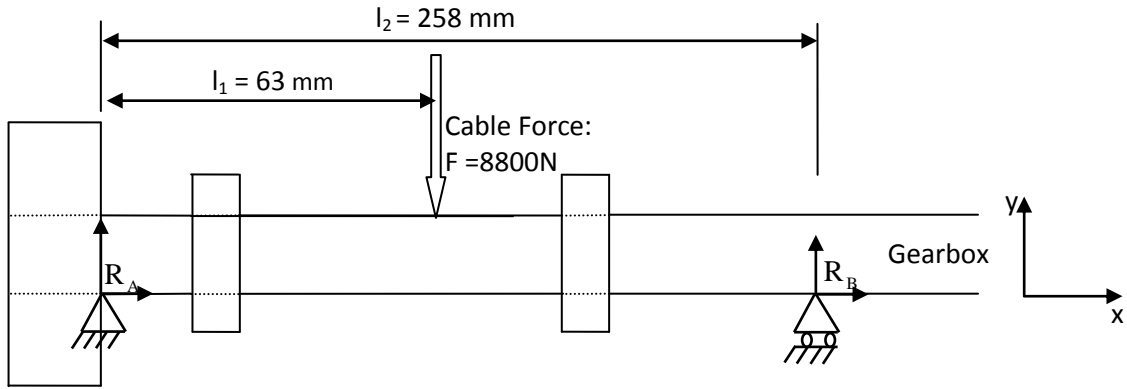


Figure 13: Free body diagram, cable drum

$$\begin{aligned} \sum M_A = 0 \text{ Nm} &= \begin{bmatrix} l_1 \\ 0 \end{bmatrix} \times \begin{bmatrix} 0 \\ -F \end{bmatrix} + \begin{bmatrix} l_2 \\ 0 \end{bmatrix} \times \begin{bmatrix} 0 \\ R_{B_y} \end{bmatrix} = l_2 \cdot R_{B_y} - l_1 \cdot F_{B_y} \\ &= 258 \text{ mm} \cdot R_{B_y} - 63 \text{ mm} \cdot F \end{aligned} \quad (2.7)$$

$$R_{B_y} = \frac{63 \text{ mm} \cdot F}{258 \text{ mm}} = \frac{63 \cdot 8800 \text{ N}}{258} = 2150 \text{ N}$$

$$\sum F_y = 0 \text{ N} = R_{A_y} - F + R_{B_y} \quad (2.8)$$

$$R_{A_y} = F - R_{B_y} = 8800 \text{ N} - 2150 \text{ N} = 6650 \text{ N}$$

The force experienced by the fillet weld is estimated to be 6650N. This force will in turn be used to determine the stress experienced by the fillet weld.

Bearing housing plus block

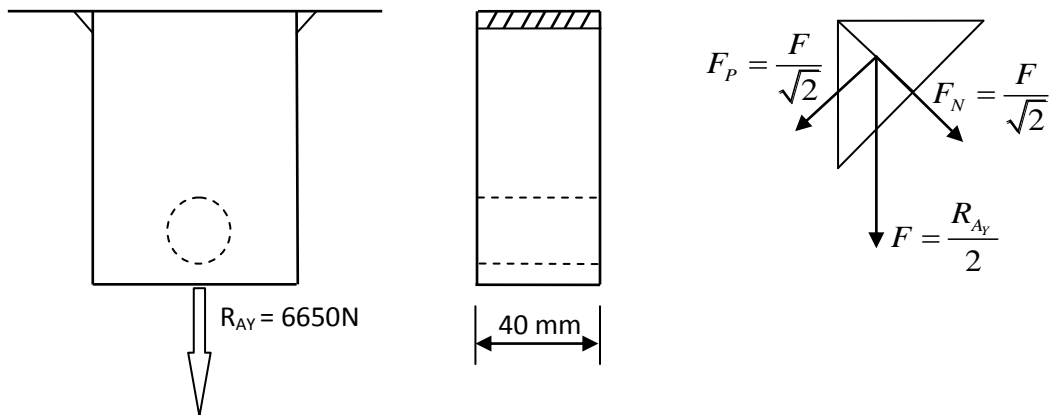


Figure 14: Weld Figure

Assuming : $a = 3mm$

$$L_e = L - 2 \cdot a = 40mm - 2 \cdot 3mm = 34mm \quad (2.9)$$

From (2.8), the effective length of a single fillet weld is estimated to be 34mm.

$$F_p = F_n = \frac{F}{\sqrt{2}} = \frac{R_{Ay}}{2 \cdot \sqrt{2}} = \frac{6650N}{2 \cdot \sqrt{2}} = 2351N \quad (2.10)$$

The forces causing yield stress and shear stress are equal and are therefore calculated as shown above at (2.9).

$$\sigma_{N\perp} = \tau_{N\perp} = \frac{F_p}{a \cdot L_e} = \frac{2351N}{3mm \cdot 34mm} = 23MPa \quad (2.11)$$

$$\sigma_{\perp} = \tau_{\perp} = \sigma_{N\perp} = 23MPa \quad (2.12)$$

Further, with no bending stress affecting the weld, the strain can be expressed as shown at (2.12).

$$\sigma_e = \sqrt{\sigma_{\perp}^2 + 3\tau_{\perp}^2} = \sqrt{4 \cdot \sigma_{\perp}^2} = \sqrt{4 \cdot (23MPa)^2} = 46MPa \quad (2.13)$$

$$\eta_w = \frac{\sigma_f}{\sigma_e} = \frac{235MPa}{46MPa} = 5.1 \quad (2.14)$$

The calculations assure the use of fillet weld with a thickness of three millimetres to be sufficient. Three millimetres is considered the minimum size of a fillet weld, the entire construction was therefore welded with this size. However, the minimum plate thickness of the pipes used in this construction is four millimetres, thereby conflicting with the rule stating the weld thickness should not exceed 0.7 times the minimum plate thickness. The group considered this rule to be superseded by the three millimetre thickness rule. In order to avoid increasing the pipe dimensions, the rule of having the maximum weld thickness of 0.7 times the plate thickness was discarded for this project.

3 Hydraulic Design

This chapter addresses the hydraulic part of the project. The hydraulic system engines the rotational components of the mechanical system. Hereby, lifting or lowering the beam and payload as desired. The first sub-chapter, Hydraulic components, covers the use and function of the various components. The students received guidelines from Michael Rygaard Hansen regarding component selection. The sub-chapter also examines the calculations required as basis for component selection. The second sub-chapter, Hydraulic circuit, illustrates the flow diagram and explains the compound function of all components.

3.1 Hydraulic components

The selection of hydraulic components is based on availability, function and cost. The group used electrically actuated components regulated by a control system and controlled by a computer.

3.1.1 Pump

The pump can be seen as the heart in the hydraulic circuit. It is usually driven by an electric motor, or a petrol or diesel engine and delivers flow to the system. There are different types and design of hydraulic pumps. The most common are the gear-, vane- and piston pumps. These pumps have the ability to displace fluid from the inlet- to the outlet port. The inlet is often connected to a reservoir and transforms low pressure fluid into high pressure fluid, and transports the fluid through the system [4]. The group could choose among three different pumps in this project. The pumps are fixed on three different HPU's, see Table 1 for specifications.

Pump number	Hydraulic specifications		Electrical specifications	
	Flow	Pressure	Supply voltage	Effect
1	14.5 l/min	100 bar	220 V	3.0 kW
2	23.0 l/min	240 bar	380 V	11.0 kW
3	210.0 l/min	350 bar	380 V	37.0 kW

Table 1: HPU specifications



Figure 15: Pump

3.1.2 Motor

The purpose of hydraulic motors is transforming hydraulic power into mechanical rotational force. There are several different types of hydraulic motors. The three most basic motors available are the same as for pumps, gear-, vane- and piston motors. For this project the group used two AA2FM 32 fixed motors. The motors are used to drive the gear boxes.

The piston motor works by pumping hydraulic fluid into the inlet of the motor. The hydraulic pressure from the fluid acts on the ends of pistons and hereby generating a force on an angled plate. The plate then rotates the output shaft. The torque created is based on the angle of the plate and the area of the pistons. Piston motors and piston pumps are basically designed in the same matter. However, there is a difference considering the motors receive flow and pressure from the system and deliver torque, whereas the pumps receive torque and deliver flow and pressure to the system [4].

The calculations below give an overview of the pressure drop over the motors and are used in chapter 3.2. The maximum and minimum pressure drop over the motors are found by attaching the load at the edge of the beam [5]. The calculations found the basis for selection of HPU size.

$$T_{L,\max} = T_L(0) = \left(\frac{m_B}{2} + m_L \cdot \left(\frac{L_B - 0}{L_B} \right) \right) \cdot r \cdot g = \underline{\underline{267.8 \text{Nm}}} \quad (3.1)$$

$$T_{L,\min} = T_L(L_B) = \left(\frac{m_B}{2} + m_L \cdot \left(\frac{L_B - L_B}{L_B} \right) \right) \cdot r \cdot g = \underline{\underline{6.9 \text{Nm}}} \quad (3.2)$$

$$\Delta p_{M,\max} (\text{negload}) = \frac{T_{L,\max}}{N \cdot \gamma} \cdot \frac{2 \cdot \pi \cdot \eta_{hmM}}{D} = \underline{\underline{29.2 \text{bar}}} \quad (3.3)$$

$$\Delta p_{M,\min} (\text{negload}) = \frac{T_{L,\min}}{N \cdot \gamma} \cdot \frac{2 \cdot \pi \cdot \eta_{hmM}}{D} = \underline{\underline{0.752 \text{bar}}} \quad (3.4)$$

$$\Delta p_{M,\max} (\text{posload}) = \frac{T_{L,\max}}{N \cdot \gamma} \cdot \frac{2 \cdot \pi}{D \cdot \eta_{hmM}} = \underline{\underline{35.2 \text{bar}}} \quad (3.5)$$

$$\Delta p_{M,\min} (\text{posload}) = \frac{T_{L,\min}}{N \cdot \gamma} \cdot \frac{2 \cdot \pi}{D \cdot \eta_{hmM}} = \underline{\underline{0.908 \text{bar}}} \quad (3.6)$$

The efficiency coefficients, η_{hmM} and η_{vM} , were given in a previous bachelor project using the same motors. In consultation with Michael Rygaard Hansen, the group decided to use the same constants. For more details on the motors see Appendix C.6.



Figure 16: Motor

3.1.3 Overcenter valve

The overcenter valve has several purposes. The valve controls an overrunning load. The overcenter valve can hold a load at steady state because it is depending on a pilot pressure to actuate. The valve also prevents the load from falling should a hose or a pipeline break. The valve also gives the system the ability to decelerate the load if necessary, and prevent cavitation.

In normal position, the overcenter valve is closed in the flow direction p_3 to p_2 and open in the opposite direction, as illustrated in Figure 17. In order to receive flow from p_3 to p_2 , the pressure at point p_3 must exceed the crack pressure in addition to the required pilot pressure. In case of breakage in either pipe or hose line connected to the valve input, a spring will return the valve to the closed position [6].

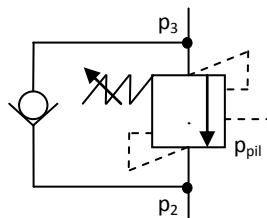


Figure 17: Overcenter valve

The students decided to use an overcenter valve with a pilot ratio of 3. The overcenter valves with a ratio of 3 require higher pilot pressure than those with higher ratio. However, a valve with ratio of 3 is more accurate with varying load [7].

The pressure drop computed in the negative direction (3.3 and 3.4), is used to calculate the size of the overcenter valve. Further, to avoid cavitation, is it important to keep the pressure at p_3 and p_{pil} within a certain limit. The group used a crack pressure (p_{cr}) equal to 150bar and the result is given in the following equations [4].

$$p_{cr} = p_3 + \rho_p \cdot p_{Pil} - (1 + \rho_p) p_2 \quad (3.7)$$

$$p_3 = p_{Pil} - \Delta p_M$$

$$p_2 = 10 \text{ bar}$$

$$p_{cr} = 150 \text{ bar}$$

$$p_{cr} = p_3 + \rho_p \cdot p_{Pil} - (1 + \rho_p) p_2$$

$$p_{cr} + \Delta p_M + (1 + \rho_p) p_2 = p_{Pil} \cdot (1 + \rho_p)$$

$$p_{Pil} = \frac{p_{cr} + \Delta p_M}{1 + \rho_p} + p_2$$

Max load(neg):

$$p_{Pil} = \frac{150 + (-29.2)}{4} + 10 = \underline{\underline{40.2 \text{ bar}}} \quad (3.8)$$

$$p_3 = 40.2 - (-29.2) = \underline{\underline{69.4 \text{ bar}}}$$

Min load(neg):

$$p_{Pil} = \frac{150 + (-0.752)}{4} + 10 = \underline{\underline{47.3 \text{ bar}}} \quad (3.9)$$

$$p_3 = 47.3 - (-0.752) = \underline{\underline{48.1 \text{ bar}}}$$

As seen in the calculations, the lowest pressure is at p_{pil} with a pressure of 40.2bar. To overcome all these parameters and to avoid cavitation the group had to use an overcenter valve. The valve used was the overcenter valve MHB-015-LBAH-51E from Parker, see Appendix C.7.

3.1.4 Proportional valve group

The proportional valve group (PVG) is a hydraulic load sensing valve designed to perform several tasks. The test stand uses the PVG 32 from Sauer Danfoss. The valve system is constructed with a module design, which makes it suitable for different tasks such as hoisting and lowering a load.

The proportional valve can be actuated either mechanically or electrically [8]. While using the electrical actuator the voltage signal applied to the valve will give the operator control of the flow or the pressure. In other words, an electrical actuator gives the operator a large margin for adjustment and flexibility [9]. The group used two electrically operated valves that were available in the workshop, illustrated in Figure 18. The PVG_M is a 4/3-way valve and closed in neutral position. The other valve (PVG_S) is also a 4/3-way valve, but is throttled and open in neutral position. For more details of the PVG see Appendix C.8.



Figure 18: Proportional valves, normally closed and normally open, respectively

3.1.5 Pressure transducer

The pressure transducer transforms pressure into a readable and manageable electric signal. There are numerous types of transducers on the market. The strain-gauge based transducer is the most common.

The aforementioned electrical signal is obtained when pressure causes a physical deformation of the strain gauges bonded into a membrane of the pressure transducer and wired to a Wheatstone bridge configuration. The pressure transducer produces strain to the gauges as pressure is applied. This strain in turn creates an electrical resistance alternating proportional to the pressure applied [10].



Figure 19: Pressure transducer

3.1.6 Pressure relief valve

The purpose of the pressure relief valve, illustrated in Figure 20, is to keep an acceptable system pressure. The pressure relief valve is necessary in every hydraulic system to prevent overloading of the components. The valve is placed close to the pump in order to keep the pressure at an acceptable level before the fluid flows through the valves [11].

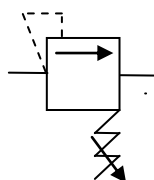


Figure 20: Pressure relief valve

3.1.7 Hydraulic lines

The hydraulic lines are used to transfer fluid through the hydraulic system. The system consists of both hoses and pipes. The velocity of the fluid is measured as the average speed of its particles past a given point in the lines. It is important to keep in mind the velocity of the fluid prior to sizing the lines. It is essential to have the fluid velocity at its minimum acceptable limit in order to keep turbulence and friction as low as possible [4].

The fluid used in the system, shown in Figure 21, is Texaco Radon HDZ 32. The constants for viscosity, ν and μ , and the density, ρ , are received from Chevron marine products [12]. The Reynolds number was calculated in order to determine whether the flow is laminar or turbulent. Furthermore, the pressure drop is calculated using the Hagen-Poiseuille equation at (3.11) [4]. The results are shown in Table 2.

Velocity:

$$\nu = \frac{Q}{A} \quad (3.8)$$

Reynolds number:

$$\text{Re} = \frac{\nu \cdot d_h}{\nu} \quad (3.9)$$

$$\text{Re}_T = 2300$$

if $\text{Re} \leq \text{Re}_T \Rightarrow$ Laminar flow
 if $\text{Re} > \text{Re}_T \Rightarrow$ Turbulent flow

Friction factor:

$$\lambda = \frac{64}{\text{Re}} \quad (3.10)$$

Hagen-Poiseuille equation:

$$Q = \frac{\pi \cdot d^4}{128 \cdot \mu \cdot L} \cdot \Delta p \quad \Rightarrow \quad \Delta p = \frac{Q \cdot 128 \cdot \mu \cdot L}{\pi \cdot d^4} \cdot 10^{-5} \quad (3.11)$$

Hose ["]	3/8	1/2	5/8	3/4	1	1 1/4
Inside d [mm]	9,5	12,7	15,9	19,1	25,4	31,8
A [mm ²]	70,9	126,7	198,6	286,5	506,7	794,2
v_{Q_n} [m/s]	5,41	3,03	1,93	1,34	0,76	0,48
$v_{Q_{M_max}}$ [m/s]	1,18	0,66	0,42	0,29	0,16	0,10
$v_{Q_{S_max}}$ [m/s]	1,29	0,72	0,46	0,32	0,18	0,12
Re [-]	1605,5	1201,0	959,3	798,6	600,5	479,6
λ [-]	0,0399	0,0533	0,0667	0,0801	0,1066	0,1334
Δp_{Q_p} [bar]	1,44	0,45	0,18	0,09	0,03	0,011
$\Delta p_{Q_{M_Max}}$	0,31	0,10	0,04	0,02	0,006	0,002
$\Delta p_{Q_{S_Max}}$ [bar]	0,34	0,11	0,04	0,02	0,007	0,003

Table 2: Calculation of hydraluc lines

As displayed in Table 2, all the calculations of the Reynolds number result in a laminar flow. Also, the pressure drop is acceptable for all of the given sizes. The hose sizes $\frac{3}{4}"$ and $1"$ was considered the best option based on the coupling to the valves as well as recommendation from our supervisor. The different sizes can be seen in Figure 21.

3.2 Hydraulic circuit

The hydraulic power unit (HPU) delivers flow and pressure to the system. According to the calculations in chapter 3.1, the group found the smallest HPU able to supply the system with sufficient pressure and flow. However, the HPU able to deliver a flow of 23.0l/min and a pressure of 240bar were provided by the supervisor. The master valve (PVG_M) is a manually operated from computer software and can deliver a flow from 0 to 5l/min. When the valve is operated in positive direction a signal is transmitted to the slave valve (PVG_S) and the spool will open equal to the spool of the master valve. Furthermore, the fluid flows through the check valve and into the overcenter valve, hereby turning the motors and hoisting the load. The pressure can be measured using pressure transducers at the inlet and the outlet of the motors. The fluid then flows through the PVG 's and back to the reservoir. If the PVG is operated in the negative direction, the fluid will flow to the motors, lowering the load. The overcenter valve will open when the crack pressure reaches the pre-set value of 150bar. The fluid will then flow through the overcenter valve and the PVG , and back to the reservoir.

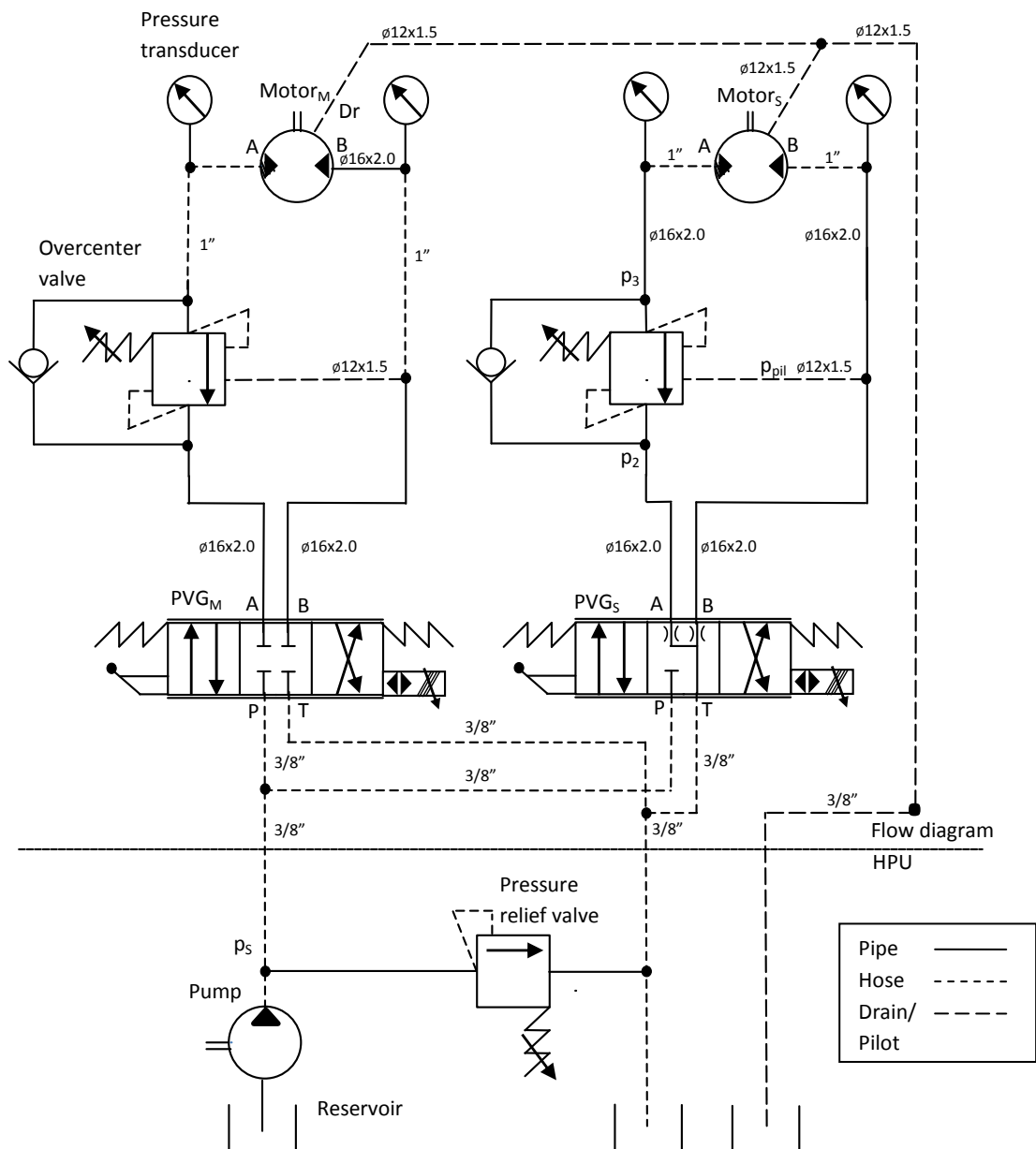


Figure 21: Hydraulic flow diagram

4 Instrumentation

The electrical part in this project seems insignificant to the rest of the construction considering size. However, the electrical part is crucial to resolve the bachelor thesis. The instrumentation is essential to monitor the system. By using the information from the instruments it is possible to control and adjust the system accordingly. The first sub-chapter, Instruments, explain how the sensors work, and their function for this project. The second subchapter, Electrical wiring, explain how the components are connected.

4.1 Instruments

In order to control the motions in the system the group had to use different instruments. There are several instruments on the market. The accuracy depends on the sensor type and cost. The group decided to use an accelerometer to measure the beam angle. Furthermore, in concern of safety it was considered ideal to use a distance sensor to prevent the beam from crashing into the winch. The angle of the beam is the key concept behind the thesis, it was therefore considered advisable to use an accurate sensor for the angle measurement.

4.1.1 National Instrument

In order to control the motion of the beam National Instrument NI USB-6211 is used as hardware and LabVIEW as software. The NI USB-6211 is a USB-powered data acquisition module. It has sixteen analogue inputs and two analogue outputs with a sampling rate of 250kS/s and range of 16-bit. It also offers four digital inputs, four digital outputs and two 32-bit counters. The voltage range of the module is $\pm 10V$ [13].

Seen in Table 3 the PVES modules are operating with input voltages in a higher range than the $\pm 10V$ range of the NI USB-6211 module. Therefore, the output signal voltage from the module must be amplified in order to reach the required input voltage range of the PVES modules. For more information about NI USB-6211, see Appendix C.10

Device	Quantity	Supply Voltage, U_{DC}	Current Consumption	Signal Current	Device Input Signal	Device Output Signal
PVG 32, 5l/min PVES module	1	22...30 V	330 mA	0.5mA	6V...18V (Analogue)	
PVG 32, 25l/min PVES module	1	22...30 V	330 mA	0.5mA	6V...18V (Analogue)	
Distance sensor, 2Y0A02	1	5 V	33 mA			0.4V...2.5V (Analogue)
Accelerometer, KAS901-04A	1	7...36 V	4...20mA			0.5...4.5 V (Analogue)
Pressure transducer, SCP01-400-44-07	4	12...30 V	2.4...6 mA			0...10 V (Analogue)

Table 3: Electrical signal specifications

4.1.2 Horizontal accelerometer

Accelerometers are used to measure acceleration or vibration in a structure. When accelerated, an internal mass in the accelerometer “squeezes” a piezoelectric material which produces an electrical charge. This electrical charge is proportional to the force acting on the mass. The mass is constant and thereby the charge is proportional to the acceleration [14].

In this project a horizontal accelerometer is used to measure inclination in the lifting beam. When tilted to one side the mass will act as if accelerated due to gravity. The accelerometer transmits feedback to the slave PVG block. The PVG block adjusts the flow ensuring no inclination. For more details on the accelerometer see Appendix C.11.

4.1.3 Distance sensor

The distance sensor is used as a safety requirement. It is mounted on the same level as the winch and measures the distance to the beam. The sensor will give a signal to the PVG valve if the beam is closer than 20cm from the sensor, and stop the system. The group has decided to use a Sharp distance sensor. This sensor measures within a range of 20cm to 150cm, and at a distance of 80cm this sensor will have a detection accuracy of $\pm 10\text{cm}$. Due to the sensors function as to prevent crashing, a resolution of 20cm is considered acceptable [15]. For more details on the sensor see Appendix C.12.

4.1.4 Pressure transducer

Four pressure transducers of the type Parker SCP01-400-44-07 are used in the hydraulic lines. The purpose of the pressure transducers is purely to monitor the pressure at the inlet and the outlet line of both motors. The pressure transducers deliver a voltage signal from 0 to 10V. The conversion from voltage to bar pressure is linear where 1V corresponds to 40bar. For more details, see chapter 3.1.5 or Appendix C.13.

4.1.5 Voltage amplifier

As mentioned in chapter 4.1.1, amplifiers are required in order to achieve higher output voltages from the NI USB-6211. The amplifiers are made using operational amplifiers (OpAmps) and resistors. The OpAmps used are the LM6142 17MHz Rail-to-Rail. These OpAmps have the capacity of two amplifiers with a single supply of +24V. For more information, see Appendix C.14.

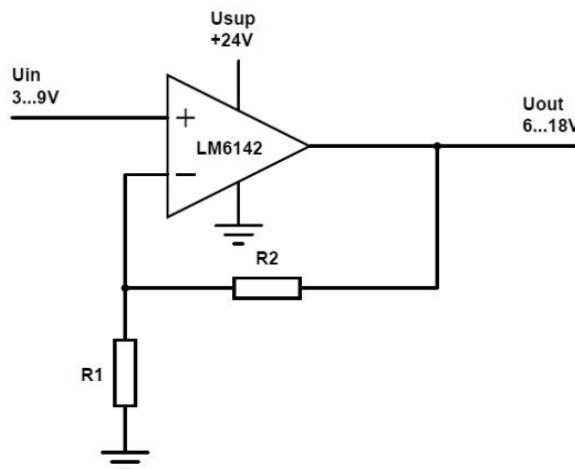


Figure 22: Amplifier Sketch

The amplifier is designed as a non-inverting amplifier to give a gain of 2, see Figure 22. The relationship between output and input voltage is shown at (4.1)

$$\frac{U_{out}}{U_{in}} = 1 + \frac{R_2}{R_1} \quad (4.1)$$

From equation (4.1) it is evident the resistors R_1 and R_2 , have to be equal in order to receive a gain of 2. The size of the resistors had to be somewhere in the $k\Omega$ range, as the voltage is much greater than the current at the output on the OpAmp.

The common formula for voltage drop across a resistor in relation to the current is expressed at (4.2).

$$\Delta U_R = I \cdot R \quad (4.2)$$

Knowing the resistors and the current flow through them are equal, the voltage drop across the resistors are equal as well and can be expressed as U_{out} .

$$\begin{aligned} R &= R_1 = R_2 \\ I &= I_{R_1} = I_{R_2} \\ U_{out} - \Delta U_{R1} - \Delta U_{R2} &= 0V \\ \Rightarrow U_{out} - 2 \cdot \Delta U_R &= 0V \\ \Rightarrow \Delta U_R &= \frac{1}{2} \cdot U_{out} \end{aligned} \quad (4.3)$$

The size of the resistors is selected in the range of the computation of equations (4.2) and (4.3).

$$R = \frac{\Delta U_R}{I} = \frac{1}{2} \cdot \frac{U_{out}}{I} = \frac{1}{2} \cdot \frac{[6...18]V}{0.5mA} = [6...18]k\Omega \quad (4.4)$$

The resistors R_1 and R_2 chosen for the amplifier are $6.8 k\Omega$.

4.2 Electrical wiring

The electrical wiring required multiple connections. Each component in Table 3 have three essential connection cords. These are the supply voltage cord, 0 volt supply cord and signal cord. See Appendix B for the electrical wiring chart.

The distance sensor is supplied with 5V. All the other components including the amplifier are supplied with 24V. The current consumption of the distance sensor is on average 33mA at the given voltage. The total current consumption of the 24V supply devices is approximately 700mA. All of the cords from the 24V supplied sensors and actuators are connected to a terminal block. The supply voltage terminals (terminal 94 to 100) are coupled in parallel with the 24V channel on the supply source. Likewise, the 0V supply terminals (terminal 87 to 93) are coupled in parallel with the 0V channel on the supply source. In case of overload, there is placed a 500mA fuse between the 24V supply source and the supply cord for both of the PVES modules.

The signal cords are coupled via the terminal and to the corresponding I/O connection on the NI USB-6211 as seen in Table 4. Read the connection steps in the table from left to right.

Signal cord	Terminal port	Amplifier	I/O connection
PVG 32, 5l/min, PVES module	80	Yes	AO1
PVG 32, 25l/min, PVES module	81	Yes	AO0
Accelerometer	82		AI1
Pressure transducer #1	83		AI9
Pressure transducer #2	84		AI2
Pressure transducer #3	85		AI10
Pressure transducer #4	86		AI3

Table 4: Signal cord connections

The amplifiers are connected with the U_{out} cord to the terminal, and the U_{in} cord to I/O connection. The distance sensors supply cords are directly connected to the 5V supply source and the signal cord is directly coupled to the I/O connection port AI11.

5 Control design

This chapter addresses the design of the controller for synchronizing the velocity of the two motors and also the inclination of the beam. LabVIEW is the software used in this project to create a control system and to do control simulations. LabVIEW is a graphical programming environment producing virtual instruments (VI's). The VI's can consist of various controls and indicators, which become inputs and outputs, respectively, to a program. Underlying each control and indicator is an associated block of code that defines its operation [16].

The first sub-chapter examines the mathematical model, founding the basis of the control system. The second sub-chapter explains the control system created based on the mathematical model. The final sub-chapter illustrates the simulation results acquired.

5.1 Mathematical model

A mathematical model describing the dynamics of the system is essential when designing a controller. The model described in this chapter is mainly based on chapter 7 of the compendium "Hydraulic Components and Systems" by M.R. Hansen and T.O. Andersen.

The first three sections describe the governing equations of the mechanical and the hydraulic system. The fourth section examines the mathematical model of the entire hydro-mechanical system.

5.1.1 Mechanical system applied to hydraulic system

The mechanical part of the system acting on the motors via the gearboxes is sketched in Figure 23. From this sketch the relations between the three angles are computed in (5.5) from equation (5.1) to (5.4).

$$\sin(\theta_{acc}) = \frac{y_e}{L_B} \quad (5.1)$$

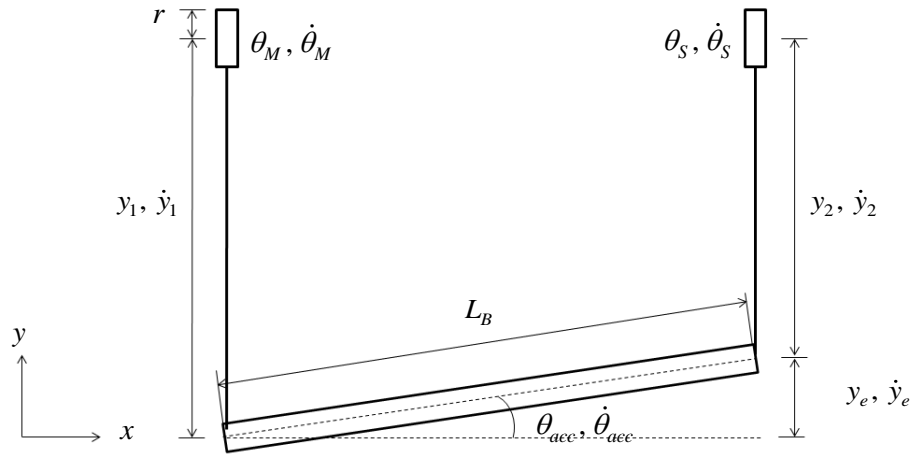
$$\theta_M \cdot r = y_1 \quad (5.2)$$

$$\theta_S \cdot r = y_2 \quad (5.3)$$

$$y_e = y_1 - y_2 \quad (5.4)$$

$$\frac{L_b}{r} \cdot \theta_{acc} = \theta_M - \theta_S \quad (5.5)$$

At equation (5.5), $\sin(\theta_{acc})$ is approximately equal to θ_{acc} and therefore expressed as seen in (5.5). This approximation is valid for small values of θ_{acc} .

**Figure 23:** Mechanical lifting system, angles and lengths

The forces acting from the beam to the wires, F_1 and F_2 , are computed from equilibrium considerations of forces and bending moments.

$$\sum M_c^{CW} = M_1 - M_2 = J \cdot \ddot{\theta}_{acc} \quad (5.6)$$

$$\sum F_y = F_1 + F_2 - (m_B + m_L) \cdot g = (m_B + m_L) \cdot a_c \quad (5.7)$$

The moments and forces acting on the mechanical lifting system are illustrated in Figure 24.

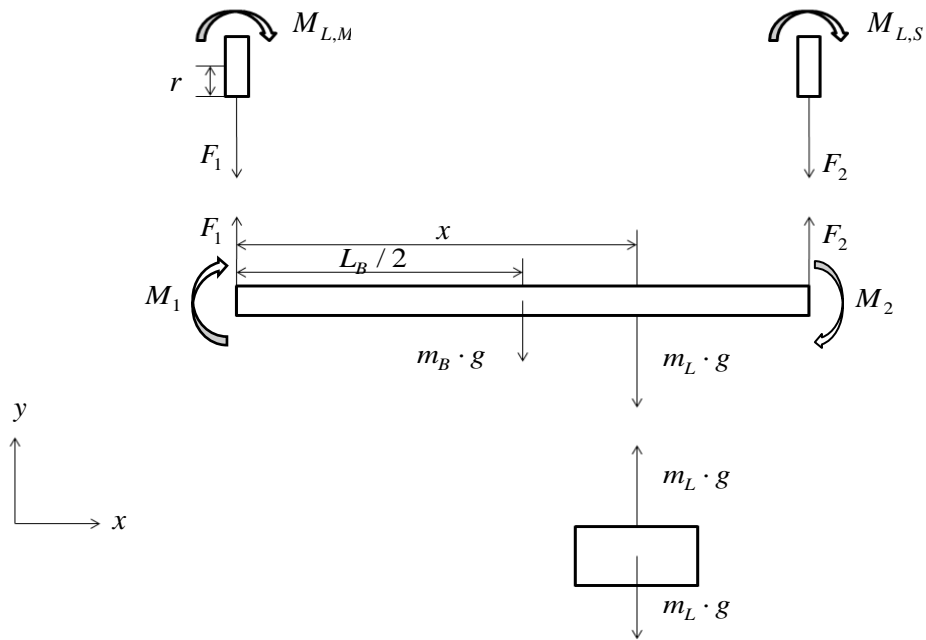


Figure 24: Mechanical lifting system, moments and forces

The mass moment of inertia is computed using Steiner's statement.

$$J = J_B + m_L \left(\frac{L_B}{2} - x \right)^2 = \frac{1}{12} \cdot m_B \cdot L_B^2 + m_L \left(\frac{L_B}{2} - x \right)^2 \quad (5.8)$$

The centre of mass (CM) is preferably calculated in the x-direction of the beam, making it easier to calculate.

$$x_c = \frac{\frac{L_B}{2} \cdot m_B + x \cdot m_L}{m_B + m_L} \quad (5.9)$$

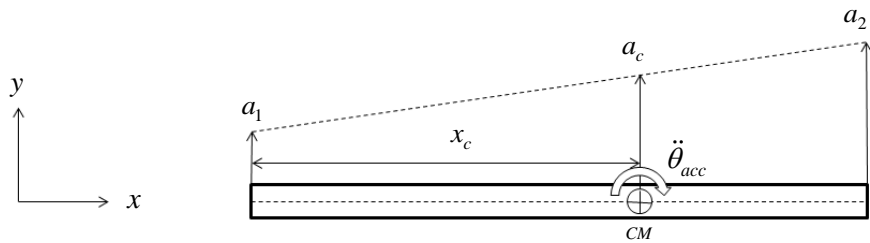


Figure 25: Mechanical lifting system, accelerations and angular acceleration

The acceleration of the centre of mass is expressed by the accelerations a_1 and a_2 on either edges of the beam. The equation is found by using trigonometry and Pythagoras' theorem concerning Figure 25.

$$\begin{aligned} \frac{a_1 - a_2}{L_B} &= \frac{a_c - a_2}{L_B - x_c} \\ \Rightarrow a_c &= \frac{a_1(L_B - x_c) + a_2 \cdot x_c}{L_B} \end{aligned} \quad (5.10)$$

The bending moments are expressed by the forces F_1 and F_2 at (5.11) and (5.12).

$$M_1 = F_1 \cdot x_c \quad (5.11)$$

$$M_2 = F_2 \cdot (L_B - x_c) \quad (5.12)$$

F_1 is expressed by inserting equation (5.11) and (5.12) into (5.6).

$$F_1 = \frac{J \cdot \ddot{\theta}_{acc} + F_2 \cdot (L_B - x_c)}{x_c} \quad (5.13)$$

F_2 is defined in (5.14) by inserting (5.13) into (5.7).

$$F_2 = \frac{x_c(m_B + m_L) \cdot (a_c + g) - J \cdot \ddot{\theta}_{acc}}{L_B} \quad (5.14)$$

Further, the final equation for F_2 is expressed in (5.15) by adding equation (5.8) to (5.10) into (5.15).

$$\begin{aligned} F_2 &= \frac{(L_B \cdot m_B + 2 \cdot x \cdot m_L)(L_B \cdot m_B + 2 \cdot m_L(L_B - x))}{4 \cdot L_B^2 \cdot (m_B + m_L)} a_1 + \frac{(L_B \cdot m_B + 2 \cdot x \cdot m_L)^2}{4 \cdot L_B^2 \cdot (m_B + m_L)} a_2 \\ &\quad + \frac{(L_B \cdot m_B + 2 \cdot x \cdot m_L)}{2 \cdot L_B} g - \frac{(m_B \cdot L_B^2 + 3 \cdot m_L(L_B - 2 \cdot x)^2)}{12 \cdot L_B} \ddot{\theta}_{acc} \\ F_2 &= (9.875 + 422.5 \cdot x - 234.7 \cdot x^2) a_1 + (0.125 + 10.83 \cdot x + 234.7 \cdot x^2) a_2 \\ &\quad + (98.1 + 4251 \cdot x) - (354 - 780 \cdot x + 433.3 \cdot x^2) \ddot{\theta}_{acc} \end{aligned} \quad (5.15)$$

Finally, F_1 is found by inserting equation (5.8), (5.9) and (5.15) into (5.16).

$$\begin{aligned} F_1 &= \frac{(L_B \cdot m_B + 2 \cdot m_L(L_B - x))^2}{4 \cdot L_B^2 (m_B + m_L)} a_1 + \frac{(L_B \cdot m_B + 2 \cdot x \cdot m_L)(L_B \cdot m_B + 2 \cdot m_L(L_B - x))}{4 \cdot L_B^2 (m_B + m_L)} a_2 \\ &\quad + \frac{(L_B \cdot m_B + 2 \cdot m_L(L_B - x))}{2 \cdot L_B} g + \frac{(m_B \cdot L_B^2 + 3 \cdot m_L(L_B - 2 \cdot x)^2)}{12 \cdot L_B} \ddot{\theta}_{acc} \\ F_1 &= (762.5 - 846.1 \cdot x + 234.7 \cdot x^2) a_1 + (9.875 + 422.5 \cdot x - 234.7 \cdot x^2) a_2 \\ &\quad + (7749.9 - 4251x) + (354 - 780 \cdot x + 433.3 \cdot x^2) \ddot{\theta}_{acc} \end{aligned} \quad (5.16)$$

As seen in the calculations (5.15) and (5.16), the forces are expressed by the variable accelerations and the distance from the wire to the load, x . The static load is expressed by the gravitational constant g .

The torque applied to the load-holding shaft on the gearbox is given by the radius of the drum multiplied the force from the wire. Equation (5.17) and (5.18) describes the torque on the load-holding shaft on the master- and slave side, respectively.

$$M_{L,M} = r \cdot F_1 \quad (5.17)$$

$$\begin{aligned} M_{L,M} = & 0.035 \cdot \left(\left(762.5 - 846.1 \cdot x + 234.7 \cdot x^2 \right) a_1 + \left(9.875 + 422.5 \cdot x - 234.7 \cdot x^2 \right) a_2 \right. \\ & \left. + \left(7749.9 - 4251x \right) + \left(354 - 780 \cdot x + 433.3 \cdot x^2 \right) \ddot{\theta}_{acc} \right) \end{aligned}$$

$$M_{L,S} = r \cdot F_2 \quad (5.18)$$

$$\begin{aligned} M_{L,S} = & 0.035 \cdot \left(\left(9.875 + 422.5 \cdot x - 234.7 \cdot x^2 \right) a_1 + \left(0.125 + 10.83 \cdot x + 234.7 \cdot x^2 \right) a_2 \right. \\ & \left. + \left(98.1 + 4251 \cdot x \right) - \left(354 - 780 \cdot x + 433.3 \cdot x^2 \right) \ddot{\theta}_{acc} \right) \end{aligned}$$

5.1.2 Motor equations

The pressure drop across the motors are depending on the torque from the shaft of the motors. The torque is reduced proportional to the ratio of the gearbox. The pressure drop across the master- and slave motor are given accordingly.

$$\begin{aligned} M_{M,M} &= \frac{M_{L,M}}{\gamma \cdot N} \\ M_{M,M} &= \eta_{hmM} \cdot \frac{D \cdot \Delta p_{M,M}}{2\pi \cdot 10^6} \\ \Rightarrow \Delta p_{M,M} &= \frac{M_{L,M}}{\gamma \cdot N} \cdot \frac{2\pi \cdot 10^6}{\eta_{hmM} \cdot D} \end{aligned} \quad (5.19)$$

$$\begin{aligned} M_{M,S} &= \frac{M_{L,S}}{\gamma \cdot N} \\ M_{M,S} &= \eta_{hmM} \cdot \frac{D \cdot \Delta p_{M,S}}{2\pi \cdot 10^6} \\ \Rightarrow \Delta p_{M,S} &= \frac{M_{L,S}}{\gamma \cdot N} \cdot \frac{2\pi \cdot 10^6}{\eta_{hmM} \cdot D} \end{aligned} \quad (5.20)$$

The angular velocities of the motor shafts are expressed as the velocity of the beam, and the relation between the fluid flow and the velocity of the beam is defined in (5.21) and (5.22).

$$\begin{aligned} Q_{M,M} &= \frac{D \cdot \omega_M}{2\pi \cdot 10^6 \cdot \eta_{vM}} \\ \omega_M &= N \cdot \dot{y}_1 \\ Q_{M,M} &= \frac{D \cdot N \cdot \dot{y}_1}{2\pi \cdot 10^6 \cdot \eta_{vM} \cdot r} \end{aligned} \quad (5.21)$$

$$\begin{aligned}
 Q_{M,S} &= \frac{D \cdot \omega_s}{2\pi \cdot 10^6 \cdot \eta_{vM}} \\
 \omega_s &= N \cdot \dot{y}_2 \\
 Q_{M,S} &= \frac{D \cdot N \cdot \dot{y}_2}{2\pi \cdot 10^6 \cdot \eta_{vM} \cdot r}
 \end{aligned} \tag{5.22}$$

The speed difference, \dot{y}_e , between the edges of the beam can be considered in Figure 23 as the velocity of a circular movement centred in the x position of the velocity \dot{y}_2 by extracting \dot{y}_2 from \dot{y}_1 .

$$\dot{y}_e = \dot{y}_1 - \dot{y}_2 = L_B \cdot \dot{\theta}_{acc} \tag{5.23}$$

The flow through the slave motor is computed in equation (5.24) from (5.23) by inserting (5.21) and (5.22).

$$Q_{M,S} = Q_{M,M} - \frac{D \cdot N}{2\pi \cdot 10^6 \cdot \eta_{vM} \cdot r} \cdot L_B \cdot \dot{\theta}_{acc} \tag{5.24}$$

The effective mass pulling the wire is defined in (5.25) and (5.26) for master- and slave side respectively.

$$m_1 = \frac{(L_B - x_c)}{L_B} \cdot (m_B + m_L) \tag{5.25}$$

$$m_2 = \frac{x_c}{L_B} \cdot (m_B + m_L) \tag{5.26}$$

From Steiner's sentence the effective mass moment of inertia on the motor shaft may be computed from the inertia of the drum and the effective mass acting on the wire.

$$\begin{aligned}
 J_{eff,M} &= \frac{J_d}{(\gamma \cdot N)^2} + \frac{m_1 \cdot r^2}{(\gamma \cdot N)^2} \\
 &= \left(\frac{r}{\gamma \cdot N} \right)^2 \left(\frac{m_d}{2} + \frac{(L_B - x_c) \cdot (m_B + m_L)}{L_B} \right)
 \end{aligned} \tag{5.27}$$

$$\begin{aligned}
 J_{eff,S} &= \frac{J_d}{(\gamma \cdot N)^2} + \frac{m_2 \cdot r^2}{(\gamma \cdot N)^2} \\
 &= \left(\frac{r}{\gamma \cdot N} \right)^2 \left(\frac{m_d}{2} + \frac{x_c \cdot (m_B + m_L)}{L_B} \right)
 \end{aligned} \tag{5.28}$$

5.1.3 Valve equations

The PVG 32 valve is symmetric, meaning the discharge area is equal for the same absolute value of the spool travel u . Due to this symmetry the pressure drop across both port A and port B are equal while neglecting the leakage in the motor. Considering Figure 26, the following equations are set up describing the pressure drop in the circuit.

$$\begin{aligned}\Delta p_v + \Delta p_M + \Delta p_{cv} + \Delta p_v &= p_s \\ \Delta p_v &= \frac{1}{2}(p_s - \Delta p_{cv} - \Delta p_M)\end{aligned}\quad (5.29)$$

$$\begin{aligned}\Delta p_v - \Delta p_M + \Delta p_{ocv} + \Delta p_v &= p_s \\ \Delta p_v &= \frac{1}{2}(p_s - \Delta p_{ocv} + \Delta p_M)\end{aligned}\quad (5.30)$$

Equation (5.29) and (5.30) estimates the pressure drop across the PVG valve for hoisting and lowering the load, respectively. The pressure drop over the check valve and the load-holding valve are approximately the same with a flow of 5l/min, according to the datasheet for the overcenter valve, see Appendix C.7. The common equation for both hoisting and lowering the load is expressed at (5.31).

$$\Delta p_v = \frac{1}{2} \left(p_s - \Delta p_{ocv} - \frac{u}{|u|} \cdot \Delta p_M \right) \quad (5.31)$$

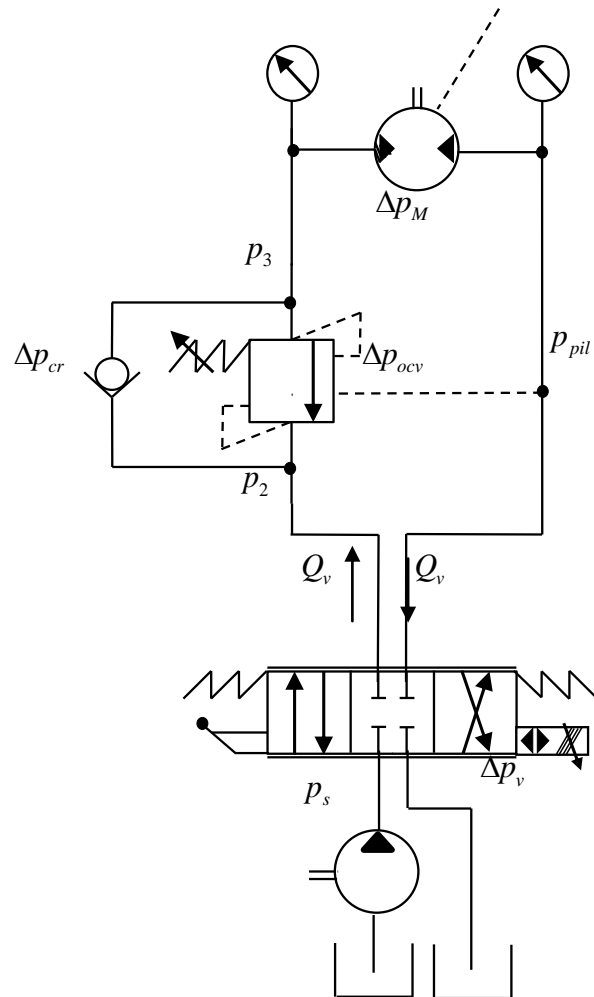


Figure 26: Hydraulic system

The orifice equation in (5.32) describes the relation between the flow through the valve, the discharge area and the pressure drop across the valve.

$$Q_v = C_d \cdot A_{d0} \cdot u \cdot \sqrt{\frac{2}{\rho} \Delta p_v} \quad (5.32)$$

The flow through the valve can be expressed by combining the equations (5.31) and (5.32).

Equation (5.33) include a non-linear variable, and can therefore not be Laplace-transformed directly. The solution to this inconvenience is examined in chapter 6.1.4.

$$Q_v = C_d \cdot A_{d0} \cdot u \cdot \sqrt{\frac{1}{\rho} \left(p_s - \Delta p_{ocv} - \frac{u}{|u|} \cdot \Delta p_M \right)} \quad (5.33)$$

The discharge areas of the two PVG valves used in this system are different and non-linear. The producer provided the students with a flow track chart containing data relating the discharge area and the spool. From this chart the following two polynomial equations are calculated from curve fittings of the data.

$$A_{d,M} = -2.6134 + 2.8582 \cdot x_v - 0.9083 \cdot x_v^2 + 0.13458 \cdot x_v^3 - 0.006165 \cdot x_v^4 \quad (5.34)$$

$$A_{d,S} = -5.916 + 10.25 \cdot x_v - 4.618 \cdot x_v^2 + 1.164 \cdot x_v^3 - 0.1357 \cdot x_v^4 + 0.006051 \cdot x_v^5 \quad (5.35)$$

Further, the equations (5.34) and (5.35) are linearized at (5.36) and (5.37).

$$A_{d,M} = 0.6839 \cdot x_v - 1.1602 \quad (5.36)$$

$$A_{d,S} = 2.243 \cdot x_v - 1.4334 \quad (5.37)$$

5.1.4 Hydro-mechanical system

The hydro-mechanical system include the non-linearized equation (5.33). It is essential to linearize the non-linearities in order to perform a Laplace transform of the equation. This was achieved by introducing the coefficients K_{qu} and K_{qp} .

The coefficient K_{qu} given in (5.38) emerges from the steady state value of the equation at (5.33) derived with respect to u . In other words, K_{qu} represents the flow behaviour during spool displacement and constant pressure drop over the motor.

$$K_{qu} = \left. \frac{\partial Q_v}{\partial u_M} \right|_{ss} = C_d \cdot A_{d0} \cdot \sqrt{\frac{1}{\rho} \left(p_s - \Delta p_{ocv} - \frac{u^{(ss)}}{|u^{(ss)}|} \cdot \Delta p_M^{(ss)} \right)} \quad (5.38)$$

The second coefficient K_{qp} is seen in (5.39). This coefficient emerges from the steady state value of the equation at (5.33) derived with respect to Δp_M . In other words, K_{qp} represents the flow behaviour depending on the pressure drop over the motor and with spool displacement held at constant.

$$K_{qp} = -\frac{\partial Q_v}{\partial \Delta p_M} \Big|_{ss} = \frac{C_d \cdot A_{d0} \cdot |u^{(ss)}|}{2 \cdot \sqrt{\rho \cdot \left(p_s - \Delta p_{ocv} - \frac{|u^{(ss)}|}{|u^{(ss)}|} \Delta p_M^{(ss)} \right)}} \quad (5.39)$$

Further, the total capacity of the hydraulic fluid is introduced at (5.40).

$$C = \frac{D + V_{L,in} + V_{L,out}}{4 \cdot \beta} \quad (5.40)$$

At this point, all the parameters required are computed and the hydro-mechanical system is described at (5.41) as a second order system. The gain K_{mh} , the eigenfrequency ω_{mh} and the damping ξ_{mh} , are defined in (5.42) to (5.44).

$$G_{mh}(s) = \frac{s \cdot \theta}{u} = \frac{K_{mh}}{s^2 + 2 \cdot \xi_{mh} \cdot \omega_{mh} \cdot s + \omega_{mh}^2} \quad (5.41)$$

$$K_{mh} = \frac{K_{qu}}{D_\omega} \quad (5.42)$$

$$\omega_{mh} = \frac{D_\omega}{\sqrt{J_{eff} \cdot C}} \quad (5.43)$$

$$\xi_{mh} = \frac{K_{qp}}{2 \cdot D_\omega} \cdot \sqrt{\frac{J_{eff}}{C}} \quad (5.44)$$

$$D_\omega = \frac{D}{2 \cdot \pi} \quad (5.45)$$

This concludes the mathematical model. The following section examines the control system based on the calculations reviewed.

5.2 Control system

This section addresses the design of the PID controller for the simulation of the hydro-mechanical plant. The control system is created on basis of the mathematical model reviewed in chapter 5.1.

Figure 27 illustrates the block diagram principle sketch of the valve operations. The operator inserts a desired set point value in the software. The desired value is directly given to the master valve. This set point value is multiplied with a gain K, representing the linear conversation between master and slave valve discharge area. Furthermore, the set point value multiplied with K is subtracted by the compensated accelerometer value. This subtraction forms the value transmitted to the slave valve.

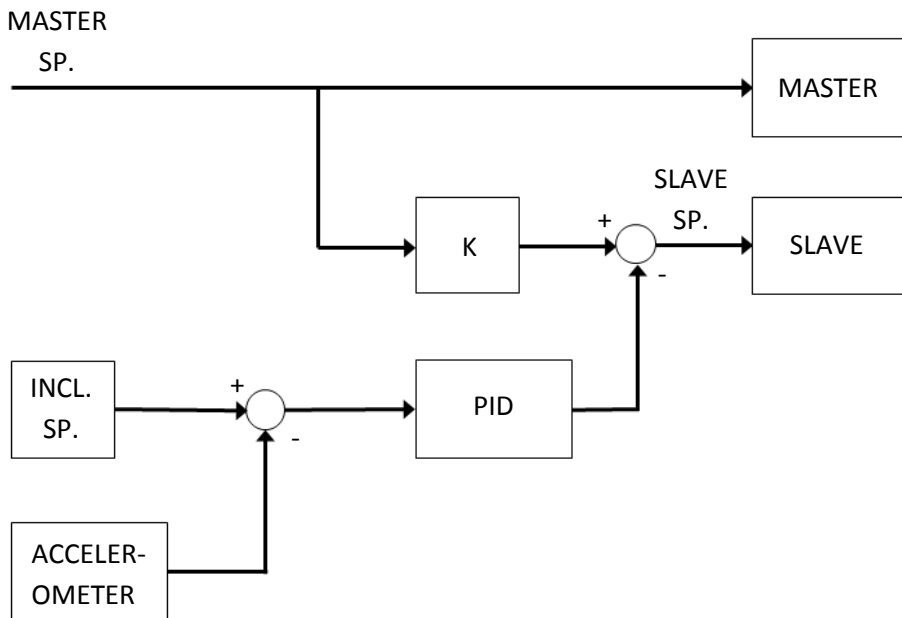


Figure 27: Valve operations block diagram

The PID controller manages the value received by the slave by comparing the value from the accelerometer and the desired constant value. The constant value is in this case is 0rad inclination in the beam. The measured inclination from the accelerometer is subtracted from the inclination set point value, hereby increasing or decreasing the slave valves' set point value. The PID controller primarily enhances the performance considering reaction time.

5.2.1 Closed loop control

The closed loop (CL) had to be simulated in order to design the controller. The controller is compensating for the inclination value read by the accelerometer. The value from the accelerometer is the feedback of the loop.

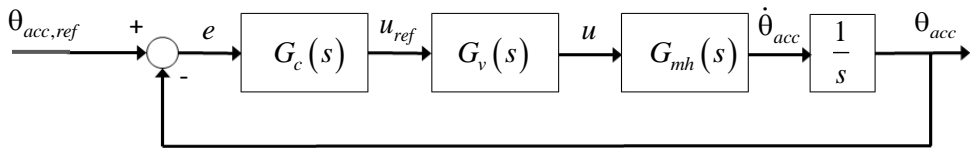


Figure 28: Closed loop of inclination

Figure 28 illustrates the loop consisting of the PID controller, the PVG valve block, the hydro-mechanical block and an integrator. The newly introduced PVG valve block, $G_v(s)$, represents the closed loop of the spool position control inside the electrical-mechanical valve. The equation at (5.47) can be expressed because of the assumption expressed at (5.46). The assumption is possible due to the high performance of the PVES module.

$$\omega_v \geq 3 \cdot \omega_{mh} \quad (5.46)$$

$$G_{vmh}(s) = \frac{K_{mh}}{s^2 + 2 \cdot \xi_{mh} \cdot \omega_{vmh} \cdot s + \omega_{vmh}^2} \approx G_v(s) \cdot G_{mh}(s) \quad (5.47)$$

$$\omega_{vmh} = 0.9 \cdot \omega_{mh} \quad (5.48)$$

The time delay of the valve is introduced in the new closed loop, illustrated in Figure 29.

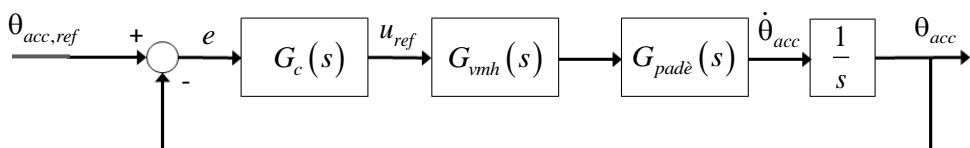


Figure 29: Closed loop with time delay of inclination

The time-delay block, $G_{padé}(s)$, introduced in Figure 29, is an approximation of the irrational transfer function for time-delay in (5.49).

$$T(s) = e^{-\tau \cdot s} \quad (5.49)$$

The approximation at (5.50) is a second order Padè-approximation [17].

$$\begin{aligned} T(s) &\approx G_{padé}(s) \\ e^{-\tau \cdot s} &\approx \frac{1 - \frac{\tau}{2} \cdot s + \frac{\tau^2}{12} \cdot s^2}{1 + \frac{\tau}{2} \cdot s + \frac{\tau^2}{12} \cdot s^2} \end{aligned} \quad (5.50)$$

The time-delay constant τ , is listed in the datasheet for the valve in Appendix C.9. The value τ in the approximation is the rated time response of 0.120s.

$$G_{padé}(s) = \frac{1 - 0.06 \cdot s + 0.0012 \cdot s^2}{1 + 0.06 \cdot s + 0.0012 \cdot s^2}$$

The hydro-mechanical-valve block, $G_{vmh}(s)$ represent the values calculated from chapter 5.1 on the slave side of the system. The block is included in this loop because the accelerometer regulates the slave valve. The system is simulated in three load position states $x=0$, $x=0.9$ and $x=1.8$ for both lifting and lowering the load.

Hoisting

The constant K_{mh} was calculated in the formulas of chapter 5.1. The pulling force, F_2 , exists only as the static force, as the force is included in the steady state coefficient, K_{qu} . The constant K_{mh} is directly calculated and all the balances are omitted.

$$\begin{aligned} K_{mh}(x) &= 0.06099 \cdot \sqrt{(97 \cdot 10^5 - 1255 \cdot (36 + 1560 \cdot x))} \\ K_{mh}(0) &= \underline{189.5} \\ K_{mh}(0.9) &= \underline{171.3} \\ K_{mh}(1.8) &= \underline{151.0} \end{aligned}$$

The bandwidth ω_{vmh} is computed from the equation at (5.48) and equations calculated in the mathematical model. The bandwidth is dependent on the load position x .

$$\begin{aligned} \omega_{vmh}(x) &= 4126 \cdot \sqrt{\frac{1}{(27.1 + x \cdot 866.7)}} \\ \omega_{vmh}(0) &= \underline{792.6} \\ \omega_{vmh}(0.9) &= \underline{145.2} \\ \omega_{vmh}(1.8) &= \underline{103.6} \end{aligned}$$

The same criteria for the load position x , and the pulling force F_2 applies to the steady state coefficient K_{qp} as for the constant $K_{qu,h}$.

$$\xi_{mh}(x) = 8.924 \sqrt{\frac{(27.1 + 866.7 \cdot x)}{(97 \cdot 10^5 - 1255 \cdot (36 + 1560 \cdot x))}}$$

$$\xi_{mh}(0) = \underline{0.01495}$$

$$\xi_{mh}(0.9) = \underline{0.09024}$$

$$\xi_{mh}(1.8) = \underline{0.1436}$$

Finally, the transfer functions for hoisting load in the two loading positions are computed as seen below.

$$G_{vmh,1}(s) = \frac{s \cdot \theta}{u} = \frac{K_{mh}(0)}{s^2 + 2 \cdot \xi_{mh}(0) \cdot \omega_{vmh}(0) \cdot s + (\omega_{vmh}(0))^2}$$

$$G_{vmh,1}(s) = \frac{s \cdot \theta}{u} = \frac{189.5}{\underline{s^2 + 23.7 \cdot s + 6.282 \cdot 10^5}}$$

$$G_{vmh,2}(s) = \frac{s \cdot \theta}{u} = \frac{K_{mh}(0.9)}{s^2 + 2 \cdot \xi_{mh}(0.9) \cdot \omega_{vmh}(0.9) \cdot s + (\omega_{vmh}(0.9))^2}$$

$$G_{vmh,2}(s) = \frac{s \cdot \theta}{u} = \frac{171.3}{\underline{s^2 + 26.21 \cdot s + 2.108 \cdot 10^4}}$$

$$G_{vmh,3}(s) = \frac{s \cdot \theta}{u} = \frac{K_{mh}(1.8)}{s^2 + 2 \cdot \xi_{mh}(1.8) \cdot \omega_{vmh}(1.8) \cdot s + (\omega_{vmh}(1.8))^2}$$

$$G_{vmh,3}(s) = \frac{s \cdot \theta}{u} = \frac{151}{\underline{s^2 + 29.75 \cdot s + 1.073 \cdot 10^4}}$$

Lowering

The constant K_{mh} was calculated in the formulas of chapter 5.1. The pulling force, F_2 , exists only as the static force, as the force is included in the steady state coefficient, K_{qu} . The constant K_{mh} is directly calculated and all the balances are omitted.

$$K_{mh}(x) = 0.06099 \cdot \sqrt{(97 \cdot 10^5 + 1255 \cdot (36 + 1560 \cdot x))}$$

$$K_{mh}(0) = \underline{190.4}$$

$$K_{mh}(0.9) = \underline{206.9}$$

$$K_{mh}(1.8) = \underline{222.2}$$

The bandwidth ω_{vmh} is computed from the equation at (5.48) and equations calculated in the mathematical model. The bandwidth is dependent on the load position x .

$$\begin{aligned}\omega_{vmh}(x) &= 4126 \cdot \sqrt{\frac{1}{(27.1 + x \cdot 866.7)}} \\ \omega_{vmh}(0) &= \underline{792.6} \\ \omega_{vmh}(0.9) &= \underline{145.2} \\ \omega_{vmh}(1.8) &= \underline{103.6}\end{aligned}$$

The same criteria for the load position x , and the pulling force F_2 applies to the steady state coefficient K_{qp} as for the constant $K_{qu,h}$.

$$\begin{aligned}\xi_{mh}(x) &= 8.924 \sqrt{\frac{(27.1 + 866.7 \cdot x)}{(97 \cdot 10^5 + 1255 \cdot (36 + 1560 \cdot x))}} \\ \xi_{mh}(0) &= \underline{0.01488} \\ \xi_{mh}(0.9) &= \underline{0.07474} \\ \xi_{mh}(1.8) &= \underline{0.09760}\end{aligned}$$

Finally, the transfer functions for hoisting load in the two loading positions are computed as seen below.

$$\begin{aligned}G_{vmh,4}(s) &= \frac{s \cdot \theta}{u} = \frac{K_{mh}(0)}{s^2 + 2 \cdot \xi_{mh}(0) \cdot \omega_{vmh}(0) \cdot s + (\omega_{vmh}(0))^2} \\ G_{vmh,4}(s) &= \frac{s \cdot \theta}{u} = \frac{190.4}{\underline{s^2 + 23.59 \cdot s + 6.282 \cdot 10^5}} \\ \\ G_{vmh,5}(s) &= \frac{s \cdot \theta}{u} = \frac{K_{mh}(0.9)}{s^2 + 2 \cdot \xi_{mh}(0.9) \cdot \omega_{vmh}(0.9) \cdot s + (\omega_{vmh}(0.9))^2} \\ G_{vmh,5}(s) &= \frac{s \cdot \theta}{u} = \frac{206.9}{\underline{s^2 + 21.70 \cdot s + 2.108 \cdot 10^4}} \\ \\ G_{vmh,6}(s) &= \frac{s \cdot \theta}{u} = \frac{K_{mh}(1.8)}{s^2 + 2 \cdot \xi_{mh}(1.8) \cdot \omega_{vmh}(1.8) \cdot s + (\omega_{vmh}(1.8))^2} \\ G_{vmh,6}(s) &= \frac{s \cdot \theta}{u} = \frac{222.2}{\underline{s^2 + 20.22 \cdot s + 1.073 \cdot 10^4}}\end{aligned}$$

The closed loop is simulated in LabVIEW for all six different hydro-mechanical-valve blocks. The time-response simulations use a step input as the signal generator. The simulation results are shown in Figure 30.

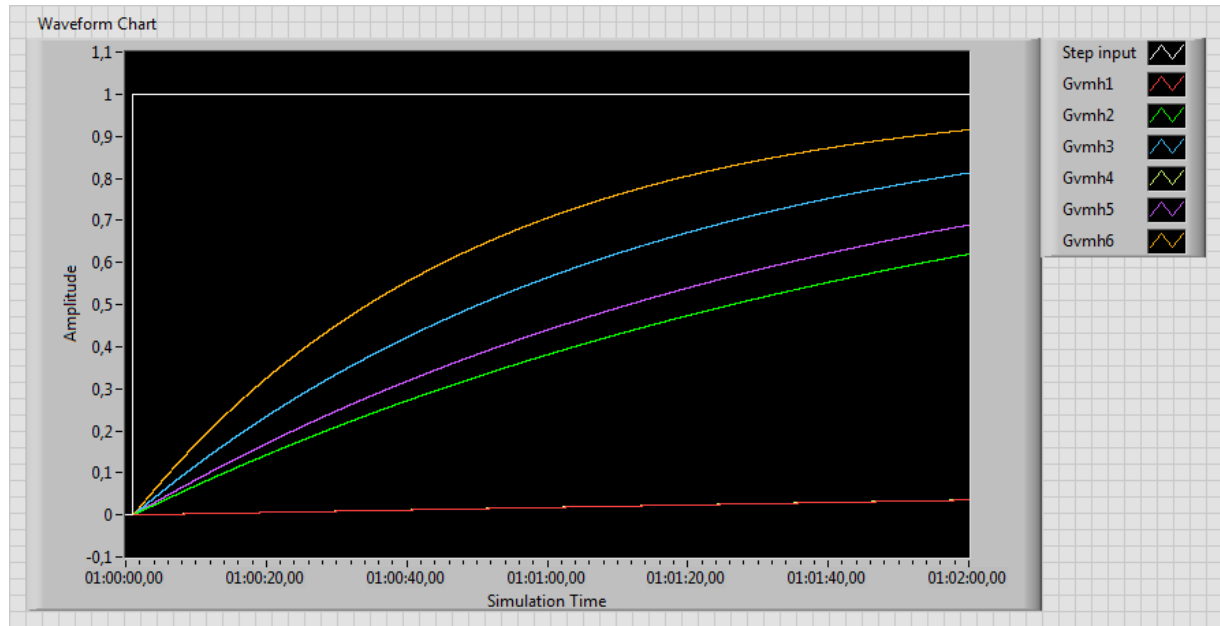


Figure 30: Simulation of the uncompensated systems Gvmh

The simulations shown in Figure 30, illustrate a very slow system. The simulation time is 120s, though none of the graphs reaches the set point value of 1. These results indicate the uncompensated system is not acceptable. A controller was made in order to obtain a better time response. The controller is examined in the following chapter.

5.2.2 Controller design

The first controller designed was a PI controller, using the Ziegler-Nichols method. The first step was to add a gain, K_u , ensuring the system oscillate with the same amplitude. Simulation of the middle loaded hoisting block, $G_{vhm,2}(s)$, show $K_u = 1593$. The period of the oscillating system, P_u , is 0.475. The PI controller is designed from these two values in the following equations.

$$K_c = 0.45 \cdot K_u = 716.9 \quad (5.51)$$

$$T_i = \frac{P_u}{1.2} = 0.3958 \quad (5.52)$$

$$T_d = 0 \quad (5.53)$$

Next, the uncompensated system is simulated with a PI controller containing the values from (5.51) to (5.53).

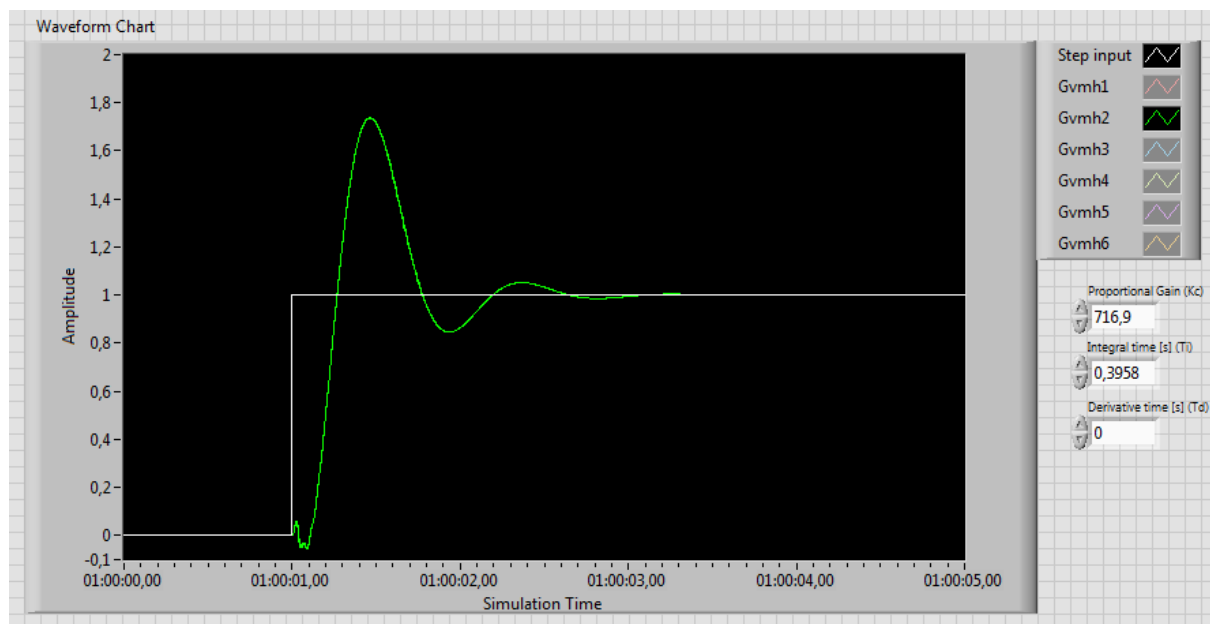


Figure 31: Simulation of the PI compensated systems Gvmh

The undershoot in simulation time 01:00:01,00 is an effect of the Padé-approximation due to the right half-plane zero $\left(-\frac{\tau}{2} \cdot s\right)$. The time response was improved with a settling time of 1.6s, but the overshoot of 80% is unacceptable. Experimental tuning of the PI controller was done in order to improve the performance.

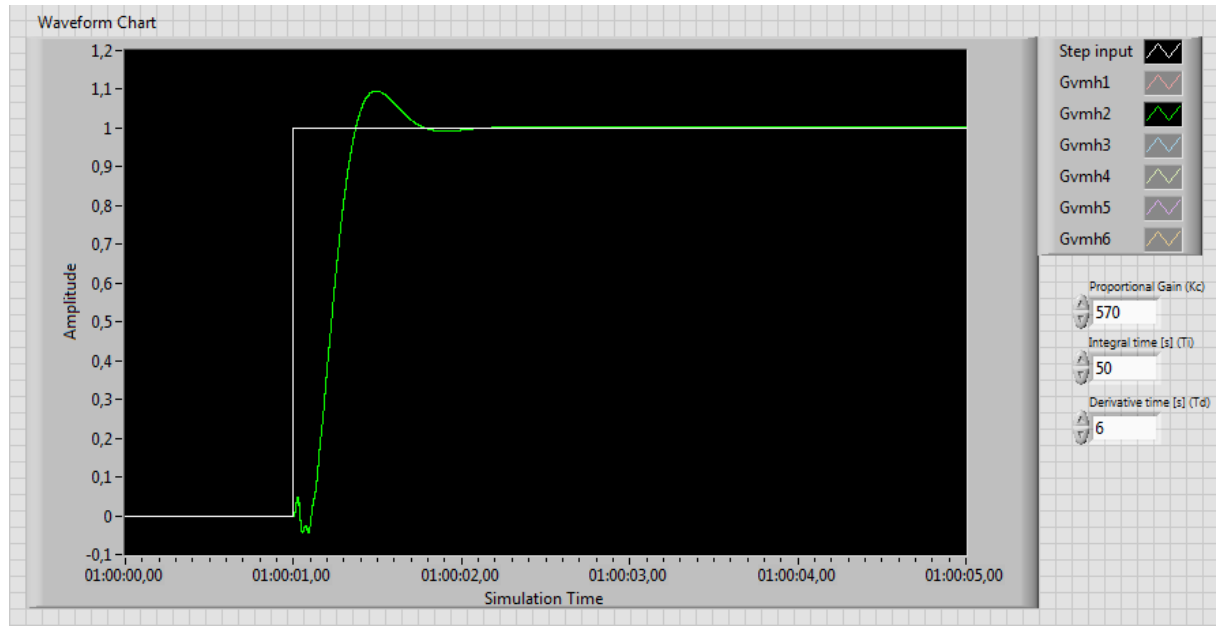


Figure 32: Simulation of the PID compensated systems Gvmh

The time response in Figure 32 are improved by using a PID controller with the values below.

$$K_c = 570$$

$$T_i = 50$$

$$T_d = 6$$

The settling time is 0.7s and with an overshoot on the acceptable value of 10%.

The PID controller designed above use the load position $x=0.9$. Using this controller in the other two load positions results in unacceptable values. The PID controller with the two other load situations are tuned by regulating the compensator gain, K_c .

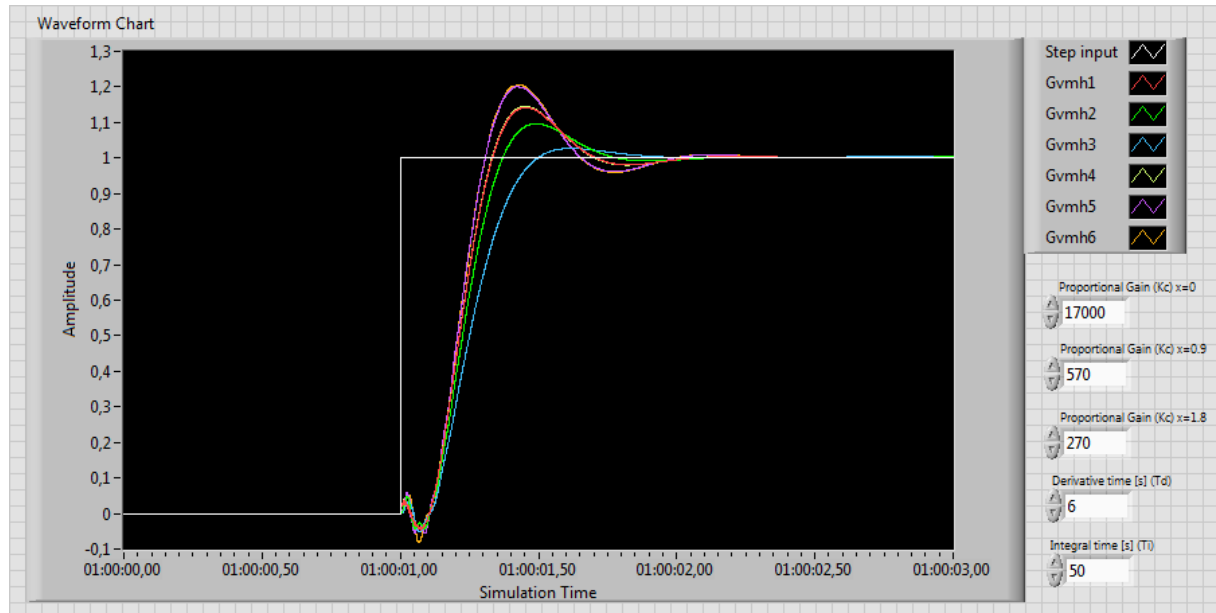


Figure 33: Simulations of the three PID controllers

The three different controllers have three separate load positions. The values are as following.

$x = 0$	$x = 0.9$	$x = 1.8$
$K_c = 17000$	$K_c = 570$	$K_c = 270$
$T_i = 50$	$T_i = 50$	$T_i = 50$
$T_d = 6$	$T_d = 6$	$T_d = 6$

The high values of K_c is due to the relation between beam angle and drum shaft angle in equation (5.5). The relation $\frac{L_B}{r}$ gives a factor of 51.4.

5.3 Real time simulations

This section addresses the simulation results during testing of the stand. The real time simulations showed good results in relation to synchronization. However, the controller was experimentally tuned during testing. Tuning was necessary partially because the load attached during testing was 400kg and not 800kg as simulated.

The first simulation shown in Figure 34 illustrates lifting of the beam with no additional load attached. The minor variations in the beam inclination illustrate the compensator regulating the slave motor, hereby stabilizing the beam. The graphs are divided into sections with green stapled lines. Each section is described with a brief explanation.

Section 1: Show the start-up process. The beam at initial state is slightly inclined and the accelerometer starts decreasing the voltage to the slave valve.

Section 2: The master signal is increased to 9V, thus hoisting the load at maximum speed. The accelerometer registers an inclination and increases the slave voltage signal.

Section 3: The system runs at constant velocity. Small variations in the inclination can be seen, but highly acceptable.

Section 4: The master signal is decreased from 9V to 6V, hereby stopping the velocity. The slave signal respond very well as the inclinations graph show only slight variations caused by vibrations.

Section 5: The master signal is decreased to 3V, implying the load being lowered at maximum velocity. This sudden change causes an inclination of -0.005rad, followed by oscillations slowly flattening.

Section 6: The master signal is changed to 6V, halting the velocity. The inclination is acceptable.

Section 7: The master signal is increased to 9 volt. The inclination responds similarly as in section 3.

Section 8: The master signal is decreased to approximately 8V. There are no major changes in the inclination.

Section 9: The signal is changed to 6V, stopping the velocity of the beam. The inclination is 0rad, apart from minor noise. The end of section 9 displays the system shutting down.

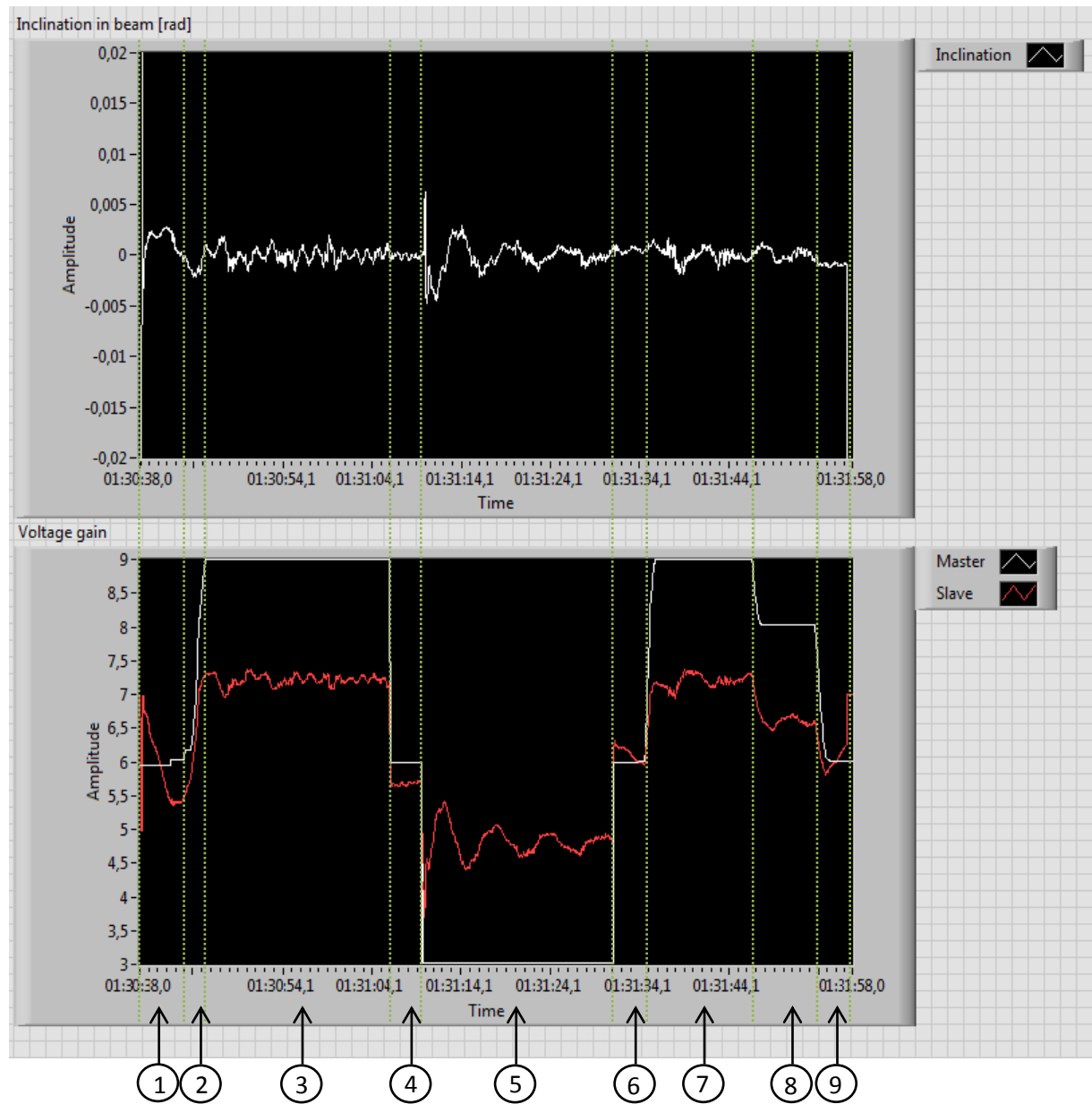


Figure 34: Real time simulation, unloaded

Figure 35 display the sequence of hoisting and lowering the load of 400kg attached to the lifting brackets in position $x = 0.44$. The inclinations are slightly higher than without load. The additional inclination is mainly caused by a malfunction in the slave motor detected during testing with the load attached. The slave motor, received from the University, may behave irregularly during lifting.

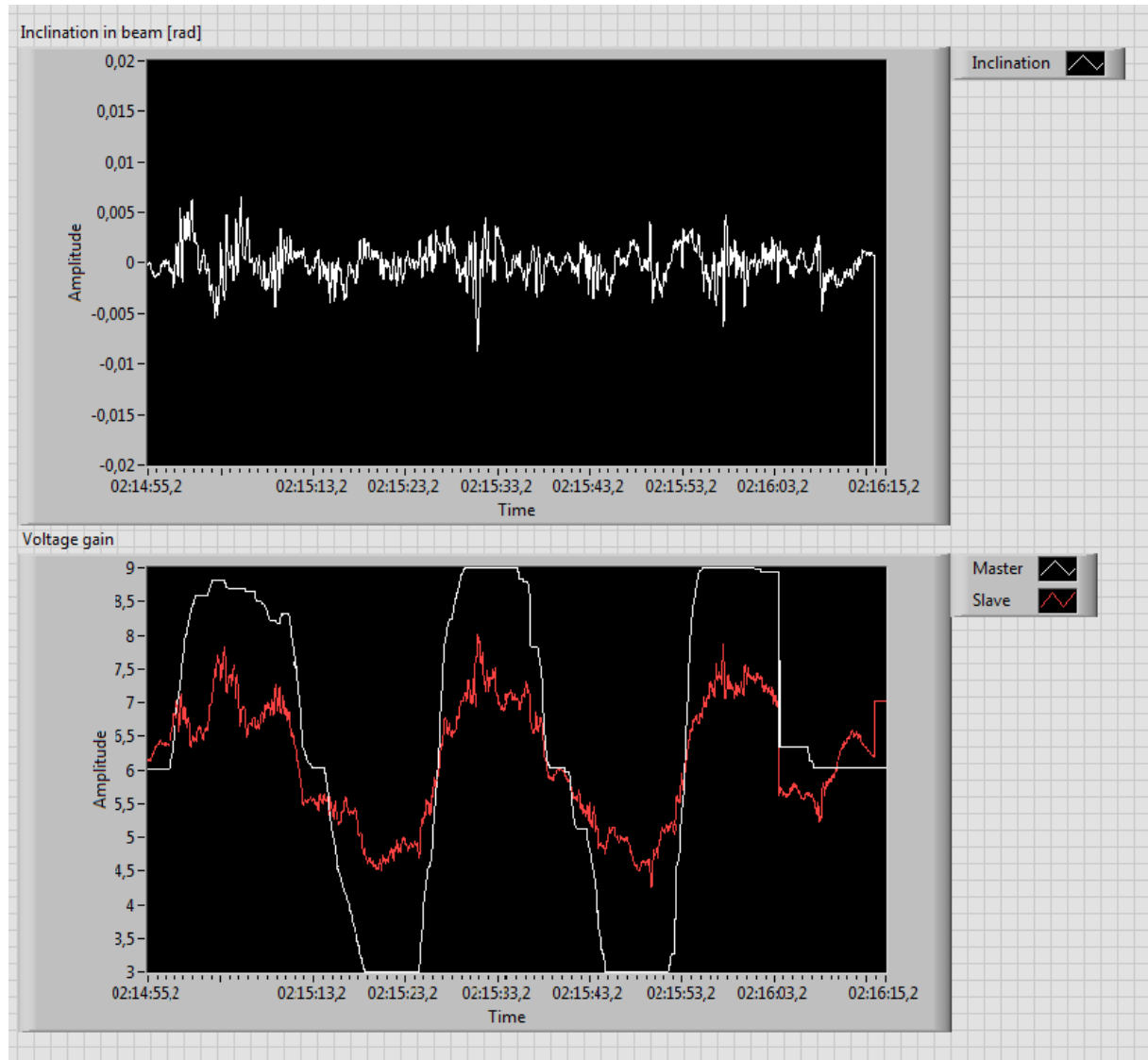


Figure 35: Real time simulation, 400kg in position $x=0.44$

The test software used to make the real time situations is shown in Figure 36 and Figure 37 as the coded block diagram and the user front panel, respectively.

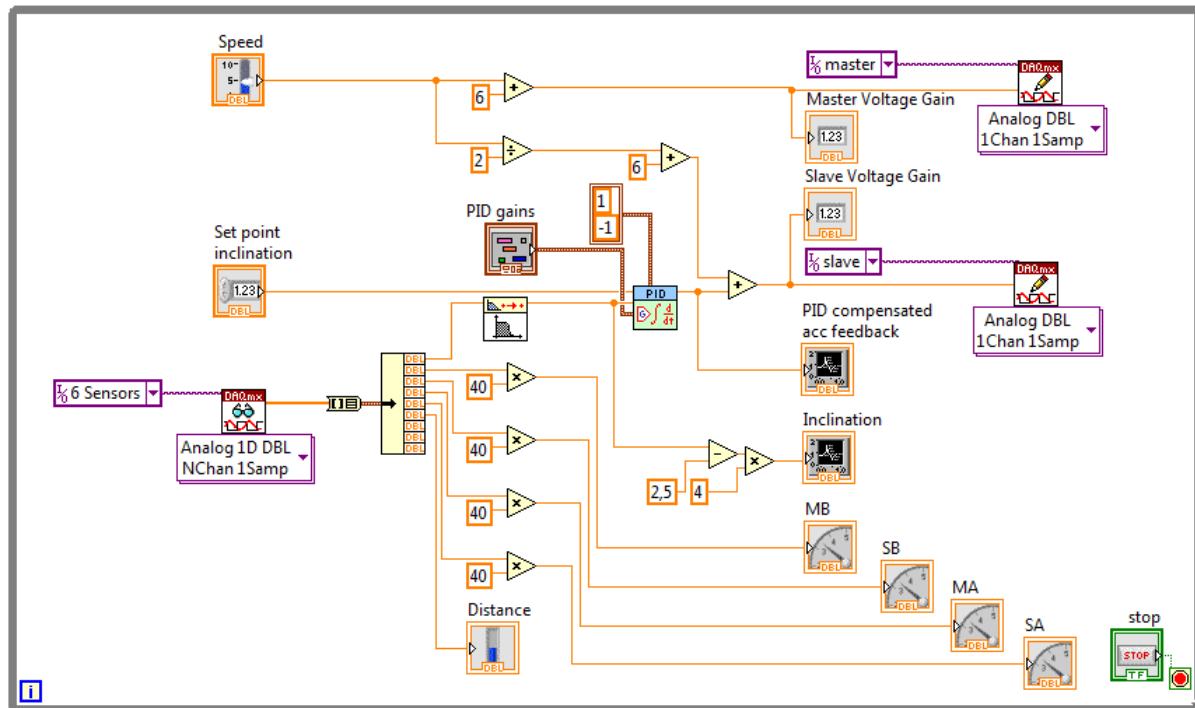


Figure 36: Block Diagram

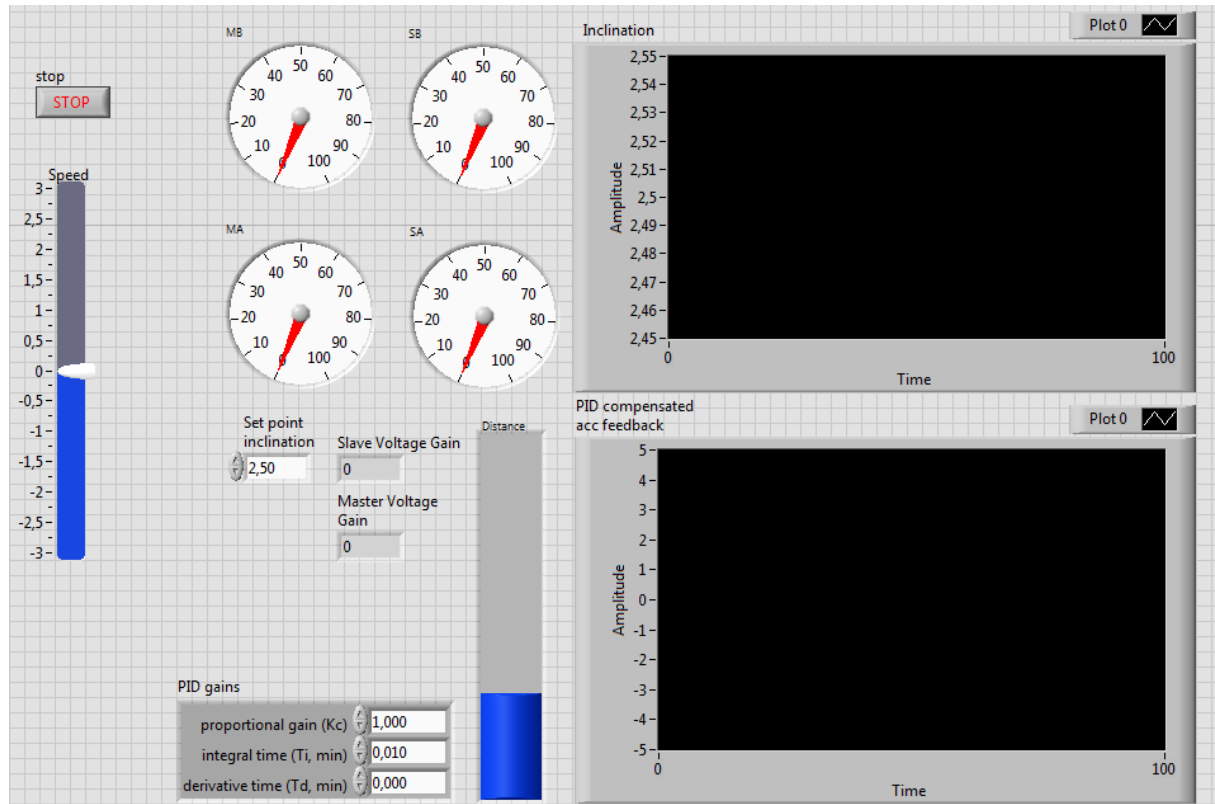


Figure 37: Front Panel

6 Concluding remarks

6.1 Results

Test running the stand showed positive results, with no sign of malfunction in the mechanical components. Also, the hydraulic system worked as intended, though the hydraulic motors turned out to be worn from previous usage. This resulted in occasional lag during lifting. Further, the electrical instruments operated properly. However, the distance sensor was not functioning as intended by end date. The control system worked as planned. The inclination in the beam was consistently close to zero.

6.2 Discussion

Regarding the mechanical construction the students had an advantage by having practical experience in the past. In hindsight, this practical experience has been considered essential to the task. The construction was expected to be built after completed design. However, the design was altered weekly throughout the project. These alterations did not however affect the end result negatively. The building process was more time consuming than expected, hereby reducing time for testing. Further, the payload used was half of the proposed load. This load reduction made it possible for simplifications. These simplifications resulted in faster completion, but reduced lifting capacity.

The overcenter valves were not adjusted as intended. As this would be a time consuming process, the group decided to ignore the adjustments due to the system working by all expectations. Further, the PVG-valve consisted of two modules with different discharge areas. If the group had used identical modules, they would have a linear correlation and be easier to control manually. Regarding instrumentation, the accelerometer proved to be reliable for completing the task.

The control system was not given a lot of time for experimental testing and tuning due to unexpected long building process. Nonetheless, the control system worked to all expectations. The accelerometer ensured not only the ability to run the motors synchronized, but also adjusted the beam to the desired angle. The PID-controller had to be adjusted manually depending on the given load. In hindsight, a loading cell could be attached between wire and beam in order to have automatic load regulation in the PID-controller.

6.3 Conclusion

The development of the mechanical structure began at an early stage of the project. All ordered components arrived on schedule and functioned well. The hydraulic system worked as intended, but one of the motors had a malfunction causing irregular behaviour. The Master and Slave principle adopted in the control system ensured a successful relationship between the motors.

The students achieved creating a product able to synchronize the two hydraulic motors. After testing, the students can conclude the ability to synchronize multiple actuators with a non-mechanical connection to be entirely possible. However, compared to the solution conducted, a mechanical connection would be able to respond faster and more accurately to varying load- magnitude and location. In conclusion, a mechanical connection would not only be simpler, but also a more accurate solution.

7 Reference list

- [1] K. D. Decker, "Low-tech Magazine," 25 03 2010. [Online]. Available: <http://www.lowtechmagazine.com/2010/03/history-of-human-powered-cranes.html>. [Accessed 21 01 2013].
- [2] structural drafting net expert, "European Standard Beams," 2013. [Online]. Available: <http://www.structural-drafting-net-expert.com/steel-sections-IPE.html>. [Accessed 12 02 2013].
- [3] K. Nice, "How stuff works," n.d.. [Online]. Available: <http://science.howstuffworks.com/transport/engines-equipment/gear5.htm>. [Accessed 12 02 2013].
- [4] M. R. Hansen and T. O. Andersen, Hydraulic Components and Systems, Grimstad: University of Agder, 2012.
- [5] J. Haugan, Formler og tabeller, Bekkestua: NKI Forlaget AS, 2010.
- [6] Hydex systemhydraulikk, Hydraulikkurs, Hydex systemhydraulikk, 2007.
- [7] Sauer Danfoss, "Counterbalance valve," Sauer Danfoss, 03 2003. [Online]. Available: http://www.sauer-danfoss.com/Catalog/Old/Section9_Counterbalance%20valves.pdf. [Accessed 04 02 2013].
- [8] Sauer Danfoss, *PVG 32 Proportional Valves*, Sauer Danfoss, 2009.
- [9] Parker Hannifin Corporation, Hydraulic Cartridge Systems, Lincolnshire, 2010.
- [10] Omega, "omega.com," Omega, 2013. [Online]. Available: <http://www.omega.com/prodinfo/pressuretransducers.html>. [Accessed 16 01 2013].
- [11] E. Herø, E. Johansen, R. Kristenen, H. Strømme and B. Tennung, Reparasjon og vedlikeholdsteknikk, Oslo: Gyldendal, 2009.
- [12] Chevron Products Company, 01 2008. [Online]. Available: http://www.chevronmarineproducts.com/docs/Chevron_RandoHDZ_PDS1_Lo.pdf. [Accessed 26 04 2013].
- [13] National Instruments, "National Instruments," [Online]. Available: <http://sine.ni.com/nips/cds/print/p/lang/no/nid/203224>. [Accessed 24 4 2013].
- [14] Omega, "omega.com," [Online]. Available: <http://www.omega.com/prodinfo/accelerometers.html>. [Accessed 22 01 2013].
- [15] Sharp, "Elfa distrelec," 2006. [Online]. Available: https://www1.elfa.se/data1/wwwroot/assets/datasheets/gpSharp_Distanzsensoren-GP-

- 2Y0A02YKOF_EN.pdf. [Accessed 11 02 2013].
- [16] N. S. Nise, Control Systems Engineering, Asia: John Wiley & Sons, 2011.
- [17] J.-P. Corriou, "Process Control: Theory and Applications," Springer, London, 2004.
- [18] Moog, "Moog," 2012. [Online]. Available: <http://www.moog.com/products/servovalves-servo-proportional-valves/>. [Accessed 15 01 2013].
- [19] Moog, "Moog," [Online]. Available: <http://www.moog.com/literature/ICD/d765seriesvalves.pdf>. [Accessed 16 01 2013].
- [20] T. O. A. Michael Rygaard Hansen, Hydraulic Components and Systems, compressed, Grimstad: University of Agder, 2012.
- [21] Kelag, Singel Axis Acceleration Sensor, Schwerzenbach: KELAG Künzli Elektronik AG, 2011.
- [22] K. G. Robbersmyr, Maskinkonstruksjon - Konstruksjonsanalyse, Grimstad: Kjell G. Robbersmyr.
- [23] Leif Hübert, Leif Hübert, [Online]. Available: <http://hubert.no/shop.php?controller=category>. [Accessed 03 05 2013].
- [24] KTR Kupplungstechnik, "www.ktrcouplings.co.uk," [Online]. Available: <http://www.ktrcouplings.co.uk/products/brands/rotex>. [Accessed 06 05 2013].

Appendix A, Final Accounts

Steel

Component	Size	Length	Total Cost	Order date	Delivery date
Square pipe S355J2H	40x40x4	30000	1 500 NOK	07.03.2013	12.03.2013
Square pipe S355J2H	80x40x4	6000	460 NOK	07.03.2013	12.03.2013
Beam IPE 100 mm S355J2G3	100mm	6000	725 NOK	07.03.2013	12.03.2013
Steel Plate	700x360x6		180 NOK*	NA	NA
Steel Plate	700x320X10		550 NOK*	NA	NA

Sensors

Component	Type	Quantity	Total Cost	Order date	Delivery date
Sharp Distance Sensor	GP 2Y0A02YK0F	1	119 NOK	NA	NA
Accelerometer	KAS901-04A	1	1 254 NOK	NA	NA
Pressure transducer	SCP01-400-44-07	4	NA *	NA	NA

Mechanical components

Component	Size	Quantity	Total Cost	Order date	Delivery date
Gear	620 NM	2	20 000 NOK	08.02.2013	13.03.2013
Wire lock	5-6 mm	4	216 NOK	02.04.2013	15.03.2013
Wire	5 mm	7000 mm	54 NOK	02.04.2013	15.03.2013
Shackle	1000 WLL/Kg	2	150 NOK	02.04.2013	15.03.2013
Rotex coupling	3138k98	2	252 NOK	12.03.2013	12.03.2013

Hydraulic components

Component	Size	Quantity	Total cost	Order date	Delivery date
Overcentre valve	MHB-015-LBAH-51E	2	2 515 NOK	08.02.2013	03.04.2013
PVG	32	1	NA*	NA	NA
Motor	AA2FM 32	2	NA*	NA	NA
HPU		1	NA*	NA	NA
Pipes & Couplings			NOK	NA	NA

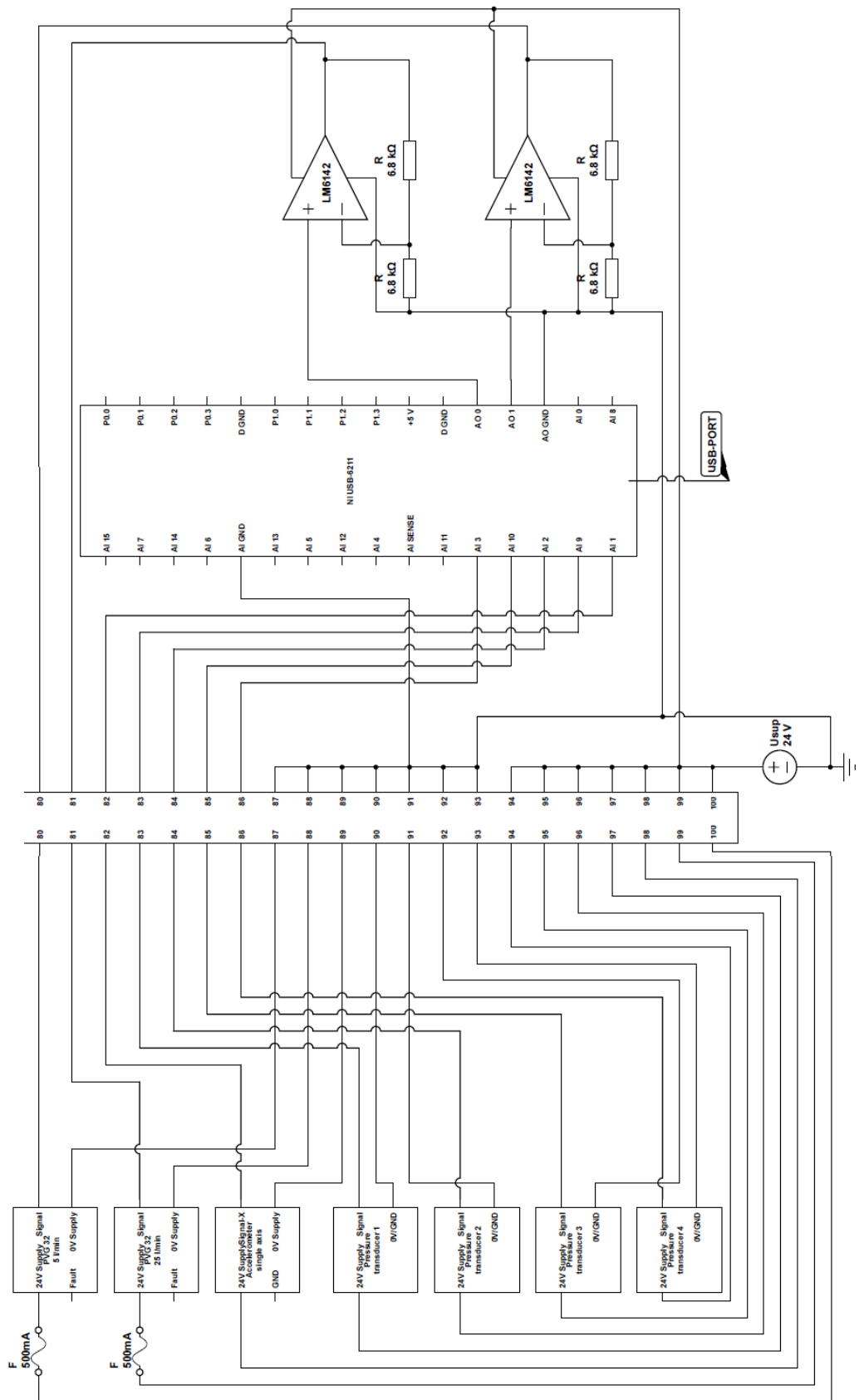
Control system

Component	Size	Quantity	Cost	Order date	Delivery date
National Instrument	NI USB - 6211	1	7 000*	NA	NA

Total cost	35 000 NOK
------------	------------

* Already available at the workshop.

Appendix B, Electrical wiring diagram



Appendix C, Data sheets

C.1 Hydromec, Worm Drive

110 Rightangle - Gear 620Nm

Rating - Cast Iron WORM GEARBOXES



- QUICK SELECTION / Selezione veloce

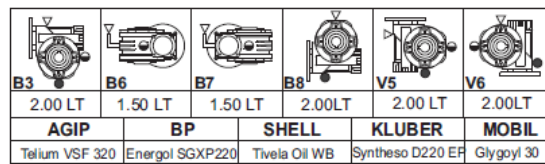
Output Speed n_2 [min ⁻¹]	Ratio i	Motor power P_{M} [kW]	Output torque M_{M} [Nm]	Service factor f.s.	Nominal power P_{N} [kW]	Nominal torque M_{N} [Nm]	Available B5 motor flanges				Available B14 motor flanges				Dynamic efficiency	Tooth Module	Ratios code
							C	D	E	F	71	80	90	100			
200	7	4.0	168	2.7	10.9	460	B	B		B	B			88	5.5	01	
140	10	4.0	235	2.1	8.5	500	B	B		B	B			86	5.4	02	
88	16	4.0	358	1.4	5.7	510	B	B		B	B			82	5.3	03	
70	20	4.0	447	1.2	4.6	520	B	B		B	B			82	4.5	04	
61	23	3.0	377	1.3	3.9	490	B	B		B	B			80	3.9	05	
47	30	3.0	467	1.3	4.0	620	B	B		B	B			76	5.6	06	
37	38	3.0	583	1.0	3.1	610	B	B		B	B			75	4.7	07	
31	45	2.2	493	1.2	2.5	570	B	B		B	B			73	4.0	08	
26	53	2.2	557	1.1	2.3	590	B	B		B	B			70	3.5	09	
22	64	1.5	452	1.1	1.7	510	B	B		B	B			69	2.9	10	
16.7	84	1.1	410	1.1	1.3	470	B	B		B	B			65	2.2	11	
14.1	99	1.1	446	1.0	1.1	460	B	B		B	B			60	1.9	12	

■ Motor Flanges Available Flange Motore Disponibili

○ B) Supplied with Reduction Bushing Fornito con Bussola di Riduzione

B) Available on Request without reduction bushing Disponibile a Richiesta senza Bussola di Riduzione

C) Motor Flange Holes Position Posizione Fori Flangia Motore



tab. 1

- RADIAL AND AXIAL LOADS

Output shaft Albero di uscita		
n_2 [min ⁻¹]	FA [N]	FR [N]
200	600	2900
150	700	3300
100	750	3600
75	800	4000
50	920	4600
25	1200	6000
15	1400	7000

Input shaft albero in entrata

n_1 [min ⁻¹]	FA [N]	FR [N]
1400	228	1140

*Strong axial loads in the DX direction are not allowed.
Non sono consentiti forti carichi assiali con direzione DX.

tab. 2

EN Unit 110 is supplied without lubricant and equipped with a breather, level and drain plugs. User can add mineral oil keeping existing plugs. Should the user wish to fill it with synthetic oil, it is recommended to replace the existing plugs with a closed plug. See table 1 for lubrication and recommended quantity. In table 2 please see possible radial loads and axial loads on the gearbox. For complete documentation please visit our web site.

I Il riduttore tipo 110 è fornito privo di lubrificazione con tappi di sfiato, livelli e scarico olio. L'utente può immettere olio minerale mantenendo i tappi esistenti. Se immetterà olio sintetico, dovrà sostituire i tappi esistenti con altri tipo chiuso. Tab.1 per oli e quantità consigliati. Tab.2 carichi radiali e assiali applicabili al riduttore. Per la documentazione completa consulta il nostro sito.

D Das Getriebe der Baugröße 110 wird ohne Schmiermittel geliefert. Es ist jedoch mit Einfüllschraube, Überdruckventil und Abläufschraube ausgerüstet. Das benötigte mineralische Öl kann über die Einfüllschraube eingefüllt werden. Sollte synthetisches Öl bevorzugt werden, so ist sind das eingebaute Überdruckventil durch eine geschlossenen Schraube zu ersetzen. In Tabelle 1 ist die Schmiernenge und das empfohlene Schmiermittel angegeben. In Tabelle 2 sind die zulässigen Radial- und Axialbelastungen des Getriebes aufgeführt. Die komplette Dokumentation, Wartungs- und Inbetriebnahmeanleitungen finden Sie unter.

E El reductor tamaño 110 se suministra sin lubricante, provisto de tapones de respiración, nivel y descarga de aceite. El usuario puede utilizar aceite mineral, manteniendo los tapones existentes. Si prefiere utilizar aceite sintético deberá sustituir los tapones existentes por tapones ciegos. La prereducción se suministra con tapones ciegos, lubricado de por vida con aceite sintético. Ver tabla 1, para cantidades y aceites recomendados. En la tabla 2, se encuentran las cargas radiales y axiales admitidas por el reductor. Para documentación completa, consultar nuestra Web.

SELECT THIS TYPE AND THIS SPECIFIC SIZE ON THE WEB PAGES TO GET COMPLETE TECHNICAL DATA.
Selezionare tipo e gandezza specifica nel sito web per la documentazione completa.

Rightangle - Gear 620Nm 110

3D dimensions on the Web

P110FB... Basic wormbox Riduttore base

M. flanges	Kit code	ϕF	A
71B5	K023.4.041	160	135.5
80/90B5	K023.4.042	200	137.5
100/112B5	K023.4.043	250	143.5
80B14	K085.4.046	120	135.5
90B14	K085.4.045	140	135.5
100/112B14	K023.4.041	160	135.5

Wormbox weight peso riduttore 35.00 kg

P110PA... Feet Piedini

P110PB... Feet Piedini

P110PV... Feet Piedini

	H	R	S	T	U	V	Y	W	ϕZ	kit code
type B	170	180	22	224	200	240	286	333	$\phi 13$	K110.9.022
type S	172	160	18	190	200	240	288	335	$\phi 14$	KS110.9.023

P110FC... Output flange Flangia uscita

	ϕD	E	G	L	N	O	P	Q	kit code
FC	170 ^{+0.083} / _{-0.045}	11	16.5	131.5	54	230	270	13	① K110.9.010 ② -
FL	170 ^{+0.083} / _{-0.043}	11	16.5	179.5	102	230	270	13	① K110.9.011 ② -

P110BR... Reaction arm Braccio di reazione

P110...S... Single Shaft Albero lento semplice

① kit cod. K110.5.028 type B ② kit cod. K110.5.029 type B

P110....D... Double Shaft Albero lento bisp.

	b1	c1	d1	e1	f1	I1	m1	n1	t2	$\phi 1$
type B	12	75	42 ^{+0.005} / _{-0.005}	96.5	155	348	163.5	260	45	M12x32
type S	-	-	-	-	-	-	-	-	-	-

R110FB... Input shaft Albero in entrata

	ϕd	e	g	l	m	x	kit code
type B	25 h6	28	8	50	131.5	M8x20	① K085.5.007 PAM90 ② K085.5.008 PAM100
type S	24 h6	27	8	50	131.5	M8x20	① K085.5.009 PAM90 ② K085.5.011 PAM100

C.2 Rotex coupling

ROTEX® Torsionally flexible coupling

Made for Motion

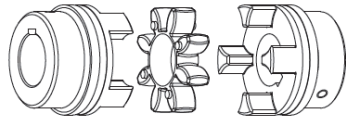


ROTEX®

Description of coupling

ROTEX® couplings are characterized by small dimensions, low weight and low mass moments of inertia yet transmit high torques. Running quality and service life of the coupling are improved by accurate all-over machining.

Their application is ideal for transmitting torque while damping torsional vibrations and absorbing shocks produced by the uneven operation of certain prime movers.



General description

ROTEX® couplings are torsionally flexible and designed for positive torque transmission. They are fail-safe. Operational vibrations and shocks are efficiently damped and reduced. The two congruent coupling halves with concave claws on the inside are peripherally offset in relation to one another by half a pitch. In addition, they are designed in such a way as to enable an involute spider to be located between them.

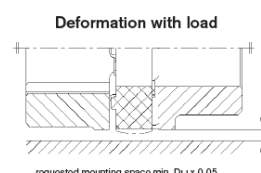
The teeth of the spider are crowned to avoid edge pressure if the shafts are misaligned. ROTEX® couplings are capable of compensating for axial, radial and angular displacements of the shafts to be connected.



Performance

In contrast to other flexible couplings, the intermediate members of which are subject to bending stress and are therefore prone to earlier wear, the flexible teeth of ROTEX® couplings are subject to pressure only. This gives the additional advantage of the individual teeth being able to accept considerably higher loads. The elastomer parts show deformation with load and excessive speeds. Sufficient space for expansion should be ensured (see drawing – deformation with load).

The maximum torsion angle with ROTEX® couplings of any size amounts to 5°. They can be fitted both horizontally and vertically.



Spiders – our innovation T-PUR®

KTR has developed a new standard material for its spiders. The improved polyurethane material T-PUR® is resistant to significantly higher temperatures and has a considerably longer service life than the previous polyurethane material. From the visual point of view we have characterized the material T-PUR® by the colours orange (92 Shore-A), purple (98 Shore-A) and pale green (64 Shore-D). The previous spiders made of polyurethane in yellow, red and natural white with green ends will still be available.

Up to size ROTEX® 180 inclusive single-parted spiders are used as a standard. Optionally the DZ tooth elements continue to be available for ROTEX® couplings sizes 100-180.

Spider
Standard from size 14 - 180

Explosion-proof use

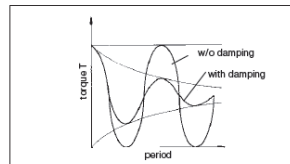
ROTEX® couplings are suitable for power transmission in drives in hazardous areas. The couplings are certified and confirmed according to EC standard 94/9/EC (ATEX 95) as units of category 2G/2D and thus suitable for the use in hazardous areas of zone 1, 2, 21 and 22. Please read through our information included in the respective Type Examination Certificate and the operating and mounting instructions at www.ktr.com.

In addition to the ATEX marking an inspection certificate by DNV, Bureau Veritas or ABS can be ordered for ROTEX® couplings.

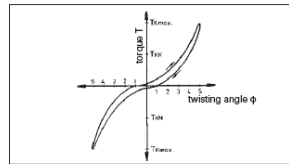


ISO 9001
ISO 16001
BUREAU VERITAS
Certification

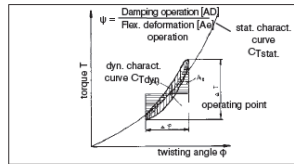
Comparison of loads



Twisting angle



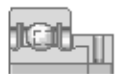
Damping



You will find continuously updated data in our online catalogue at www.ktr.com.

19

C.3 Bearing GAY45-NPP-B



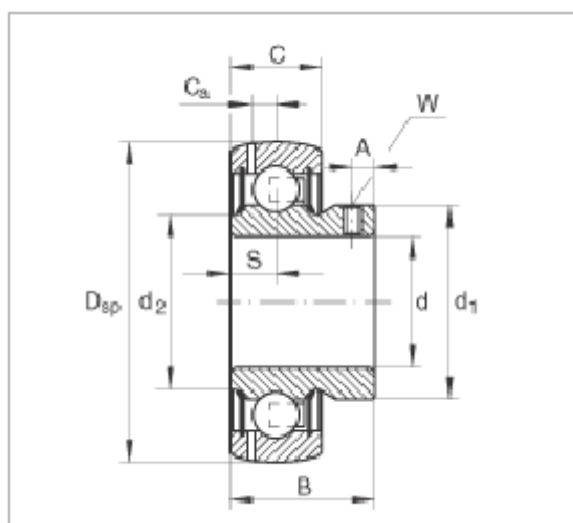
Radial insert ball bearings GAY45-NPP-B (Series GAY..-NPP-B)



spherical outer ring, location by grub screws, P seals on both sides

The datasheet is only an overview of dimensions and basic load ratings of the selected product. Please always observe all the guidelines in these overview pages. Further information is given on many products under the menu item "Description". You can also order comprehensive information via the Catalogue ordering system (<http://www.ina.de/content.ina.de/en/médiathèque/library/library.jsp>) or by telephone on +49 (91 32) 82 - 28 97.

d	45 mm
D _{sp}	85 mm
B	41,5 mm
A	8 mm
C	22 mm
C _a	6,4 mm
d ₁	57 mm
d ₂	54,3 mm
S	11 mm
W	4 mm
m	0,6 kg Mass
C _r	32500 N Basic dynamic load rating, radial
C _{or}	20400 N Basic static load rating, radial
	6209 Reference bearing for determining the equivalent bearing load.



C.4 Bearing Housing, PASEY45



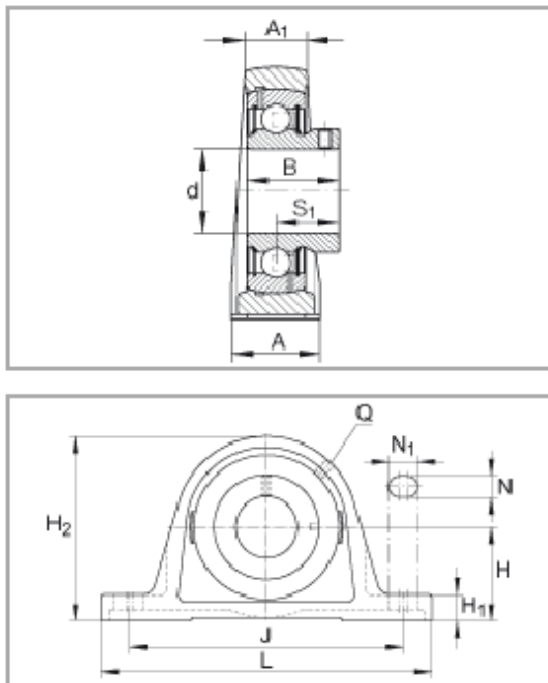
Plummer block housing units PASEY45 (Series PASEY)

cast iron housing, radial insert ball bearing with grub
screws in inner ring, P seals



The datasheet is only an overview of dimensions and basic load ratings of the selected product. Please always observe all the guidelines in these overview pages. Further information is given on many products under the menu item "Description". You can also order comprehensive information via the Catalogue ordering system (<http://www.ina.de/content.ina.de/en/mediathek/library/library.jsp>) or by telephone on +49 (91 32) 82 - 28 97.

d	45 mm
L	192 mm
H ₂	107 mm
A	48 mm
A ₁	32 mm
B	41,5 mm
H	54 mm
H ₁	21,5 mm
J	150 mm
N	14 mm
N ₁	29 mm
Q	Rp 1/8
S ₁	30,5 mm
m	2,06 kg Mass
C _r	32500 N Basic dynamic load rating, radial
C _{0r}	20400 N Basic static load rating, radial
GG.ASE09 Designation of housing	
GAY45-NPP-B Designation of bearing	



C.5 Iron Grip BG-100

BG-100 Wire Clamp Fitting Instructions

EN

Use

IronGrip's BG-100 wire clamp can be used for all types of lifting device and suspended load. It is intended for use with steel wire ropes with a steel or fibre core for general applications up to and including strength class 1,960 N/mm². Plastic-coated wires are not suitable for lifting applications using IronGrip wire clamps.

Restrictions and requirements

In use for lifting applications, **two** wire clamps per attachment must be used in accordance with these instructions. This applies to all dimensions with BG-600, BG-800, BG-1000, BG-1200, BG-1600, BG-2000, BG-2500 and BG-3400.

The BG-100 can be used with steel wire ropes for general lifting purposes including lifts etc. up to and including strength class 1,960 N/mm². Note that lifting application refers to both static lifting (suspended loads) and dynamic lifting.

Standards

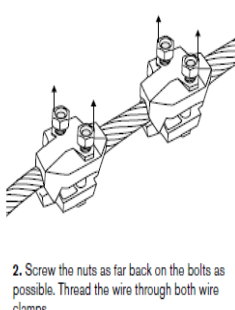
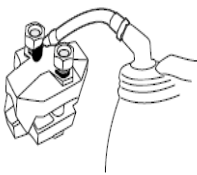
For approval of IronGrip's BG-100 wire clamp for lifting applications the standard SS-EN 13411-3 regarding ferrules has been used. The IronGrip BG-100 wire clamp has been tested in accordance with the same standards, and easily meets the requirements for ferrules, provided the right number of wire clamps per attachment are fitted in accordance with these instructions.

Wire clamp	Wire (mm)	Torque (Nm)	Bending length (mm)	Weight (kg)	Key width (mm)
BG-600	5-6	9,5	180	0,09	10
BG-800	7-8	9,5	220	0,12	10
BG-1000	9-10	22	270	0,20	13
BG-1200	11-12,5	44	330	0,39	16
BG-1600	13-16	75	430	0,72	18
BG-2000	17-20	120	530	1,18	21
BG-2500	21-25	260	700	2,80	27
BG-3400	26-34	350	1100	7,70	30

WARNING

- Failure to follow these fitting instructions may have serious consequences and may cause injury/damage.
- Read the instructions carefully before you start the fitting.
- Tighten using a torque wrench so as to achieve the correct tension in the wire clamps.
- Always oil the bolt threads before tightening. If you do not do this the stipulated torque will not create the right tension.
- Test-load the application with the maximum permissible force, then check the torque again.
- Inspect the attachment regularly.
- Note that the wire clamp's teeth can absorb minor displacement forces. If a tooth breaks off, this is an important sign that undesirable sliding has occurred. Reduce the load immediately, check the attachment and replace the wire clamp.

1. Check that the cable and the wire clamps are undamaged and that the threads are clean and lubricated. Thread lubrication is particularly important in lifting applications, so as to achieve the right traction in the screws.



3. Measure out the requisite bending length in accordance with the table. Bend the wire and feed the end back through the wire clamps.



4. Tighten the nuts a little on the wire clamp nearest the end.

5. Insert the thimble, squeeze together the cable and push the wire clamp as close to the thimble as possible. Press against the first fixed clamp.

The distance from the thimble must be about one wire diameter. The wire clamp nearest the thimble must be so close that there is no risk of the thimble loosening when the wire clamp is tightened.

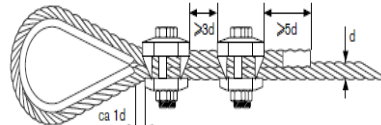
6. Make sure the wire clamp is as straight and symmetrical on the wire as possible.

7. Tighten the nuts alternately so that the teeth fit into the recesses on each side. **NB: Use a torque wrench!** Tighten until the right torque has been achieved.

When tightening the BG-3400, the middle nuts must first be tightened alternately until the right torque has been achieved. The two outer nuts must then be tightened. Finally ensure that all nuts are tightened to the right torque.

8. When the wire clamp closest to the thimble is well tightened, the wire clamp closest to the end can be loosened and if necessary adjusted so that it is at a suitable distance from the other clamp. Tighten the nuts on this lock in accordance with 7) above.

9. The distances between wire clamp, thimble and free end must be as follows:



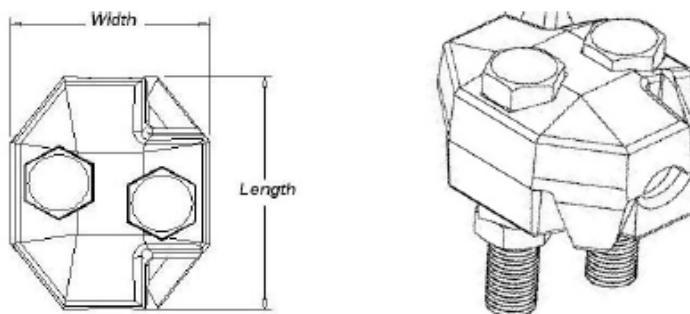
 IRONGRIP®
www.irongrip.se +46(0)8-661 91 70



IronGrip BG-100 Wire Clamps

Technical Specifications

Name	Wire Diameter (mm)	Length (mm)	Width (mm)	Weight (kg)	No. of Bolts	Bolt Dimension	Rec. Torque (Nm)
BG-600	5-6	32	26	0.09	2	M6*35	9.5
BG-800	7-8	36	28	0.12	2	M6*40	9.5
BG-1000	9-10	44	34	0.20	2	M8*50	22.5
BG-1200	11-12,5	54	42	0.39	2	M10*60	44
BG-1600	13-16	68	52	0.72	2	M12*75	75
BG-2000	17-20	82	60	1.18	2	M14*90	120
BG-2500	21-25	122	80	2.80	2	M18*110 f.t.	260
BG-3400	26-34	214	94	7.70	4	M20*150 f.t.	360


Material Specification:

Castings in ductile cast iron

Strength class for bolts: 8.8 in accordance with ISO 3506

Rustproofing of castings: Hot dip galvanisation in accordance with ISO 1461

Rustproofing of bolts: Electrically galvanised in accordance with ISO 2081

Recommended for all kinds of lifting applications with two wire clamps per fixation
for wire ropes of tenacity class including 1960 N/mm²

Tested and approved according to EN 13411-3:2004

C.6 Rexroth, AA2FM 32

RA 91001/09.07 | AA2FM

Bosch Rexroth Corp. 7/36

Technical Data

Table of values (theoretical values, ignoring η_{mh} and η_v ; values rounded)

Size		5	10	12	16	23	28	32	45	56	63	80	
Displacement	V _g	in ³	0.30	0.63	0.73	0.98	1.40	1.71	1.95	2.78	3.42	3.84	4.91
		cm ³	4.93	10.3	12	16	22.9	28.1	32	45.6	56.1	63	80.4
Max. Speed	n _{max}	rpm	10000	8000	8000	8000	6300	6300	6300	5600	5000	5000	4500
	n _{max} intermit. ¹⁾	rpm	11000	8800	8800	8800	6900	6900	6900	6200	5500	5500	5000
Max. flow	q _v max	gpm	13	21.8	25.3	33.9	38.2	46.6	52.2	67.4	74.0	83.1	95.6
		L/min	49	82	96	128	144	176	201	255	280	315	360
Torque at	Δp = 5100 psi T	lb·ft	18 ²⁾	42	49	66	94	115	132	188	231	259	332
	Δp = 350 bar T	Nm	24.7 ²⁾	57	67	88	126	156	178	254	312	350	445
	Δp = 5800 psi T	lb·ft	—	48	56	75	107	131	150	213	263	295	377
	Δp = 400 bar T	Nm	—	65	76	100	144	178	204	290	356	400	508
Rotary stiffness	c	Nm/rad	625	922	1250	1590	2560	2930	3120	4180	5940	6250	8730
Moment of inertia for rotary group	J _{TW}	lbs·ft ²	0.0014	0.0095	0.0095	0.0095	0.0285	0.0285	0.0285	0.0569	0.0997	0.0997	0.1708
		kgm ²	0.00006	0.0004	0.0004	0.0004	0.0012	0.0012	0.0012	0.0024	0.0042	0.0042	0.0072
Angular acceleration maximum α		rad/s ²	5000	5000	5000	5000	6500	6500	6500	14600	7500	7500	6000
Filling capacity	V	gal	0.045	0.045	0.045	0.053	0.053	0.053	0.053	0.087	0.119	0.119	0.145
		L	0.17	0.17	0.17	0.20	0.20	0.20	0.20	0.33	0.45	0.45	0.55
Mass (approx.)	m	lbs	5.5	12	12	12	21	21	21	30	40	40	51
		kg	2.5	5.4	5.4	5.4	9.5	9.5	9.5	13.5	18	18	23

Size		90	107	125	160	180	200	250	355	500	710	1000	
Displacement	V _g	in ³	5.49	6.51	7.63	9.79	10.98	12.20	15.25	21.66	30.51	43.33	61.02
		cm ³	90	106.7	125	160.4	180	200	250	355	500	710	1000
Max. Speed	n _{max}	rpm	4500	4000	4000	3600	3600	2750	2700	2240	2000	1600	1600
	n _{max} intermit. ¹⁾	rpm	5000	4400	4400	4000	4000	3000	—	—	—	—	—
Max. flow	q _v max	gpm	106.9	112.7	132.1	152.5	1711	145.2	178	210	264	300	422
		L/min	405	427	500	577	648	550	675	795	1000	1136	1600
Torque at	Δp = 5100 psi T	lb·ft	371	440	516	662	742	825	1030	1465	2063	2930	4127
	Δp = 350 bar T	Nm	501	595	697	889	1001	1114	1393	1978	2785	3955	5570
	Δp = 5800 psi T	lb·ft	422	500	587	753	844	938	—	—	—	—	—
	Δp = 400 bar T	Nm	572	680	796	1016	1144	1272	—	—	—	—	—
Rotary stiffness	c	Nm/rad	9140	11200	11900	17400	18200	57300	73100	96100	144000	270000	324000
Moment of inertia for rotary group	J _{TW}	lbs·ft ²	0.1708	0.2753	0.2753	0.5221	0.5221	0.8377	1.4475	2.4205	4.2240	13.052	13.052
		kgm ²	0.0072	0.0116	0.0116	0.0220	0.0220	0.0353	0.061	0.102	0.178	0.55	0.55
Angular acceleration maximum α		rad/s ²	6000	4500	4500	3500	3500	11000	10000	8300	5500	4300	4000
Filling capacity	V	gal	0.145	0.211	0.211	0.291	0.291	0.713	0.660	0.925	1.110	2.113	2.113
		L	0.55	0.8	0.8	1.1	1.1	2.7	2.5	3.5	4.2	8	8
Mass (approx.)	m	lbs	51	71	71	99	99	145	161	242	342	715	741
		kg	23	32	32	45	45	66	73	110	155	325	336

¹⁾ Intermittent maximum speed: overspeed at discharge and over-running travel operations, t < 5 s and Δp < 2200 psi (150 bar)²⁾ Torque at Δp = 4550 psi (315 bar)

Caution: Exceeding the permissible limit values may result in a loss of function, a reduction in service life or in the destruction of the axial piston unit.

Other permissible limit values with respect to speed variation, reduced angular acceleration as a function of the frequency and the permissible startup angular acceleration (lower than the maximum angular acceleration) can be found in data sheet RE 90261.

Technical Data

Determining the size

$$\text{Flow} \quad q_v = \frac{V_g \cdot n}{231 \cdot \eta_v} \quad \text{gpm} \quad \left(q_v = \frac{V_g \cdot n}{1000 \cdot \eta_v} \quad \text{l/min} \right)$$

$$\text{Speed} \quad n = \frac{q_v \cdot 231 \cdot \eta_v}{V_g} \quad \text{rpm} \quad \left(n = \frac{q_v \cdot 1000 \cdot \eta_v}{V_g} \quad \text{rpm} \right)$$

$$\text{Torque} \quad T = \frac{V_g \cdot \Delta p \cdot \eta_{mh}}{24 \cdot \pi} \quad \text{lb-ft} \quad \left(T = \frac{V_g \cdot \Delta p \cdot \eta_{mh}}{20 \cdot \pi} \quad \text{Nm} \right)$$

$$\text{Power} \quad P = \frac{2 \pi \cdot T \cdot n}{33\,000} = \frac{q_v \cdot \Delta p \cdot \eta_t}{1714} \quad \text{HP} \quad \left(P = \frac{2 \pi \cdot T \cdot n}{60\,000} = \frac{q_v \cdot \Delta p \cdot \eta_t}{600} \quad \text{kW} \right)$$

V_g = Displacement per revolution in in^3 (cm^3)

Δp = Differential pressure in psi (bar)

n = Speed in rpm

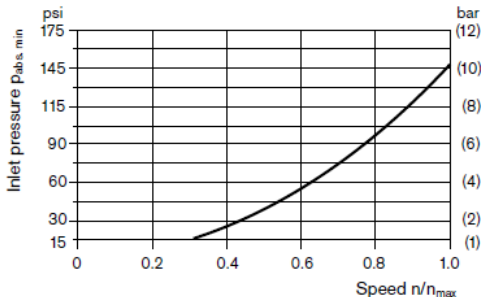
η_v = Volumetric efficiency

η_{mh} = Mechanical-hydraulic efficiency

η_t = Overall efficiency

Minimum inlet pressure on service line port A (B)

To prevent damage to the motor, there must be a minimum inlet pressure in the inlet area. The minimum inlet pressure is dependent on the speed of the fixed motor.



Please contact us if these conditions cannot be satisfied

Technical Data

Permissible radial and axial loading on the drive shaft

The specified values are maximum values and do not apply to continuous operation.

Size		5	10	12	16	23	28	32	45	56	63	80
Radial force, max. ¹⁾ at distance a (from shaft collar)	$F_q \text{ max}$	lbf	160	472	562	730	865	1079	1214	1630	1832	2057
		N	710	2100	2500	3250	3850	4800	5400	7250	8150	9150
	a	in	0.47	0.63	0.63	0.63	0.63	0.63	0.71	0.71	0.71	0.79
		mm	12	16	16	16	16	16	18	18	18	20
Axial force, max. ³⁾	$+F_{ax} \text{ max}$	lbf	40	72	72	72	112	112	112	142	180	180
		N	180	320	320	320	500	500	500	630	800	800
	$-F_{ax} \text{ max}$	lbf	40	72	72	72	112	112	112	142	180	180
		N	180	320	320	320	500	500	500	630	800	800
Permissible axial force/psi (bar) operating pressure	$\pm F_{ax} \text{ per/psi}$ (bar)	lbf/psi N/bar	0.023	0.05	0.05	0.05	0.08	0.08	0.08	0.11	0.13	0.13
			1.5	3.0	3.0	3.0	5.2	5.2	5.2	7.0	8.7	10.6

Size		90	107	125	160	180	200	250	355	500	710	1000
Radial force, max. ¹⁾ at distance a (from shaft collar)	$F_q \text{ max}$	lbf	2574 ²⁾	2720	3170	3664	4114	5148	270	337	427	674
		N	11450	12100	14100	16300	18300	22900	1200 ⁴⁾	1500 ⁴⁾	1900 ⁴⁾	3000 ⁴⁾
	a	in	0.79	0.79	0.79	0.98	0.98	0.98	1.61	2.07	2.07	2.66
		mm	20	20	20	25	25	25	41	52.5	52.5	67.5
Axial force, max. ³⁾	$+F_{ax} \text{ max}$	lbf	225	281	281	360	360	360	450	562	674	989
		N	1000	1250	1250	1600	1600	1600	2000	2500	3000	4400
	$-F_{ax} \text{ max}$	lbf	225	281	281	360	360	360	450	562	674	989
		N	1000	1250	1250	1600	1600	1600	2000	2500	3000	4400
Permissible axial force/psi (bar) operating pressure	$\pm F_{ax} \text{ per/psi}$ (bar)	lbf/psi N/bar	0.16	0.20	0.20	0.26	0.26	0.26	5)	5)	5)	5)

1) During intermittent operation (sizes 5 to 200)

2) Value for Q-shaft: $F_q \text{ max} = 2023 \text{ lbf}$ (9000 N)

3) Max. permissible axial force when at a standstill or when axial piston unit working in pressureless conditions

4) When at a standstill or when axial piston unit operating in depressurized condition. Higher forces are permissible when under pressure. Please contact us.

5) Please contact us

When considering the permissible axial force, the force-transfer direction must be taken into account.

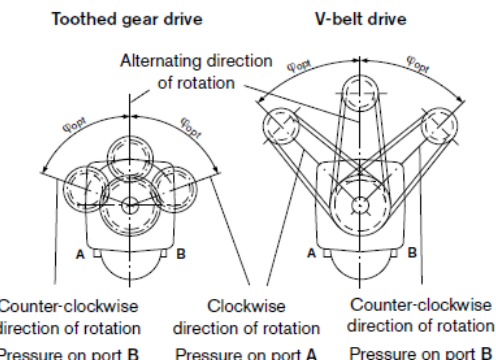
- $F_{ax} \text{ max}$ = increase in service life of bearings

+ $F_{ax} \text{ max}$ = reduction in service life of bearings (avoid)

Effect of radial force F_q on the service life of the bearings

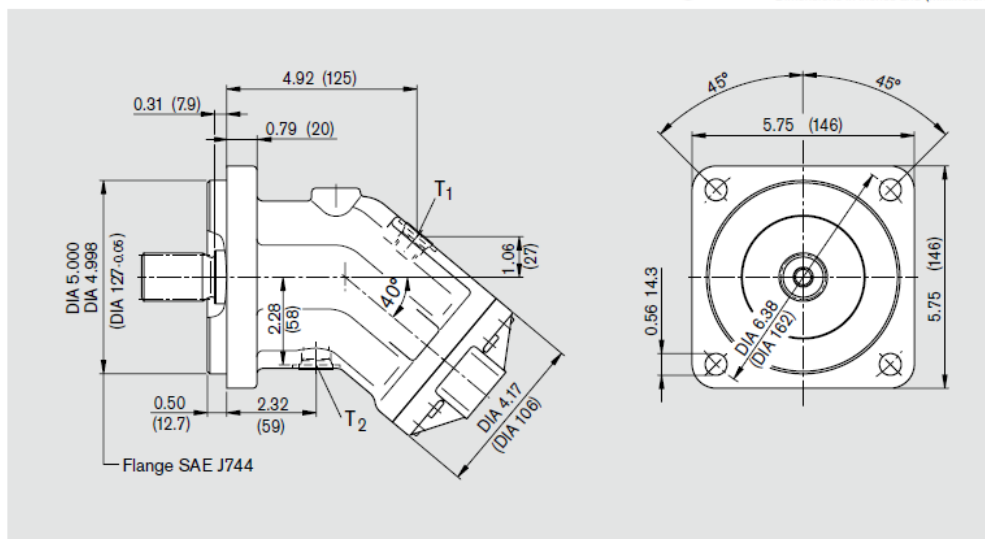
By selecting a suitable force-transfer direction of F_q , the stress on the bearings caused by the internal transmission forces can be reduced, thus achieving the optimum service life for the bearings. Recommended position of mating gear is dependent on direction of rotation. Examples:

Size	Toothed gear drive	V-belt drive
10 to 180	$\pm 70^\circ$	$\pm 45^\circ$
200 to 1000	$\pm 45^\circ$	$\pm 70^\circ$



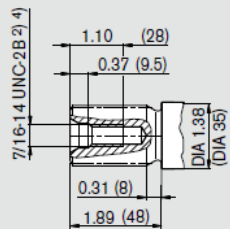
Unit Dimensions, Sizes 23, 28, 32 – SAE Design

Before finalizing your design, please request a binding installation drawing.
Dimensions in inches and (millimeters)

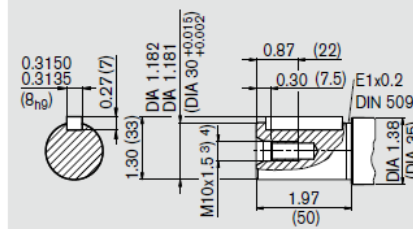


Shaft ends

S Splined shaft 1 1/4 in 14T 12/24 DP¹
(SAE J744 – 32-4 (C))
 $p_N = 5800 \text{ psi}$ (400 bar)



B Parallel keyed shaft
DIN 6885 – AS8x7x40 (mm)
 $p_N = 5100 \text{ psi}$ (350 bar)



Ports

A, B Service line ports (see port plates)

T₁, T₂ Case drain ports (T₂ plugged) ISO 11926 3/4 in -16 UNF-2B; 0.59 (15) deep 120 lb-ft (160 Nm)⁴

¹) ANSI B92.1a-1976, 30° pressure angle, flat root, side fit, tolerance class 5

²) Thread according to ISO 68

³) Center bore according to DIN 332 (thread according to DIN 13)

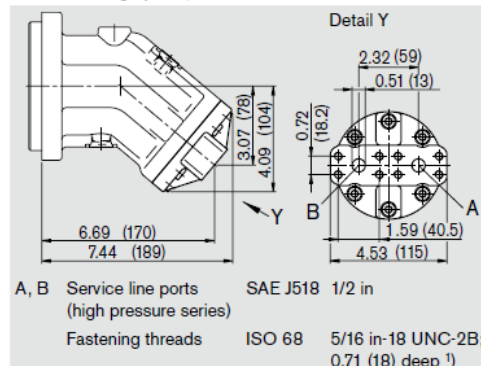
⁴) Please observe the general notes for the max. tightening torques on page 36

Unit Dimensions, Sizes 23, 28, 32 – SAE Design

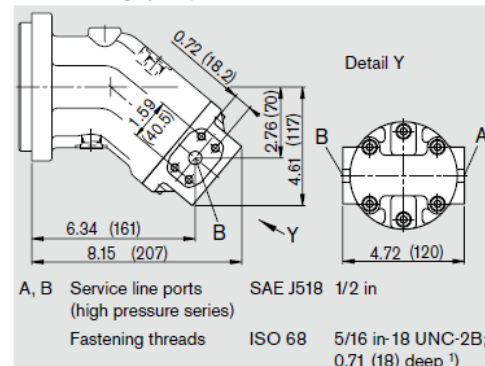
Port plates

Before finalizing your design, please request a binding installation drawing.
Dimensions in inches and (millimeters)

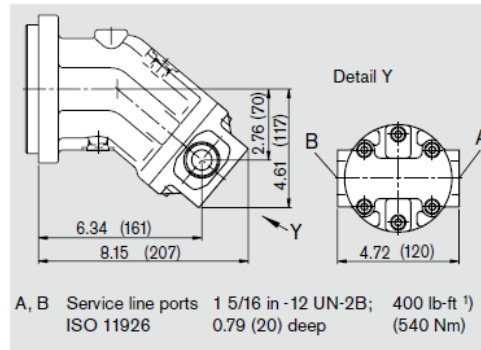
51 SAE flange ports, rear



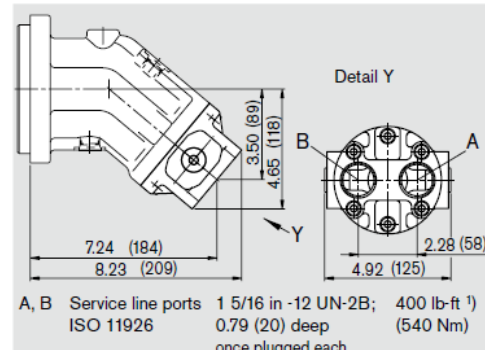
52 SAE flange ports, at side



53 Threaded ports, at side



54 Threaded ports, at side and rear



1) Please observe the general notes for the max. tightening torques on page 36

Note: port plates 18 and 19 see pages 31, 32

C.7 Parker, Overcenter valve

**Catalog HY15-3502/US
Technical Information**

CV
Check Valves

SH
Shuttle Valves

LM
Load/Motion Controls

FC
Flow Controls

PC
Pressure Controls

LE
Elements Logic

DC
Directional Controls

MV
Manual Valves

SV
Solenoid Valves

PV
Proportional Valves

CE
Electronics

BC
Bodies & Cavities

TD
Technical Data

General Description
Body Style Counterbalance Valve. For additional information see Technical Tips on pages LM1-LM4.

Features

- Conical Poppet design provides longer metering stroke for stable operation
- Hardened seat provides reliable load holding
- External vent option available for high back pressure applications
- Tamper resistant cap for added safety and security
- Various pilot ratios available for application flexibility

Specifications

Rated Flow	46.25 LPM (15 GPM)
Maximum Inlet Pressure	210 Bar (3000 PSI)
Leakage at 150 SSU (32 cSt)	5 drops/min. (.33 cc/min.) @ 80% of thermal crack pressure
Valve Material	All parts steel. All operating parts hardened steel.
Body Material	Aluminum
Operating Temp. Range/Seals	-31.7°C to +121.1°C (Fluorocarbon) (-25°F to +250°F)
Fluid Compatibility/ Viscosity	Mineral-based or synthetic with lubricating properties at viscosities of 45 to 2000 SSU (6 to 420 cSt)
Filtration	ISO Code 16/13, SAE Class 4 or better
Approx. Weight	Single 0.68 kg (1.5 lbs.) Double 1.36 kg (3.0 lbs.)

Counterbalance Valve Series MHB-015

Performance Curve
Flow vs. Pressure Drop (Through cartridge only)

Hydraulic Oil 150 SSU @ 100°F (32 cSt)

Flow (GPM)	Controlled Flow 6:1 (PSI)	Controlled Flow 6:1 (Bar)	Free Flow (PSI)	Free Flow (Bar)
0	0	0	0	0
15	~150	~10.5	~150	~10.5
30	~300	~21	~300	~21
45	~450	~31.5	~450	~31.5
60	~600	~42	~600	~42
75	~750	~52.5	~750	~52.5
83	~830	~60.5	~830	~60.5

Ordering Information

MHB — 015 — — — — —

Counterbalance Parts In Body	Nominal Flow Rating	Vent Setting	Pilot Ratio	Body Style	Holding Pressure	Porting	Pilot Port
------------------------------	---------------------	--------------	-------------	------------	------------------	---------	------------

Code	Nominal Flow Rating
015	46.3 LPM (15 GPM)

Code	Pilot Ratio
*A	1:1 Equal Area
B	3:1
E	6:1
J	10:1

Code	Body Style
A / Single Inline	D / Double Inline
B / Single Gasket	E / Double Gasket

Code	Porting
51	SAE-6
52	SAE-8 (Gasket mount only)

Code	Vent Setting
L	Non-Vented
W	Vent

*Equal Area does not have a thermal relief

Code	Holding Pressure
*C	17.2 to 34.5 Bar (250 to 500 PSI) 1:1 Pilot Crack Pressure
E	34.5 to 103.4 Bar (500 to 1500 PSI)
H	105 to 210 Bar (1500 to 3000 PSI)

*Equal Area does not have a thermal relief

Code	Pilot Port
N	Internal Pilot (Dual valve only)
E	SAE-6 (Code 51 & 52 bodies only)

Seal Kits:
Single 711708
Double 711709



LM11

Parker Hannifin Corporation
Hydraulic Cartridge Systems

Catalog HY15-3502/US
Dimensions

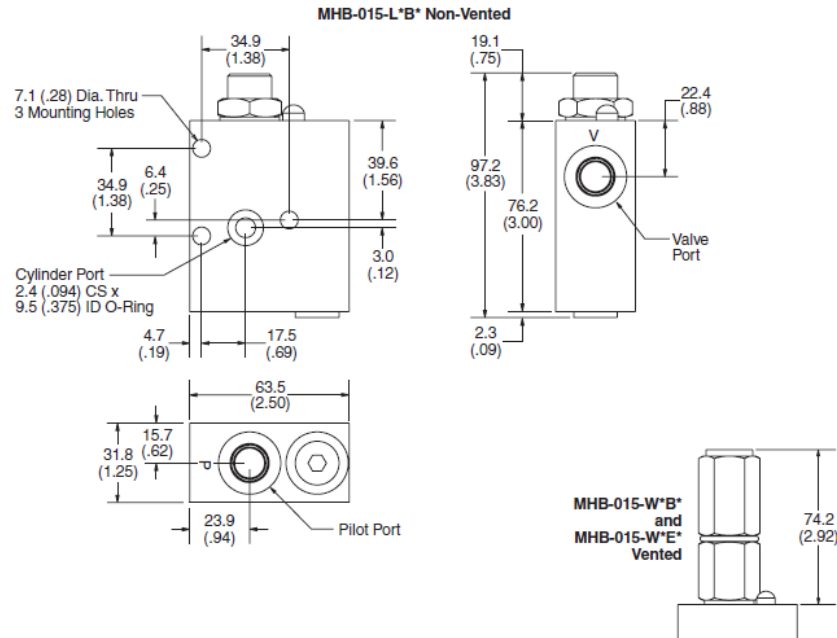
Counterbalance Valve
Series MHB-015

CV	
Check Valves	
SH	
Shuttle Valves	
LM	Load/Motor Controls
FC	Flow Controls
PC	Pressure Controls
LE	Logic Elements
DC	Directional Controls
MV	Manual Valves
SV	Solenoid Valves
PV	Proportional Valves
CE	Electronics
BC	Bodies & Cartridges
TD	Technical Data

*Inch equivalents for millimeter dimensions are shown in (**)

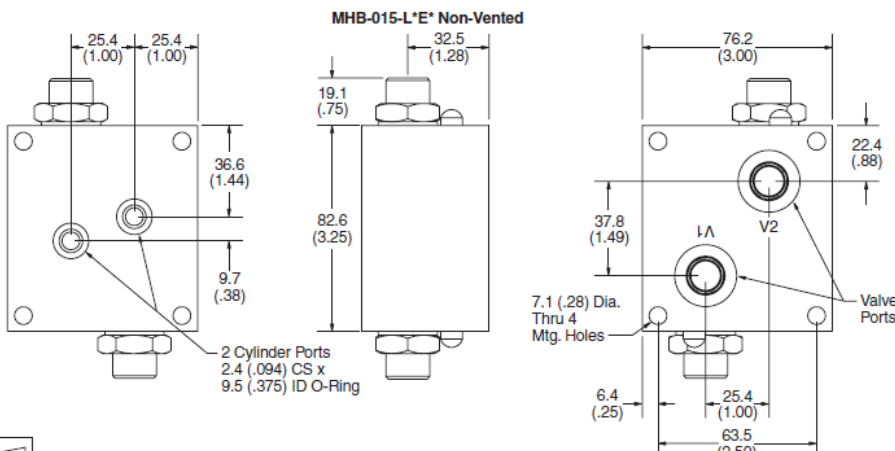
Series MHB-015-L*B* Single Counterbalance, Non-Vented, Gasket Mount

Series MHB-015-W*B* Single Counterbalance, Vented, Gasket Mount



Series MHB-015-L*E* Dual Counterbalance, Non-Vented, Gasket Mount

Series MHB-015-W*E* Dual Counterbalance, Vented, Gasket Mount



LM13

Parker Hannifin Corporation
Hydraulic Cartridge Systems

C.8 Sauer Danfoss, Proportional valve PVG 32

Proportional Valve PVG 32						PVG No. 11021079		
SAUER DANFOSS Specification						SAP: Subsidiary/Dealer Sauer-Danfoss AS		
Customer Aker Kværner MH AS			Application 100682, BC381, Spinner					
Function			A-Port			B-Port		
Inlet	▽		▽		▽			
	a 157B _____		0 157B 2014	157B _____	c 157B _____			
Motor	b 157B _____		1 157B 5937	157B _____	b 157B _____	b 157B _____		
	a 157B 4853Em		2 157B 6233	157B 9784	13 157B 3184	c 157B 3184		
Clamp A front	b 157B 2001		LS_A ____ bar	LS_B ____ bar	157B 2001	b 157B 2001		
	a 157B 4853Em		3 157B 6203	157B 9784	13 157B 3184	c 157B 3184		
Clamp B back	b 157B _____		LS_A ** bar	LS_B ** bar	157B _____	b 157B _____		
	a 157B 4853Em		4 157B 6203	157B 9783	13 157B 3184	c 157B 3184		
Clamp back C	b 157B _____		LS_A ** bar	LS_B ** bar	157B _____	b 157B _____		
	a 157B 4853Em		5 157B 6203	157B 9783	13 157B 3184	c 157B 3184		
Elevation	b 157B _____		LS_A ** bar	LS_B ** bar	157B _____	b 157B _____		
	a 157B 4853Em		6 157B 6203	157B 9781	13 157B 3184	c 157B 3184		
Rotameter	b 157B 2032		LS_A ** bar	LS_B ** bar	157B 2001	b 157B 2001		
	a 157B _____		7 157B 6233	157B 7025	13 157B 3184	c 157B 3184		
	b 157B _____		LS_A ** bar	LS_B ** bar	157B _____	c 157B _____		
	a 157B _____		8 157B _____	157B _____	13 157B _____	c 157B _____		
	b 157B _____		LS_A ____ bar	LS_B ____ bar	157B _____	b 157B _____		
	a 157B _____		9 157B _____	157B _____	13 157B _____	c 157B _____		
	b 157B _____		LS_A ____ bar	LS_B ____ bar	157B _____	b 157B _____		
	a 157B _____		10 157B _____	157B _____	13 157B _____	c 157B _____		
Marinisert og tectylert			11 157B 2014			=159U6549.09		
** LS setting ref flowdiagram (MH intern)			12 157B 8026			_____		
Filled in by EAU						Date 22.11.2006		



PVG 32 Proportional Valve Group
Technical Information
Module Selection Chart

Standard FC Spools

To be used when PVB is with LS _{A/B} shuttle valve							Code number 157B....		To be used when PVB is without LS _{A/B} shuttle valve								
Size									Size								
Press. compensated flow l/min [US gal/min]							ISO symbol	Symbol	Press. compensated flow l/min [US gal/min]								
F 130 [34.3]	E 100 [26.4]	D 65 [17.2]	C 40 [10.6]	B 25 [6.6]	A 10 [2.6]	AA 5 [1.3]			AA 5 [1.3]	A 10 [2.6]	B 25 [6.6]	C 40 [10.6]	D 65 [17.2]	E 100 [26.4]	F 130 [34.3]		
7026	7024	7023	7022	7021	7020	7025			157-02,10 4-way, 3-position Closed neutral position	157-26,10	7005	7000	7001	7002	7003	7004	7006
7126	7124	7123	7122	7121	7120	7125			157-03,10 4-way, 3-position Throttled, open neutral position	157-27,10	7105	7100	7101	7102	7103	7104	7106
-	-	-	-	-	-	-			157-04,10 3-way, 3-position Closed neutral position, P → A	157-28,10	-	7200	7201	7202	7203	7204	-
-	-	-	-	-	-	-			157-05,10 3-way, 3-position Closed neutral position, P → B	157-29,10	-	-	7301	7302	7303	7304	-



PVG 32 Proportional Valve Group
Technical Information
Module Selection Chart

FC Spools with Linear Flow Characteristic

To be used when PVB is with LS _{A/B} shuttle valve							Code number 157B....		To be used when PVB is without LS _{A/B} shuttle valve								
Size									Size								
Press. compensated flow l/min [US gal/min]							ISO symbol	Symbol	Press. compensated flow l/min [US gal/min]								
F 130 [34.3]	E 100 [26.4]	D 65 [17.2]	C 40 [10.6]	B 25 [6.6]	A 10 [2.6]	AA 5 [1.3]			AA 5 [1.3]	A 10 [2.6]	B 25 [6.6]	C 40 [10.6]	D 65 [17.2]	E 100 [26.4]	F 130 [34.3]		
-	9774	9773	9772	9771	-	-			157-02,10	157-26,10	-	9750	9751	9752	9753	9754	-
-	9784	9783	9782	9781	-	-			157-03,10	157-27,10	-	9760	9761	9762	9763	9764	-
-	-	-	-	-	-	-			157-06,10	157-30,10	-	-	-	-	-	9794	-
-	-	-	-	-	-	-			157-07,10	157-31,10	-	-	-	-	-	9804	-



PVG 32 Proportional Valve Group
Technical Information
Module Selection Chart

PVB, basic valves

Description	No facilities for shock valves A and B		Facilities for shock valves A and B	
	G 1/2	1/8 - 14 UNF	G 1/2	7/8 - 14 UNF
Without compensator /check valve	157B6000	157B6400	157B6030	157B6430
With check valve	157B6100	157B6500	157B6130	157B6530
With check valve and LS _{A/B} shuttle valve	-	-	157B6136	157B6536
With compensator valve	157B6200	157B6600	157B6230	157B6630
With damped compensator valve	157B6206	-	157B6236	-
With compensator valve, LS _{A/B} relief valve and LS _{A/B} shuttle valve	157B6203	157B6603	157B6233	157B6633
With damped compensator valve, LS _{A/B} relief valve and LS _{A/B} shuttle valve	157B6208	-	157B6238	-
Weight kg [lb]	3.1 [6.8]		3.0 [6.6]	

PVPC, plugs

Description	G 1/2	1/2 in - 20	Weight kg [lb]
External pilot supply	157B5400	—	0.05 0.1
External pilot supply incl. check valve	157B5600	157B5700	0.05 0.1

PVM, mechanical actuation

Description	Alu		Alu anodized	Cast iron	Angle
	with stop screws	without stop screws	with stop screws	with stop screws	
Standard	157B3171	157B3191	157B3184	157B3161	22,5°/37,5°
Standard with base, without arm and button	157B3174	157B3194	—	—	22,5°/37,5°
Standard without base, without arm and button	157B3173	157B3193	157B3186	—	—
Weight kg [lb]	0.4 [0.9]		0.8 [1.8]		

PVAS, assembly kit

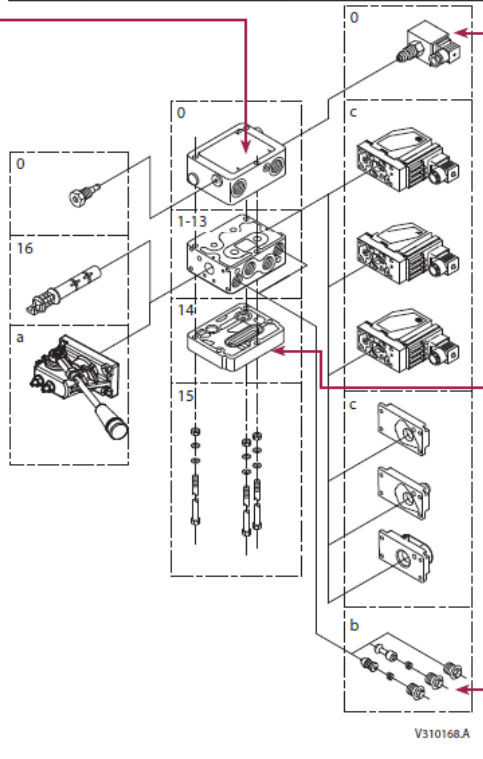
Code no.	0	1	2	3	4	5	6	7	8	9	10	11	12
PVB's	157B8000	157B8001	157B8002	157B8003	157B8004	157B8005	157B8006	157B8007	157B8008	157B8009	157B8010	157B8061	157B8062
PVB + PVPVM	-	157B8021	157B8022	157B8023	157B8024	157B8025	157B8026	157B8027	157B8028	157B8029	157B8030	157B8081	157B8082
Weight kg [lb]	0.1[0.2]	0.15[0.3]	0.25[0.6]	0.30[0.7]	0.40[0.9]	0.45[1.0]	0.50[1.1]	0.60[1.3]	0.65[1.4]	0.70[1.6]	0.80[1.7]	0.85[1.8]	0.9[2.0]



PVG 32 Proportional Valve Group
Technical Information
Module Selection Chart

PVP, pump side module

Description		Without pilot supply		With pilot supply			
		for PVE	for PVE with facilit. for PVPX	for PVE	for PVE and facilit. for PVPX	for PVE and pilot oil pressure take-off	for PVH and pilot oil pressure take-off
Open center	$P = G\frac{1}{2}, T = G\frac{3}{4}$	157B5000	-	157B5010	157B5012	-	-
	$P = \frac{7}{8} - 14, T = 1\frac{1}{16} - 12$	157B5200	-	157B5210	157B5212	-	-
	$P = G\frac{3}{4}, T = G\frac{3}{4}$	157B5100	157B5102	157B5110	157B5112	157B5180	157B5190
Closed center	$P = 1\frac{1}{16} - 12, T = 1\frac{1}{16} - 12$	157B5300	-	157B5310	157B5312	157B5380	157B5390
	$P = G\frac{1}{2}, T = G\frac{3}{4}$	157B5001	-	157B5011	157B5013	-	-
	$P = \frac{7}{8} - 14, T = 1\frac{1}{16} - 12$	157B5201	-	157B5211	157B5213	-	-
Weight	$P = G\frac{3}{4}, T = G\frac{3}{4}$	157B5101	157B5103	157B5111	157B5113	157B5181	157B5191
	$P = 1\frac{1}{16} - 12, T = 1\frac{1}{16} - 12$	157B5301	-	157B5311	157B5313	157B5381	157B5391
Weight		3 [6.6]					



PVPX, electrical LS pressure relief valves

Description/ Supply voltage	Code No. Hirsch.	Code No. AMP	Weight kg [lb]
Normally open	12 V	157B4236	157B4981
	24 V	157B4238	157B4982
	12 V	157B4246	157B4983
	24 V	157B4248	157B4984
	12 V	157B4256	157B4985
Normally open with manual override	24 V	157B4258	157B4986
Plug			0.06 [.13]

PVS and PVSI, End plate

Description	BSP	SAE	Weight kg [lb]
PVS, without connections	157B2000	157B2020	0.5 [1.1]
PVS, with LX connection G 1/8 [3/8-24 UNF]	157B2011	157B2021	
PVSI, without connections	157B2014	157B2004	1.7 [3.6]
PVSI, with LX connections G 1/4 [1/2-20 UNF]	157B2015	157B2005	

PVLP, shock/ and anti-cavitation valves

Code no.	157B2032	157B2050	157B2063	157B2080	157B2100	157B2125	157B2140	157B2150	157B2160	157B2175	157B2190	
Settings	bar [psi]	32 460	50 725	63 914	80 1160	100 1450	125 1813	140 2031	150 2175	160 2320	175 2538	190 2755
Weight for all											0.05 kg [0.17 lb]	
Code no.	157B2210	157B2230	157B2240	157B2250	157B2265	157B2280	157B2300	157B2320	157B2350	157B2380	157B2400	
Settings	bar [psi]	210 3045	230 3335	240 3480	250 3625	265 3845	280 4061	300 4351	320 4641	350 5075	380 5511	400 5801



PVG 32 Proportional Valve Group
Technical Information
Module Selection Chart

PVE, electrical actuation

Description	Code No.			Weight kg [lb]
	Hirsch	AMP	Deut.	
PVEO, on-off 12 V	157B4216	157B4901	157B4291	0.6 [1.3]
24 V	157B4228	157B4902	157B4292	
PVEO-R, on/off 12 V	157B4217	157B4903	-	
24 V	157B4229	157B4904	-	
PVEM, prop. medium – Standard 12 V	157B4116	-	-	0.9 [2.0]
24 V	157B4128	-	-	
PVEM, prop. medium – Float -> B 12 V	157B4416	-	-	1.0 [2.2]
24 V	157B4428	-	-	
PVEA, active fault mon.	-	157B4734	157B4792	
PVEA, passive fault mon.	-	157B4735	-	
PVEA-DI, active fault mon.	-	157B4736	157B4796	0.9 [2.0]
PVEA-DI, passive fault mon.	-	157B4737	-	
PVEH active fault mon. 157B4032	157B4034	157B4092		
PVEH passive fault mon. 157B4033	157B4035	157B4093		
PVEH float -> B, act. fault 157B4332	-	157B4392	1.0 [2.2]	
PVEH float -> A, act. fault	-	157B4338		
PVEH- DI active fault mon. 157B4036	157B4096			
PVEH - DI passive fault mon. 157B4037	-			
PVES, active fault mon. 157B4832	157B4834	157B4892		
PVES, passive fault mon. 157B4833	157B4835	-		

PVMD, PVMR, PVMF, PVH covers

Description	Code No.	Material	Anodized	Weight kg [lb]
PVMD Cover for PVB	157B0001 157B0009 157B0021	aluminium yes cast iron	no yes N/A	0.1 [0.2] 0.9 [2.0]
PVMR (Frict. Detent)	157B0004 157B0012 157B0024	aluminium yes cast iron	no yes N/A	0.3 [0.6]
PVMF (Mech. float position)	157B0005	aluminium	no	
Hydraulic actuation PVH 9/16-18 UNF	157B0007 157B0010 157B0014	aluminium yes cast iron	no yes N/A	0.2 [0.4]
Hydraulic actuation PVH G1/4	157B0008 157B0011 157B0016	aluminium yes cast iron	no yes N/A	

PVLA, anti-cavitation valve

Description	Code No.	Weight	
		kg	[lb]
Plug A or B	157B2002	0.04	0.09
Valve A or B	157B2001	0.05	0.1

C.9 Sauer Danfoss, PVG 32, Electrical actuators



3. Spesifikasjon

3. Specifications

PVE 32 Reaksjonstid (21 mm²/s)

PVE 32 reaction time (21 mm²/s)

Voltage	Spennin	Function	Funksjon	PVEO ON/OFF s	PVEH Prop. high s	PVES Prop. super s
Neutral switch	Nøytral bryter	Reaction time from neutral position to max. spool travel	Reaksjonstid fra nøytral posisjon til maks sleide utstyring	Max.	0,235	0,230
				Rated	0,180	0,150
				Min.	0,120	0,120
Neutral switch	Nøytral bryter	Reaction time from max. spool travel to neutral position	Reaksjonstid fra maks utstyrt sleide tilbake til nøytral	Max.	0,175	0,175
				Rated	0,090	0,090
				Min.	0,065	0,065
Constant voltage	Konstant spenning	Reaction time from neutral position to max. spool travel	Reaksjonstid fra nøytral posisjon til maks sleide utstyring	Max.	-	0,200
				Rated	-	0,120
				Min.	-	0,050
Constant voltage	Konstant Spenning	Reaction time from max. spool travel to neutral position	Reaksjonstid fra maks utstyrt sleide tilbake til nøytral	Max.	-	0,100
				Rated	-	0,090
				Min.	-	0,065

PVE 32 Oljeforbruk og hysterese

PVE 32 Oil consumption and hysteresis

Voltage	Spennin	Function	Funksjon	PVEO ON/OFF l/min	PVEH Prop. high l/min	PVES Prop. super l/min
Without voltage	Uten spenning	Pilot oil flow per PVE	Pilot olje flow per PVE (l/min)	Neutral	0,0	0,0
With voltage	Med spenning	Pilot oil flow per PVE	Pilot olje flow per PVE (l) (l/min)	Locked	0,1	0,1
				1actu.	0,002	0,002
				actu.s	0,7	1,1
		Hysteresis ¹⁾	Hysterese ¹⁾	Rated	-	<1%

¹⁾ Hysteresis is indicated at rated voltage and f=0,02 Hz fore one cycle. A cycle incl. N>full A>N>full B>N.

¹⁾ Hysteresen er oppgitt ved rated spenning og f=0,02 Hz for en syklus. En syklus inkl. N>full A>N>full B>N.

PVE 32 Elektrisk aktivering

PVE 32 Electrical actuation

Actuation Aktivering		PVEO, PVEH, PVES
Grade of enclosure EN 60529		IP 67
Tetthet iht EN 60529		
Ambient temp min		-35 °C
Ambient temp max		60 °C
Rated voltage		24 VDC
Rated spenning		
Supply voltage (UDC)	Voltage range	22-30 VDC
Forsyningsspenning (UDC)	Max. Ripple	5%
Current consumtion at rated voltage		0,33 A
Spenningsforbruk ved rated spenning		
Signal voltage at rated current (PVEH, PVES)	Neutral/Nøytral	0,5 x UDC
Signal spenning ved rated spenning (PVEH, PVES)	Regulating/regulering	0,25 x UDC - 0,75 x UDC
Signal current (PVEH, PVES)		0,5 mA
Signal strøm (PVEH, PVES)		
Input impedance in relation 0,5 x UDC		12kΩ
Ingangsimpedans i relasjon til 0,5 x UDC		
Power consumption		8W
Effekt forbruk		
Fault monitoring (PVEH, PVES)	Max load	60 mA
Feilovervåking (PVEH, PVES)	Reaction time at fault	250 ms

**6. Elektrisk tilslutning****6. Electrical connection**

Aktiveringene leveres standard med 5 meter 2x2x0,5mm² Skipskabel
 Alternativt kan aktiveringene leveres med 5 meter BFOU MUD 1x3x0,75mm² kabel.

As standard the actuators are delivered with 5 meter 2x2x0,5mm² Ship cable.
 As option the actuation can be delivered with 5 meter BFOU MUD 1x3x0,75mm² cable.

Standard kabel -- Standard cable				
Type	Leder nr.	Wire nr	Funksjon	Function
PVEO on/off	1	1	+24VDC signal/A-port	+24VDC signal/A-port
	2	2	+24VDC signal/B-port	+24VDC signal/B-port
	3	3	Ikke i bruk	Not used
	4 grønn/gul	4 green/yellow	0VDC forsyningsspenning	0VDC supply voltage

Type	Leder nr.	Wire nr	Funksjon	Function
PVEH PVES prop.	1	1	+24VDC forsyningsspenning	+24VDC supply voltage
	2	2	Us styre spenning	Us signal voltage
	3	3	Feil indikering	Fault indication
	4 grønn/gul	4 green/yellow	0VDC forsyningsspenning	0VDC supply voltage

Alternativ BFOU kabel -- Option BFOU cable				
Type	Leder farge	Wire color	Funksjon	Function
PVEO on/off	Blå	Blue	+24VDC signal/A-port	+24VDC signal/A-port
	Sort	Black	+24VDC signal/B-port	+24VDC signal/B-port
	Brun	Brown	0VDC forsyningsspenning	0VDC supply voltage
PVEH PVES prop.	Blå	Blue	+24VDC forsyningsspenning	+24VDC supply voltage
	Sort	Black	Us styre spenning	Us signal voltage
	Brun	Brown	0VDC forsyningsspenning	0VDC supply voltage

Spesiell Ex- beskyttelseshenvisninger: Utstyret må ha en forankoblet sikring med verdi In=0,5A. Sikringen må ha bryteevne på minst 1500A .

Special Ex protection instructions: The equipment must be connected to an external fuse with a value of In=0,5A. The fuse must have a breaking capacity of at least 1500A.

NI USB-621x Specifications

Specifications listed below are typical at 25 °C unless otherwise noted. Refer to the *NI USB-621x User Manual* for more information about USB-621x devices.



Caution The input/output ports of this device are not protected for electromagnetic interference due to functional reasons. As a result, this device may experience reduced measurement accuracy or other temporary performance degradation when connected cables are routed in an environment with radiated or conducted radio frequency electromagnetic interference.

To ensure that this device functions within specifications in its operational electromagnetic environment and to limit radiated emissions, care should be taken in the selection, design, and installation of measurement probes and cables.

Français	Deutsch	日本語	한국어	简体中文
ni.com/manuals				

Analog Input

Number of channels		Input range.....	±10 V, ±5 V, ±1 V, ±0.2 V
USB-6210/6211/6212/ 6215/6216.....	8 differential or 16 single ended	Maximum working voltage for analog inputs (signal + common mode).....	±10.4 V of AI GND
USB-6218.....	16 differential or 32 single ended	CMRR (DC to 60 Hz)	100 dB
ADC resolution	16 bits	Input impedance	
DNL	No missing codes guaranteed	Device on	
INL.....	Refer to the <i>AI Absolute Accuracy Tables</i>	AI+ to AI GND	>10 GΩ in parallel with 100 pF
Sampling rate		AI- to AI GND.....	>10 GΩ in parallel with 100 pF
Maximum		Device off	
USB-6210/6211/6215/6218 ...	250 kS/s single channel, 250 kS/s multichannel (aggregate)	AI+ to AI GND	1200 Ω
USB-6212/6216	400 kS/s single channel, 400 kS/s multichannel (aggregate)	AI- to AI GND	1200 Ω
Minimum	0 S/s	Input bias current.....	±100 pA
Timing accuracy	50 ppm of sample rate	Crosstalk (at 100 kHz)	
Timing resolution	50 ns	Adjacent channels	-75 dB
Input coupling.....	DC	Non-adjacent channels	-90 dB
		Small signal bandwidth (-3 dB)	
		USB-6210/6211/6215/6218	450 kHz
		USB-6212/6216	1.5 MHz



Input FIFO size.....	4,095 samples
Scan list memory	4,095 entries
Data transfers.....	USB Signal Stream, programmed I/O
Overtoltage protection (AI <0..31>, AI SENSE)	
Device on	±30 V for up to two AI pins
Device off	±20 V for up to two AI pins
Input current during overtoltage condition	±20 mA max/AI pin

Settling Time for Multichannel Measurements

Accuracy, full scale step, all ranges

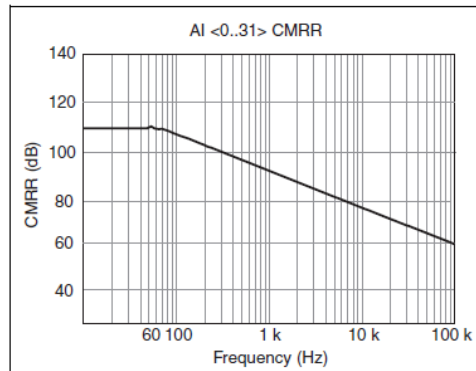
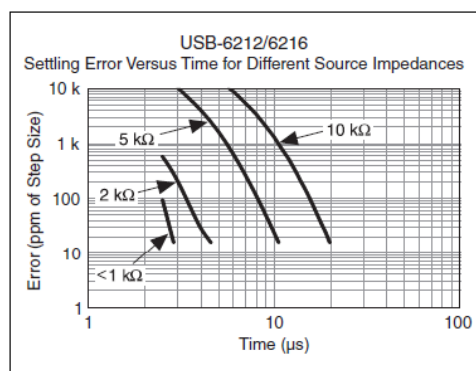
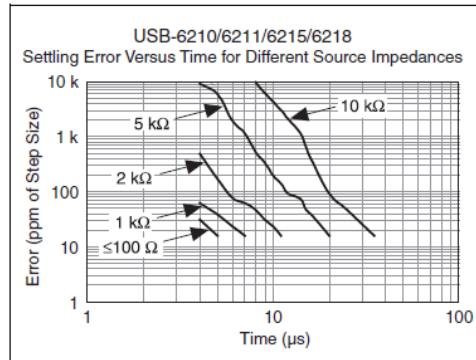
USB-6210/6211/6215/6218

- ±90 ppm of step (±6 LSB).....4 µs convert interval
- ±30 ppm of step (±2 LSB).....5 µs convert interval
- ±15 ppm of step (±1 LSB).....7 µs convert interval

USB-6212/6216

- ±90 ppm of step (±6 LSB).....2.5 µs convert interval
- ±30 ppm of step (±2 LSB).....3.5 µs convert interval
- ±15 ppm of step (±1 LSB).....5.5 µs convert interval

Typical Performance Graphs



Analog Output

Number of channels

USB-6210..... 0

USB-6211/6212/6215/

6216/6218..... 2

DAC resolution..... 16 bits

DNL ±1 LSB

Monotonicity..... 16 bit guaranteed

Maximum update rate

1 channel..... 250 kS/s

2 channels..... 250 kS/s per channel

Timing accuracy 50 ppm of sample rate

Timing resolution..... 50 ns

Output range ±10 V

Output coupling DC

Output impedance 0.2 Ω

Output current drive..... ±2 mA

Overdrive protection ±30 V

Overdrive current..... 2.4 mA

Power-on state..... ±20 mV

Power-on glitch..... ±1 V for 200 ms

Output FIFO size 8,191 samples shared
among channels used

Data transfers USB Signal Stream,
programmed I/O

AO waveform modes:

- Non-periodic waveform
- Periodic waveform regeneration mode from onboard FIFO
- Periodic waveform regeneration from host buffer including dynamic update

Settling time, full scale step

15 ppm (1 LSB) 32 μs

Slew rate 5 V/μs

Glitch energy

Magnitude..... 100 mV

Duration..... 2.6 μs

Calibration (AI and AO)

Recommended warm-up time 15 minutes

Calibration interval 1 year

Bachelor project MAS302

AI Absolute Accuracy Table (USB-6210/6211/6215/6218)

Nominal Range		Residual Gain Error (ppm of Reading)	Gain Tempo (ppm/°C)	Reference Tempo	Residual Offset Error (ppm of Range)	Offset Tempo (ppm of Range/°C)	INL Error (ppm of Range)	Random Noise, σ (µVRms)	Absolute Accuracy at Full Scale ¹ (µV)	Sensitivity ² (µV)
Positive Full Scale	Negative Full Scale									
10	-10	75	7.3	5	20	34	76	229	2,690	91.6
5	-5	85	7.3	5	20	36	76	118	1,410	47.2
1	-1	95	7.3	5	25	49	76	26	310	10.4
0.2	-0.2	135	7.3	5	40	116	76	12	88	4.8
AbsoluteAccuracy = Reading · (GainError) + Range · (OffsetError) + NoiseUncertainty GainError = ResidualAIGainError + GainTempco · (TempChangeFromLastInternalCal) + ReferenceTempco · (TempChangeFromLastExternalCal) OffsetError = ResidualAIOffsetError + OffsetTempco · (TempChangeFromLastInternalCal) + INL_Error $\text{NoiseUncertainty} = \frac{\text{RandomNoise} \cdot 3}{\sqrt{100}}$ For a coverage factor of 3 σ and averaging 100 points.										
¹ Absolute accuracy at full scale on the analog input channels is determined using the following assumptions: TempChangeFromLastExternalCal = 10 °C TempChangeFromLastInternalCal = 1 °C number_of_readings = 100 CoverageFactor = 3 σ For example, on the 10 V range, the absolute accuracy at full scale is as follows: $\text{GainError} = 75 \text{ ppm} + 7.3 \text{ ppm} \cdot 1 + 5 \text{ ppm} \cdot 10 \quad \text{GainError} = 132 \text{ ppm}$ $\text{OffsetError} = 20 \text{ ppm} + 34 \text{ ppm} \cdot 1 + 76 \text{ ppm} \quad \text{OffsetError} = 130 \text{ ppm}$ $\text{NoiseUncertainty} = \frac{229 \mu\text{V} \cdot 3}{\sqrt{100}} \quad \text{NoiseUncertainty} = 68.7 \mu\text{V}$ $\text{AbsoluteAccuracy} = 10 \text{ V} \cdot (\text{GainError}) + 10 \text{ V} \cdot (\text{OffsetError}) + \text{NoiseUncertainty} \quad \text{AbsoluteAccuracy} = 2,690 \mu\text{V}$ ² Sensitivity is the smallest voltage change that can be detected. It is a function of noise. Accuracies listed are valid for up to one year from the device external calibration.										

AI Absolute Accuracy Table (USB-6212/6216)

Nominal Range		Residual Gain Error (ppm of Reading)	Gain Tempo (ppm/°C)	Reference Tempo	Residual Offset Error (ppm of Range)	Offset Tempo (ppm of Range/°C)	INL Error (ppm of Range)	Random Noise, σ (µVRms)	Absolute Accuracy at Full Scale ¹ (µV)	Sensitivity ² (µV)
Positive Full Scale	Negative Full Scale									
10	-10	75	7.3	5	20	34	76	295	2,710	118.0
5	-5	85	7.3	5	20	36	76	149	1,420	59.6
1	-1	95	7.3	5	25	49	76	32	310	12.8
0.2	-0.2	135	7.3	5	40	116	76	13	89	5.2
AbsoluteAccuracy = Reading · (GainError) + Range · (OffsetError) + NoiseUncertainty GainError = ResidualAIGainError + GainTempco · (TempChangeFromLastInternalCal) + ReferenceTempco · (TempChangeFromLastExternalCal) OffsetError = ResidualAIOffsetError + OffsetTempco · (TempChangeFromLastInternalCal) + INL_Error $\text{NoiseUncertainty} = \frac{\text{RandomNoise} \cdot 3}{\sqrt{100}}$ For a coverage factor of 3 σ and averaging 100 points.										
¹ Absolute accuracy at full scale on the analog input channels is determined using the following assumptions: TempChangeFromLastExternalCal = 10 °C TempChangeFromLastInternalCal = 1 °C number_of_readings = 100 CoverageFactor = 3 σ For example, on the 10 V range, the absolute accuracy at full scale is as follows: $\text{GainError} = 75 \text{ ppm} + 7.3 \text{ ppm} \cdot 1 + 5 \text{ ppm} \cdot 10 \quad \text{GainError} = 132 \text{ ppm}$ $\text{OffsetError} = 20 \text{ ppm} + 34 \text{ ppm} \cdot 1 + 76 \text{ ppm} \quad \text{OffsetError} = 130 \text{ ppm}$ $\text{NoiseUncertainty} = \frac{295 \mu\text{V} \cdot 3}{\sqrt{100}} \quad \text{NoiseUncertainty} = 88.5 \mu\text{V}$ $\text{AbsoluteAccuracy} = 10 \text{ V} \cdot (\text{GainError}) + 10 \text{ V} \cdot (\text{OffsetError}) + \text{NoiseUncertainty} \quad \text{AbsoluteAccuracy} = 2,710 \mu\text{V}$ ² Sensitivity is the smallest voltage change that can be detected. It is a function of noise. Accuracies listed are valid for up to one year from the device external calibration.										

AO Absolute Accuracy Table

Nominal Range		Residual Gain Error (ppm of Reading)	Gain Tempco (ppm/°C)	Reference Tempco	Residual Offset Error (ppm of Range)	Offset Tempco (ppm of Range/°C)	INL_Error (ppm of Range)	Absolute Accuracy at Full Scale ¹ (µV)
Positive Full Scale	Negative Full Scale							
10	-10	90	11	5	60	12	128	3,512

¹ Absolute Accuracy at full scale numbers is valid immediately following internal calibration and assumes the device is operating within 10 °C of the last external calibration. Accuracies listed are valid for up to one year from the device external calibration.

AbsoluteAccuracy = OutputValue · (GainError) + Range · (OffsetError)
GainError = ResidualGainError + GainTempco · (TempChangeFromLastInternalCal) + ReferenceTempco · (TempChangeFromLastExternalCal)
OffsetError = ResidualOffsetError + AOOOffsetTempco · (TempChangeFromLastInternalCal) + INL_Error

Digital I/O/PFI

Static Characteristics

Number of channels

Digital input

- USB-6210/6211/6215 4 (PFI <0..3>/P0.<0..3>)
- USB-6218 8 (PFI <0..3>/P0.<0..3>, PFI <8..11>/P0.<4..7>)

Digital output

- USB-6210/6211/6215 4 (PFI <4..7>/P1.<0..3>)
- USB-6218 8 (PFI <4..7>/P1.<0..3>, PFI <12..15>/P1.<4..7>)

Digital input or output

- USB-6212/6216
- Screw Terminal 32 total, 16 (P0.<0..15>), 16 (PFI <0..7>/P1.<0..7>, PFI <8..15>/P2.<0..7>)

USB-6212/6216

- Mass Termination/BNC 24 total, 8 (P0.<0..7>), 16 (PFI <0..7>/P1.<0..7>, PFI <8..15>/P2.<0..7>)

Ground reference D GND

Pull-down resistor

- USB-6210/6211/6215/6218..... 47 kΩ ±1%
- USB-6212/6216..... 50 kΩ typical, 20 kΩ minimum

Input voltage protection¹ ±20 V on up to 8 pins

PFI Functionality

USB-6210/6211/6215/6218

PFI <0..3>, PFI <8..11>/Port 0

Functionality Static digital input, timing input

Debounce filter settings 125 ns, 6.425 μs, 2.56 ms, disable; high and low transitions; selectable per input

PFI <4..7>, PFI <12..15>/Port 1

Functionality Static digital output, timing output

Timing output sources Many AI, AO, counter timing signals

USB-6212/6216 PFI <0..15>

Functionality Static digital input, static digital output, timing input, timing output

Timing output sources Many AI, AO, counter timing signals

Debounce filter settings 125 ns, 6.425 μs, 2.56 ms, disable; high and low transitions; selectable per input

Maximum Operation Conditions

Level	Min	Max
I _{OL} output low current	—	16 mA
I _{OH} output high current	—	-16 mA

Digital Input Characteristics (USB-6210/6211/6215/6218)

Level	Min	Max
V _{IL} input low voltage	0 V	0.8 V
V _{IH} input high voltage	2 V	5.25 V
I _{IL} input low current (V _{in} = 0 V)	—	-10 μA
I _{IH} input high current (V _{in} = 5 V)	—	120 μA

Digital Input Characteristics (USB-6212/6216)

Level	Min	Max
V _{IL} input low voltage	0 V	0.8 V
V _{IH} input high voltage	2.2 V	5.25 V
I _{IL} input low current (V _{in} = 0 V)	—	-10 μA
I _{IH} input high current (V _{in} = 5 V)	—	250 μA
Positive-going threshold (VT+)	—	2.2 V
Negative-going threshold (VT-)	0.8 V	—
Delta VT hysteresis (VT+ - VT-)	0.2 V	—

Digital Output Characteristics (USB-6210/6211/6215/6218)

Parameter	Voltage Level	Current Level
V _{OL}	0.6 V	6 mA
V _{OH}	2.7 V	-16 mA
	3.8 V	-6 mA

¹ Stresses beyond those listed under *Input voltage protection* may cause permanent damage to the device.

External Digital Triggers

Source	
USB-6210/6211/6215/6218.....	PFI <0..3>, PFI <8..11>
USB-6212/6216.....	PFI <0..15>
Polarity.....	Software-selectable for most signals
Analog input function	Start Trigger, Reference Trigger, Pause Trigger, Sample Clock, Convert Clock, Sample Clock Timebase
Analog output function	Start Trigger, Pause Trigger, Sample Clock, Sample Clock Timebase
Counter/timer functions	Gate, Source, HW_Arm, Aux, A, B, Z, Up_Down,

Bus Interface

USB.....	USB 2.0 Hi-Speed or Full-Speed ¹
USB Signal Stream (USB).....	4, can be used for analog input, analog output, counter/timer 0, counter/timer 1

Power Limits

+5 V terminal as output ²	
Voltage	4.6 to 5.2 V
Current (internally limited)	50 mA max, shared with digital outputs
+5 V terminal as input ²	
Voltage	4.75 to 5.35 V
Current.....	350 mA max, self-resetting fuse
Protection.....	±10 V



Caution Do not exceed 16 mA per DIO pin.

Power Requirements

Input voltage on USB-621x	
USB port.....	4.5 to 5.25 V in configured state
Maximum inrush current.....	500 mA
No load typical current.....	320 mA at 4.5 V
Maximum load	
Typical current.....	400 mA at 4.5 V
Suspend current.....	260 µA, typical

Physical Characteristics

Enclosure dimensions (includes connectors)	
USB-621x Screw Terminal.....	16.9 × 9.4 × 3.1 cm (6.65 × 3.70 × 1.20 in.)
USB-621x Mass Termination	19.3 × 9.4 × 3.1 cm (7.61 × 3.68 × 1.20 in.)
USB-621x BNC	23.5 × 11.2 × 6.4 cm (9.25 × 4.40 × 2.50 in.)

Weight

USB-621x Screw Terminal.....	206 g (7.2 oz)
USB-6212 Mass Termination	227 g (8.0 oz)
USB-6216 Mass Termination	231 g (8.1 oz)
USB-6212/6216/6218 BNC.....	950 g (33.5 oz)
USB-6210 OEM	73 g (2.5 oz)
USB-6212/6216/6218 OEM	76 g (2.6 oz)

I/O connectors

USB-6210/6211/6215	Two 16-position combicon
USB-6212/6216/6218	
Screw Terminal.....	Four 16-position combicon
USB-6212/6216	
Mass Termination	One 68-pin SCSI
USB-6212/6216/6218 BNC	19 BNCs and 26 screw terminals
USB connector	Series B receptacle
Screw terminal wiring	16 to 28 AWG
Torque for screw terminals	0.22–0.25 N · m (2.0–2.2 lb · in.)

¹ If you are using a USB M Series device in Full-Speed mode, device performance will be lower and you will not be able to achieve maximum sampling/update rates.

² USB-621x Screw Terminal/BNC devices have a self-resetting fuse that opens when current exceeds this specification. USB-621x Mass Termination devices have a user-replaceable socketed fuse that opens when current exceeds this specification. Refer to the *NI USB-621x User Manual* for information about fuse replacement.

Environmental

Operating temperature	0 to 45 °C
Storage temperature.....	-20 to 70 °C
Humidity.....	10 to 90% RH, noncondensing
Maximum altitude	2,000 m
Pollution Degree (indoor use only)	2

Maximum Working Voltage¹

USB-6210/6211/6212 Rated Voltage

Channel-to-earth ground.....11 V,
Measurement Category I



Caution Do not use for measurements within Categories II, III, or IV.

USB-6215/6216/6218 Rated Voltage

Channel-to-earth ground²

Continuous	≤60 VDC, Measurement Category I ³
Withstand	≤1000 Vrms, verified by a 5 s dielectric withstand test

Analog channel to AI GND/AO GND
(in Figure 1, $|V_a - V_c|$).....≤11 V,
Measurement Category I³

Digital channel to D GND
(in Figure 1, $V_b - V_c$).....≤5.25 V,
Measurement Category I³



Caution This device is rated for Measurement Category I and the voltage across the isolation barrier is limited to no greater than 30 Vrms/ 60 VDC/42.4 V_{pk} continuous. Do not use for measurements within Categories II, III, or IV.

Figure 1 illustrates the maximum working voltage specifications.

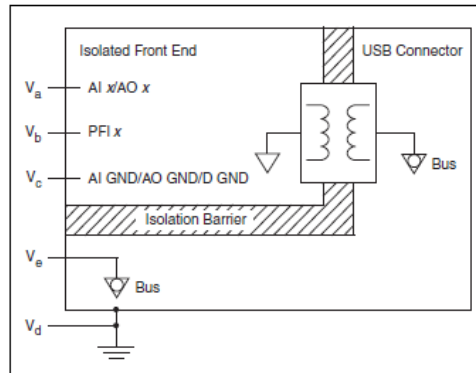


Figure 1. USB-6215/6216/6218 Maximum Working Voltage

Safety

This product meets the requirements of the following standards of safety for electrical equipment for measurement, control, and laboratory use:

- IEC 61010-1, EN 61010-1
- UL 61010-1, CSA 61010-1



Note For UL and other safety certifications, refer to the product label or the [Online Product Certification](#) section.

Electromagnetic Compatibility

This product meets the requirements of the following EMC standards for electrical equipment for measurement, control, and laboratory use:

- EN 61326 (IEC 61326): Class A emissions;
Basic immunity
- EN 55011 (CISPR 11): Group 1, Class A emissions
- AS/NZS CISPR 11: Group 1, Class A emissions
- FCC 47 CFR Part 15B: Class A emissions
- ICES-001: Class A emissions

¹ Maximum working voltage refers to the signal voltage plus the common-mode voltage.

² In Figure 1, $|V_a - V_d|$, $|V_b - V_d|$, and $|V_c - V_d|$.

³ Measurement Category I is for measurements performed on circuits not directly connected to the electrical distribution system referred to as **MAINS** voltage. MAINS is a hazardous live electrical supply system that powers equipment. This category is for measurements of voltages from specially protected secondary circuits. Such voltage measurements include signal levels, special equipment, limited-energy parts of equipment, circuits powered by regulated low-voltage sources, and electronics.



Note For the standards applied to assess the EMC of this product, refer to the *Online Product Certification* section.



Note For EMC compliance, operate this product according to the documentation.



Note For EMC compliance, operate this device with shielded cables.

CE Compliance

This product meets the essential requirements of applicable European Directives as follows:

- 2006/95/EC; Low-Voltage Directive (safety)
- 2004/108/EC; Electromagnetic Compatibility Directive (EMC)

Online Product Certification

Refer to the product Declaration of Conformity (DoC) for additional regulatory compliance information. To obtain product certifications and the DoC for this product, visit ni.com/certification, search by model number or product line, and click the appropriate link in the Certification column.

Environmental Management

NI is committed to designing and manufacturing products in an environmentally responsible manner. NI recognizes that eliminating certain hazardous substances from our products is beneficial to the environment and to NI customers.

For additional environmental information, refer to the *NI and the Environment* Web page at ni.com/environment. This page contains the environmental regulations and directives with which NI complies, as well as other environmental information not included in this document.

Waste Electrical and Electronic Equipment (WEEE)



EU Customers At the end of their life cycle, all products *must* be sent to a WEEE recycling center. For more information about WEEE recycling centers and National Instruments WEEE initiatives, visit ni.com/environment/weee.htm.

电子信息产品污染控制管理办法（中国 RoHS）



中国客户 National Instruments 符合中国电子信息产品中限制使用某些有害物质指令 (RoHS)。关于 National Instruments 中国 RoHS 合规性信息, 请登录 ni.com/environment/rohs_china。
(For information about China RoHS compliance, go to ni.com/environment/rohs_china.)

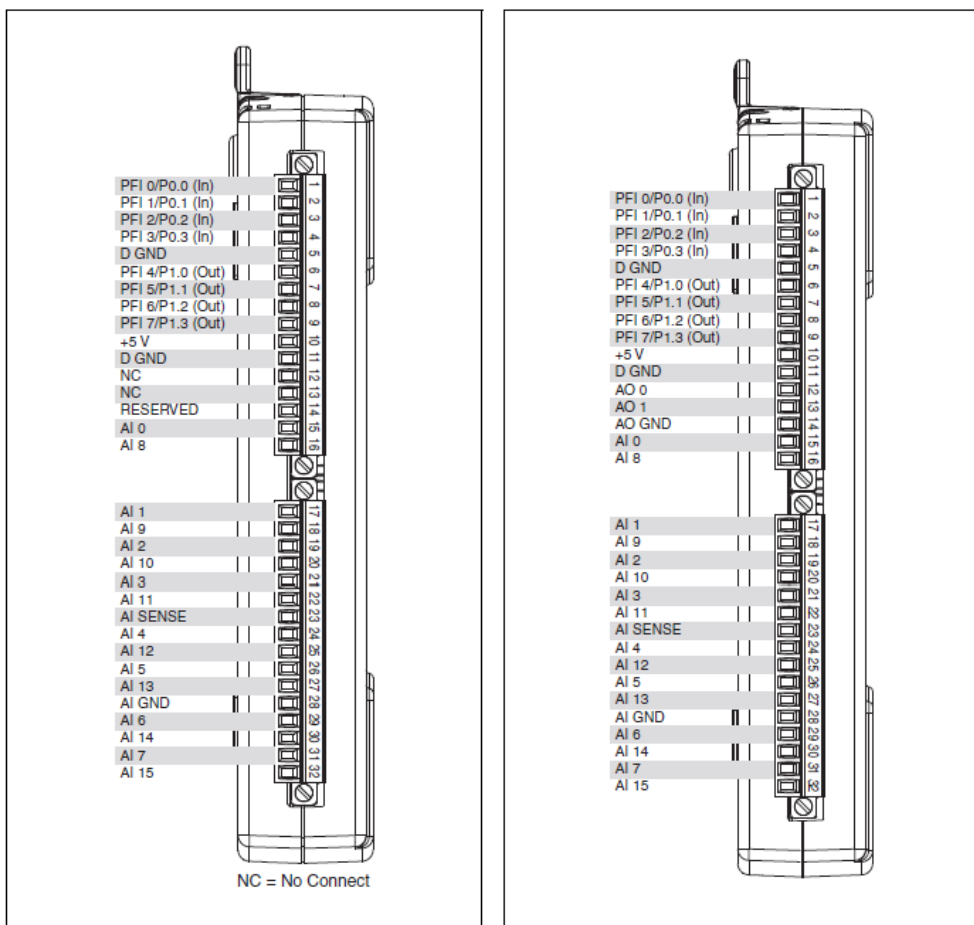


Figure 2. USB-6210 Pinout

Figure 3. USB-6211/6215 Pinout

C.11 Kelag Acceleration sensor

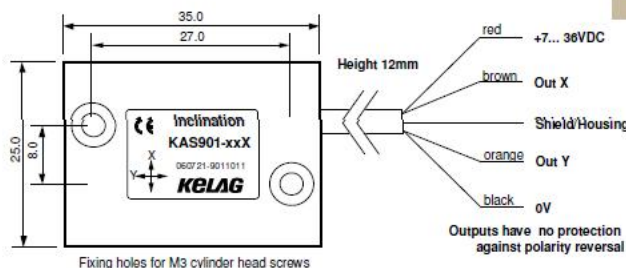
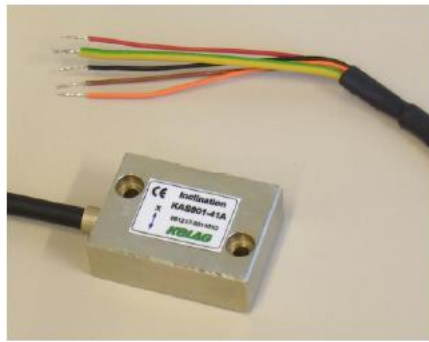
KELAG Künzli Elektronik AG Telefon +41 (0)44 806 22 00
 Ringstrasse 5 Fax +41 (0)44 806 22 08
 Ch-8603 Scherzenbach E-Mail kelag@kelag.ch
 Schweiz / Switzerland www.accelerometer.ch/en



Single Axis Acceleration Sensor KAS901- 04

The sensors are based one an advanced "bulk micro machined" technology. The three dimensional structure of these sensors comprise a pendulum made of mono crystalline silicon. The pendulum is hermetically enclosed between two silicon discs. From this construction results a long term stable, high resolution und shock resistant sensor. A gas damping prevents overshooting and interfering resonance oscillation. An ASIC measures the capacitive change caused by the movement of the pendulum.

- senses in positive and negative direction
- static and dynamic acceleration measured
- high repeatability up to 0,05% over range
- high resolution: up to 0,005% over range
- shock resistance of the pendulum min. 50'000g
- temperature range -30 .. +85 °C
- passive temperature compensation
- small, solid brass housing with fixing holes
- rugged PVC cable
- large output span: 0.5 .. 4.5V output over measuring range
- power supply requirement: 7... 36 VDC, stabilized



Other versions:

- single and dual axis sensors in IP67 housing with cable or connector and standardized output 4... 20mA, 2...10V and Modbus
- smaller cases and sensors for higher temperatures ranges

Parameter	Conditions	KAS901-04	Unit
Measuring range ⁴⁾		+/- 1,7 +/- 90	G °
Repeatability at 0° (horizontal position) ¹⁾	at 0...40 °C, 20°C typ	4 0,2	mg °
Resolution at 0°/ 1g	DC .. 1Hz	0,2 0,01	mg °
typ. Offset temperature dependency	20...60 °C	0,6	mg/°
long term stability ⁶⁾	10 years ⁶⁾	approx. 1,5	mg
Measuring direction		x-axis	
Cross axis sensitivity ²⁾		4	%
damping	-3 dB	50	Hz ⁵⁾
Operating temperature range		-30 ⁷⁾ .. +85	°C
Shock resistance (Chip)		20'000	g
Output signal V _{out}		0,5 .. 4,5	V
Offset = V _{out} in 0%1gposition		2,5	V
Sensitivity		4	V/g
Power supply ³⁾		7... 36	VDC

1) **Repeatability:** maximum offset occurring with position change after return to initial position (corresponds to achievable precision, including temperature hysteresis after temperature compensation and linearization).

2) **Cross axis sensitivity:** maximum error occurring with (additional) inclination or acceleration from another direction than the measuring plane

3) **Supply stabilized**

4) **Measuring range:** Trigonometric function:

$$\text{angle} = \arcsin\left(\frac{V_{out} - 2,5 \text{ (Offset)}}{\text{Sensitivity}}\right)$$

(paste values without units)

5) Typical values;

6) **Long term stability:** calculated values from HTB tests. Test results available at request.

7) Cable is specified for -15 °C for dynamic and -30 °C for static applications.

C.12 Sharp, Optoelectronic device

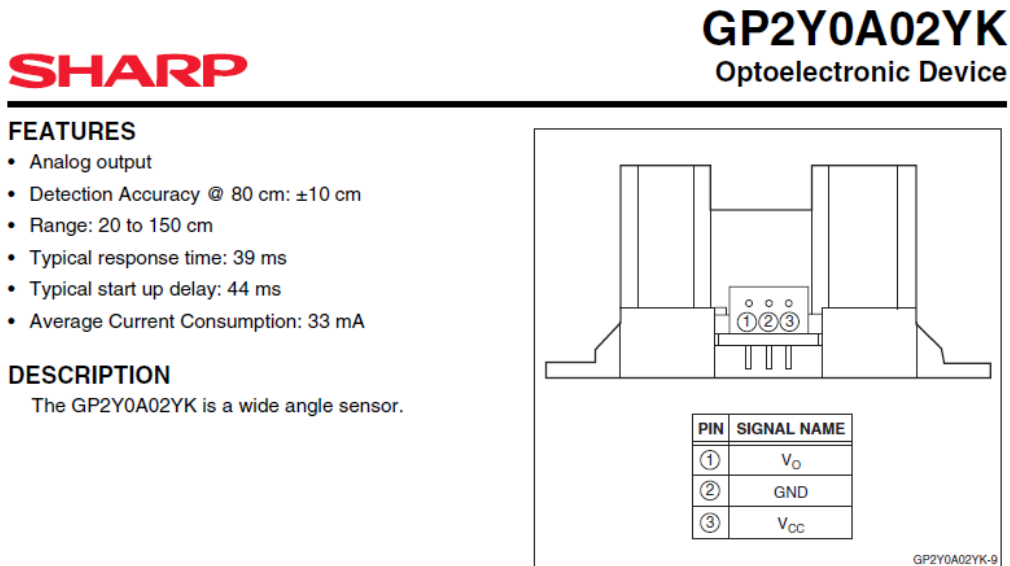


Figure 1. Pinout

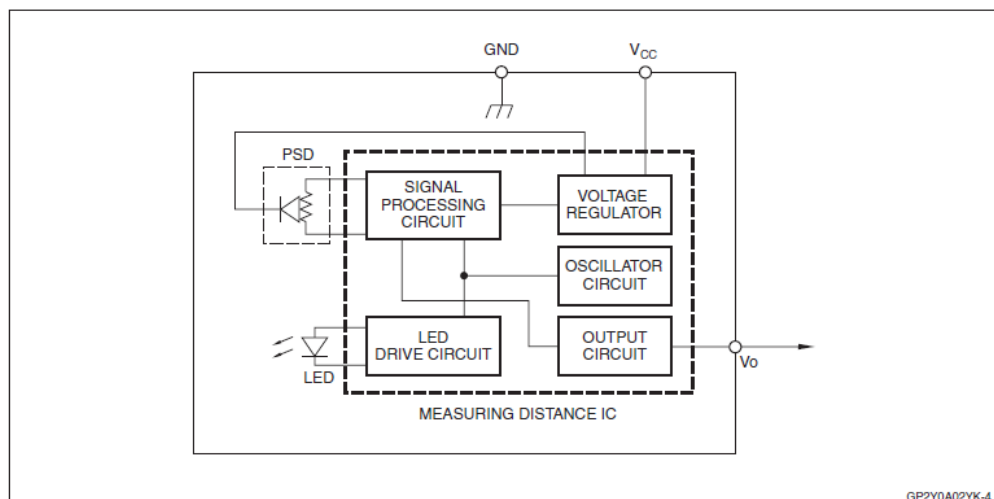


Figure 2. Block Diagram

ELECTRICAL SPECIFICATIONS**Absolute Maximum Ratings**Ta = 25°C, V_{CC} = 5 VDC

PARAMETER	SYMBOL	RATING	UNIT
Supply Voltage	V _{CC}	-0.3 to +7.0	V
Output Terminal Voltage	V _O	-0.3 to (V _{CC} + 0.3)	V
Operating Temperature	Topr	-10 to +60	°C
Storage Temperature	Tstg	-40 to +70	°C

Operating Supply Voltage

PARAMETER	SYMBOL	RATING	UNIT
Operating Supply Voltage	V _{CC}	4.5 to 5.5	V

Electro-optical CharacteristicsTa = 25°C, V_{CC} = 5 VDC

PARAMETER	SYMBOL	CONDITIONS	MIN.	TYP.	MAX.	UNIT	NOTES
Measuring Distance Range	ΔL		20	—	150	cm	1
Output Terminal Voltage	V _O	L = 150 cm	0.25	0.4	0.55	V	1
Output Voltage Difference	ΔV _O	Output change at L change (150 cm – 20 cm)	1.8	2.05	2.3	V	1
Average Supply Current	I _{CC}	L = 150 cm	—	33	50	mA	1, 2

NOTES:

1. Measurements made with Kodak R-27 Gray Card, using the white side, (90% reflectivity).
2. L = Distance to reflective object.

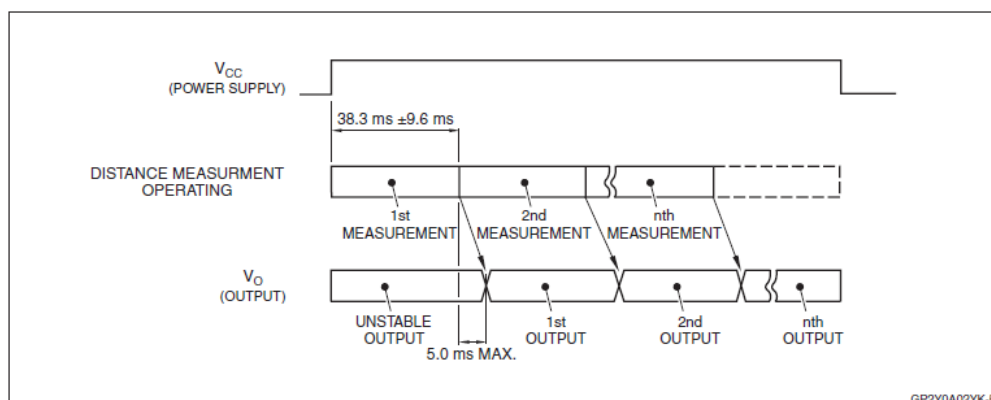


Figure 3. Timing Diagram

REALIABILITY

The reliability requirements of this device are listed in Table 1.

Table 1. Reliability

TEST ITEMS	TEST CONDITIONS	FAILURE JUDGEMENT CRITERIA	SAMPLES (n), DEFECTIVE (C)
Temperature Cycling	One cycle -40°C (30 min.) to +70°C in 30 minutes, repeated 25 times	Initial $\times 0.8 > V_O$ $V_O >$ Initial $\times 1.2$	n = 11, C = 0
High Temperature and High Humidity Storage	+40°C, 90% RH, 500h		n = 11, C = 0
High Temperature Storage	+70°C, 500h		n = 11, C = 0
Low Temperature Storage	-40°C, 500h		n = 11, C = 0
Operation Life (High Temperature)	+60°C, V _{CC} = 5 V, 500h		n = 11, C = 0
Mechanical Shock	100 m/s ² , 6.0 ms 3 times/ $\pm X, \pm Y, \pm Z$ direction		n = 6, C = 0
Variable Frequency Vibration	10-to-55-to-10 Hz in 1 minute Amplitude: 1.5 mm 2h in each X, Y, Z direction		n = 6, C = 0

NOTES:

1. Test conditions are according to Electro-optical Characteristics, shown on page 2.
2. At completion of the test, allow device to remain at nominal room temperature and humidity (non-condensing) for two hours.
3. Confidence level: 90%, Lot Tolerance Percent Defect (LTPD): 20%/40%.

MANUFACTURER'S INSPECTION

Inspection Lot

Inspection shall be carried out per each delivery lot.

Inspection Method

A single sampling plan, normal inspection level II based on ISO 2859 shall be adopted.

Table 2. Quality Level

DEFECT	INSPECTION ITEM and TEST METHOD	AQL (%)
Major Defect	Electro-optical characteristics defect	0.4
Minor Defect	Defect on appearance and dimension (crack, split, chip, scratch, stain)*	1.0

NOTE: *Any one of these that affects the Electro-optical Characteristics shall be considered a defect.

SHARP

GP2Y0A02YK

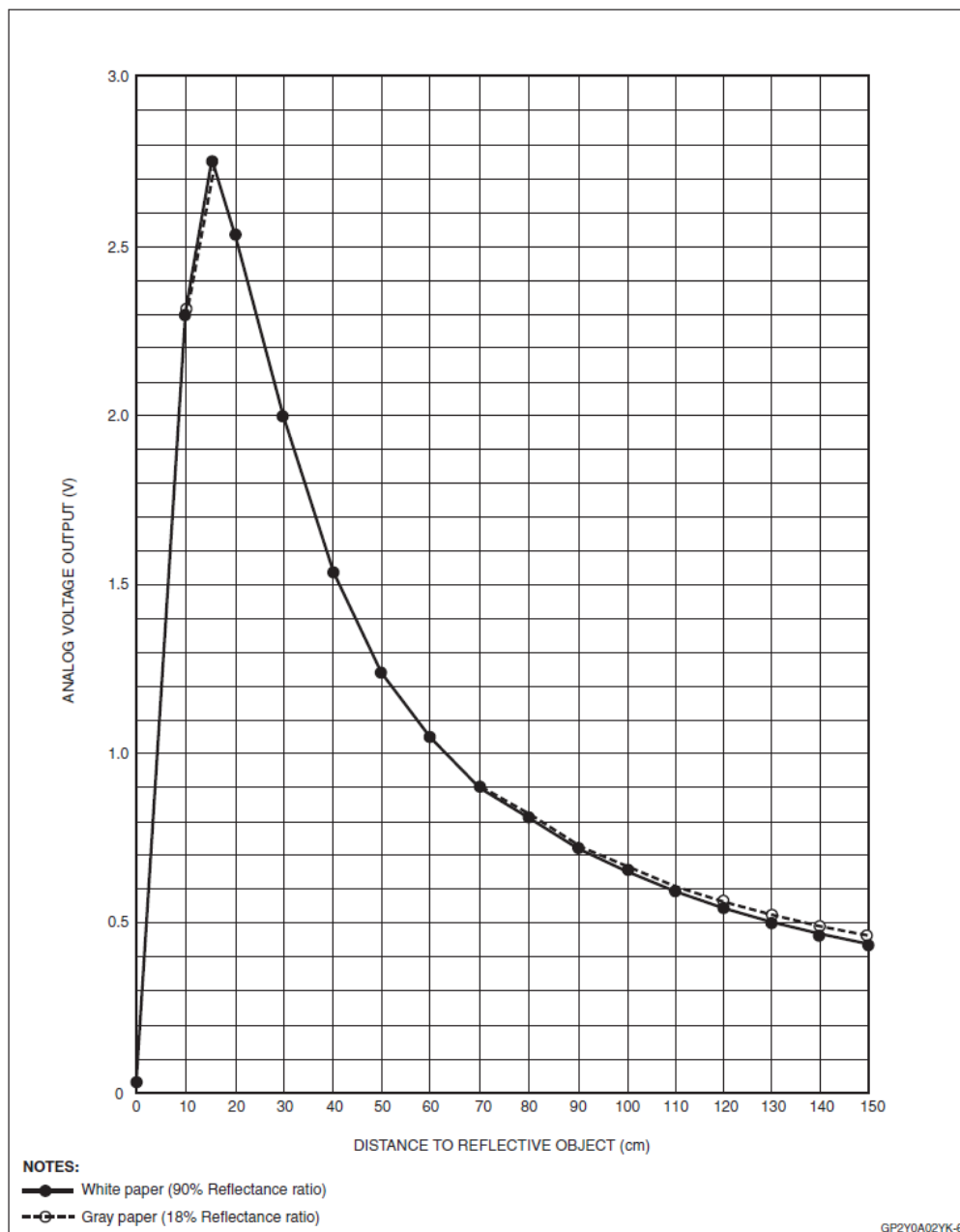


Figure 4. GP2Y0A02YK Example of Output Distance Characteristics

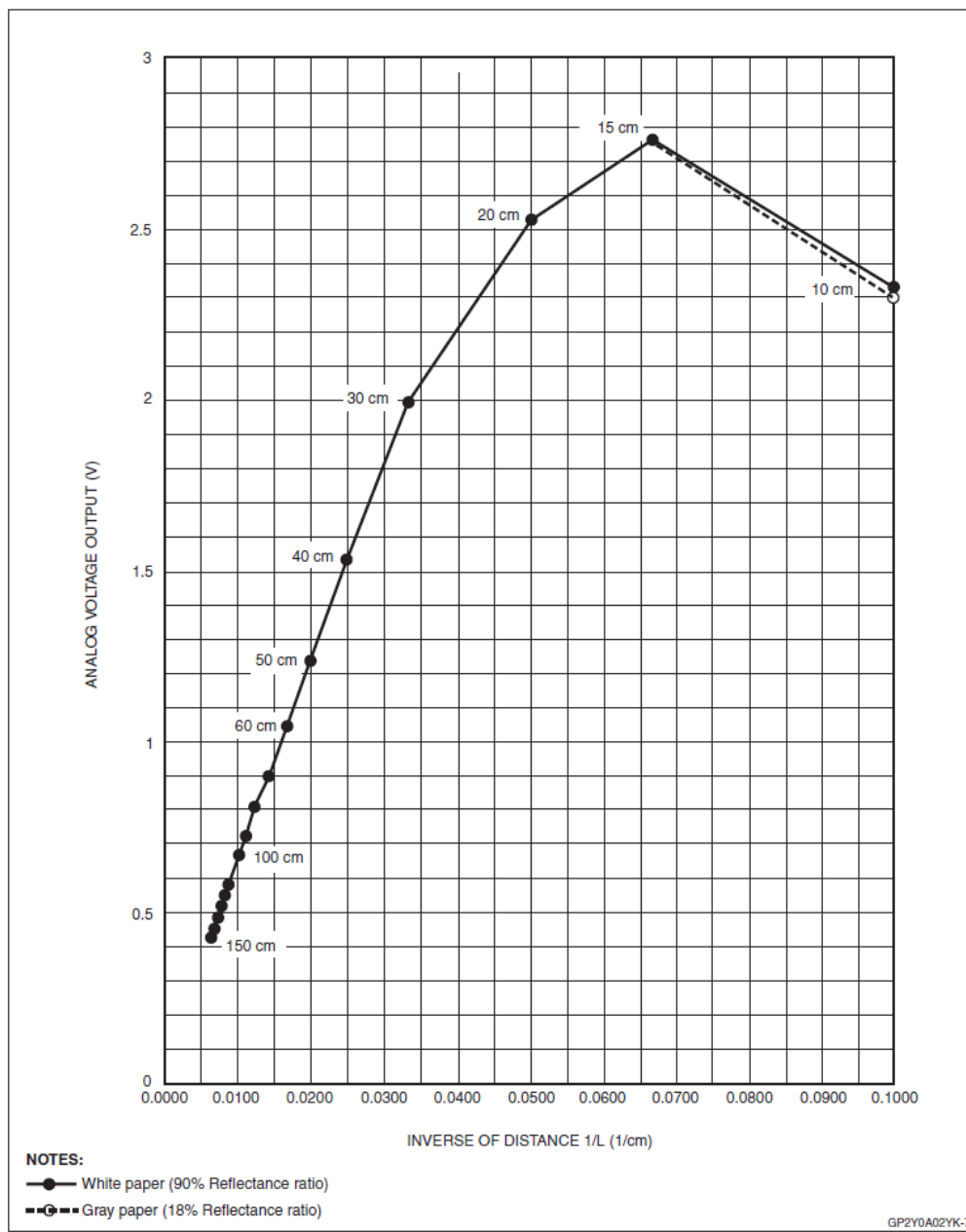
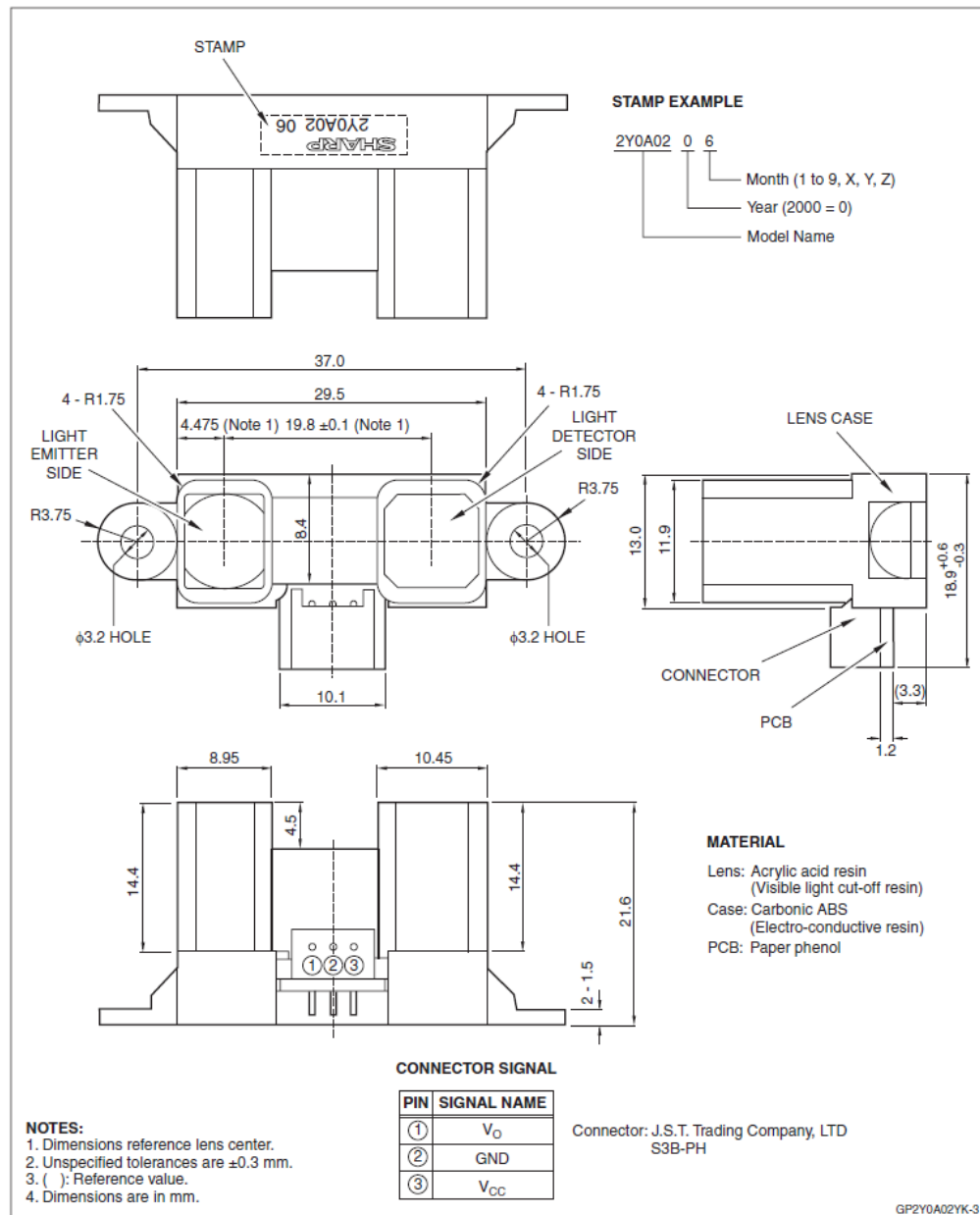


Figure 5. GP2Y0A02YK Example of Output Characteristics with Inverse Number of Distance

PACKAGE SPECIFICATIONS

C.13 Parker, Pressure transducer

SCP01 pressure sensors

Device features

- Small design
- Stainless steel measuring cell
- Stainless steel housing
- Shock and vibration proof
- Wide range of compatible substances
- High linearity
- Long-term stability
- Substance temperature -40 to 125 °C
- Up to 1000 bar
- High burst pressure
- 1 ms
- Eroding milling
- Encapsulated electronics

The SCP01 pressure sensor was designed to meet industrial requirements and is used in control, regulating and monitoring systems.

The SCP01 is characterised by its compact design, high linearity and excellent interference immunity. It is suitable for quick control solutions because of its fast response speed. The compact stainless steel housing is good for harsh environmental conditions. All components which come into contact with the substance are made from stainless steel. This feature, combined with the welded, thin-layer measuring cell, ensure optimal compatibility with the substance. The electronics are encapsulated for protection against vibration damage and moisture.

In order to ensure an exact pressure measurement and to avoid disturbances, an EDM hole is integrated. This minimises the cavitation of air and dirt, thus preventing the measuring cell from being influenced by pressure surges and pressure peaks.

This product is ideal for permanent series usage in hydraulic applications because of its long lifespan, high accuracy, high reliability and sturdy stainless steel construction.



Typical application range

- General machine construction
- Injection-mould machines
- Die-casting machines
- Press construction
- Test benches
- Tool-making machines



SCP01 pressure sensors

Technical data

SCP01-xxx-x4-0x (bar / G1/4" BSPP)

SCP01-	010	016	025	040	060	100	160	250	400	600	1000
Pressure range P _n relative 0... (bar)	10	16	25	40	60	100	160	250	400	600	1000
Overload pressure* P _{max} relative (bar)							2 × P _n				1.5 × P _n
Burst pressure** P _{burst} relative (bar)							4 × P _n				2.5 × P _n

SCP01-xxxxP-x5-0x (psi / 1/4 NPT) & **SCP01-xxxxP-x7-0x** (psi / 7/16-20 UNF)

SCP01-	0150P	0250P	1000P	3000P	5000P	9000P***
Pressure range P _n relative 0... (psi)	150	250	1000	3000	5000	9000
Overload pressure* P _{max} relative (psi)				2 × P _n		
Bursting pressure** P _{burst} relative (psi)				4 × P _n		

* DIN EN 60770-1 / ** DIN 16086 / *** only 1/4 NPT

General		Ambient conditions	
Response time	≤1 ms	Ambient temperature range	-40...+85 °C
Long-term stability	< 0.2 % FS / a	Fluid temperature range	-40 to +125 °C
Load change	> 20 million	Compensated range	0 to +85 °C
Weight	Approx. 80 g	Storage temperature	-40 to +125 °C
MTTFd	> 100 years	Vibration resistance	IEC 60068-2-6: 20 g
Accuracy		Shock resistance	
Non-linearity	BFSL according to IEC 61298-2 ≤± 0.25 %FS	IEC 60068-2-27: 500 g	
Accuracy	Type ≤± 0.25 %FS Max. ≤± 0.5 %FS	Electrical protection	
Total error at 0 to 85 °C	≤±1 %FS	Short-circuit, signal to GND, reverse polarity protection	
Temperature coefficient		EM compatibility	
Zero point	Max. ≤± 0.2 %FS/10 K	Disturbance emissions	EN 61000-6-3
Output range	Max. ≤± 0.2 %FS/10 K	Resistance to interference	EN 61000-6-2
Material		Process connection	
Housing	Stainless steel 1.4404	Eroding milling	0.6 mm
		Tightening torque	Max. 35 Nm

Process connection	G1/4A BSPP; DIN 3852 T11, Form E	SAE 7/16 UNF Male O ring	1/4 NPT
Seal	Sealing ring DIN 3869-14-FKM	O ring 8,12x1,83 FKM	
Parts in contact with substances	FKM Stainless steel 1.4404 Stainless steel 1.4548	FKM Stainless steel 1.4404 Stainless steel 1.4548	FKM Stainless steel 1.4404 Stainless steel 1.4548

Output signal	0 to 20 mA	4 to 20 mA (3-wire)	4 to 20 mA (2-wire)	0 to 10 V
Auxiliary power V ₊	+9 to 36 VDC	+9 to 36 VDC	+9 to 36 VDC	+14 to 36 VDC
Max. load	≥50 to ≤500 Ω (V ₊ - 9 V) / 28 mA	≥50 to ≤500 Ω (V ₊ - 9 V) / 28 mA	≥50 to ≤500 Ω (V ₊ - 9 V) / 20 mA	≥10 kΩ

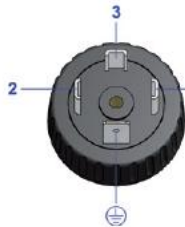


SCP01 pressure sensors

Pin assignment

Device plug DIN EN 175301-803 Form A 4-pole (old 43650)

SCP01-xxx-xx-06



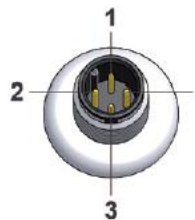
PIN	0 to 20 mA	4 to 20 mA (3-wire)	4 to 20 mA (2-wire)	0 to 10 V
1	P signal	P signal	P signal	P signal
2	0 V / GND	0 V / GND	n.c.*	0 V / GND
3	V ₊	V ₊	V ₊	V ₊
(n.c.*	

Protection class

IP65

Circular connector M12x1 4-pole

SCP01-xxx-xx-07



PIN	0 to 20 mA	4 to 20 mA (3-wire)	4 to 20 mA (2-wire)	0 to 10 V
1	V ₊	V ₊	V ₊	V ₊
2	P signal	P signal	P signal	P signal
3	0 V / GND	0 V / GND	n.c.*	0 V / GND
4			n.c.*	

Material

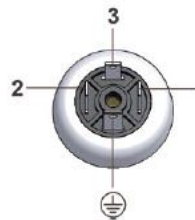
Plastic PBT-GF30 Ultradur B4300 G6 black

Protection class

IP67

Device plug Industrial Micro DIN 9.4 mm

SCP01-xxx-xx-0C



PIN	0 to 20 mA	4 to 20 mA (3-wire)	4 to 20 mA (2-wire)	0 to 10 V
1	P signal	P signal	P signal	P signal
2	V ₊	V ₊	V ₊	V ₊
3			n.c.*	
(0 V / GND	0 V / GND		0 V / GND

Protection class

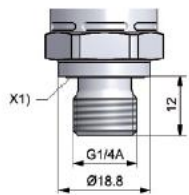
IP65

*) n.c. = not connected

Dimensioned drawings

SCP01-xxx-x4-0x

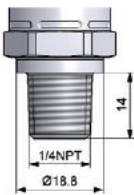
G1/4 BSPP ED



X1) = ED-seal

SCP01-xxxP-x5-0x

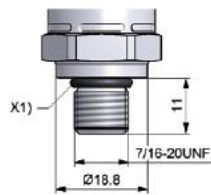
1/4 NPT



X1) = O ring 8.92 x 1.83

SCP01-xxxP-x7-0x

SAE 7/16-20UNF



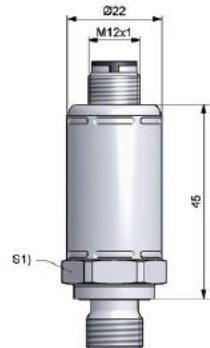
X1) = O ring 8.92 x 1.83



SCP01 pressure sensors

Dimensioned drawings

SCP01-xxx-xx-07



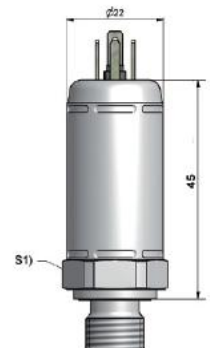
S1) = SW22

SCP01-xxx-xx-06



S1) = SW22

SCP01-xxx-xx-0C



S1) = SW22

Order code

Pressure sensor SCP01 (bar)

SCP01-xxxx-xx-0x

Pressure range (bar)

0...10 bar	010
0...16 bar	016
0...25 bar	025
0...40 bar	040
0...60 bar	060
0...100 bar	100
0...160 bar	160
0...250 bar	250
0...400 bar	400
0...600 bar	600
0...1000 bar	1000

Output signal

0 to 20 mA	1
4 to 20 mA (3-wire)	2
4 to 20 mA (2-wire)	3
0 to 10 V	4

Connecting plug

Circular connector M12x1 4-pole	7
Device connector DIN EN 175301-803 Form A 4-pole	6
Device plug industrial micro DIN 9.4mm	C

Pressure sensor SCP01 (psi)

SCP01-xxxx-xx-0x

Pressure range (psi)

0 to 150 psi	0150P
0 to 250 psi	0250P
0 to 1000 psi	1000P
0 to 3000 psi	3000P
0 to 5000 psi	5000P
0 to 9000 psi	9000P

Output signal

0 to 20 mA	1
4 to 20 mA (3-wire)	2
4 to 20 mA (2-wire)	3
0 to 10 V	4

Process connection

SAE 7/16 UNF Male O ring (P_n max. = 400 bar)	7
1/4 NPT (P_n max. = 600 bar)	5

Connecting plug

Circular connector M12x1 4-pole	7
Device connector DIN EN 175301-803 Form A 4-pole	6

Pressure and temperature sensors



C.14 National Semiconductor, LM6142

National Semiconductor

November 2004

LM6142/LM6144
17 MHz Rail-to-Rail Input-Output Operational Amplifiers

General Description

Using patent pending new circuit topologies, the LM6142/LM6144 provides new levels of performance in applications where low voltage supplies or power limitations previously made compromise necessary. Operating on supplies of 1.8V to over 24V, the LM6142/LM6144 is an excellent choice for battery operated systems, portable instrumentation and others.

The greater than rail-to-rail input voltage range eliminates concern over exceeding the common-mode voltage range. The rail-to-rail output swing provides the maximum possible dynamic range at the output. This is particularly important when operating on low supply voltages.

High gain-bandwidth with 650 μ A/Amplifier supply current opens new battery powered applications where previous higher power consumption reduced battery life to unacceptable levels. The ability to drive large capacitive loads without oscillating functionally removes this common problem.

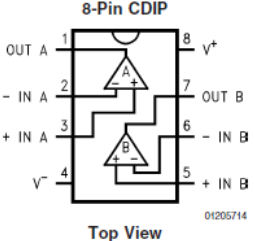
Features

- At $V_S = 5V$. Typ unless noted.
- Rail-to-rail input CMVR -0.25V to 5.25V
- Rail-to-rail output swing 0.005V to 4.995V
- Wide gain-bandwidth: 17MHz at 50kHz (typ)
- Slew rate:
 - Small signal, 5V/ μ s
 - Large signal, 30V/ μ s
- Low supply current 650 μ A/Amplifier
- Wide supply range 1.8V to 24V
- CMRR 107dB
- Gain 108dB with $R_L = 10k$
- PSRR 87dB

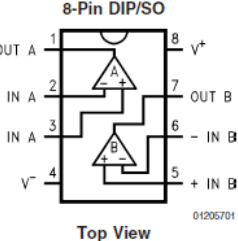
Applications

- Battery operated instrumentation
- Depth sounders/fish finders
- Barcode scanners
- Wireless communications
- Rail-to-rail in-out instrumentation amps

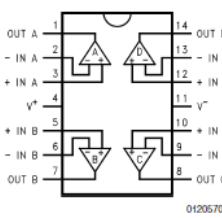
Connection Diagrams



8-Pin CDIP
Top View
01205714



8-Pin DIP/SO
Top View
01205701



14-Pin DIP/SO
Top View
01205702

© 2004 National Semiconductor Corporation DS012057

www.national.com

LM6142/LM6144

Absolute Maximum Ratings (Note 1)

If Military/Aerospace specified devices are required, please contact the National Semiconductor Sales Office/ Distributors for availability and specifications.	
ESD Tolerance (Note 2)	2500V
Differential Input Voltage	15V
Voltage at Input/Output Pin	(V ⁺) + 0.3V, (V ⁻) - 0.3V
Supply Voltage (V ⁺ - V ⁻)	35V
Current at Input Pin	±10mA
Current at Output Pin (Note 3)	±25mA
Current at Power Supply Pin	50mA
Lead Temperature (soldering, 10 sec)	260°C
Storage Temp. Range	-65°C to +150°C
Junction Temperature (Note 4)	150°C

Operating Ratings (Note 1)

Supply Voltage	1.8V ≤ V ⁺ ≤ 24V
Temperature Range	-40°C ≤ T _A ≤ +85°C
LM6142, LM6144	N Package, 8-Pin Molded DIP
Thermal Resistance (θ _{JA})	115°C/W
M Package, 8-Pin Surface Mount	193°C/W
N Package, 14-Pin Molded DIP	81°C/W
M Package, 14-Pin Surface Mount	126°C/W

5.0V DC Electrical Characteristics (Note 8)

Unless otherwise specified, all limits guaranteed for T_A = 25°C, V⁺ = 5.0V, V⁻ = 0V, V_{CM} = V_O = V⁺/2 and R_L > 1 MΩ to V⁺/2. Boldface limits apply at the temperature extremes.

Symbol	Parameter	Conditions	Typ (Note 5)	LM6144AI LM6142AI Limit (Note 6)	LM6144BI LM6142BI Limit (Note 6)	Units
V _{OS}	Input Offset Voltage		0.3	1.0 2.2	2.5 3.3	mV max
TCV _{OS}	Input Offset Voltage Average Drift		3			µV/°C
I _B	Input Bias Current		170	250	300	nA
		0V ≤ V _{CM} ≤ 5V	180	280	526	max
I _{OS}	Input Offset Current		3	30 80	30 80	nA max
R _{IN}	Input Resistance, C _M		126			MΩ
CMRR	Common Mode Rejection Ratio	0V ≤ V _{CM} ≤ 4V	107	84 78	84 78	dB min
		0V ≤ V _{CM} ≤ 5V	82 79	66 64	66 64	
PSRR	Power Supply Rejection Ratio	5V ≤ V ⁺ ≤ 24V	87	80 78	80 78	
V _{CM}	Input Common-Mode Voltage Range		-0.25 5.25	0 5.0	0 5.0	V
A _V	Large Signal Voltage Gain	R _L = 10k	270 70	100 33	80 25	V/mV min
V _O	Output Swing	R _L = 100k	0.005	0.01 0.013	0.01 0.013	V max
			4.995	4.98 4.93	4.98 4.93	V min
			0.02 4.97			V max V min
		R _L = 10k	0.06	0.1 0.133	0.1 0.133	V max
			4.90	4.86	4.86	V

24V Electrical Characteristics (Note 8)

Unless Otherwise Specified, All Limits Guaranteed for $T_A = 25^\circ\text{C}$, $V^+ = 24\text{V}$, $V^- = 0\text{V}$, $V_{CM} = V_O = V^+/2$ and $R_L > 1\text{ M}\Omega$ to $V^+/2$. **Boldface** limits apply at the temperature extreme

Symbol	Parameter	Conditions	Typ (Note 5)	LM6144AI LM6142AI	LM6144BI LM6142BI	Units
				Limit (Note 6)	Limit (Note 6)	
V_{OS}	Input Offset Voltage		1.3	2 4.8	3.8 4.8	mV max
I_B	Input Bias Current		174			nA max
I_{OS}	Input Offset Current		5			nA max
R_{IN}	Input Resistance		288			M Ω
CMRR	Common Mode Rejection Ratio	$0\text{V} \leq V_{CM} \leq 23\text{V}$	114			dB min
		$0\text{V} \leq V_{CM} \leq 24\text{V}$	100			
PSRR	Power Supply Rejection Ratio	$0\text{V} \leq V_{CM} \leq 24\text{V}$	87			
V_{CM}	Input Common-Mode Voltage Range		-0.25	0	0	V min
			24.25	24	24	V max
A_V	Large Signal Voltage Gain	$R_L = 10\text{k}\Omega$	500			V/mV min
V_O	Output Swing	$R_L = 10\text{k}\Omega$	0.07	0.15 0.185	0.15 0.185	V max
			23.85	23.81 23.62	23.81 23.62	V min
I_S	Supply Current	Per Amplifier	750	1100 1150	1100 1150	μA max
GBW	Gain-Bandwidth Product	$f = 50\text{ kHz}$	18			MHz

Note 1: Absolute Maximum Ratings indicate limits beyond which damage to the device may occur. Operating Ratings indicate conditions for which the device is intended to be functional, but specific performance is not guaranteed. For guaranteed specifications and the test conditions, see the Electrical Characteristics.

Note 2: Human body model, $1.5\text{k}\Omega$ in series with 100pF .

Note 3: Applies to both single-supply and split-supply operation. Continuous short circuit operation at elevated ambient temperature can result in exceeding the maximum allowed junction temperature of 150°C .

Note 4: The maximum power dissipation is a function of $T_{J(MAX)}$, θ_{JA} , and T_A . The maximum allowable power dissipation at any ambient temperature is $P_D = (T_{J(MAX)} - T_A)/\theta_{JA}$. All numbers apply for packages soldered directly into a PC board.

Note 5: Typical values represent the most likely parametric norm.

Note 6: All limits are guaranteed by testing or statistical analysis.

Note 7: For guaranteed military specifications see military datasheet MNLM6142AM-X.

Note 8: Electrical Table values apply only for factory testing conditions at the temperature indicated. Factory testing conditions result in very limited self-heating of the device such that $T_J = T_A$. No guarantee of parametric performance is indicated in the electrical tables under conditions of the internal self heating where $T_J > T_A$.

Production drawings

Bachelor project

MAS302

Lars Alexander Eikeland

Thomas Børseth

Kjetil Lohne Bakke

Supervisor

Hamid Reza Karimi

Eivind Arne Johansen

This Bachelor's Thesis is carried out as a part of the education at the University of Agder and is therefore approved as a part of this education. However, this does not imply that the University answers for the methods that are used or the conclusions that are drawn.

University of Agder, 2013

Faculty of Engineering and Science

Department of Mechatronics

Frame Parts

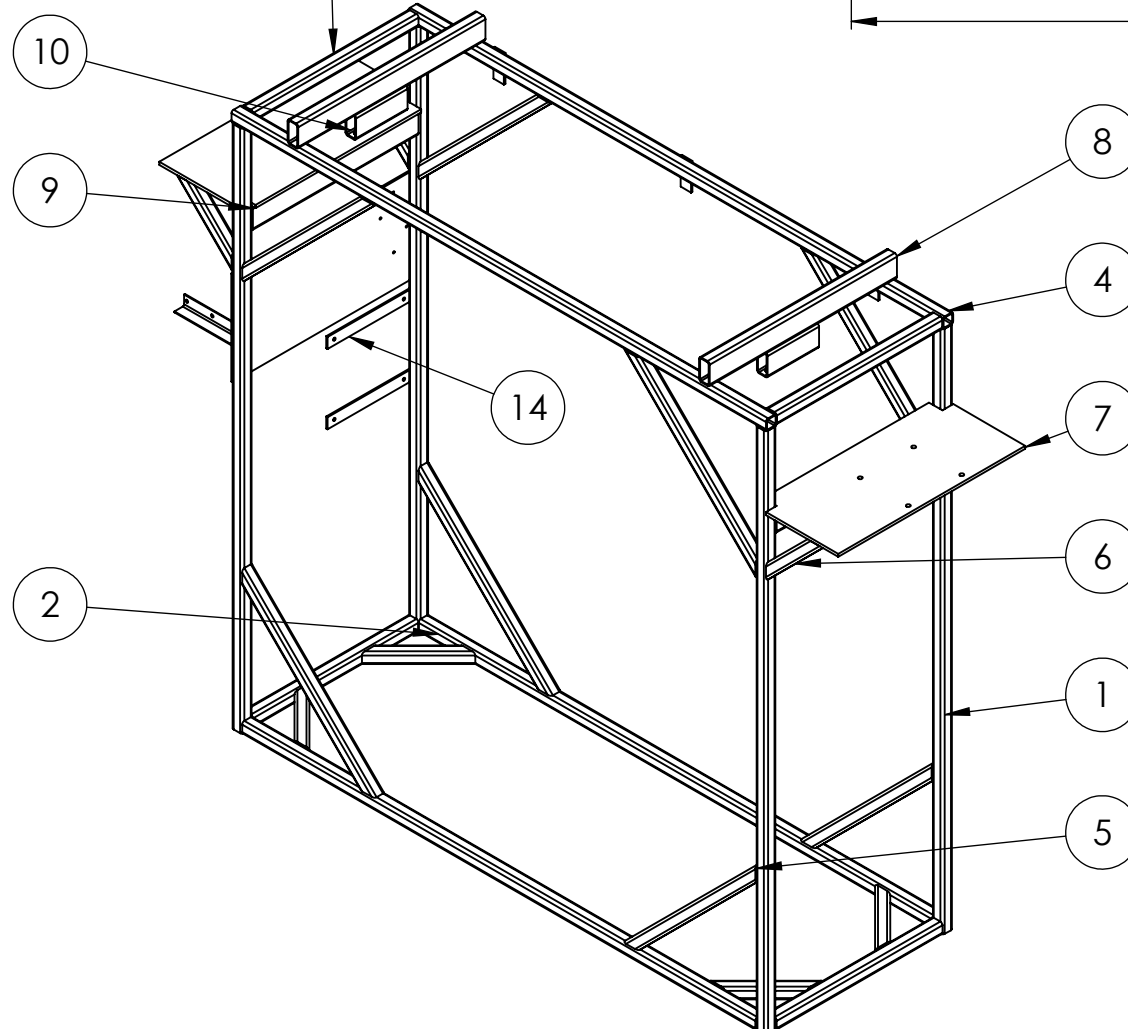
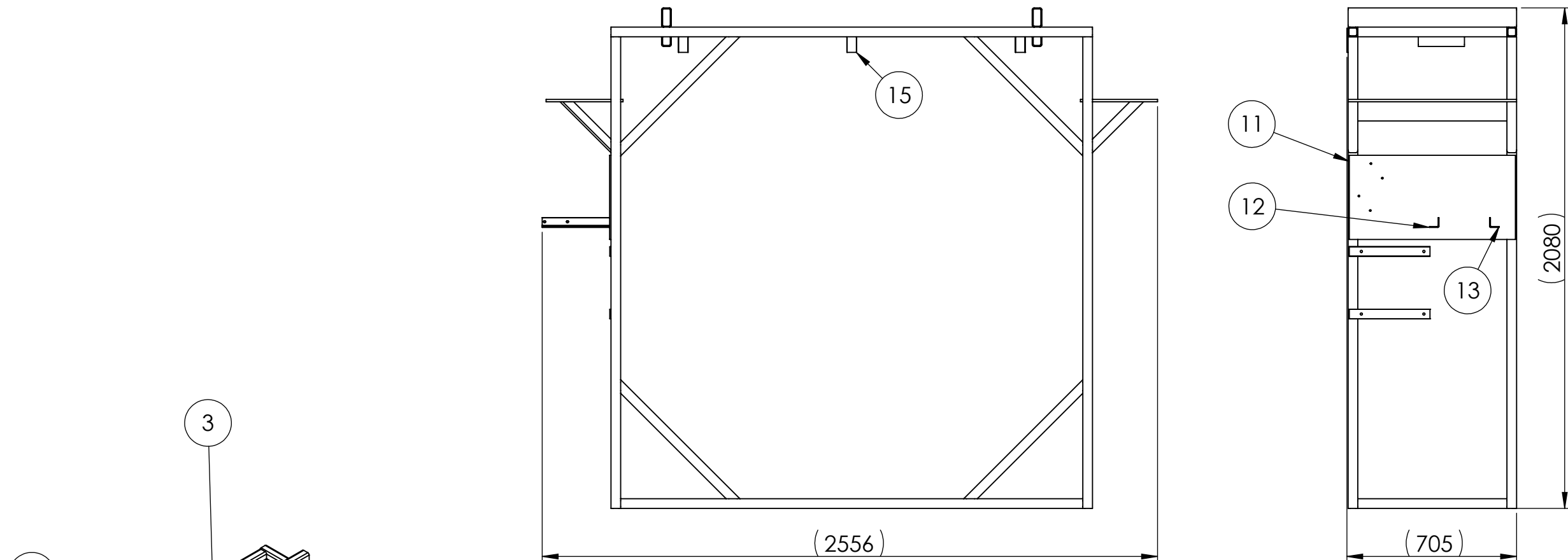
Bachelor project

MAS302

University of Agder, 2013

Faculty of Engineering and Science

Department of Mechatronics



ITEM NO.	PART TITLE	DWG NO.:	QTY.
1	Pipe Leg	F-102	4
2	Pipe Bottom Length	F-103	2
3	Pipe Width	F-104	4
4	Pipe Top Length	F-105	2
5	Pipe Support Long	F-106	8
6	Pipe Support Short	F-107	8
7	Support Plate Horizontal	F-108	2
8	Pipe Support Top	F-109	2
9	Pipe 40x80x4x620	F-110	2
10	Pipe Bracket	F-111	2
11	Control Panel	F-112	1
12	Angel Iron Support Left	F-113	1
13	Angel Iron Support Right	F-114	1
14	Bracket for Cabinet	F-115	2
15	Bracket for Pipelines	F-116	3

UNLESS OTHERWISE SPECIFIED; DIMENSIONS ARE IN MILLIMETERS SURFACE FINISH: TOLERANCES: NS-ISO 2768-1 m LINEAR: ANGULAR:				FINISH: Dark Blue, Hammerlack Art. 36-042 Biltema	DEBUR AND BREAK SHARP EDGES	DO NOT SCALE DRAWING	REVISION 1
University of Agder							
DRAWN	NAME	SIGNATURE	DATE	Projection:			
CHK'D	LAE						
CHK'D	TB						
				MATERIAL:		DWG NO.	
				WEIGHT: 174.8kg		SCALE: 1:20	
						A3	
						SHEET 1 OF 16	

DWG.: F-101



Standard dimentions
for square pipe 40x40x4

A

A

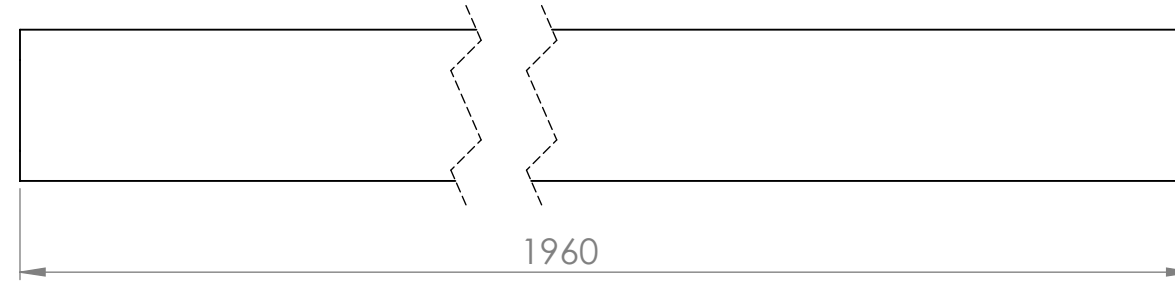
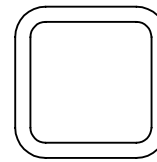
B

B

C

C

D



ITEM NO.	PART TITLE	QTY.
1	Pipe Leg	4

UNLESS OTHERWISE SPECIFIED:
DIMENSIONS ARE IN MILLIMETERS
SURFACE FINISH:
TOLERANCES: NS-ISO 2768-1 m
LINEAR:
ANGULAR:

FINISH:

DEBUR AND
BREAK SHARP
EDGES

DO NOT SCALE DRAWING

REVISION 1

University of Agder

DRAWN	NAME	SIGNATURE	DATE		Projection:
CHK'D	LAE				
CHK'D	TB				

TITLE:

Pipe Leg



MATERIAL:
S355J2H

DWG NO.

DWG.: F-102

A4

WEIGHT: 8.2kg

SCALE:1:5

SHEET 2 OF 16

Standard dimensions
for square pipe 40x40x4

A

A

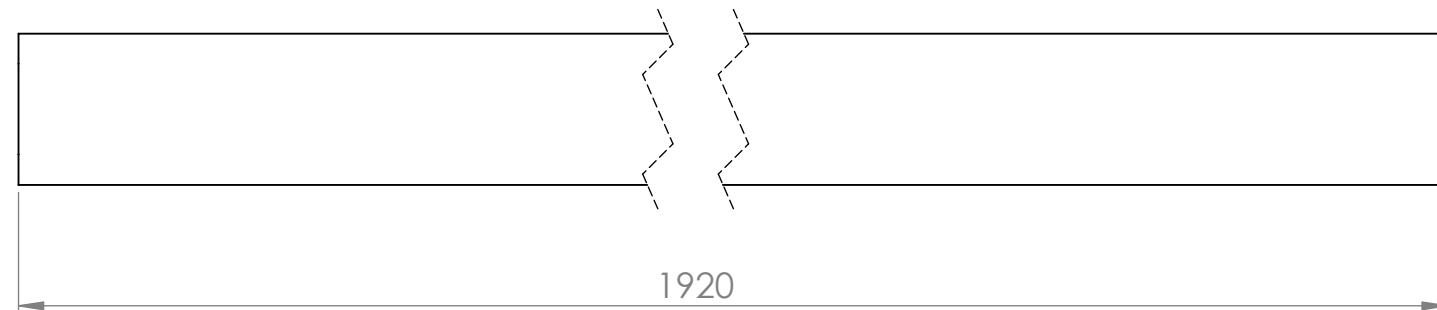
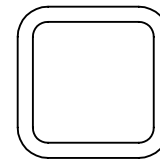
B

B

C

C

D



ITEM NO.	PART TITLE	QTY.
2	Pipe Bottom length	2

UNLESS OTHERWISE SPECIFIED:
DIMENSIONS ARE IN MILLIMETERS
SURFACE FINISH:
TOLERANCES: NS-ISO 2768-1 m
LINEAR:
ANGULAR:

FINISH:

DEBUR AND
BREAK SHARP
EDGES

DO NOT SCALE DRAWING

REVISION 1

University of Agder

DRAWN	NAME	SIGNATURE	DATE		Projection:
CHK'D	LAE				
CHK'D	TB				

TITLE:

Pipe Bottom Length



MATERIAL:
S355J2H

DWG NO.

DWG.: F-103

A4

WEIGHT: 8.0kg

SCALE:1:5

SHEET 3 OF 16

Standard dimensions
for square pipe 40x40x4

A

A

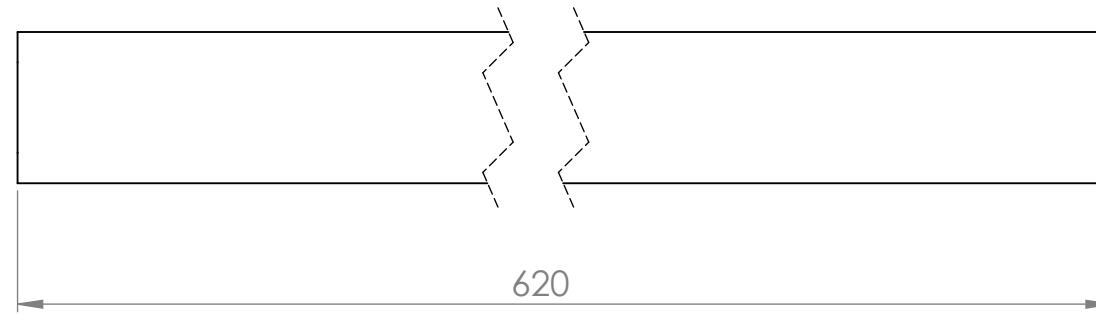
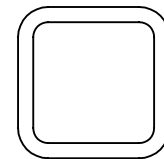
B

B

C

C

D



UNLESS OTHERWISE SPECIFIED:
DIMENSIONS ARE IN MILLIMETERS
SURFACE FINISH:
TOLERANCES: NS-ISO 2768-1 m
LINEAR:
ANGULAR:

FINISH:

ITEM NO.	PART TITLE	QTY.
3	Pipe Width	4

DO NOT SCALE DRAWING

REVISION

1

University of Agder

DRAWN KLB

CHK'D LAE

CHK'D TB

NAME

SIGNATURE

DATE

Projection:

DEBUR AND
BREAK SHARP
EDGES

TITLE:

Pipe Width



MATERIAL:
S355J2H

DWG NO.

DWG.: F-104

A4

WEIGHT: 2.6kg

SCALE:1:5

SHEET 4 OF 16

Standard dimensions
for square pipe 40x40x4

A

A

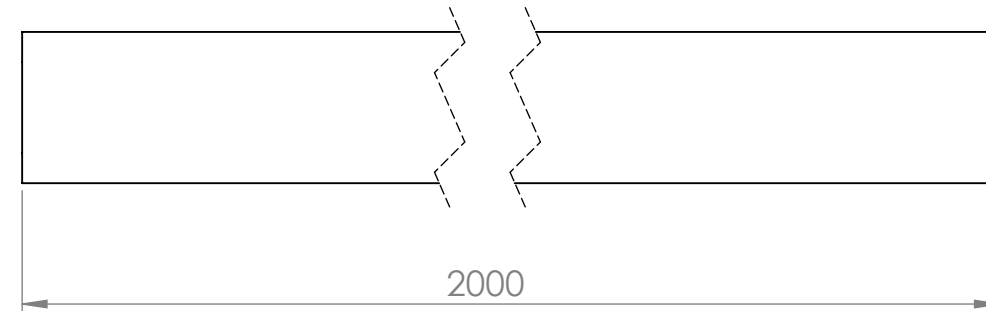
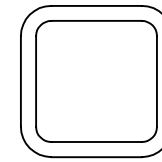
B

B

C

C

D



UNLESS OTHERWISE SPECIFIED:
DIMENSIONS ARE IN MILLIMETERS
SURFACE FINISH:
TOLERANCES: NS-ISO 2768-1 v
LINEAR:
ANGULAR:

FINISH:

DEBUR AND
BREAK SHARP
EDGES

ITEM NO.

PART TITLE

QTY.

4

Pipe Top Length

REVISION

1

University of Agder

DRAWN NAME

CHK'D SIGNATURE

DATE

Projection:



TITLE:

Pipe Top Length

MATERIAL:

S355J2H

DWG NO.

DWG.: F-105

A4

SCALE:1:5

SHEET 5 OF 16



Standard dimensions
for square pipe 40x40x4

A

A

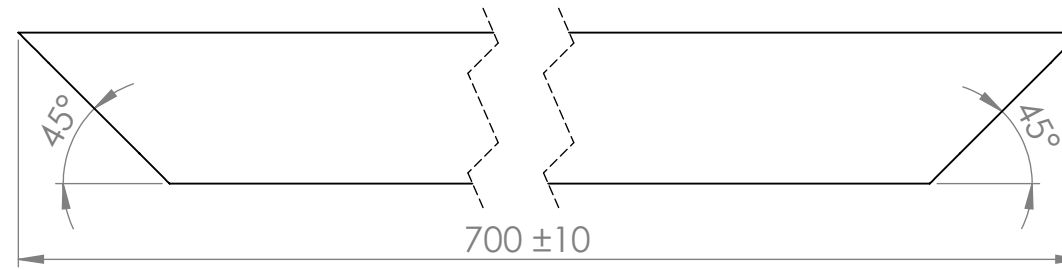
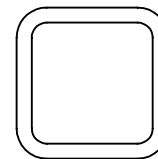
B

B

C

C

D



ITEM NO.	PART TITLE	QTY.
5	Pipe Support Long	8

UNLESS OTHERWISE SPECIFIED:
DIMENSIONS ARE IN MILLIMETERS
SURFACE FINISH:
TOLERANCES: NS-ISO 2768-1 m
LINEAR:
ANGULAR:

FINISH:

DEBUR AND
BREAK SHARP
EDGES

DO NOT SCALE DRAWING

REVISION

1

University of Agder

DRAWN	NAME	SIGNATURE	DATE		Projection:
CHK'D	LAE				
CHK'D	TB				

TITLE:

Pipe Support Long



MATERIAL:	S355J2H	DWG NO.
		DWG.: F-106

A4

Standard dimensions
for square pipe 40x40x4

A

A

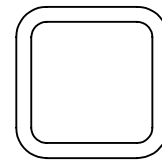
B

B

C

C

D



ITEM NO.	PART TITLE	QTY.
6	Pipe Support Short	8

UNLESS OTHERWISE SPECIFIED:
DIMENSIONS ARE IN MILLIMETERS
SURFACE FINISH:
TOLERANCES: NS-ISO 2768-1 m
LINEAR:
ANGULAR:

FINISH:

DEBUR AND
BREAK SHARP
EDGES

DO NOT SCALE DRAWING

REVISION 1

University of Agder

DRAWN	NAME	SIGNATURE	DATE		Projection:
CHK'D	LAE				
CHK'D	TB				

TITLE:

Pipe Support Short



MATERIAL:
S355J2H

DWG NO.

DWG.: F-107

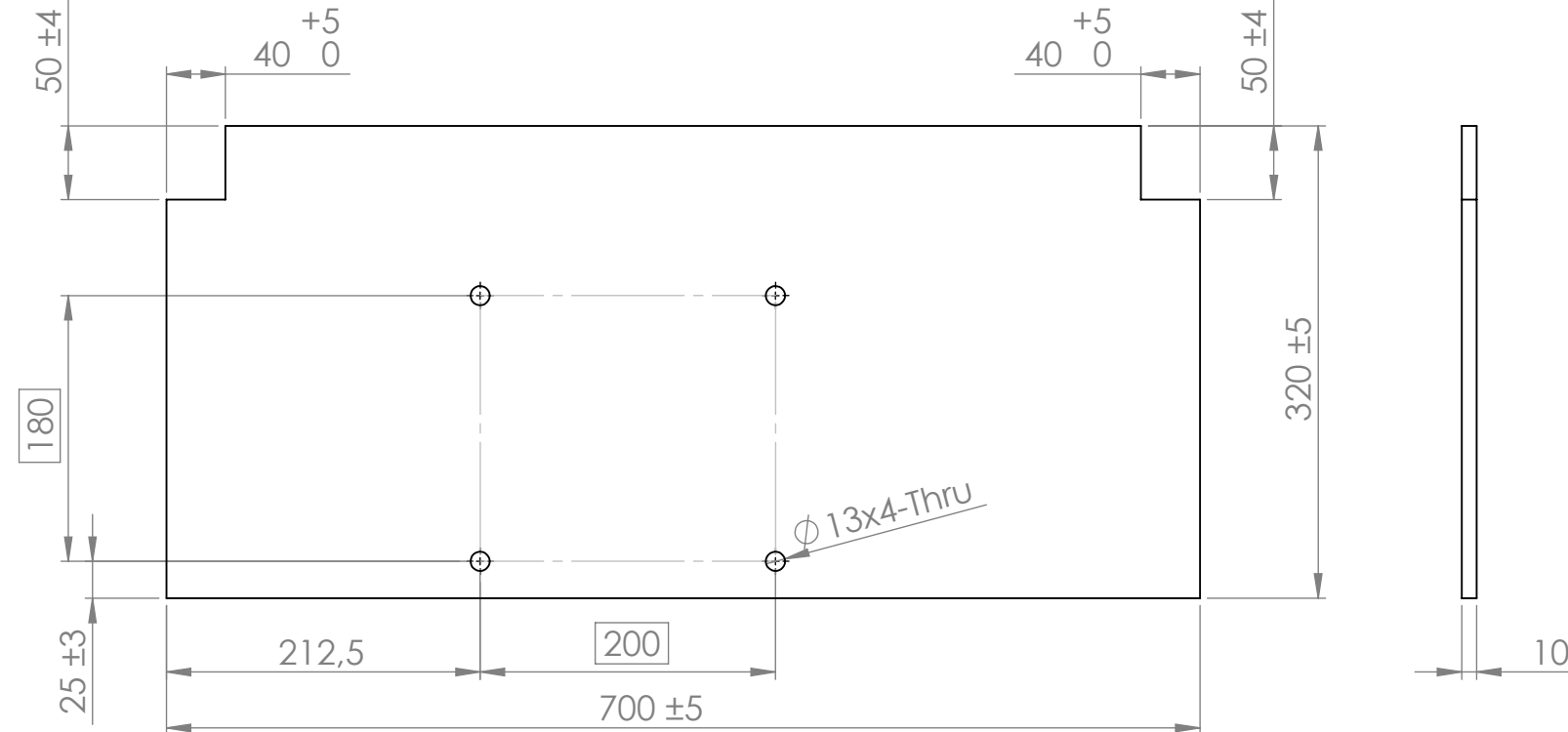
A4

WEIGHT: 1.1kg

SCALE:1:5

SHEET 7 OF 16

1 2 3 4 5 6



ITEM NO.	PART TITLE	QTY.
7	Support Plate Horizontal	2

UNLESS OTHERWISE SPECIFIED:
DIMENSIONS ARE IN MILLIMETERS
SURFACE FINISH:
TOLERANCES: NS-ISO 2768-1 m
LINEAR:
ANGULAR:

FINISH:

DEBUR AND
BREAK SHARP
EDGES

DO NOT SCALE DRAWING

REVISION

1

University of Agder

DRAWN	NAME	SIGNATURE	DATE	Projection:
CHK'D	LAE			
CHK'D	TB			

TITLE:	
Support Plate Horizontal	

MATERIAL:
S235JR

DWG NO.

DWG.: F-108

A4

Standard dimensions
for square pipe 80x40x4

A

A

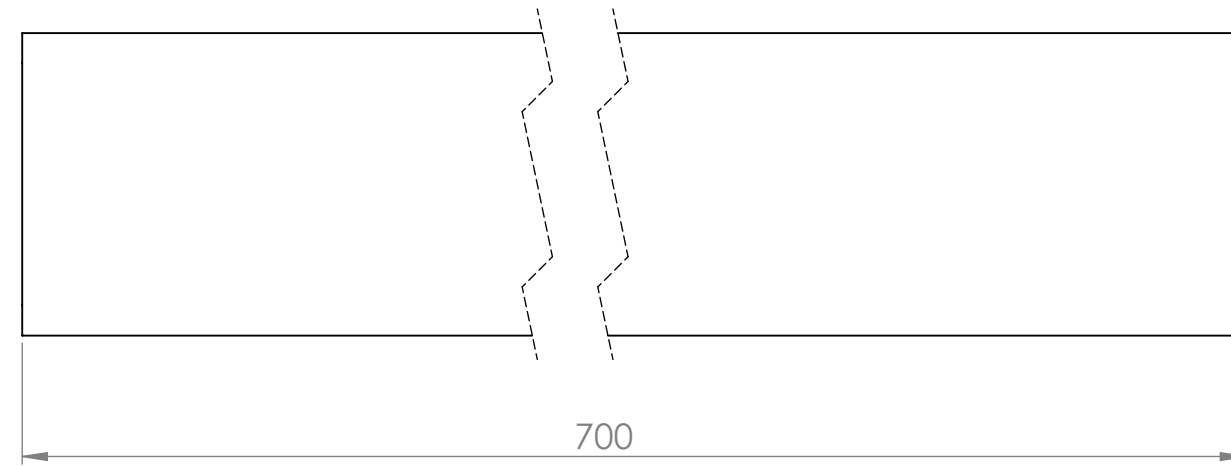
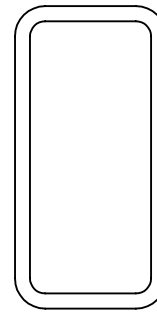
B

B

C

C

D



700

ITEM NO.	PART TITLE	QTY.
8	Pipe Support Top	2

UNLESS OTHERWISE SPECIFIED:
DIMENSIONS ARE IN MILLIMETERS
SURFACE FINISH:
TOLERANCES: NS-ISO 2768-1 v
LINEAR:
ANGULAR:

FINISH:

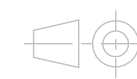
DEBUR AND
BREAK SHARP
EDGES

DO NOT SCALE DRAWING

REVISION 1

University of Agder

DRAWN	NAME	SIGNATURE	DATE	Projection	TITLE:
CHK'D	LAE				
CHK'D	TB				



TITLE:

Pipe Support Top



MATERIAL:
S335J2H

DWG NO.

DWG.: F-109

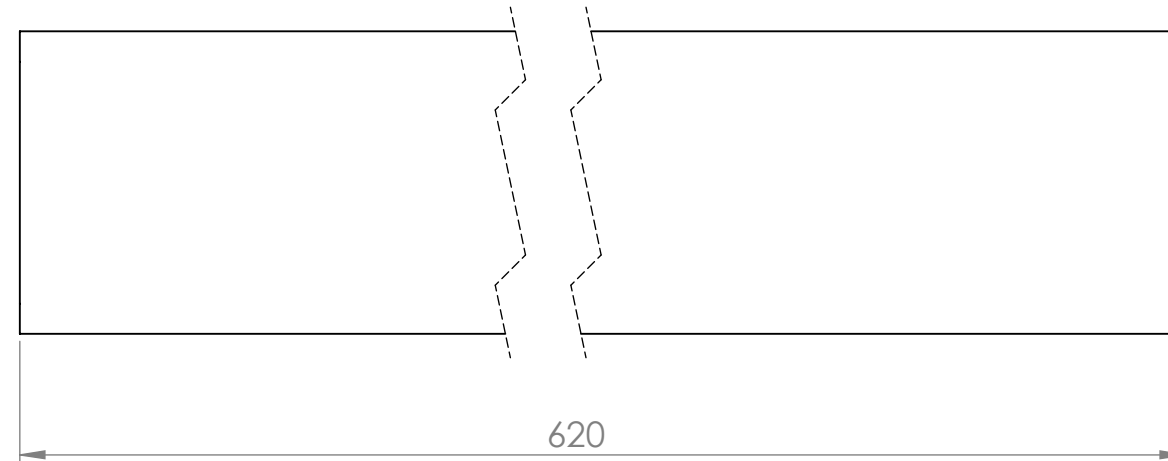
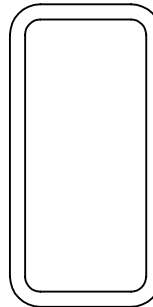
A4

WEIGHT: 4.7kg

SCALE:1:5

SHEET 9 OF 16

Standard dimensions
for square pipe 80x40x4x620



A

B

C

D

A

B

C

D

ITEM NO.	PART TITLE	QTY.
9	Pipe 80x40x4x620	2

UNLESS OTHERWISE SPECIFIED:
DIMENSIONS ARE IN MILLIMETERS
SURFACE FINISH:
TOLERANCES: NS-ISO 2768-1 m
LINEAR:
ANGULAR:

FINISH:

DEBUR AND
BREAK SHARP
EDGES

DO NOT SCALE DRAWING

REVISION 1

University of Agder

DRAWN	NAME	SIGNATURE	DATE		Projection
CHK'D	LAE				
CHK'D	TB				

TITLE:

Pipe 80x40x4x620



MATERIAL:
S335J2H

DWG NO.

DWG.: F-110

A4

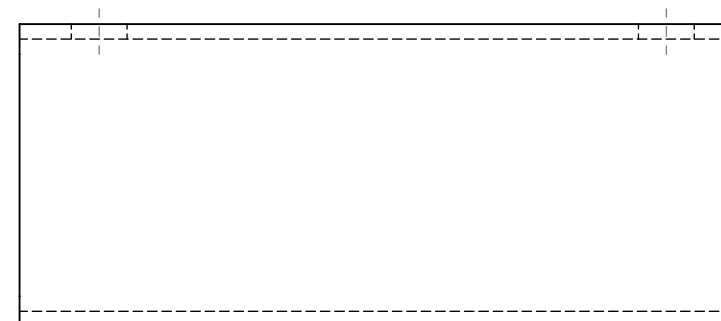
WEIGHT: 4.1kg

SCALE:1:5

SHEET 10 OF 16

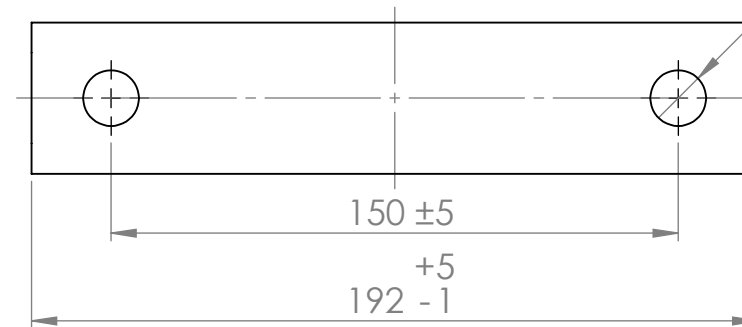
Standard dimensions
for square pipe 80x40x4

A



Ø14,75x2

B



C

D

ITEM NO.	PART TITLE	QTY.
10	Pipe Bracelet	2

UNLESS OTHERWISE SPECIFIED:
DIMENSIONS ARE IN MILLIMETERS
SURFACE FINISH:
TOLERANCES: NS-ISO 2768-1 m
LINEAR:
ANGULAR:

FINISH:

DEBUR AND
BREAK SHARP
EDGES

DO NOT SCALE DRAWING

REVISION 1

University of Agder

DRAWN	NAME	SIGNATURE	DATE	Projection	DEBUR AND BREAK SHARP EDGES
CHK'D	LAE				
CHK'D	TB				

TITLE:

Pipe Bracket



MATERIAL:
S335J2H

DWG NO.

DWG.: F-111

A4

1

2

3

4

5

6

A

A

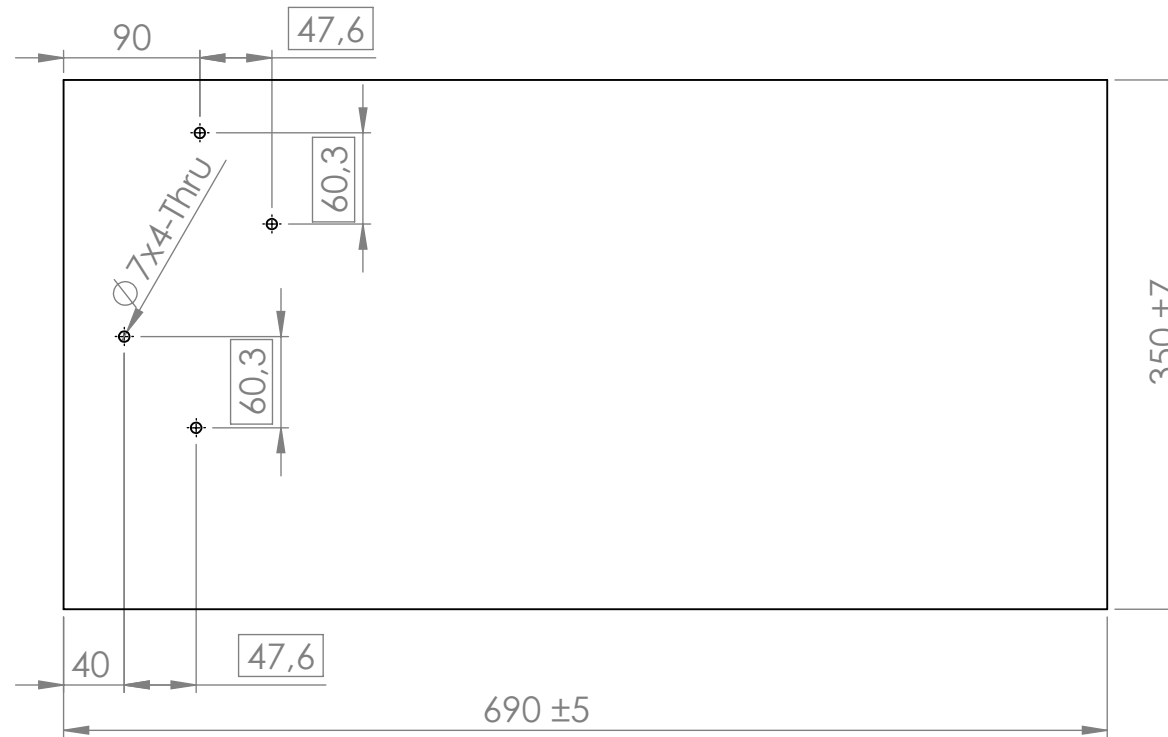
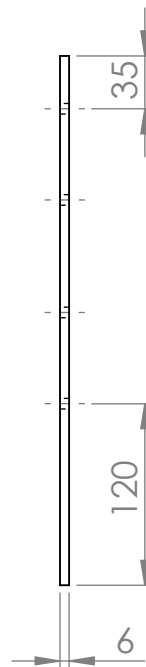
B

B

C

C

D



ITEM NO.	PART TITLE	QTY.
11	Control Panel	1

University of Agder

UNLESS OTHERWISE SPECIFIED:
DIMENSIONS ARE IN MILLIMETERS
SURFACE FINISH:
TOLERANCES: NS-ISO 2768-1 v
LINEAR:
ANGULAR:

FINISH:

DEBUR AND
BREAK SHARP
EDGES

DO NOT SCALE DRAWING

REVISION 1

DRAWN KLB

CHK'D LAE

CHK'D TB

NAME

SIGNATURE

DATE

DATE

SIGNATURE

DATE

Projection:



TITLE:

Control Panel

MATERIAL:

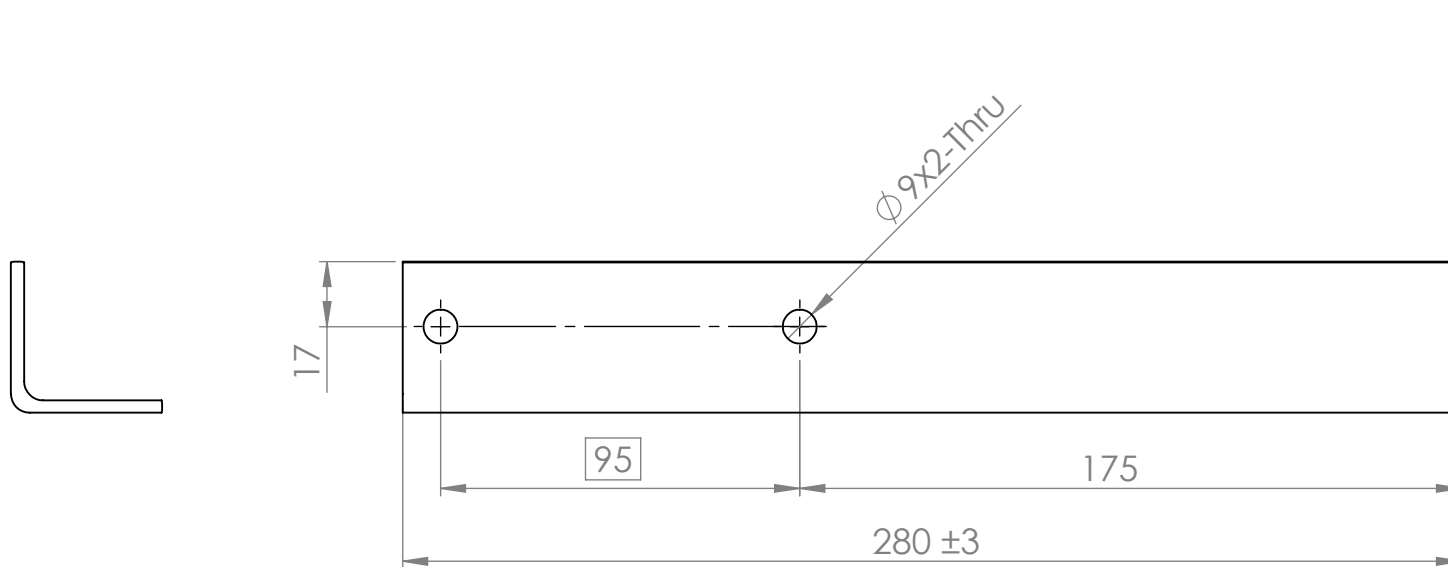
S235JR

DWG NO.

DWG.: F-112

A4

Standard dimensions
for angel iron 40x40x4



ITEM NO.	PART TITLE	QTY.
12	Angel Iron Support Left	1

UNLESS OTHERWISE SPECIFIED:
DIMENSIONS ARE IN MILLIMETERS
SURFACE FINISH:
TOLERANCES: NS-ISO 2768-1 m
LINEAR:
ANGULAR:

FINISH:

DEBUR AND
BREAK SHARP
EDGES

DO NOT SCALE DRAWING

REVISION 1

University of Agder

DRAWN	NAME	SIGNATURE	DATE		Projection:
CHK'D	LAE				
CHK'D	TB				

TITLE:

Angel Iron Support Left



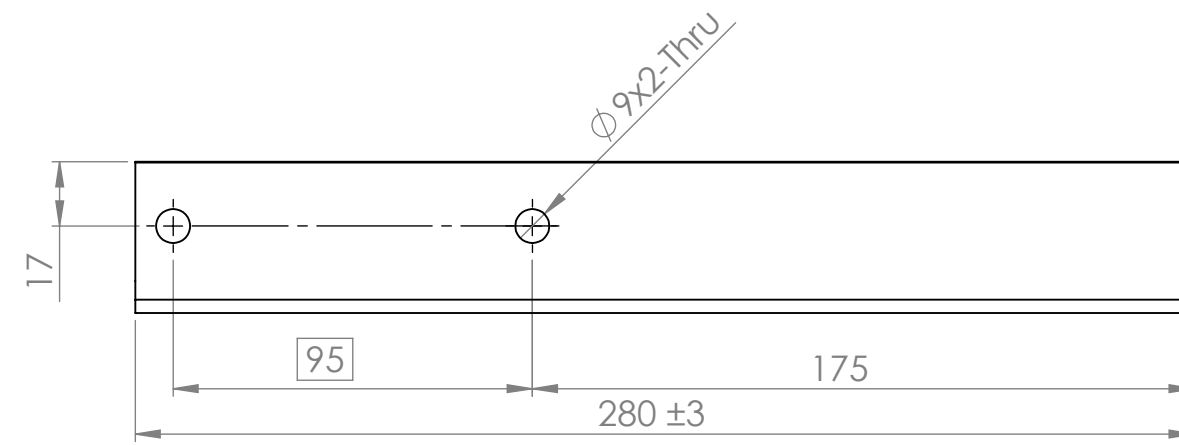
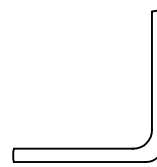
MATERIAL:
S235JR

DWG NO.

DWG.: F-113

A4

Standard dimensions
for angel iron 40x40x4



ITEM NO.	PART TITLE	QTY.
13	Angel Iron Support Right	1

UNLESS OTHERWISE SPECIFIED:
DIMENSIONS ARE IN MILLIMETERS
SURFACE FINISH:
TOLERANCES: NS-ISO 2768-1 m
LINEAR:
ANGULAR:

FINISH:

DEBUR AND
BREAK SHARP
EDGES

DO NOT SCALE DRAWING

REVISION 1

University of Agder

DRAWN	NAME KLB	SIGNATURE	DATE		Projection:
CHK'D	LAE				
CHK'D	TB				

TITLE:

Angel Iron Support Right



MATERIAL:
S235JR

DWG NO.

DWG.: F-114

A4

Standard dimensions
for iron flat bar 5x40

A

A

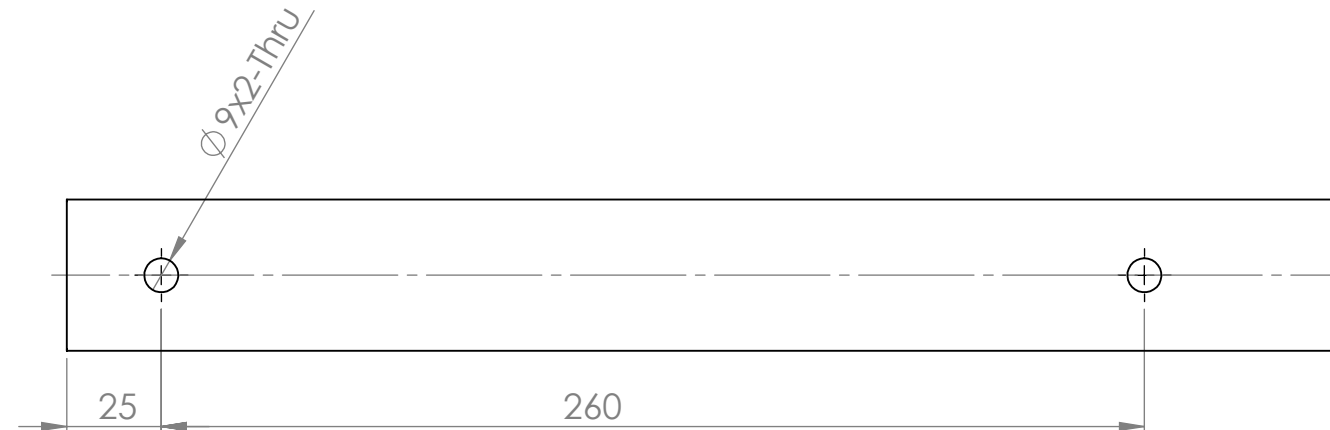
B

B

C

C

D



ITEM NO.	PART TITLE	QTY.
14	Bracket for Cabinet	2

UNLESS OTHERWISE SPECIFIED:
DIMENSIONS ARE IN MILLIMETERS
SURFACE FINISH:
TOLERANCES: NS-ISO 2768-1 c
LINEAR:
ANGULAR:

FINISH:

DEBUR AND
BREAK SHARP
EDGES

DO NOT SCALE DRAWING

REVISION

1

University of Agder

DRAWN	NAME	SIGNATURE	DATE		Projection:
CHK'D	LAE				
CHK'D	TB				

TITLE:

Bracket for Cabinet



MATERIAL:
S235JR

DWG NO.

DWG.: F-115

A4

WEIGHT: 0.5 kg

SCALE:1:2

SHEET 15 OF 16

Standard dimensions
for iron flat bar 5x40

A

A

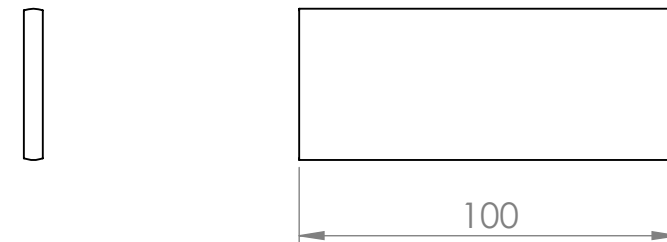
B

B

C

C

D



ITEM NO.	PART TITLE	QTY.
15	Bracket for Pipelines	3

UNLESS OTHERWISE SPECIFIED:
DIMENSIONS ARE IN MILLIMETERS
SURFACE FINISH:
TOLERANCES: NS-ISO 2768-1 v
LINEAR:
ANGULAR:

FINISH:

DEBUR AND
BREAK SHARP
EDGES

DO NOT SCALE DRAWING

REVISION

1

University of Agder

DRAWN	NAME	SIGNATURE	DATE		Projection:
CHK'D	LAE				
CHK'D	TB				

TITLE:

Bracket for Pipelines



MATERIAL:	S235JR	DWG NO.

DWG.: F-116

A4

WEIGHT: 0.2 kg

SCALE:1:2

SHEET 16 OF 16

Gear-Motor Connection Parts

Bachelor project

MAS302

University of Agder, 2013

Faculty of Engineering and Science

Department of Mechatronics

1

2

3

4

5

6

A

A

B

B

C

C

D

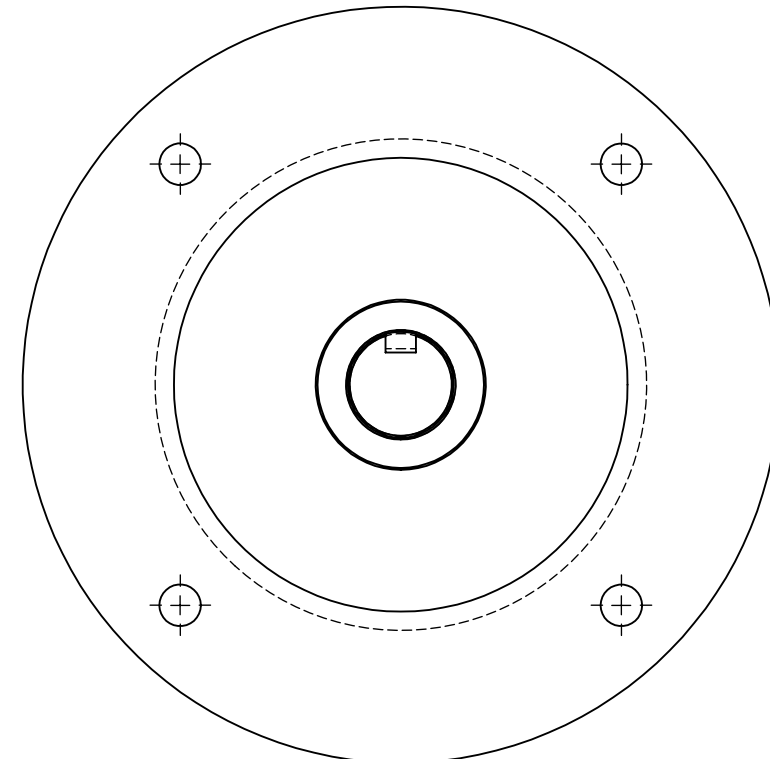
1

2

3

(193,7)

(ϕ 200)



ITEM NO.	PART TITLE	DWG NO.:	QTY.
1	Shaft between gear and motor	C-102	2
2	Gear-Motor Connection Drum	C-103	2
3	Gear-Motor Connection Side Plate	C-104	4

UNLESS OTHERWISE SPECIFIED:
DIMENSIONS ARE IN MILLIMETERS
SURFACE FINISH:
TOLERANCES: NS-ISO 2768-1 m
LINEAR:
ANGULAR:

FINISH:
Brush after welding

DEBUR AND
BREAK SHARP
EDGES

DO NOT SCALE DRAWING

REVISION

1

University of Agder

DRAWN	NAME	SIGNATURE	DATE		Projection:
CHK'D	LAE				
CHK'D	TB				

TITLE:

**Gear-Motor Connection,
assembly**



MATERIAL:	S235JR
-----------	--------

DWG NO.

DWG.: C-101

A4

1

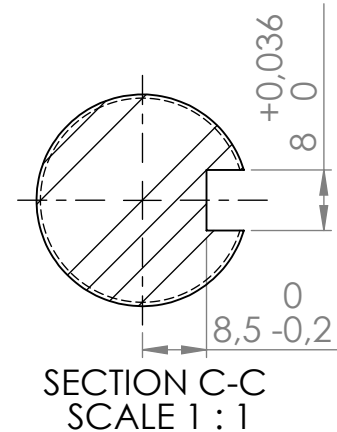
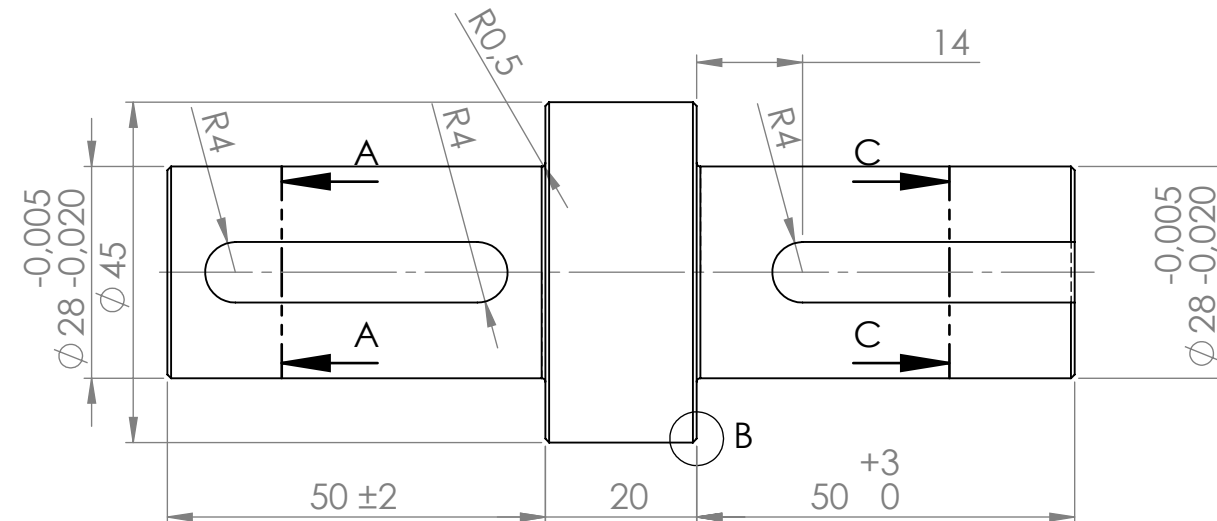
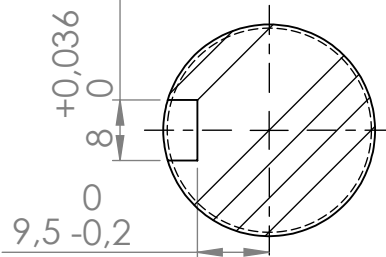
2

WEIGHT: 5.6kg

SCALE:1:2

SHEET 1 OF 4

A



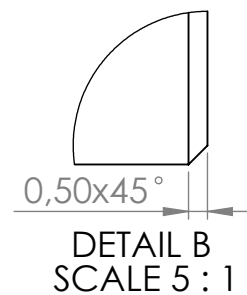
B

B

C

C

All edges have
to be chamfered



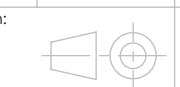
UNLESS OTHERWISE SPECIFIED:
DIMENSIONS ARE IN MILLIMETERS
SURFACE FINISH:
TOLERANCES: NS-ISO 2768-1 m
LINEAR:
ANGULAR:

FINISH:

DRAWN KLB
CHK'D LAE
CHK'D TB

DATE

ITEM NO.	PART TITLE	QTY.
1	Shaft between gear and motor	2



DO NOT SCALE DRAWING

REVISION

1

University of Agder

TITLE:

**Shaft between gear and
motor**



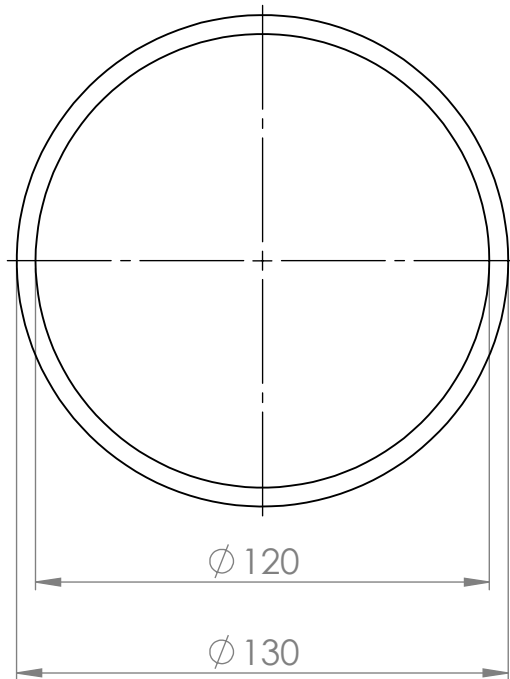
MATERIAL:
S235JR

DWG NO.

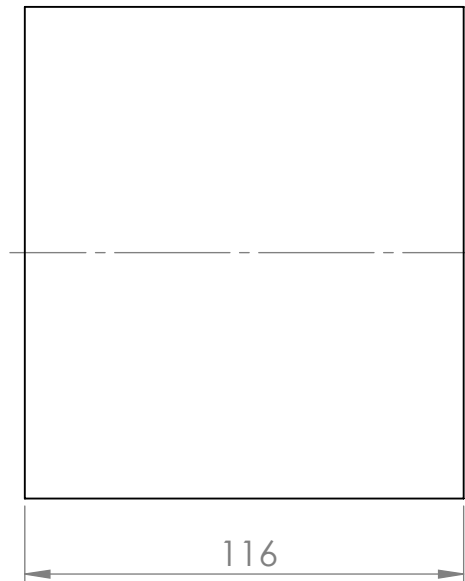
DWG.: C-102

A4

A



B



A

C

ITEM NO.	PART TITLE	QTY.
2	Gear-Motor Connection Drum	2

UNLESS OTHERWISE SPECIFIED:
DIMENSIONS ARE IN MILLIMETERS
SURFACE FINISH:
TOLERANCES: NS-ISO 2768-1 m
LINEAR:
ANGULAR:

FINISH:

DEBUR AND
BREAK SHARP
EDGES

DO NOT SCALE DRAWING

REVISION

1

University of Agder

DRAWN	NAME	SIGNATURE	DATE	Projection:
CHK'D	LAE			
CHK'D	TB			

TITLE:

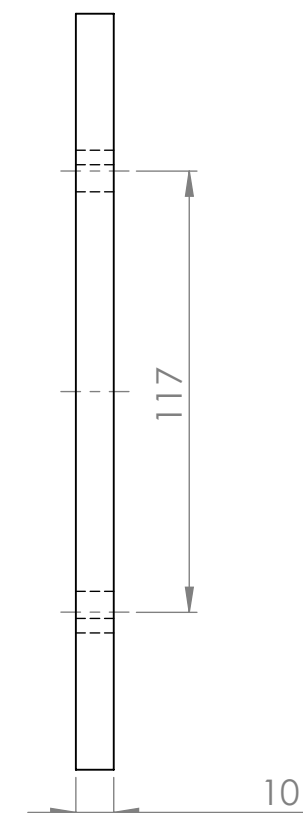
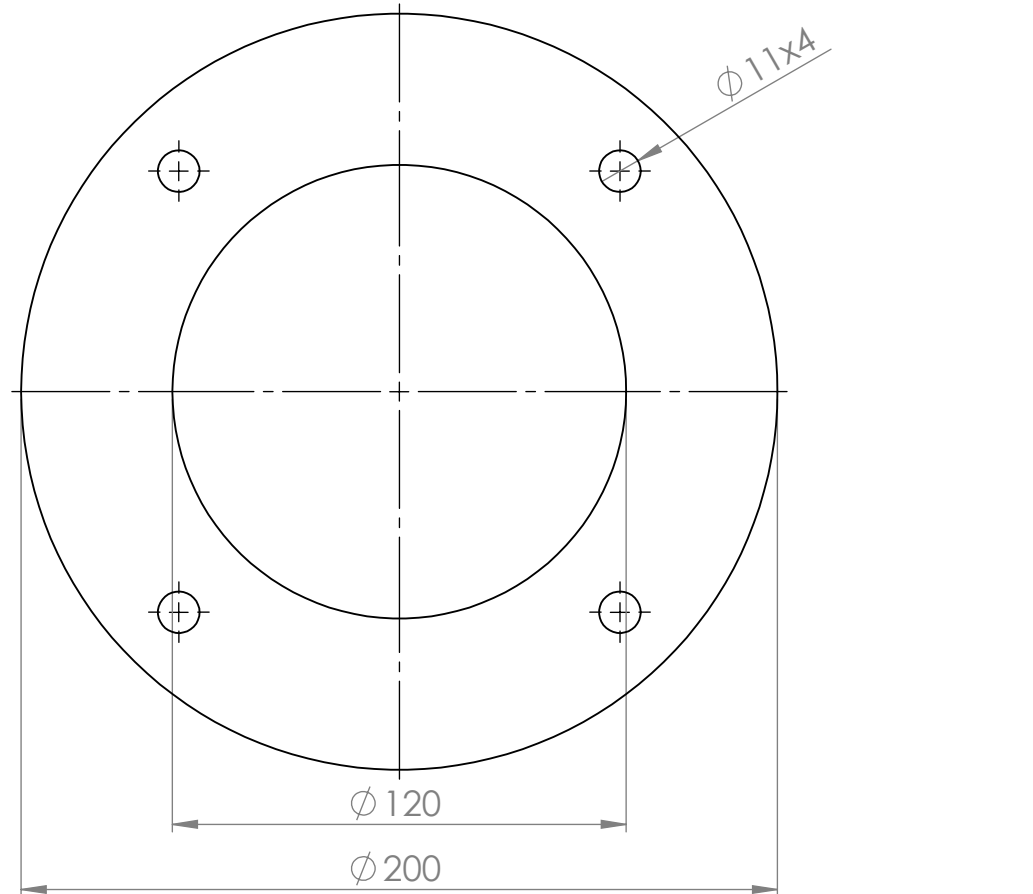
**Gear-Motor Connection
Drum**

MATERIAL:
S235JR

DWG NO.

DWG.: C-103

A4



ITEM NO.	PART TITLE	QTY.
3	Gear-Motor Connection Side Plate	4

UNLESS OTHERWISE SPECIFIED:
DIMENSIONS ARE IN MILLIMETERS
SURFACE FINISH:
TOLERANCES: NS-ISO 2768-1 m
LINEAR:
ANGULAR:

FINISH:

DRAWN	NAME	SIGNATURE	DATE	
CHK'D	LAE			
CHK'D	TB			

Projection:



DEBUR AND
BREAK SHARP
EDGES

DO NOT SCALE DRAWING

REVISION

1

University of Agder

**Gear-Motor Connection
Side Plate**



MATERIAL:
S235JR

DWG NO.

DWG.: C-104

A4

WEIGHT: 1.5kg

SCALE:1:2

SHEET 4 OF 4

Drum Parts

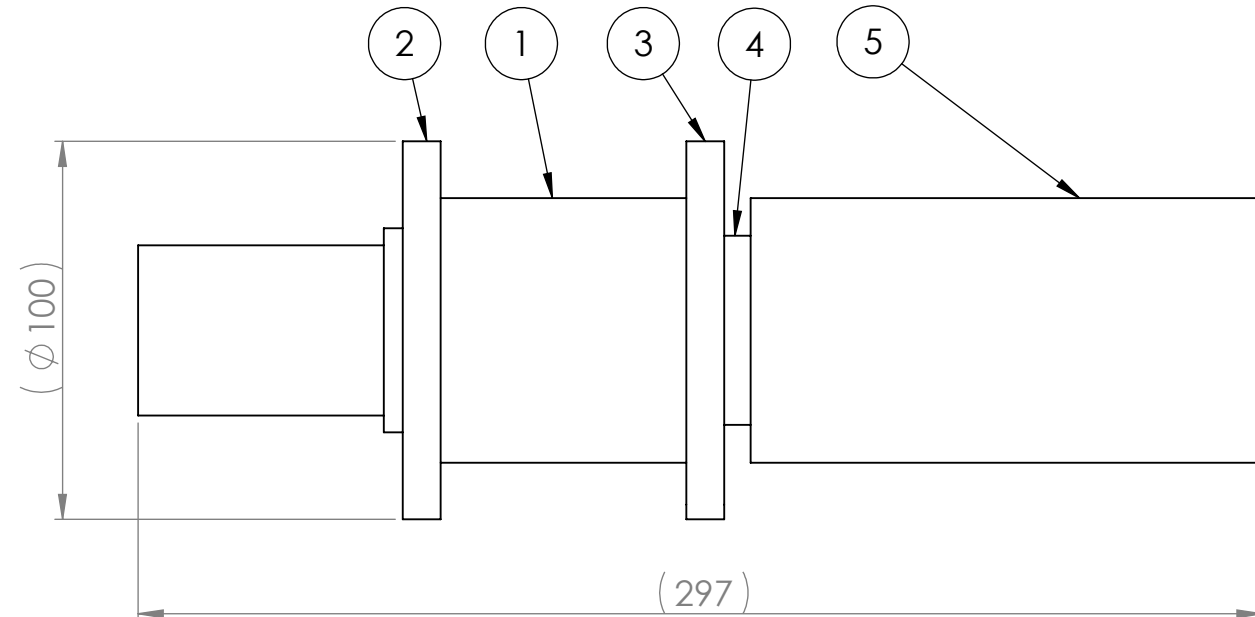
Bachelor project

MAS302

University of Agder, 2013

Faculty of Engineering and Science

Department of Mechatronics



ITEM NO.	PART TITLE	DWG NO.:	QTY.
1	Drum	D-102	2
2	Drum Side Plate Holed	D-103	2
3	Drum Side Plate	D-104	2
4	Shaft Through Drum	D-105	2
5	Sleeve	D-106	2

UNLESS OTHERWISE SPECIFIED:
DIMENSIONS ARE IN MILLIMETERS
SURFACE FINISH:
TOLERANCES: NS-ISO 2768-1 m
LINEAR:
ANGULAR:

FINISH:

DEBUR AND
BREAK SHARP
EDGES

DO NOT SCALE DRAWING

REVISION 1

University of Agder

DRAWN	NAME	SIGNATURE	DATE		Projection:
CHK'D	LAE				
CHK'D	TB				

TITLE:

Drum, assembly

MATERIAL:	DWG NO.

DWG.: D-101

A4

A

A

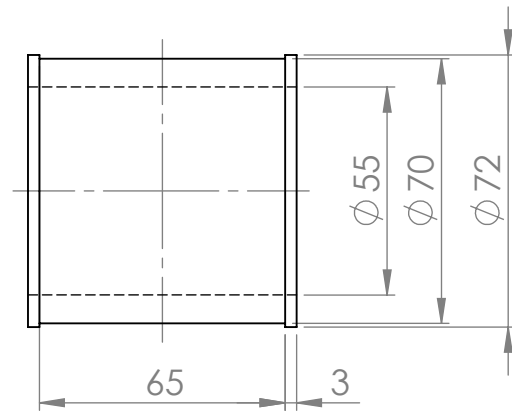
B

B

C

C

D



ITEM NO.	PART TITLE	QTY.
1	Drum	2

UNLESS OTHERWISE SPECIFIED:
DIMENSIONS ARE IN MILLIMETERS
SURFACE FINISH:
TOLERANCES: NS-ISO 2768-1 m
LINEAR:
ANGULAR:

FINISH:

DEBUR AND
BREAK SHARP
EDGES

DO NOT SCALE DRAWING

REVISION 1

University of Agder

DRAWN	NAME	SIGNATURE	DATE		Projection:
CHK'D	LAE				
CHK'D	TB				

TITLE:
Drum



MATERIAL:
S235JR

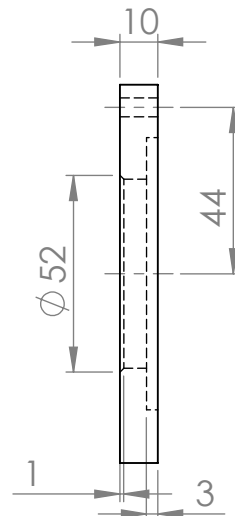
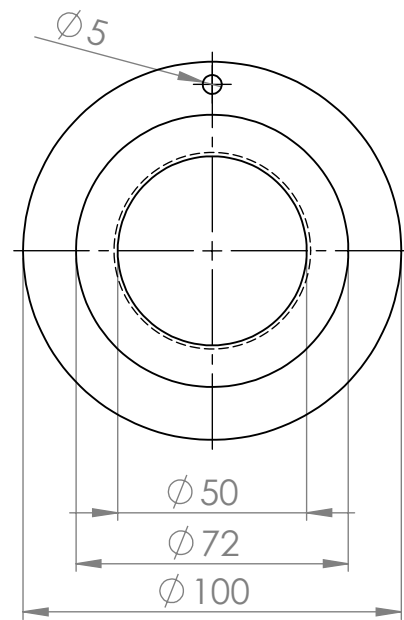
DWG NO.

DWG.: D-102

A4

A

A



E

B

6

C

ITEM NO.	PART TITLE	QTY.
2	Drum Side Plate Holed	2

UNLESS OTHERWISE SPECIFIED:
DIMENSIONS ARE IN MILLIMETERS
SURFACE FINISH:
TOLERANCES: NS-ISO 2768-1 m
LINEAR:
ANGULAR:

FINISH

DEBUR AND BREAK SHARP EDGES

DO NOT SCALE DRAWINGS

三

३

University of Agder

TITLE: **Drum Side Plate Holed Side Plate Holed**

	NAME	SIGNATURE	DATE	Projection: 
DRAWN	KLB			
CHK'D	LAE			

DWG NC

DWG.: D-103

A4

1

2

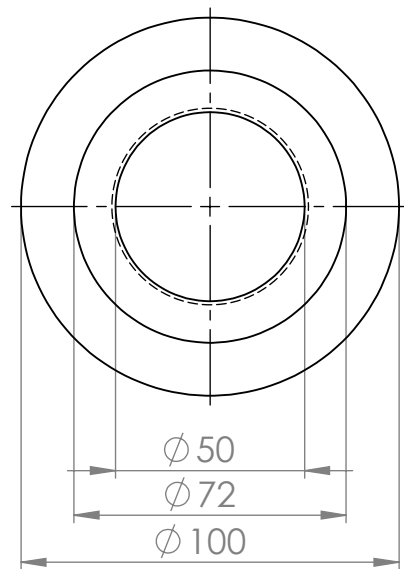
WEIGHT: 0.4kg

S235JR

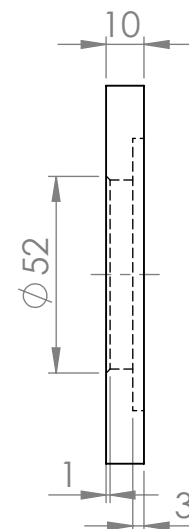
SCALE 1:2

SHEET 3 OF 6

A



B



C

ITEM NO.	PART TITLE	QTY.
2	Drum Side Plate	2

UNLESS OTHERWISE SPECIFIED:
DIMENSIONS ARE IN MILLIMETERS
SURFACE FINISH:
TOLERANCES: NS-ISO 2768-1 m
LINEAR:
ANGULAR:

FINISH:

DEBUR AND
BREAK SHARP
EDGES

DO NOT SCALE DRAWING

REVISION 1

University of Agder

DRAWN	NAME	SIGNATURE	DATE		Projection:
CHK'D	LAE				
CHK'D	TB				

TITLE:

Drum Side Plate Side Plate

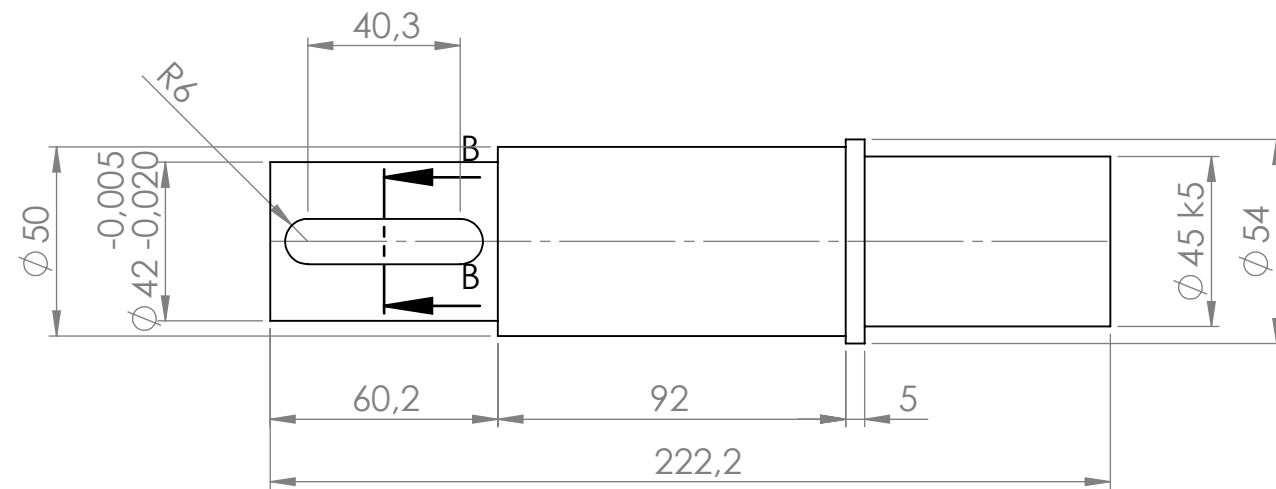
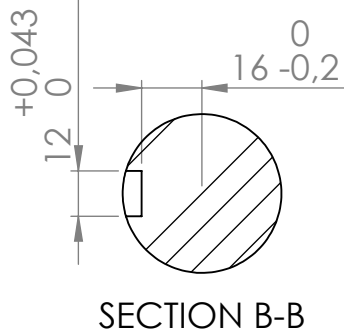
MATERIAL:
S235JR

DWG NO.

DWG.: D-104

A4

1 2 3 4 5 6



ITEM NO.	PART TITLE	QTY.
4	Shaft Through Drum	2

UNLESS OTHERWISE SPECIFIED:
DIMENSIONS ARE IN MILLIMETERS
SURFACE FINISH:
TOLERANCES: NS-ISO 2768-1 f
LINEAR:
ANGULAR:

FINISH:

DEBUR AND
BREAK SHARP
EDGES

DO NOT SCALE DRAWING

REVISION

1

University of Agder

DRAWN	NAME KLB	SIGNATURE	DATE	Projection:
CHK'D	LAE			
CHK'D	TB			

TITLE:

Shaft Through Drum

MATERIAL:	S235JR	DWG NO.
-----------	--------	---------

DWG.: D-105

A4

1

2

WEIGHT: 2.9kg

SCALE:1:2

SHEET 5 OF 6

A

A

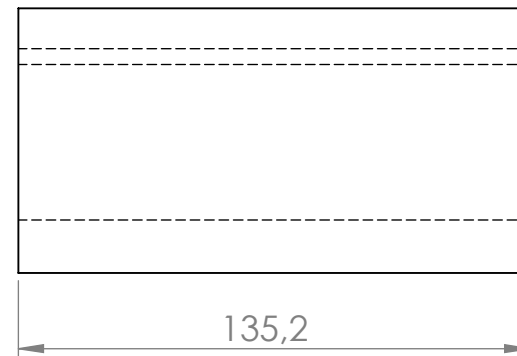
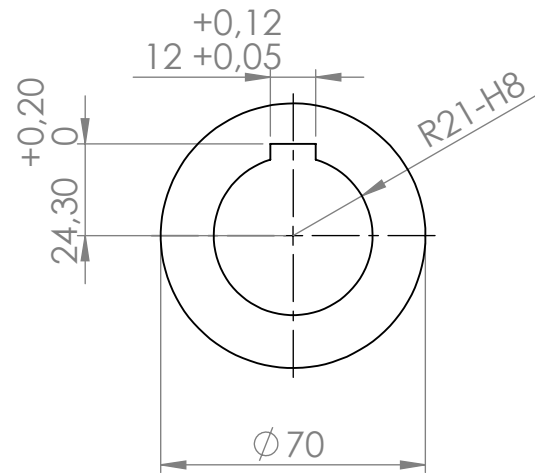
B

B

C

C

D



ITEM NO.	PART TITLE	QTY.
5	Sleeve	2

UNLESS OTHERWISE SPECIFIED:
DIMENSIONS ARE IN MILLIMETERS
SURFACE FINISH:
TOLERANCES: NS-ISO 2768-1 m
LINEAR:
ANGULAR:

FINISH:

DEBUR AND
BREAK SHARP
EDGES

DO NOT SCALE DRAWING

REVISION 1

University of Agder

DRAWN	NAME	SIGNATURE	DATE	Projection:
	KLB			
CHK'D	LAE			
CHK'D	TB			

TITLE:
Sleeve



MATERIAL:
S235JR

DWG NO.

DWG.: D-106

A4

WEIGHT: 2.6kg

SCALE:1:2

SHEET 6 OF 6

Beam Parts

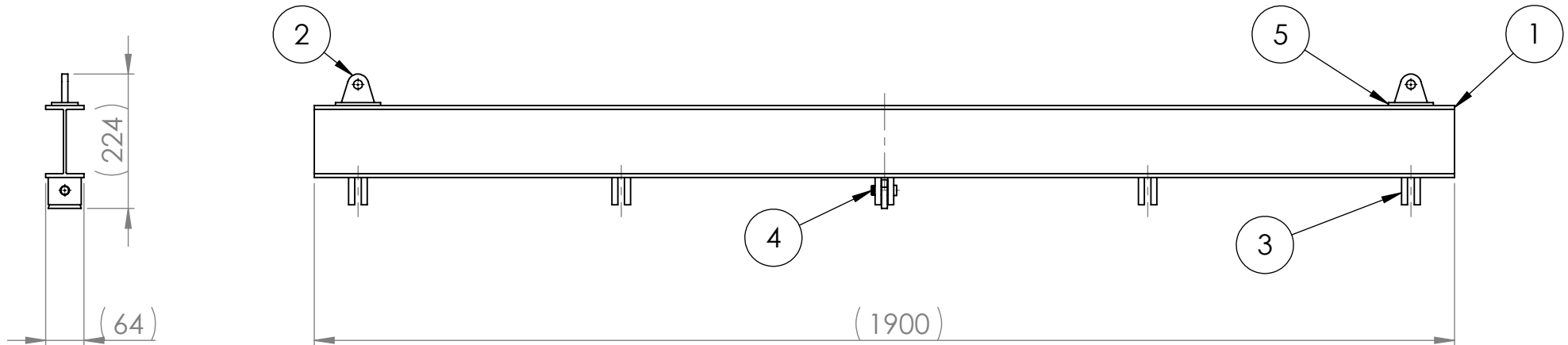
Bachelor project

MAS302

University of Agder, 2013

Faculty of Engineering and Science

Department of Mechatronics



ITEM NO.	PART TITLE	DWG NO.:	QTY.
1	Beam	B-102	1
2	Lifting Eye	B-103	3
3	Lifting Plate	B-104	10
4	Lock Shaft	B-105	1
5	Beam bracket	B-106	2

UNLESS OTHERWISE SPECIFIED:
 DIMENSIONS ARE IN MILLIMETERS
 SURFACE FINISH:
 TOLERANCES: NS-ISO 2768-1 m
 LINEAR:
 ANGULAR:

FINISH:

Black, Hammerlack
 Art. 36-023 Biftema

DEBUR AND
 BREAK SHARP
 EDGES

DO NOT SCALE DRAWING

REVISION

1

University of Agder

DRAWN	NAME	SIGNATURE	DATE		Projection:
CHK'D	LAE				
CHK'D	TB				

TITLE:

Beam Assembly



MATERIAL:

DWG NO.

DWG.: B-101

A4

Standard dimensions
for IPE 120 beam

A

A

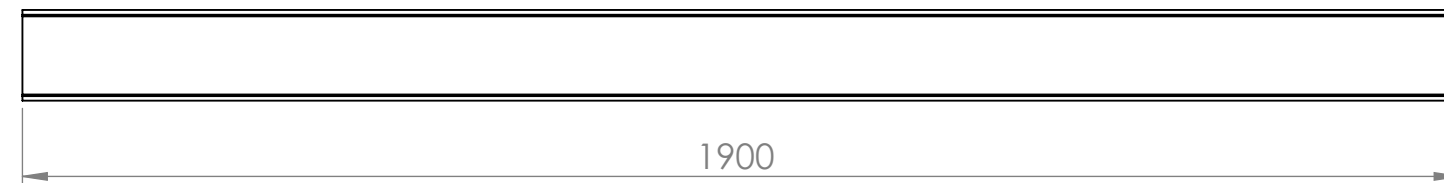
B

B

C

C

D



1900

ITEM NO.	PART TITLE	QTY.
1	Beam	1

DO NOT SCALE DRAWING REVISION 1

University of Agder

UNLESS OTHERWISE SPECIFIED: DIMENSIONS ARE IN MILLIMETERS SURFACE FINISH: TOLERANCES: NS-ISO 2768-1 v LINEAR: ANGULAR:		FINISH:			DEBUR AND BREAK SHARP EDGES	TITLE: Beam	
DRAWN	NAME KLB	SIGNATURE	DATE		Projection:		
CHK'D	LAE						
CHK'D	TB						
					MATERIAL: S355J2+M	DWG NO. DWG.: B-102	
						SCALE:1:10	
					WEIGHT: 19.0kg	SHEET 2 OF 6	
						A4	

A

A

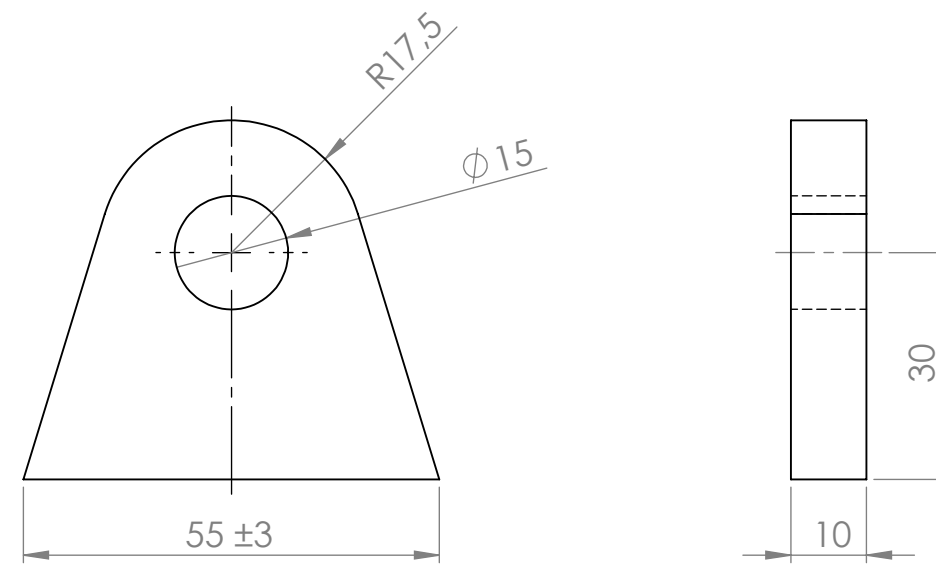
B

B

C

C

D



ITEM NO.	PART TITLE	QTY.
2	Lifting Eye	3

UNLESS OTHERWISE SPECIFIED:
DIMENSIONS ARE IN MILLIMETERS
SURFACE FINISH:
TOLERANCES: NS-ISO 2768-1 v
LINEAR:
ANGULAR:

FINISH:

DEBUR AND
BREAK SHARP
EDGES

DO NOT SCALE DRAWING

REVISION 1

University of Agder

DRAWN	NAME	SIGNATURE	DATE		Projection:
CHK'D	LAE				
CHK'D	TB				

TITLE:

Lifting Eye

MATERIAL:
S235JR

DWG NO.

DWG.: B-103

A4

A

A

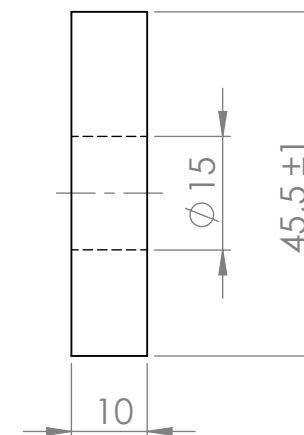
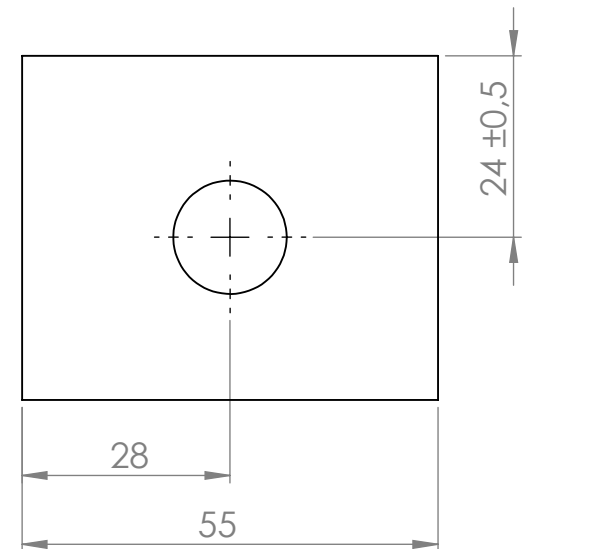
B

B

C

C

D



ITEM NO.	PART TITLE	QTY.
3	Lifting Plate	10

UNLESS OTHERWISE SPECIFIED:
DIMENSIONS ARE IN MILLIMETERS
SURFACE FINISH:
TOLERANCES: NS-ISO 2768-1 v
LINEAR:
ANGULAR:

FINISH:

DEBUR AND
BREAK SHARP
EDGES

DO NOT SCALE DRAWING

REVISION

1

University of Agder

DRAWN	NAME	SIGNATURE	DATE		Projection:
CHK'D	LAE				
CHK'D	TB				

TITLE:

Lifting Plate



MATERIAL:
S235JR

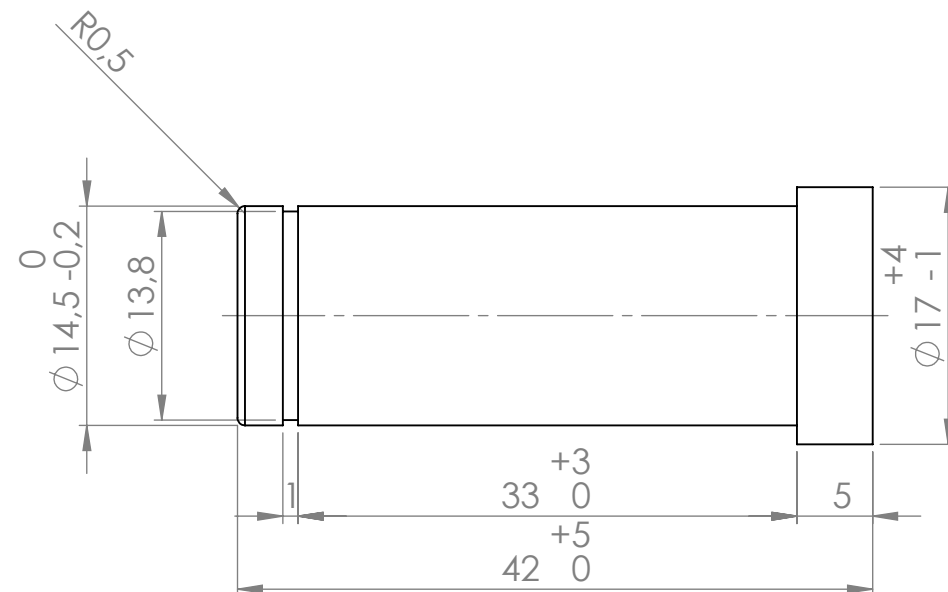
DWG NO.

DWG.: B-104

A4

A

A



B

B

C

C

ITEM NO.	PART TITLE	QTY.
4	Lock Shaft	1

UNLESS OTHERWISE SPECIFIED:
DIMENSIONS ARE IN MILLIMETERS
SURFACE FINISH:
TOLERANCES: NS-ISO 2768-1 m
LINEAR:
ANGULAR:

FINISH:

DEBUR AND
BREAK SHARP
EDGES

DO NOT SCALE DRAWING

REVISION 1

University of Agder

DRAWN	NAME	SIGNATURE	DATE	Projection:
CHK'D	LAE			
CHK'D	TB			

TITLE:

Lock Shaft



MATERIAL:
S235JR

DWG NO.

DWG.: B-105

A4

A

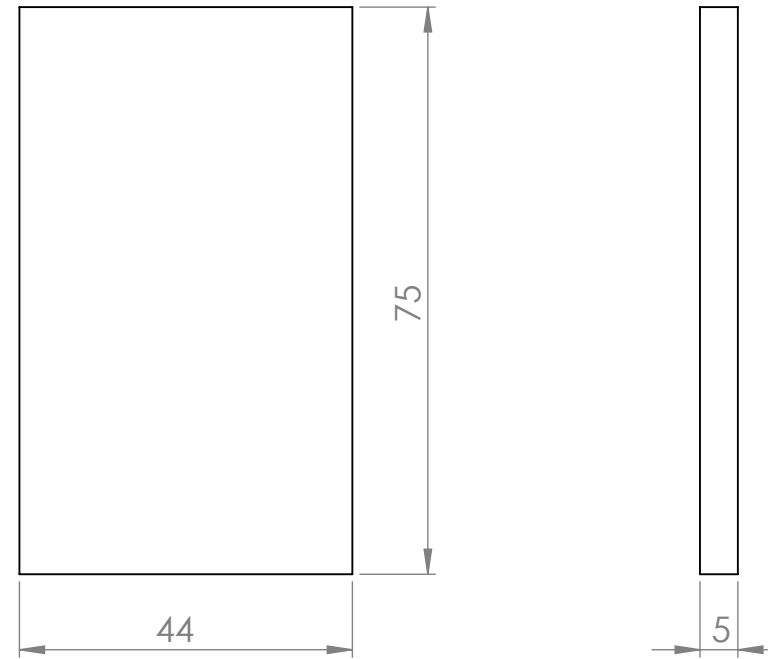
A

B

B

C

C



ITEM NO.	PART TITLE	QTY.
5	Beam Bracket	2

UNLESS OTHERWISE SPECIFIED:
DIMENSIONS ARE IN MILLIMETER.
SURFACE FINISH:
TOLERANCES: NS-ISO 2768-1 v
LINEAR:
ANGULAR:

FINISH

DEBUR AND BREAK SHAR EDGES

DO NOT SCALE DRAWING

REVISION 1

University of Agder



	NAME	SIGNATURE	DATE	Projection:
DRAWN	KLB			
CHK'D	LAE			
CHK'D	TB			

TITL

Beam Bracket

DWG.: B-106

A4

1

2

WEIGHT: 0.01kg

SCALE 1:1

SHEET 6 OF 6

Frame Assembly

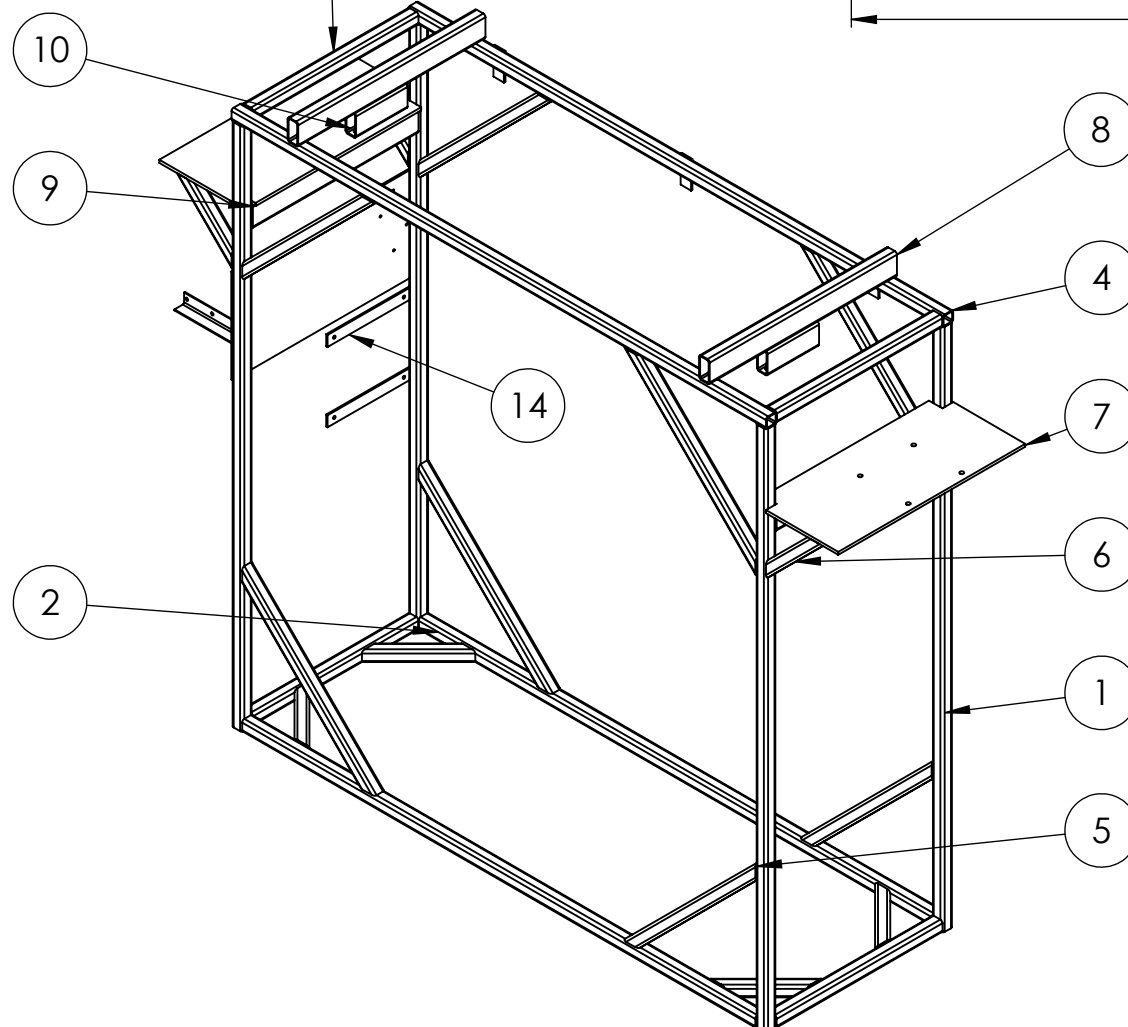
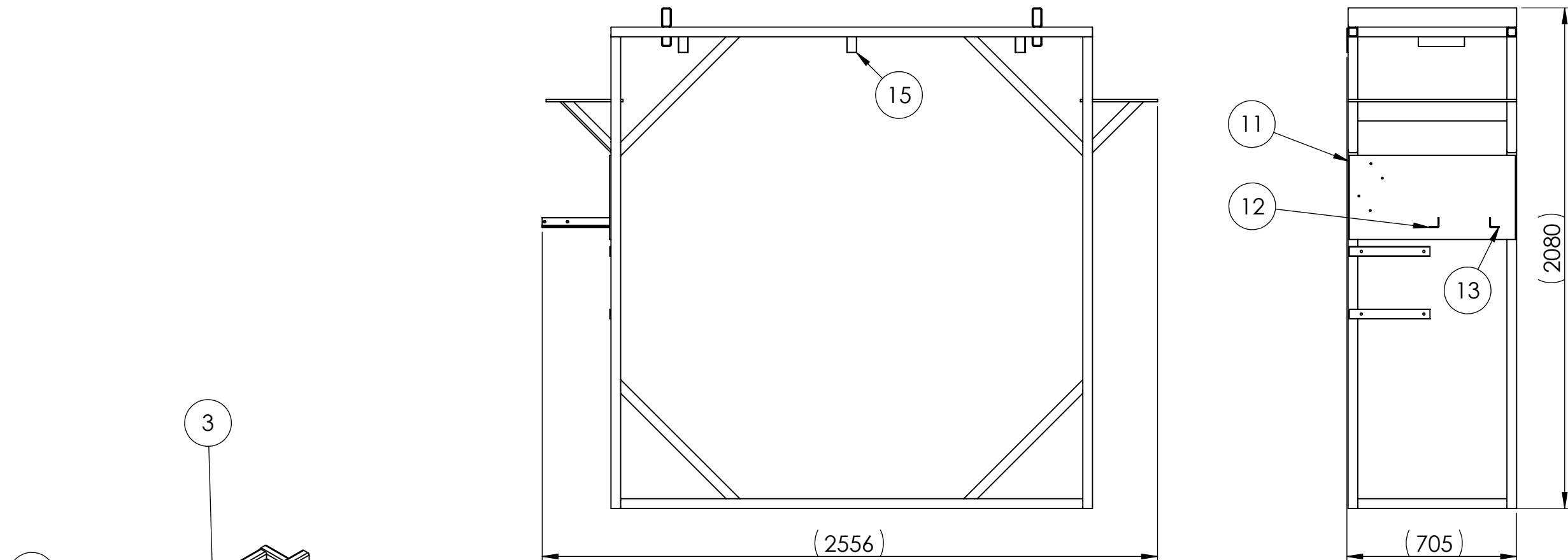
Bachelor project

MAS302

University of Agder, 2013

Faculty of Engineering and Science

Department of Mechatronics



ITEM NO.	PART TITLE	DWG NO.:	QTY.
1	Pipe Leg	F-102	4
2	Pipe Bottom Length	F-103	2
3	Pipe Width	F-104	4
4	Pipe Top Length	F-105	2
5	Pipe Support Long	F-106	8
6	Pipe Support Short	F-107	8
7	Support Plate Horizontal	F-108	2
8	Pipe Support Top	F-109	2
9	Pipe 40x80x4x620	F-110	2
10	Pipe Bracket	F-111	2
11	Control Panel	F-112	1
12	Angel Iron Support Left	F-113	1
13	Angel Iron Support Right	F-114	1
14	Bracket for Cabinet	F-115	2
15	Bracket for Pipelines	F-116	3

UNLESS OTHERWISE SPECIFIED;
DIMENSIONS ARE IN MILLIMETERS
SURFACE FINISH:
TOLERANCES: NS-ISO 2768-1 m
LINEAR:
ANGULAR:

FINISH:
Dark Blue, Hammerlack
Art. 36-042 Biltema

DEBUR AND
BREAK SHARP
EDGES

DO NOT SCALE DRAWING

REVISION 1

University of Agder

DRAWN	NAME	SIGNATURE	DATE	Projection:
CHK'D	LAE			
CHK'D	TB			
MATERIAL:			DWG NO.	
WEIGHT: 174.8kg			SCALE: 1:20	

**Synchronous Motor Drive,
Frame**

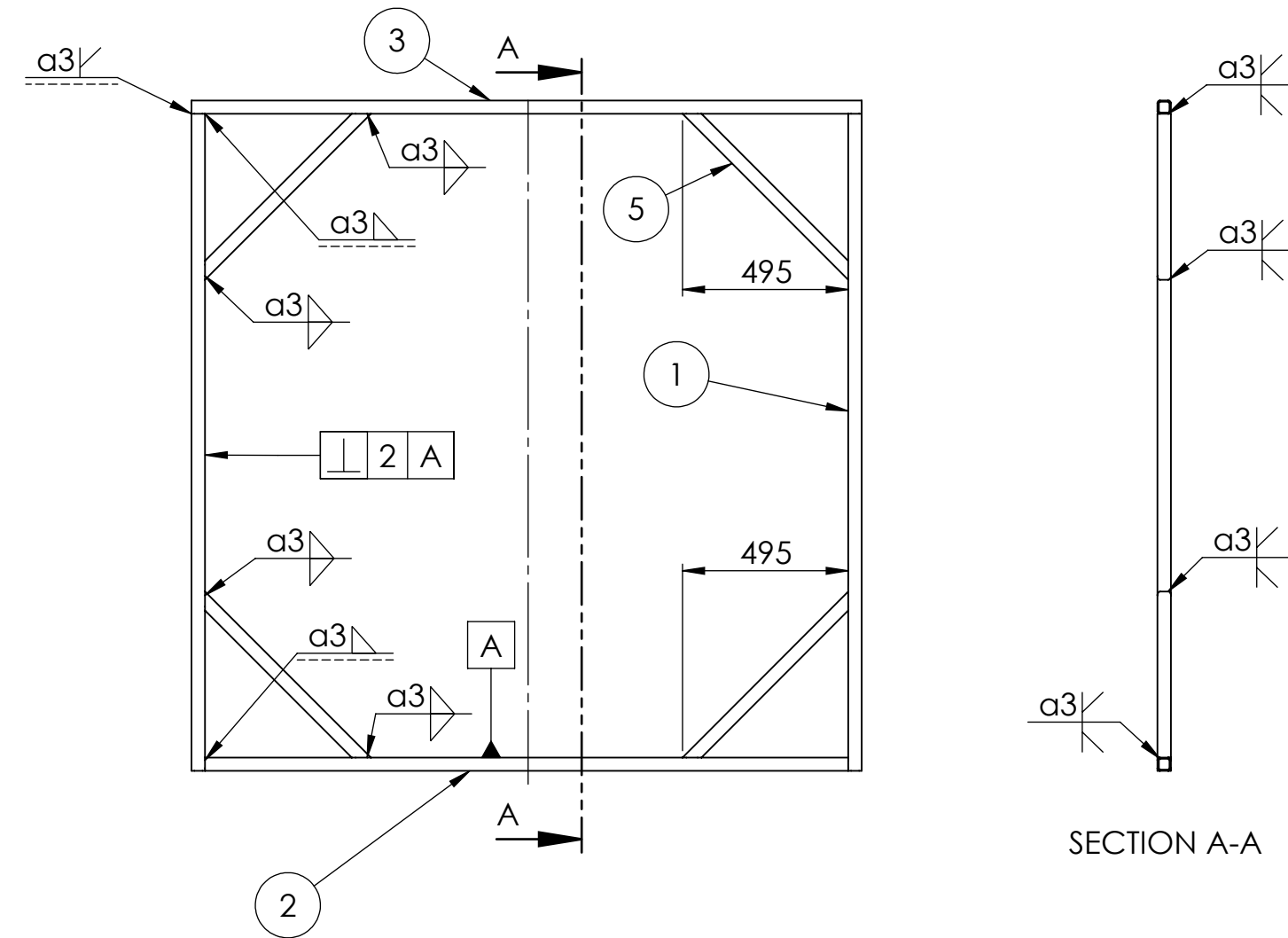


DWG.: W-F-101

A3

SHEET 1 OF 11

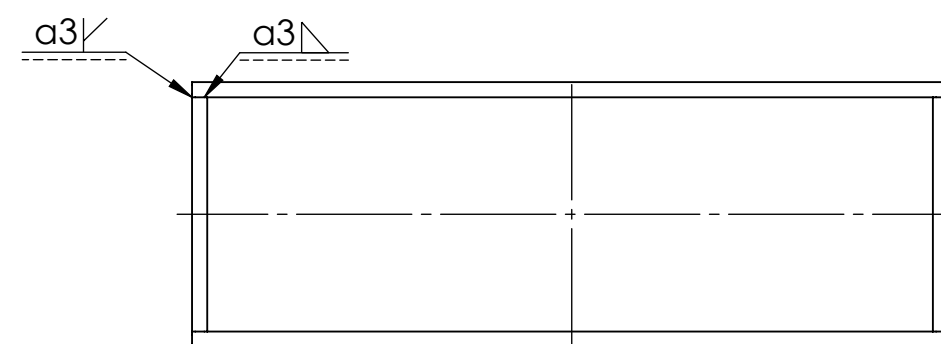
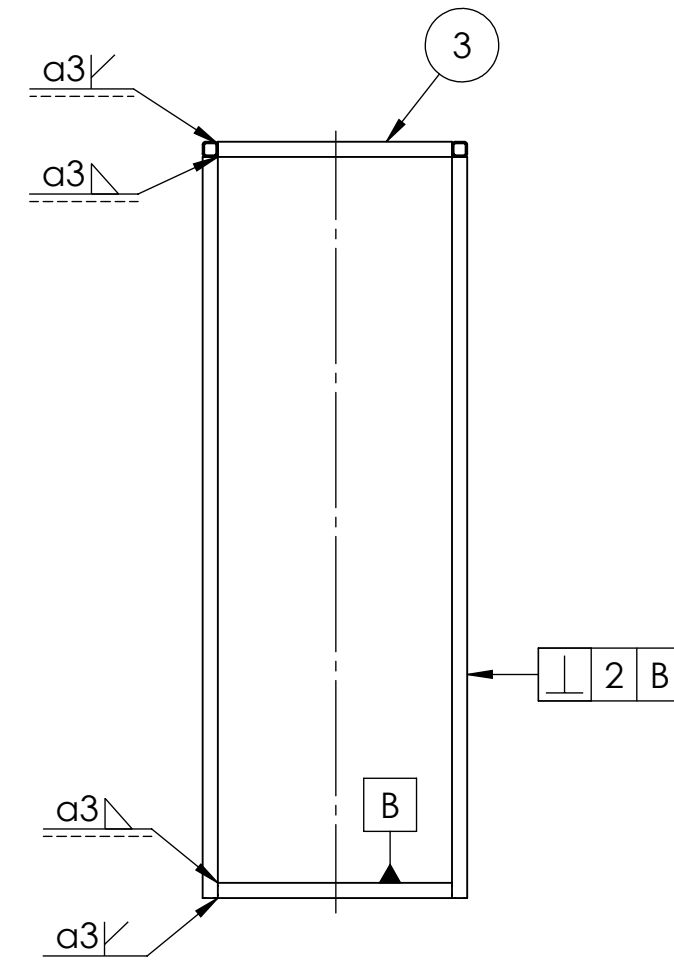
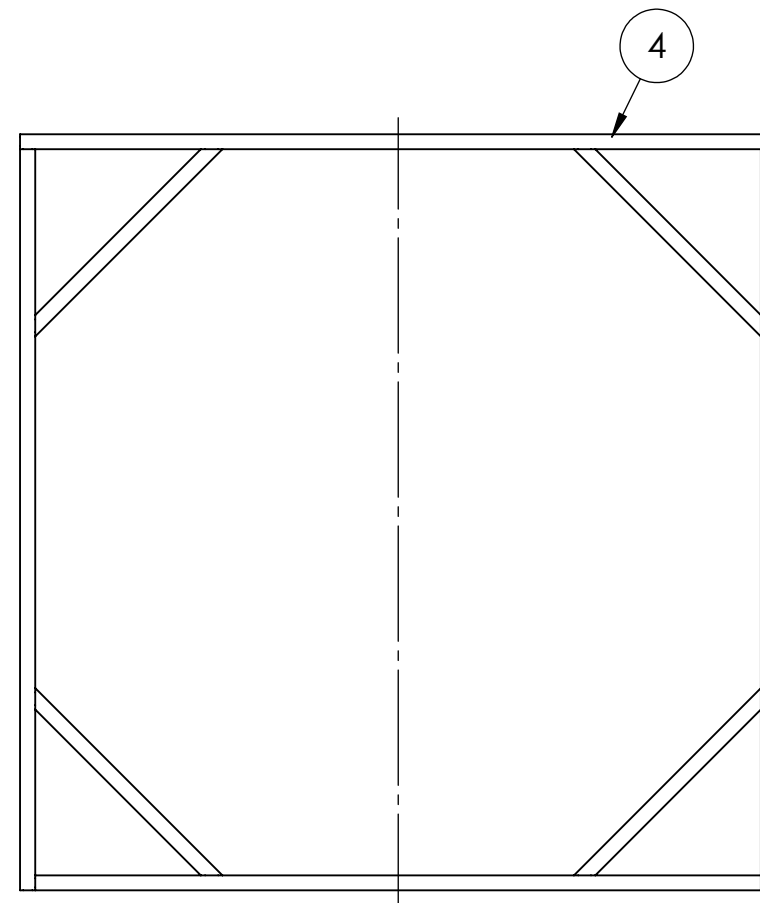
ITEM NO.	PART TITLE	DWG NO.:	QTY.
14	F/B-Frame	W-F-102	2



ITEM NO.	PART TITLE	DWG NO.:	QTY.
1	Pipe Leg	F-102	4
2	Pipe Bottom Length	F-102	2
4	Pipe Top Length	F-105	2
5	Pipe Support Long	F-106	8

UNLESS OTHERWISE SPECIFIED; DIMENSIONS ARE IN MILLIMETERS SURFACE FINISH: TOLERANCES: NS-ISO 2768-1 m LINEAR: ANGULAR:		FINISH: Dark Blue, Hammerlack Art. 36-042 Biltema	DEBUR AND BREAK SHARP EDGES	DO NOT SCALE DRAWING	REVISION 1
University of Agder					
DRAWN	NAME KLB	SIGNATURE	DATE	Projection: 	TITLE: F/B-Frame
CHK'D	LAE				
CHK'D	TB				
			MATERIAL:	DWG NO.	
				DWG.: W-F-102	
			WEIGHT: 43.7kg	SCALE: 1:20	A3
SHEET 2 OF 11					

ITEM NO.	PART TITLE	DWG NO.:	QTY.
15	Main Frame w/Pipe Width	W-F-103	1



ITEM NO.	PART TITLE	DWG NO.:	QTY.
3	Pipe Width	F-104	4
14	F/B-Frame	W-F-102	2

UNLESS OTHERWISE SPECIFIED:
DIMENSIONS ARE IN MILLIMETERS
SURFACE FINISH:
TOLERANCES: NS-ISO 2768-1 m
LINEAR:
ANGULAR:

FINISH: Dark Blue, Hammerlack Art. 36-042 Biltema

DEBUR AND BREAK SHARP EDGES

DO NOT SCALE DRAWING

REVISION 1

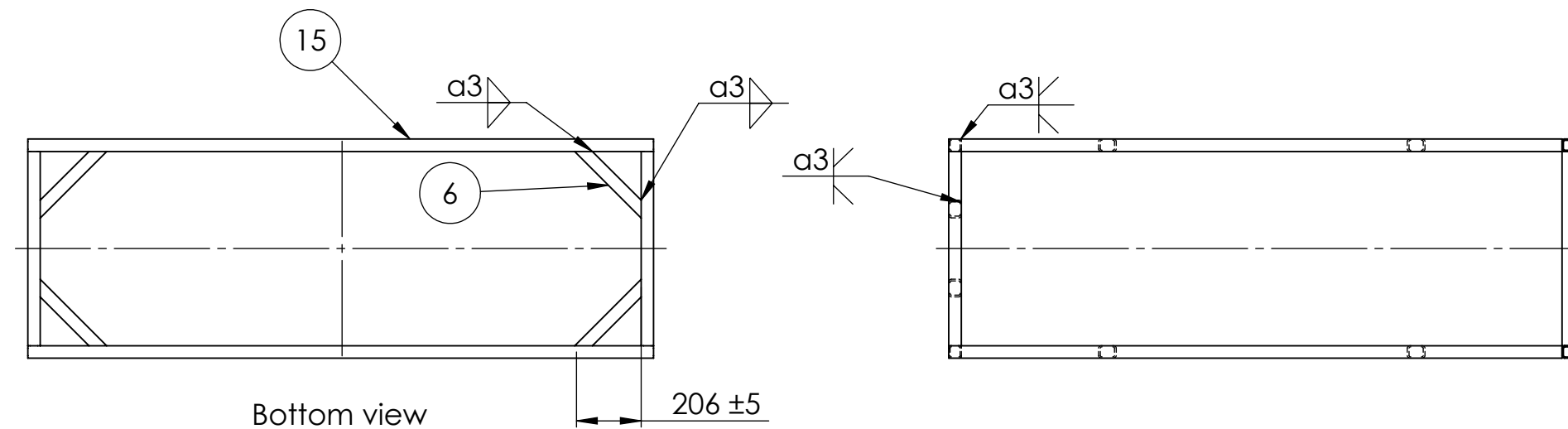
University of Agder

DRAWN	NAME	SIGNATURE	DATE	Projection:
CHK'D	LAE			
CHK'D	TB			
				MATERIAL:
				DWG NO.
				WEIGHT: 97.8kg
				SCALE: 1:20
				SHEET 3 OF 11

Main Frame w/Pipe Width

DWG.: W-F-103 A3

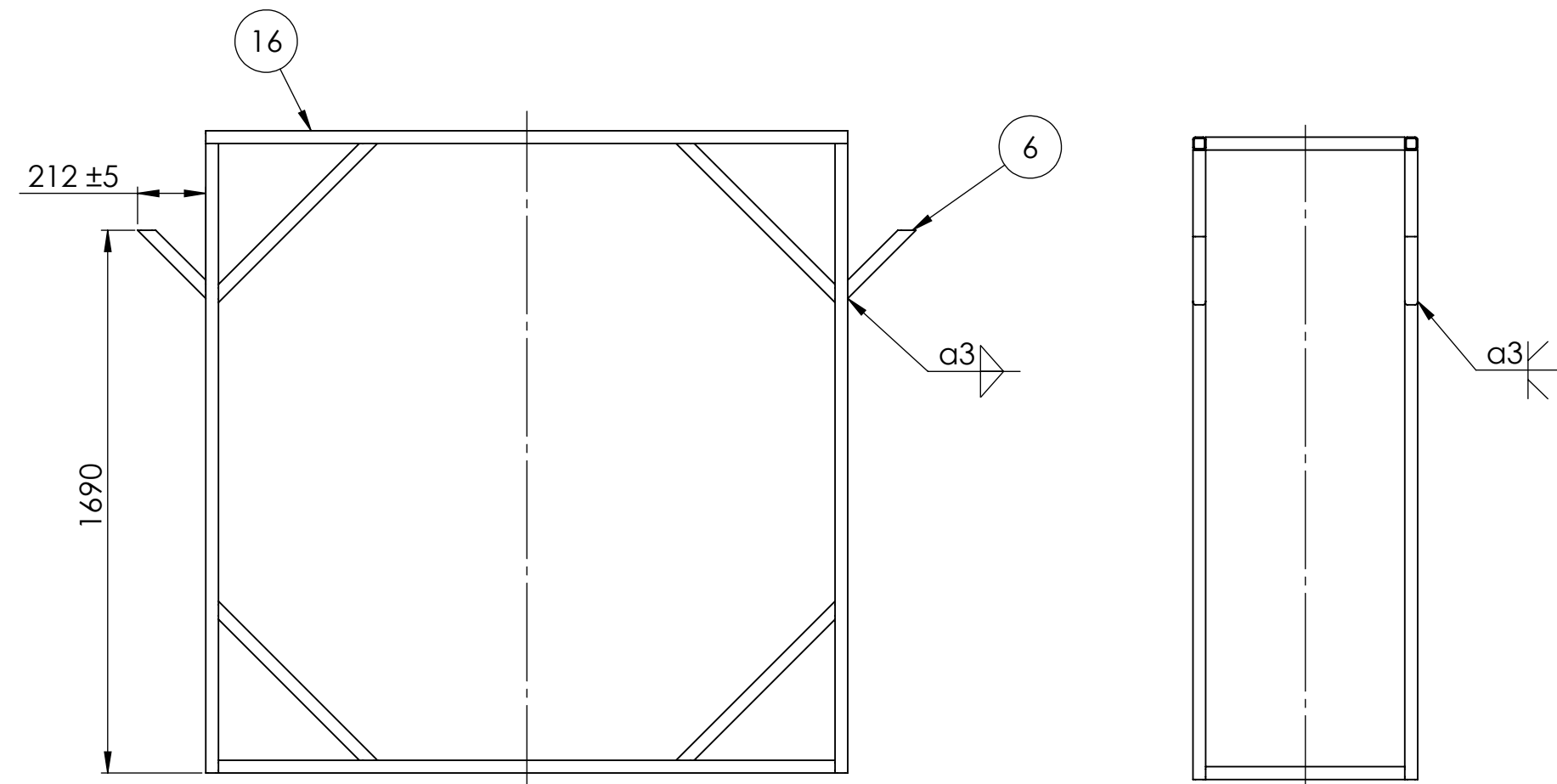
ITEM NO.	PART TITLE	DWG NO.:	QTY.
16	Main Frame w/Support	W-F-104	1



ITEM NO.	PART TITLE	DWG NO.:	QTY.
6	Pipe Support Short	F-108	4
15	Main Frame w/Pipe Width	W-F-103	1

UNLESS OTHERWISE SPECIFIED; DIMENSIONS ARE IN MILLIMETERS SURFACE FINISH: TOLERANCES: NS-ISO 2768-1 m LINEAR: ANGULAR:		FINISH: Dark Blue, Hammerlack Art. 36-042 Biltema	DEBUR AND BREAK SHARP EDGES	DO NOT SCALE DRAWING	REVISION 1
University of Agder					
DRAWN	NAME KLB	SIGNATURE	DATE	Projection: 	TITLE: Main Frame w/Support
CHK'D	LAE				
CHK'D	TB				
MATERIAL:				DWG NO.	A3
				WEIGHT: 107.9kg	
DWG.: W-F-104					
SHEET 4 OF 11					

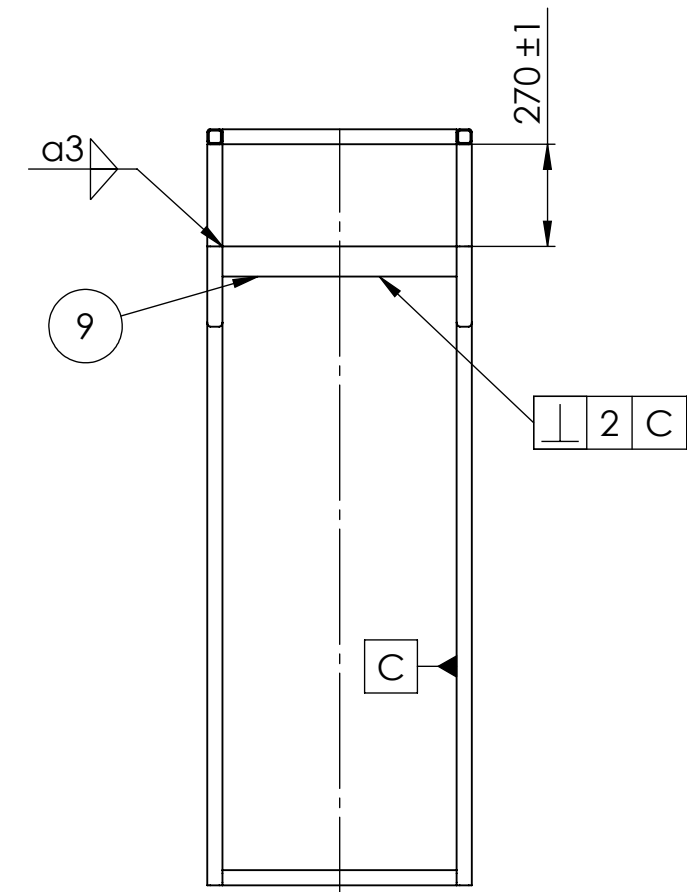
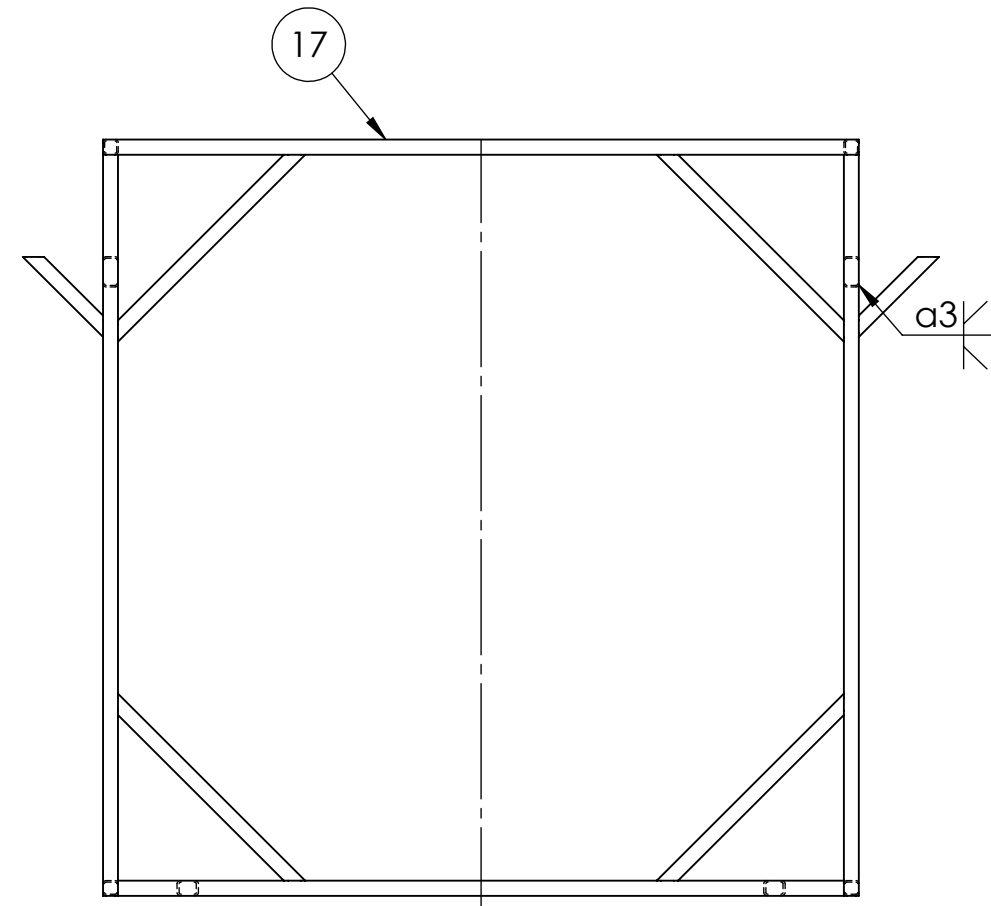
ITEM NO.	PART TITLE	DWG NO.:	QTY.
17	Main Frame w/Support Plate Leg	W-F-105	1



ITEM NO.	PART TITLE	DWG NO.:	QTY.
6	Pipe Support Short	F-108	4
16	Main Frame w/Support	W-F-104	1

UNLESS OTHERWISE SPECIFIED; DIMENSIONS ARE IN MILLIMETERS SURFACE FINISH: TOLERANCES: NS-ISO 2768-1 m LINEAR: ANGULAR:		FINISH: Dark Blue, Hammerlack Art. 36-042 Biltema	DEBUR AND BREAK SHARP EDGES	DO NOT SCALE DRAWING	REVISION 1
University of Agder					
DRAWN	NAME KLB	SIGNATURE	DATE	Projection: 	
CHK'D	LAE				
CHK'D	TB				
		MATERIAL:		DWG NO.	
				DWG.: W-F-105	A3
				SCALE:1:20	
				SHEET 5 OF 11	

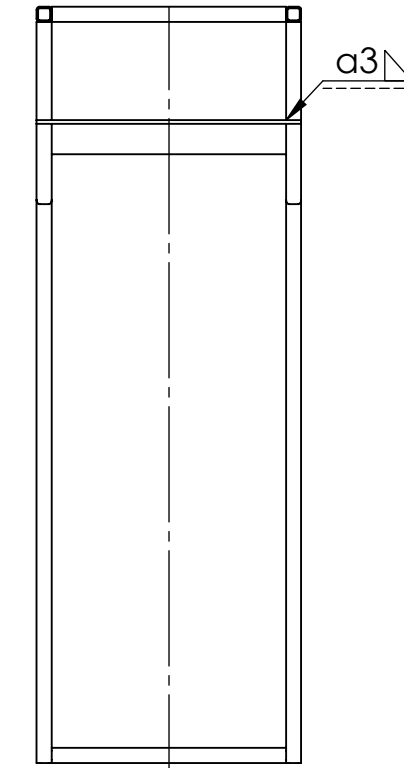
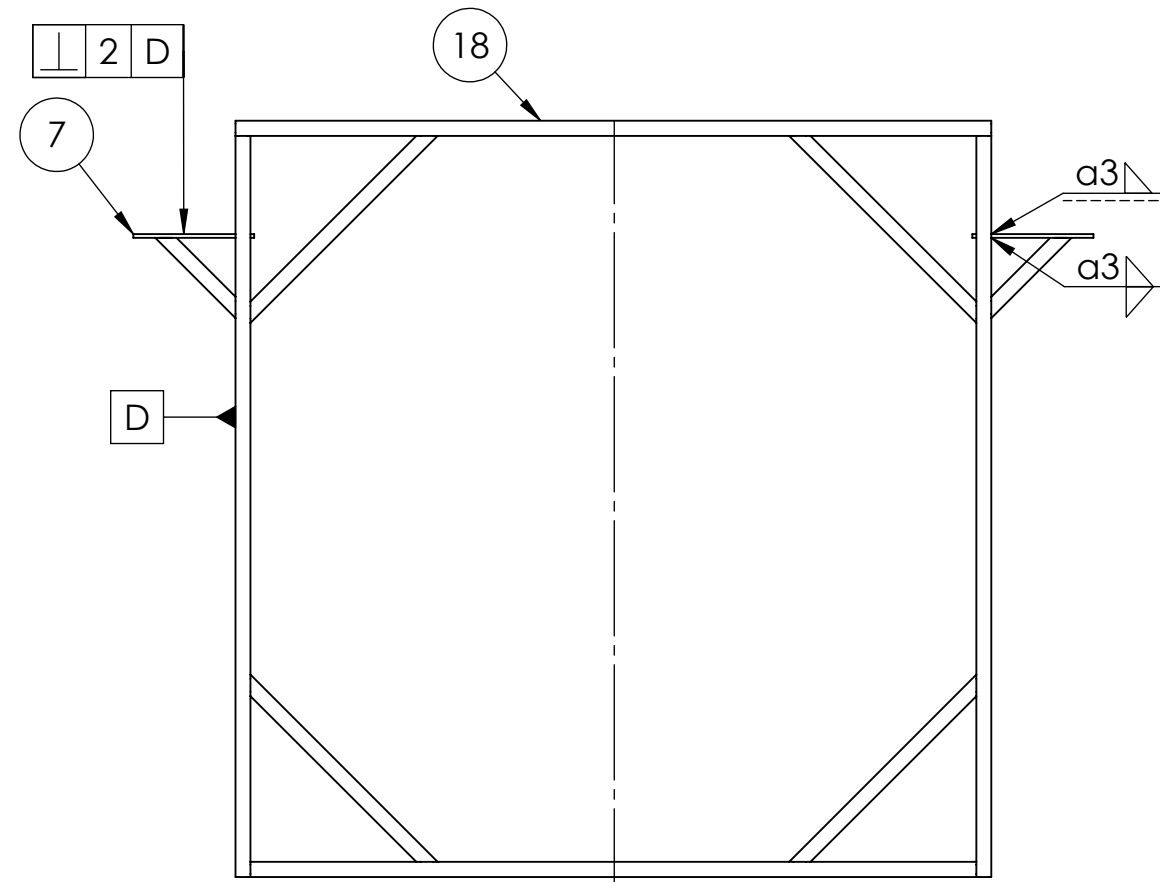
ITEM NO.	PART TITLE	DWG NO.:	QTY.
18	Main Frame w/Support Pipe	W-F-106	1



ITEM NO.	PART TITLE	DWG NO.:	QTY.
9	Pipe 40x80x4x620	F-108	2
17	Main Frame w/Support Plate Leg	W-F-105	1

UNLESS OTHERWISE SPECIFIED: DIMENSIONS ARE IN MILLIMETERS SURFACE FINISH: TOLERANCES: NS-ISO 2768-1 m LINEAR: ANGULAR:		FINISH: Dark Blue, Hammerlack Art. 36-042 Biltema	DEBUR AND BREAK SHARP EDGES	DO NOT SCALE DRAWING	REVISION 1
University of Agder					
DRAWN	NAME KLB	SIGNATURE	DATE	Projection: 	TITLE: Main Frame w/Support Pipe
CHK'D	LAE				
CHK'D	TB				
			MATERIAL:	DWG NO.	
				DWG.: W-F-106	A3
			WEIGHT: 114.7kg	SCALE: 1:20	
				SHEET 6 OF 11	

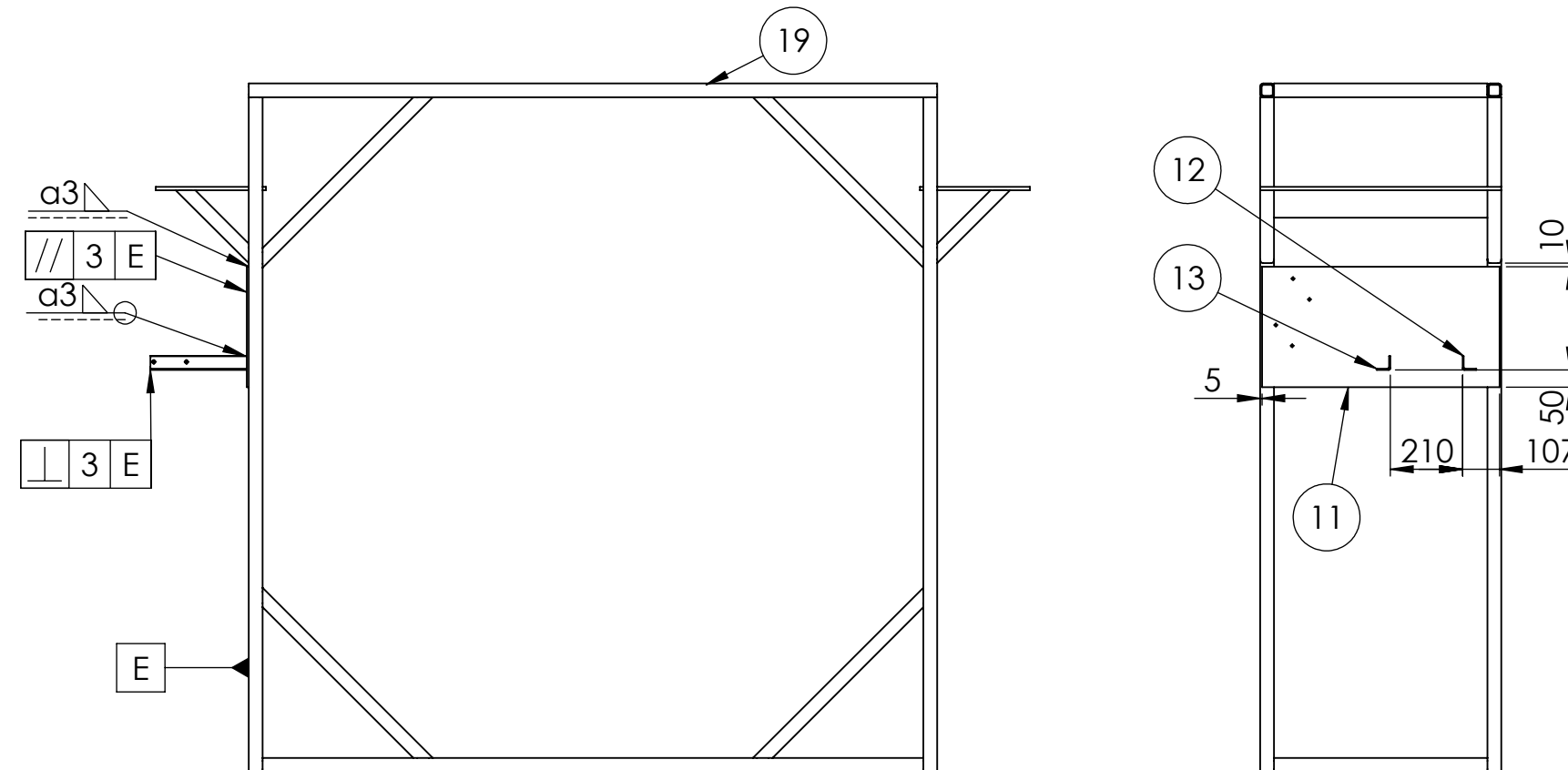
ITEM NO.	PART TITLE	DWG NO.:	QTY.
19	Main Frame w/Support Plate	W-F-107	1



ITEM NO.	PART TITLE	DWG NO.:	QTY.
7	Support Plate Horizontal	F-108	2
18	Main Frame w/Support Pipe	W-F-106	1

UNLESS OTHERWISE SPECIFIED: DIMENSIONS ARE IN MILLIMETERS SURFACE FINISH: TOLERANCES: NS-ISO 2768-1 m LINEAR: ANGULAR:		FINISH: Dark Blue, Hammerlack Art. 36-042 Biltema	DEBUR AND BREAK SHARP EDGES	DO NOT SCALE DRAWING	REVISION 1
University of Agder					
DRAWN	NAME KLB	SIGNATURE	DATE	Projection: 	TITLE: Main Frame w/Support Plate
CHK'D	LAE				
CHK'D	TB				
		MATERIAL:		DWG NO.	
				DWG.: W-F-107	A3
				SCALE: 1:20	
				SHEET 7 OF 11	
				WEIGHT: 149.0kg	

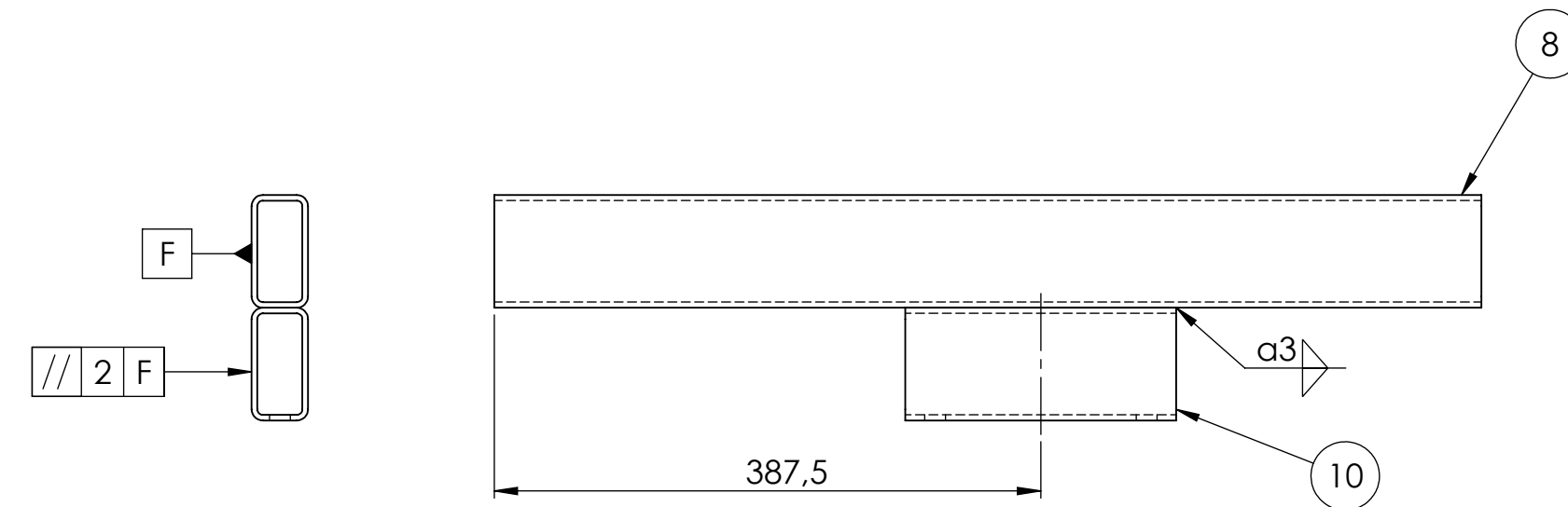
ITEM NO.	PART TITLE	DWG NO.:	QTY.
20	Main Frame w/Control Panel	W-F-108	1



ITEM NO.	PART TITLE	DWG NO.:	QTY.
11	Control Panel	F-112	1
12	Angel Iron Support Right	F-113	1
13	Angel Iron Support Left	F-114	1
19	Main Frame w/Support Plate	W-F-107	1

UNLESS OTHERWISE SPECIFIED: DIMENSIONS ARE IN MILLIMETERS SURFACE FINISH: TOLERANCES: NS-ISO 2768-1 m LINEAR: ANGULAR:		FINISH: Dark Blue, Hammerlack Art. 36-042 Biltema	DEBUR AND BREAK SHARP EDGES	DO NOT SCALE DRAWING	REVISION 1
University of Agder					
DRAWN	NAME KLB	SIGNATURE	DATE	Projection: 	TITLE: Main Frame w/Control Panel
CHK'D	LAE				
CHK'D	TB				
				MATERIAL: WEIGHT: 161.4kg	DWG NO. DWG.: W-F-108
					SCALE: 1:20
					SHEET 8 OF 11

ITEM NO.	PART TITLE	DWG NO.:	QTY.
21	Bearing House Support	W-F-109	2



ITEM NO.	PART TITLE	DWG NO.:	QTY.
8	Pipe Support Top	F-109	2
10	Pipe Bracket	F-111	2

UNLESS OTHERWISE SPECIFIED:
DIMENSIONS ARE IN MILLIMETERS
SURFACE FINISH:
TOLERANCES: NS-ISO 2768-1 m
LINEAR:
ANGULAR:

FINISH: Dark Blue, Hammerla
Art. 36-042 Biltema

University of Agder

Bearing House Support

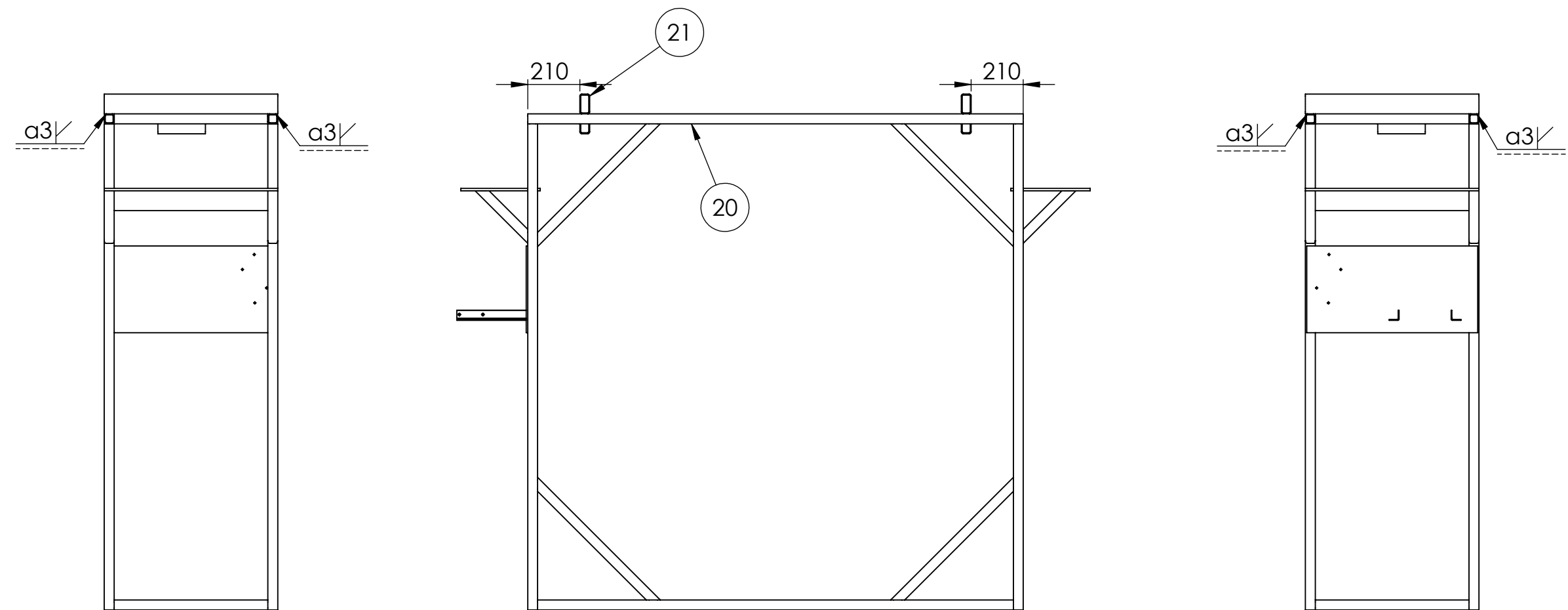


DWG.: W-F-109

A3

SHEET 9 OF 11

ITEM NO.	PART TITLE	DWG NO.:	QTY.
22	Main Frame w/Bearing House support	W-F-110	1



ITEM NO.	PART TITLE	DWG NO.:	QTY.
20	Main Frame w/Control Panel	W-F-108	1
21	Bracket for Pipelines	W-F-109	2

UNLESS OTHERWISE SPECIFIED:
DIMENSIONS ARE IN MILLIMETERS
SURFACE FINISH:
TOLERANCES: NS-ISO 2768-1 m
LINEAR:
ANGULAR:

FINISH:

DEBUR AND
BREAK SHARP

REVISION

University of Agder



	NAME	SIGNATURE	DATE		Projection: 
DRAWN	KLB				
CHK'D	LAE				
CHK'D	TB				
				MATERIAL:	
				WEIGHT:	173.3kg

1

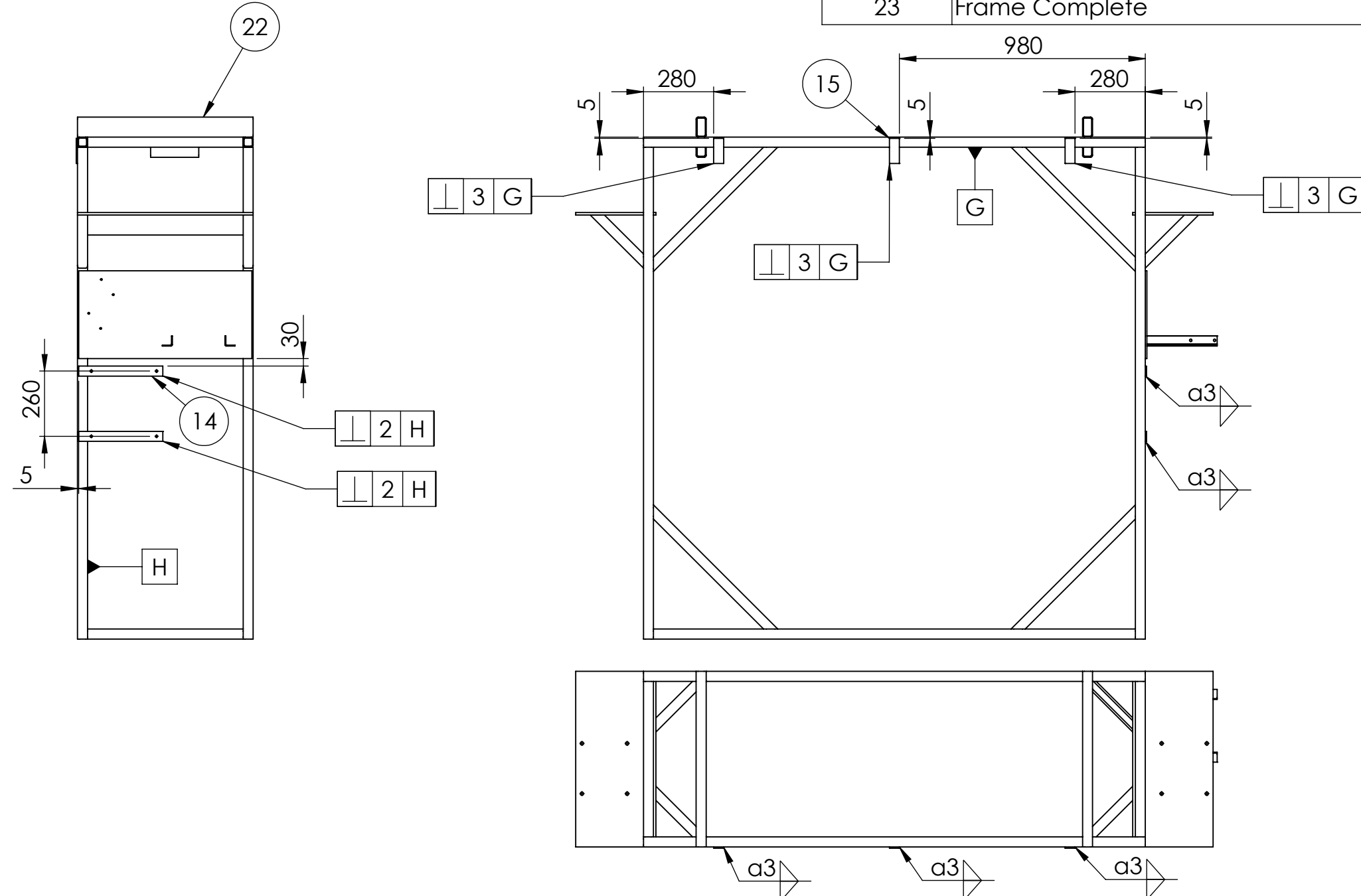
Main Frame w/Bearing House Support

DWG.: W-F-110

A3

SHEET 10 OF 11

ITEM NO.	PART TITLE	DWG NO.:	QTY.
23	Frame Complete	W-F-111	1



ITEM NO.	PART TITLE	DWG NO.:	QTY.
22	Main Frame w/Bearing House Support	W-F-110	1
14	Bracket for Cabinet	F-115	2
15	Bracket for Pipelines	F-116	3

UNLESS OTHERWISE SPECIFIED;
DIMENSIONS ARE IN MILLIMETERS
SURFACE FINISH:
TOLERANCES: NS-ISO 2768-1 m
LINEAR:
ANGULAR:

FINISH:
Dark Blue, Hammerlack
Art. 36-042 Biltema

DEBUR AND
BREAK SHARP
EDGES

DO NOT SCALE DRAWING

REVISION

1

University of Agder

DRAWN	NAME	SIGNATURE	DATE	Projection:
CHK'D	LAE			
CHK'D	TB			
MATERIAL:			DWG NO.	
			WEIGHT: 174.8kg	SCALE: 1:20
				SHEET 11 OF 11

Frame Complete



DWG.: W-F-111

A3

Drum Assembly

Bachelor project

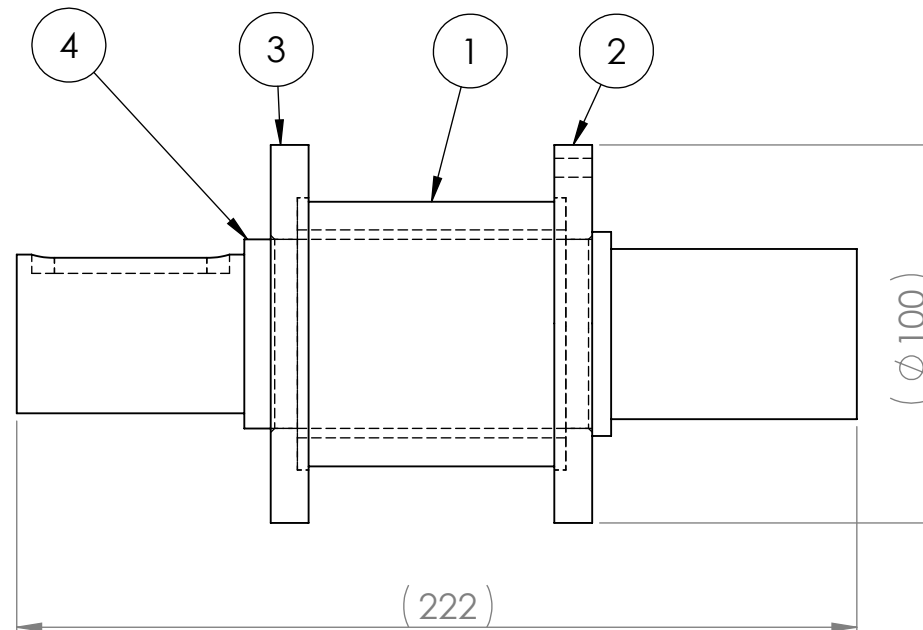
MAS302

University of Agder, 2013

Faculty of Engineering and Science

Department of Mechatronics

A



A

B

B

C

C

ITEM NO.	PART TITLE	DWG NO.:	QTY.
1	Drum	D-102	2
2	Drum Side Plate Holed	D-103	2
3	Drum Side Plate	D-104	2
4	Shaft Through Drum	D-105	2

UNLESS OTHERWISE SPECIFIED:
DIMENSIONS ARE IN MILLIMETERS
SURFACE FINISH:
TOLERANCES: NS-ISO 2768-1 m
LINEAR:
ANGULAR:

FINISH:
Machine after welding

DEBUR AND
BREAK SHARP
EDGES

DO NOT SCALE DRAWING

REVISION

1

University of Agder

DRAWN	NAME	SIGNATURE	DATE		Projection:
CHK'D	LAE				
CHK'D	TB				

TITLE:

Drum, assembly - welding

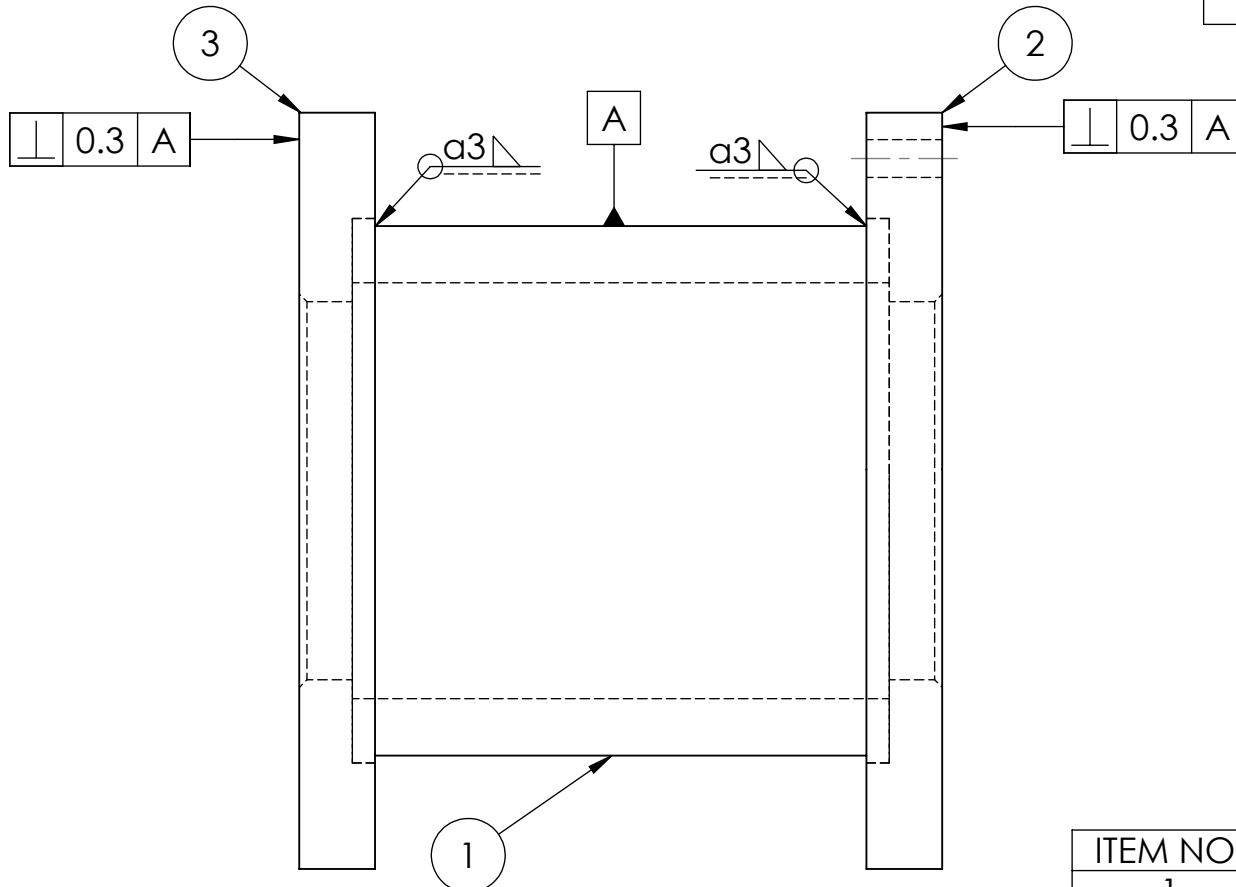


MATERIAL:	DWG NO.

DWG.: W-D-101

A4

1	2	3	4	5	6
ITEM NO.	PART TITLE	DWG NO.:	QTY.		
5	Drum w/Side Plates	W-D-102	2		



ITEM NO.	PART TITLE	DWG NO.:	QTY.
1	Drum	D-102	2
2	Drum Side Plate Holed	D-103	4
3	Drum Side Plate	D-104	4

UNLESS OTHERWISE SPECIFIED:
DIMENSIONS ARE IN MILLIMETERS
SURFACE FINISH:
TOLERANCES: NS-ISO 2768-1 m
LINEAR:
ANGULAR:

FINISH:

DEBUR AND
BREAK SHARP
EDGES

DO NOT SCALE DRAWING

REVISION 1

University of Agder

DRAWN	NAME	SIGNATURE	DATE		Projection:
CHK'D	LAE				
CHK'D	TB				

TITLE:

Drum, assembly - welding



MATERIAL:
S235JR

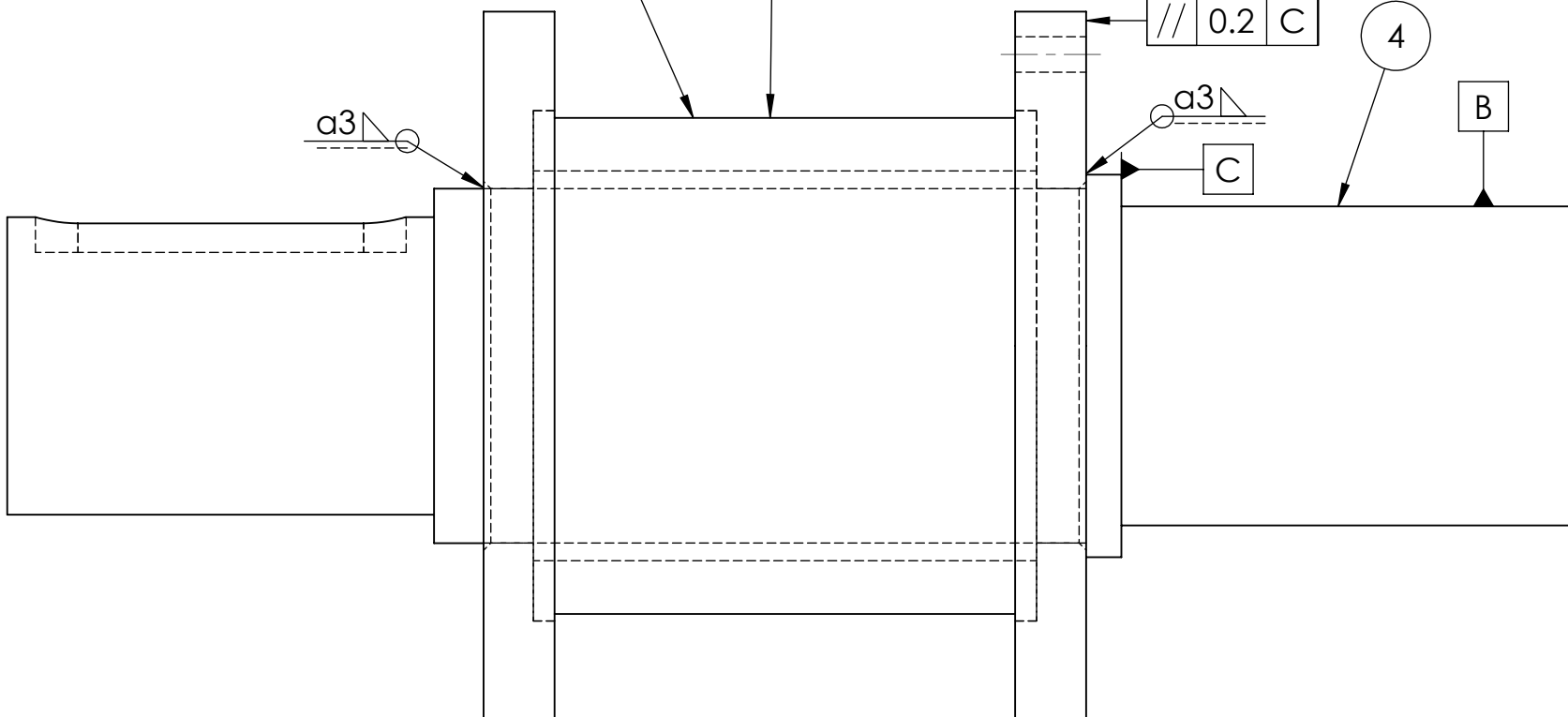
DWG NO.

DWG.: W-D-102

A4

1	2	3	4	5	6
			ITEM NO.	PART TITLE	DWG NO.: QTY.

6	Drum Shaft Complete	W-D-103	2
---	---------------------	---------	---



ITEM NO.	PART TITLE	DWG NO.:	QTY.
4	Shaft Through Drum	D-105	2
5	Drum w/Side Plates	W-D-102	2

UNLESS OTHERWISE SPECIFIED:
DIMENSIONS ARE IN MILLIMETERS
SURFACE FINISH:
TOLERANCES: NS-ISO 2768-1 m
LINEAR:
ANGULAR:

FINISH:

DEBUR AND
BREAK SHARP
EDGES

DO NOT SCALE DRAWING

REVISION 1

University of Agder

DRAWN	NAME	SIGNATURE	DATE		Projection:
CHK'D	LAE				
CHK'D	TB				

TITLE:

**Drum, assembly - welding
Side Plate Holed**



MATERIAL:
S235JR

DWG NO.

DWG.: W-D-103

A4

Beam Assembly

Bachelor project

MAS302

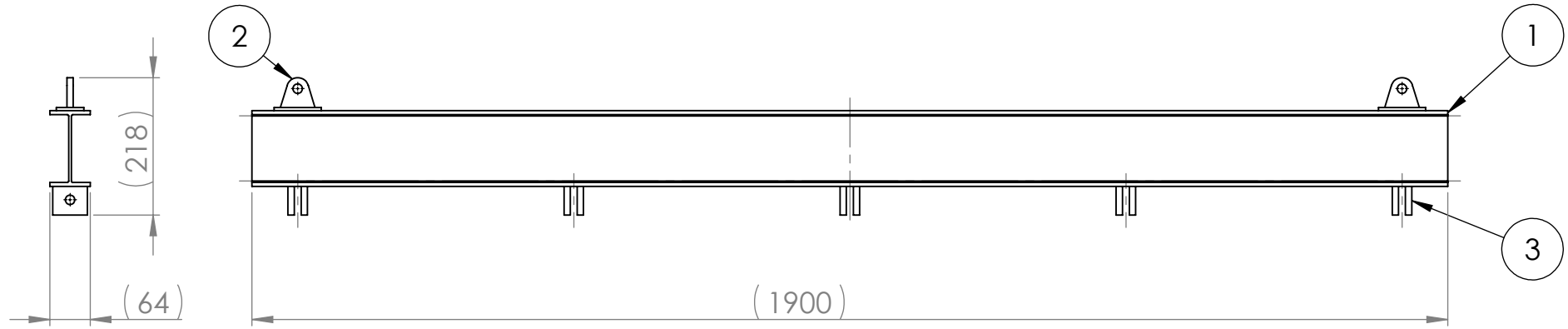
University of Agder, 2013

Faculty of Engineering and Science

Department of Mechatronics

A

A



B

B

9

C

ITEM NO.	PART TITLE	DWG NO.:	QTY.
1	Beam	B-102	1
2	Lifting Eye	B-103	3
3	Lifting Plate	B-104	10
5	Beam bracket	B-106	2

UNLESS OTHERWISE SPECIFIED:
DIMENSIONS ARE IN MILLIMETER.
SURFACE FINISH:
TOLERANCES: NS-ISO 2768-1 m
LINEAR:
ANGULAR:

FINISH:

DEBUR AND
BREAK SHAR
EDGES

DO NOT SCALE DRAWING

REVISION 1

University of Agder

	NAME	SIGNATURE	DATE	Projection:
DRAWN	KLB			
CHK'D	LAE			
CHK'D	TB			

TITLE:



MATERIAL

DWG NO.

DWG.: W-B-101

A4

1

2

3

4

5

6

ITEM NO.

PART TITLE

DWG NO.:

QTY.

6

Beam w/Lifting Plate

W-B-102

1

A

A

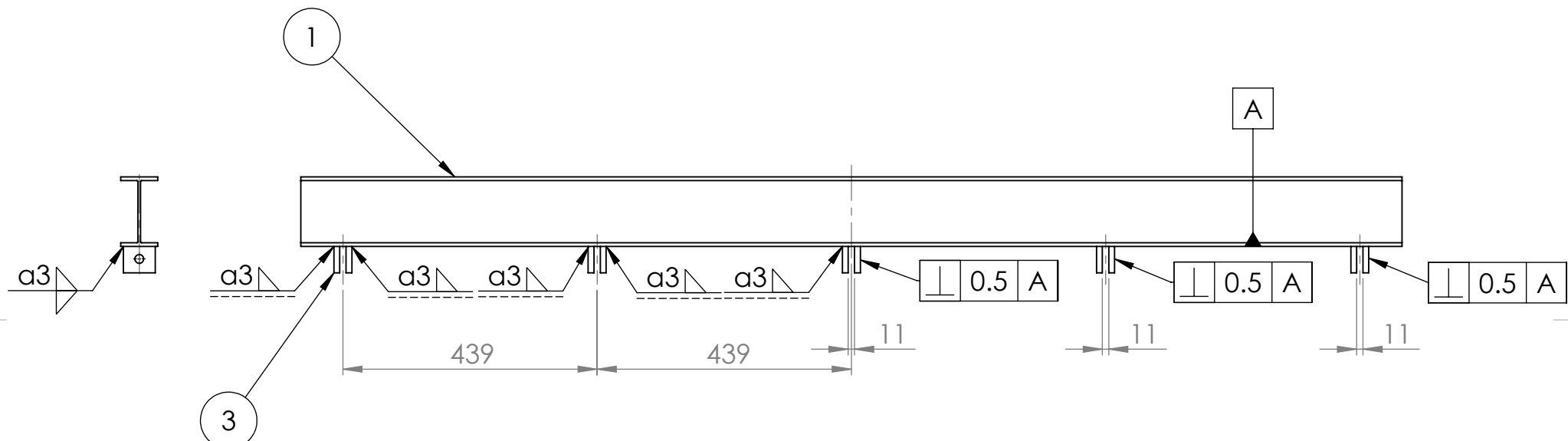
B

B

C

C

D



ITEM NO.

1

3

PART TITLE

Beam

Lifting Plate

DWG NO.:

B-102

B-104

QTY.

1

10

UNLESS OTHERWISE SPECIFIED:
DIMENSIONS ARE IN MILLIMETERS
SURFACE FINISH:
TOLERANCES: NS-ISO 2768-1 v
LINEAR:
ANGULAR:

FINISH:

DEBUR AND
BREAK SHARP
EDGES

DO NOT SCALE DRAWING

REVISION

1

University of Agder

DRAWN KLB

CHK'D LAE

CHK'D TB

SIGNATURE

DATE

Projection:



TITLE:

Beam w/Lifting Plate



MATERIAL:

S355J2+M

DWG NO.

DWG.: W-B-102

A4

1

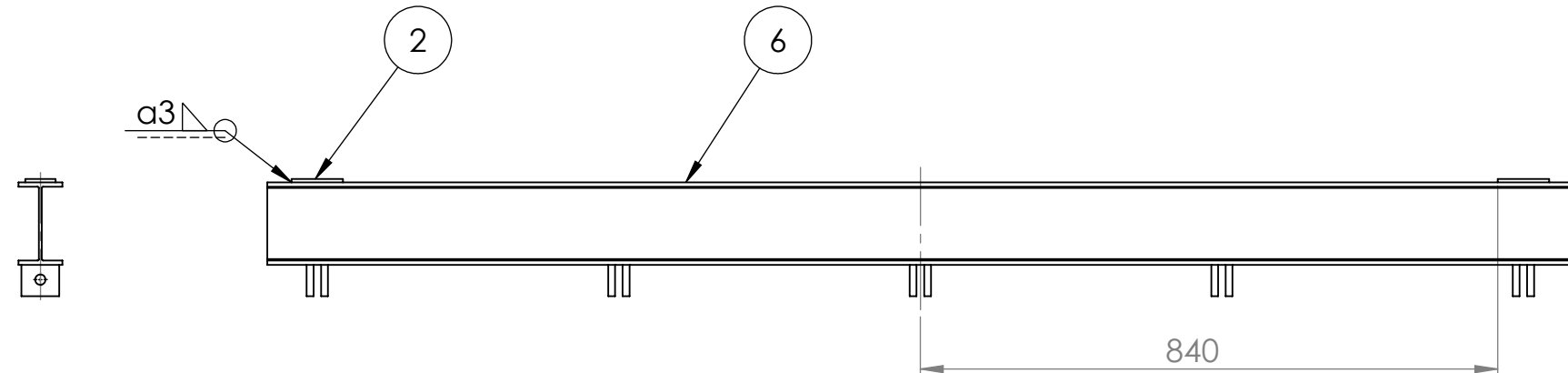
2

WEIGHT: 21.0kg

SCALE: 1:10

SHEET 2 OF 4

1	2	3	4	5	6
			ITEM NO.	PART TITLE	DWG NO.: QTY
			7	Beam w/Beam Bracket	W-B-103 1



ITEM NO.	PART TITLE	DWG NO.:	QTY.
4	Beam bracket	B-105	2
6	Beam w/Lifting Plate	W-B-102	1

UNLESS OTHERWISE SPECIFIED:
DIMENSIONS ARE IN MILLIMETER.
SURFACE FINISH:
TOLERANCES: NS-ISO 2768-1 v
LINEAR:
ANGULAR:

FINISH

DEBUR AND
BREAK SHAR
EDGES

DO NOT SCALE DRAWING

三國志

1

University of Agder



TITI

Beam w/Beam Bracket

	NAME	SIGNATURE	DATE		Projection:
DRAWN	KLB				
CHK'D	LAE				
CHK'D	TB				

DWG N

S235JF

DWG.: W-B-103

A4

1

2

WEIGHT: 21.3kg

SCALE 1:10

SHEET 3 OF 4

